



**Design and development of biologically inspired materials
based ultrafiltration membranes with enhanced antifouling
property**

By

J Antony Prince
(120537451)

Thesis submitted for the
Degree of Doctor of Philosophy in the Faculty of Science,
Agriculture and Engineering at Newcastle University

*School of Chemical Engineering and Advanced Materials,
Newcastle University
Newcastle Upon Tyne, UK
17-12-2015*

Author's declarations

This thesis is submitted in fulfillment of the requirements for the degree of Doctor of Philosophy at Newcastle University, United Kingdom. All the studies described within are solely my work unless expressly stated otherwise, and were undertaken under the guidance and supervision of Dr Kamelia Boodhoo between September 2012 and June 2015.

I certify that none of the material offered in this thesis has been previously submitted for a degree or any other qualification at the above or any other university or institute.

Neither the author nor Newcastle University accepts any liability for the contents of this document.

Abstract

One of the most pervasive problems afflicting mankind throughout the world is poor access to clean freshwater and sanitation. United Nations' FAO states that by 2025, around 1.8 billion people will be living in countries or regions with absolute water scarcity. With the growing demand for high quality water, many new technologies of water purification are being developed to cater for potable and non-potable use. The reliability and ease of operation of membrane-based filtration systems have led to their proliferation in wastewater treatment. Ultrafiltration (UF) is one such well-developed low pressure membrane separation process used in different applications. However, membrane fouling remains an inevitable problem in all pressure-driven membrane processes. Biofouling, in particular, is the most difficult type of fouling to address in terms of cleaning and regeneration of the membrane, causing deterioration of the membrane performance and leading to high operational costs, short replacement intervals and increase in chemical usage. Current trend and future direction of antifouling membranes are based on biologically inspired materials such as block copolymers with desired functional groups (amine, hydroxyl, acid), hydrogenated/hydroxylated and aminated graphene, aliened carbon nanotubes and aquaporin.

In this thesis, a novel concept is proposed and practiced to prevent bio-fouling by developing a self-cleaning membrane surface imparted with enhanced hydrophilicity via blending a newly synthesized, water-insoluble, highly hydrophilic biologically inspired co-polymers and functionalised graphene based additives with PES dope solution within the membrane matrix. The polymeric additives were developed by polymerising the highly reactive alkene monomers containing highly hydrophilic, negatively charged carboxyl (-COOH), hydroxyl (-OH) and amine (-NH₂) functional groups by a simple atom transfer radical polymerization technique. The new surface chemistry, enabled by the anchoring of antimicrobial silver nanoparticles to the functional groups of the polymeric additives, has been shown to be responsible for the self-cleaning property exhibited by the membrane surface.

Four new additives were investigated in this thesis for their effect on membrane hydrophilicity, permeability and selectivity. They include polyethylene glycol-silver (PEG-Ag) attached poly acrylonitrile-co-maleic acid (PANCMA), polyethylene imine-silver (PEI-Ag) attached PANCMA, PEG-Ag attached poly acrylonitrile-co-maleic acid co-diaminomaleio nitrile (PANCMACDAMN) and amine and carboxylated graphene attached poly acrylonitrile-co-maleimide (G-PANCMI).

These new additives were blended with PES dope solution to prepare the hollow fiber ultrafiltration membranes by dry wet spinning process. The additive G-PANCMII alone was also used to produce membrane without PES. All prepared polymeric additives and the membranes were characterized thoroughly using Fourier transform infrared (FTIR) spectroscopy, Nuclear magnetic resonance (NMR) spectroscopy, Raman spectroscopy, Gel permeable chromatography (GPC), Thermo gravimetric analysis (TGA), Differential scanning calorimetry (DSC), Energy-Dispersive X-ray Spectroscopy (EDX), Transmission Electron Microscopy (TEM), contact angle (CA), Scanning electron microscopy (SEM), Porometer, zone of inhibition test and clean water flux test. Finally, the membranes were tested for their permeability, selectivity and antifouling property in long term experiments using different feed water.

From the analytical data it was found that the hydrophilicity of all membranes prepared with these new additives are significantly increased. At the optimized condition, PEG-Ag attached PANCMADAMN reduced the contact angle of the PES membrane by 78.1% compared to the control membrane and the membrane fabricated by G-PANCMII gives a water contact angle of zero (0°) which is 100% reduction. Similarly, the water permeability of the membranes is also increased significantly with these new additives. At the optimized condition, PEG-Ag attached PANCMADAMN increases the water permeability of the PES membrane by 119.8% compared to the control membrane and the membrane prepared only with G-PANCMII gives 126% higher water permeability compared to the control PES membrane. The highest selectivity was also achieved for the G-PANCMII based membrane which was more than 99% with protein solution and the second highest selectivity was achieved for the membrane with PEG-Ag attached PANCMADAMN which was 96.2% with the same protein solution. Based on the experimental data of selectivity, permeability and antifouling property, the overall performance of the additives are in the following order; ***G-PANCMII > PEG-Ag attached PANCMADAMN > PEG-Ag attached PANCMADAMN > PEI-Ag attached PANCMADAMN***.

Development of biologically inspired materials based self-cleaning ultrafiltration membrane with long lasting properties opens up a viable solution for bio-fouling in ultrafiltration application for wastewater purification and based on the findings in this work, it can be concluded that the ultra-wetting graphene will be an ideal material for new generation water filtration membranes.

Publications

International Journals

1. **Prince J.A.**, Bhuvana S., Boodhoo K.V.K., Anbharasi V., Singh G., Synthesis and characterization of PEG-Ag immobilized PES hollow fiber ultrafiltration membranes with long lasting antifouling properties, *Journal of Membrane Science*. **454**, 538–548(2014).
2. **Prince J.A.**, Bhuvana S., Anbharasi V., Ayyanar N., Boodhoo K.V.K and Singh G., Self-cleaning Metal Organic Framework (MOF) based ultrafiltration membranes - A solution to bio-fouling in membrane separation processes. *Nature, Scientific Report*. **4**, 6555; DOI:10.1038/srep06555 (2014).
3. **Prince J.A.**, Bhuvana S., Anbharasi V., Ayyanar N., Boodhoo K.V.K and Singh G., Ultra-wetting graphene based membrane. *Journal of Membrane Science* **500**, 76–85(2016).
4. **Prince J.A.**, Bhuvana S., Anbharasi V., Boodhoo K.V.K and Singh G., Highly hydrophilic copolymer modified PES ultrafiltration (UF) membranes with robust antifouling properties. Under review in *Desalination (Manuscript ID: DES-D-15-01256)*
5. **Prince J.A.**, S. Bhuvana, V. Anbharasi, N. Ayyanar, K.V.K. Boodhoo and G. Singh: Ultra-wetting graphene-based PES ultrafiltration membrane - A novel approach for successful oil-water separation, (to be submitted to *Journal of Membrane Science*)

International Conference Proceedings/Presentations

- ❖ **Prince J.A.**, Boodhoo KVK and Siller L, Polyethersulfone (PES) hollow fiber ultrafiltration (UF) membranes with long-lasting antifouling properties. The 8th *International Membrane Science & Technology Conference (IMSTEC2013)*, Melbourne, Australia from 25 - 29 November 2013,
- ❖ **Prince J.A.**, S Bhuvana, KVK Boodhoo, V Anbharasi, N Ayyanar and G Singh, Hydrophilization of polyethersulfone (PES) hollow fiber ultrafiltration membranes with PEI-Ag grafted PANCMA to enhance the antifouling properties” (OR-2-010990), the 10th *International Congress on Membranes and Membrane Processes (ICOM2014)*” in Suzhou, China on July 20-25, 2014.
- ❖ **Prince J.A.** , S Bhuvana, V Anbharasi, N Ayyanar, KVK Boodhoo and G Singh, Highly hydrophilic block copolymer based hollow fibre ultrafiltration (UF) membranes with

enhanced permeability and antifouling properties, *2nd International Conference on Desalination using Membrane Technology*, 26-29 July 2015, Singapore, ABSTRACT REFERENCE NUMBER: MDES2015_0227

Patents

- **Prince J.A. et al.**, Graphene-based membrane and method of producing the same, International filing no: PCT/SG2015/050076, International filing date: 20-04-2015

Patents on potential future development from this thesis

- **Prince J.A. et al.**, Functionalized single-layer graphene water channel and method of producing the same, provisional patent application number: 10201503074T, Filing reference number E201504200134T, Provisional filing date: 20-04-2015

Grants

- **MOE2013-TIF-1-G-056**

Project title: Super hydrophilic polymer based UF membrane to treat oil refinery wastewater, Funding: SG\$ **394,000.00**, Role: CO- PI (**Prince J.A**), Duration: From Sep 2014 – to Oct 2016

- **NRF2015EWT-EWRP001-006**

Project title: Ultra-wetting graphene and aquaporin based biomimetic membranes for low pressure desalination, Funding: SG\$ **3,359,600.00**, Role: PI (**Prince J.A**), Duration: Jan 2016 to Jan 2019 (**Awarded**)

Awards

- European Membrane Society (EMS) “**Young Researcher Travel Award**” to the International Membrane Science and Technology Conference (IMSTEC-2013), which was held in Melbourne, Australia.
- Newcastle-Singapore institute of technology-Polytechnic (**NU-SIT-Poly**) **PhD Scholarship 2012**
- **IES-Young creator award - 2015** (for the invention titled “ultra-wetting graphene based membrane”) – *Shortlisted for presentation*

Acknowledgment

I would like to express my sincere appreciation especially to Dr Kamelia Boodhoo for her supervision, support, advice and in-depth knowledge in guiding and helping me during my studies. I am also thankful to the Dean of Postgraduate Studies Dr Bryn Jones from Newcastle University and my Director Mrs Tam Li Phin and Deputy Director Dr Gurdev Singh from EWTCOI for their support and advice.

My gratitude goes to Dr Bhuvana ‘Thala’ and Ms Anbharasi ‘Anbu’ for being good colleagues for sharing their knowledge, experiences as well as moral support. Their encouragement and kind words really helped me to go through hard times along my studies, without them it is impossible for me to complete my thesis on time.

I also wish to take this opportunity to give my sincere thanks to all the colleagues in EWTCOI especially Mr Shanmugasundaram ‘Shanmuu’, Ayyanar and staff from Newcastle University International Singapore (NUIS) for their kind assistance.

I am most grateful to my sister Antony Leema Rose, my parents and my family for their endless love, encouragement and support that enable me to continue my academic pursuits.

I gratefully acknowledge the support from Newcastle University and Environmental & Water Technology – Centre of Innovation (EWTCOI), Ngee Ann Polytechnic, Singapore, for the NU-Poly-SIT scholarship.

This work was partially supported from funding provided by Ministry of Education (MOE), Singapore under the Innovation Fund.

Table of contents

Author's declaration	ii
Abstract	iii
Publications	v
Acknowledgement	vii
Table of contents	viii
Nomenclature	xiv
List of figures	xix
List of tables	xxiv
1. Introduction	1
1.1. Increasing demand for clean fresh water	1
1.2. Membrane technology for water filtration	2
1.3. History of membrane process	3
1.4. Dissertation outline	5
2. Literature review	7
2.1. Low pressure membrane process	7
2.1.1. Microfiltration	7
2.1.2. Ultrafiltration	7
2.1.2.1. Ultrafiltration membranes	8
2.1.3. Membrane modules	10
2.1.3.1. Hollow fiber membrane modules	12
2.1.3.2. Spiral wound membrane modules	13
2.1.4. Ultrafiltration operation method	14
2.1.4.1. Dead-end flow filtration	15
2.1.4.2. Cross flow filtration	16
2.2. Membrane fouling	16
2.2.1. Biofouling	17
2.2.2. Biofilm control on membranes	19

2.3. Membrane surface modification	20
2.3.1. Membrane materials	20
2.3.1.1. Biologically inspired materials	21
2.3.1.1.1. Block copolymer based biomimetic membranes	22
2.3.1.1.2. Aquaporin based biomimetic membranes	22
2.3.1.1.3. Graphene based biomimetic membranes	22
2.3.1.2. Polyethersulfone (PES) membrane	23
2.3.1.3. Polyethersulfone membrane modification	24
2.3.2. Bulk modification of Polyethersulfone	25
2.3.2.1. Sulfonation of Polyethersulfone	25
2.3.2.2. Grafting functional groups to Polyethersulfone	27
2.3.3. Surface modification of Polyethersulfone membrane	28
2.3.3.1. Surface coating via thin film layer	28
2.3.3.2. Surface coating-interfacial polymerization	29
2.3.3.3. Photo-induced surface modification	31
2.3.3.4. Gama ray and ion beam induced grafting	34
2.3.3.5. Plasma based grafting polymerization and treatment	35
2.3.3.6. Atom transfer radical polymerization (ATRP)	36
2.3.3.7. Ozone-induced grafting	36
2.3.3.8. Ionic modification method	38
2.3.3.9. Pore filling method	39
2.3.3.10. Redox grafting method	39
2.3.3.11. Molecular imprinting	40
2.3.3.12. Thermal induced grafting and immobilization method	40
2.3.4. Blending method	42
2.3.4.1. Blending of hydrophilic additives with PES dope solution	42
2.3.4.2. Blending nanoparticle with PES dope solution	47
2.3.4.3. Blending of nanobiocides with PES dope solution	50
3. Objective and scope of this thesis	51
3.1. Scope and objective of the present work	52

4. Materials and characterization methods	55
4.1. Materials	55
4.2. Characterization methods	55
4.2.1. Streaming potential measurements	56
4.2.2. Fourier transform infrared spectroscopy (FTIR)	57
4.2.3. Thermal analysis (TGA)	57
4.2.4. Pore size analysis-capillary flow porometry	58
4.2.5. Transmission electron microscopy (TEM)	59
4.2.6. Scanning electron microscopy (SEM)	60
4.2.7. Gel permeable chromatography (GPC)	61
4.2.8. Contact angle (CA) analysis	62
4.2.9. Antibacterial activity by zone of inhibition test	63
4.2.10. Confocal microscopy analysis	63
4.2.11. Raman spectroscopy analysis	64
4.2.12. Nanomaterial leaching test	65
4.3. Membrane performance evaluation	66
4.3.1. Clean water flux test	66
4.3.2. Long term experiment with polluted wastewater	67
5. Effect of <u>hydroxyl (-OH)</u>, carboxyl (-COOH) and silver (Ag) functionalization on the antifouling properties of the prepared membranes	
5.1. Introduction	68
5.2. Experimental methods	69
5.2.1. Materials	69
5.2.2. Synthesis of poly (acrylonitrile co maleic acid) (PANCMA)	69
5.2.3. Preparation of membranes by dry wet spinning	70
5.2.4. Membrane surface modification	71
5.2.5. Membrane characterization	72
5.3. Results and discussion	72
5.3.1. Fourier Transform infra-red analysis	72

5.3.2.	Morphology of Hollow fibers	74
5.3.3.	EDX analysis	76
5.3.4.	Leaching test for Silver	78
5.3.5.	Contact angle	78
5.3.6.	Pore Size Analysis	78
5.3.7.	Zone inhibition test	79
5.3.8.	Clean water flux	80
5.3.9.	Long time performance and the fouling evaluation	80
5.4.	Summary	83
6.	Effect of <u>amine (-NH₂)</u>, carboxyl (-COOH) and silver (Ag) functionalization on the antifouling properties of the prepared membranes	
6.1.	Introduction	84
6.2.	Experimental methods	86
6.2.1.	Materials	86
6.2.2.	Synthesis of poly (acrylonitrile co maleic anhydride) (PANCMA)	86
6.2.3.	Synthesis of Ag capped PEI	87
6.2.4.	Synthesis of Ag capped PEI attached PANCMA	87
6.2.5.	Preparation of membranes by dry wet spinning	89
6.3.	Results and discussion	89
6.3.1.	TEM analysis of Ag capped PEI colloid	89
6.3.2.	FTIR analysis of PANCMA and PEI-Ag attached PANCMA	90
6.3.3.	Morphology of Hollow fibers and EDX analysis	92
6.3.4.	Leaching test for Silver	93
6.3.5.	Contact angle	93
6.3.6.	Pore Size Analysis	94
6.3.7.	Clean water flux	94
6.3.8.	Zone inhibition test	95
6.3.9.	Long time performance and the fouling evaluation	97
6.4.	Summary	99

7. Effect of hydroxyl (-OH), amine (-NH₂), carboxyl (-COOH) and silver (Ag) functionalization on the antifouling properties of the prepared membranes

7.1. Introduction	100
7.2. Experimental methods	102
7.2.1. Materials	102
7.2.2. Synthesis of PANCMACDAMN	102
7.2.3. Attachment of PEG and Ag with PANCMACDAMN	103
7.2.4. Preparation of membranes by dry wet spinning	104
7.3. Results and discussion	105
7.3.1. FTIR analysis	105
7.3.2. GPC analysis of PANCMACDAMN	107
7.3.3. Morphology of Hollow fibers and EDX analysis	107
7.3.4. Leaching test for Silver	109
7.3.5. Contact angle	109
7.3.6. Pore Size Analysis	109
7.3.7. Zone inhibition test	110
7.3.8. Clean water flux	111
7.3.9. Long time performance and the fouling evaluation	111
7.4. Summary	113

8. Effect of amine (-NH₂) functionalized graphene oxide on the antifouling properties of the prepared membranes

8.1. Introduction	115
8.2. Experimental methods	116
8.2.1. Materials	117
8.2.2. Synthesis of functionalized xGnP	117
8.2.3. Synthesis of xGnP grafted PANCFI (G-PANCFI)	117
8.2.4. Preparation of flat sheet membrane	118
8.2.5. Preparation of hollow fiber membranes by dry wet spinning	120
8.3. Results and discussion	121
8.3.1. FTIR analysis of xGnP, PANCFI and G- PANCFI	121

8.3.2.	Ram spectral analysis of xGnP, PANcMA and G- PANcMI	122
8.3.3.	Zeta potential analysis	123
8.3.4.	TGA and DSC analysis	124
8.3.5.	Contact angle analysis and dispersibility test	125
8.3.6.	Morphology analysis	127
8.3.7.	Pore Size Analysis	128
8.3.8.	Clean water flux	128
8.3.9.	Long time performance and the fouling evaluation	129
8.3.10.	Oily waste water treatment	133
8.4.	Summary	136
9.	Performance characterization of developed membranes	138
9.1.	Summary of results	138
9.2.	Comparison of various membrane prepared in this thesis	140
9.2.1.	Hydrophilicity	141
9.2.2.	Water permeability	142
9.2.3.	Selectivity	143
9.2.4.	Effect of functional groups on the anti-fouling properties	143
10.	Conclusion and recommendations	145
10.1.	Conclusions	145
10.2.	Recommendations	148
11.	References	150

Nomenclature

-COOH	Carboxyl functional group
-NH ₂	Amine functional group
-OH	Hydroxyl functional group
ΔH	Enthalpy change
ΔP	Pressure Difference
AA	Acrylic acid
AAG	2-acrylamidoglycolic acid monohydrate
AAP	2-acrylamido-2-methyl-1-propanesulfonic acid
AFM	Atomic Force Microscopy
Ag	Silver
AgNO ₃	Silver nitrate
AIBN	Azobisisobutyronitrile
AM	Acrylamide
AMPS	2-acrylamido-2-methyl-1-propanesulfonic acid
ATR	Attenuated total reflection
ATRP	Atom transfer radical polymerization
BAP	Bacterial alkaline phosphatase
BET	Bruauer, Emmett and Teller
BMA	Butyl methacrylate
BPA	Bisphenol A
BPPO	Benzoyl peroxide
BSA	Bovine serum albumin
BSA	Bovine Serum Albumin
C _f	Feed concentration
C _p	Permeate concentration
CA	Cellulose acetate
CA _{oil}	Oil contact angle
CA _w	Water contact angle

CBAP	Cyclic bacterial alkaline phosphatase
$(\text{CH}_3)_3\text{SiSO}_3\text{Cl}$	Trimethylsilylchlorosulfate
CHMA	Cyclohexyl methacrylate
CLSM	Confocal Laser Scanning Microscopy
ClSO_3H	Chlorosulfonic acid
CN	Cellulose nitrate
CO_2	Carbon dioxide
CPES	Carboxylic polyethersulfone
DEA	Diethanolamine
DEG	Diethylene glycol
DG	Degree of grafting
DLS	Dynamic light scattering
DMAC	Dimethyl acetamide
DMF	Dimethyl formamide
DMMSA	N,N-dimethyl-N-methacryloxyethyl-N-(3-sulfopropyl) ammonium
DS	Degree of sulfonation
DSC	Differential Scanning Calorimetry
EDC	Ethyl dimethyl aminopropylcarbodiimide
EDX	Energy Dispersive X-ray
EPS	Extracellular Polymeric Substances
FESEM	Field Emission Scanning Electron Microscopy
FTIR	Fourier Transform Infra-Red
G-PANCMMA	Grafted poly acrylonitrile-co-maleic acid
G-PANCFMI	Grafted poly acrylonitrile-co-maleimide
GMA-IDA	2-methacrylic acid 3-(bis-carboxymethylamino)-2-hydroxyl-propyl ester
GO	Graphene oxide
GPC	Gel permeation chromatography
H_2O	Water
H_2SO_4	Sulfuric acid
HCl	Hydrochloric acid

HEMA	(Hydroxyethyl)methacrylate
HRP	Horse radish peroxidase
ICP-OES	Inductively coupled plasma optical emission spectrometry
ID	Inner diameter
J_w	Water flux
$K_2S_2O_8$	Potassium persulfate
KBr	Potassium bromide
KOH	Potassium hydroxide
LEP	Liquid entry pressure
LMH	Liters per area per hour
MA	Maleic anhydride
MF	Micro Filtration
MIPs	Molecularly Imprinted Polymers
MOF	Metal organic framework
MPC	2-methacryloyloxyethyl phosphorylcholine
MPEG	Methylated polyethylene glycol
MWCO	Molecular Weight Cut Off
N_2	Nitrogen
Na_2SO_3	Sodium sulfite
$NaBH_4$	Sodium borohydride
NF	Nano Filtration
NH_3	Ammonia
NHS	N-hydroxysuccinimide
NMP	N-methyl-2-pyrrolidone
NMR	Nuclear Magnetic Resonance
NOMs	Natural Organic Matters
NVP	N-vinyl-2-pyrrolidinone
O_2	Oxygen
O_3	Ozone
OD	Outer diameter
PA	Polyacrylate

PAN	Polyacrylonitrile
PANCMA	Poly acrylonitrile-co-maleic acid
PANCMI	Poly acrylonitrile-co-maleimide
PDA	Phenylenediamines
PEG	Polyethylene glycol
PEGMA	poly(ethylene glycol) methyl ether methacrylate
PEI	Polyethylene imine
PEO	Polyethylene oxide
PES	Polyethersulfone
PI	Polyimine
PMAA	Poly(methacrylic acid)
PMAA-g-PES	Poly(methacrylic acid) grafted polyether sulfone
PS	Polysulfone
PSF	Polysulfone
PTAB	Phenyltrimethylammoniumtribromide
PVA	Polyvinyl alcohol
PVC	Polyvinyl chloride
PVDF	Polyvinylidene fluoride
qDMAEM	quaternary-2-dimethylaminoethyl methacrylate
R	Rejection of contaminants
RAFT	Reversible addition fragmentation chain transfer
RO	Reverse Osmosis
SDBAP	Site directed bacterial alkaline phosphate
SDS	Sodium dodecylsulfate
SFRP	Stable free radical polymerization
SMA	Styrene maleic anhydride
SMMs	Surface modifying macromolecules
SO ₃	Sulfur trioxide
SO ₃ H	Sulfonic acid
SOCl ₂	Thionyl chloride
SPES	Sulfonated polyether sulfone

SPPO	Sulfonated polypropylene oxide
SWRO	Sea Water Reverse Osmosis
TEM	Transmission electron microscopy
TETA	Trimethylenetertramine
TFL	Thin film layer
TGA	Thermogravimetric analysis
THF	Tetrahydrofuran
TiO ₂	Titanium dioxide
T _m	Melting point
TMC	Trimesoyl chloride
TMP	Trans Membrane Pressure
TOC	Total organic carbon
UF	Ultra Filtration
UPAC	Union of Pure and Applied Chemistry
UV	Ultraviolet
xGnP	Exfoliated graphene nano platelets
XPS	X-ray photoelectron spectroscopy

List of figures

CHAPTER: 1

Figure.1.1.1. Projected global water scarcity in 2025 (International Water Management Institute)

Figure.1.2. Schematic of membrane filtration process.

Figure.1.3. Scheme of different pressure-driven membrane filtration processes and rejection capacities.

Figure.1.4. Historical development of pressure driven membrane process and the future direction

CHAPTER: 2

Figure.2.1. (a) Solvent/non-solvent exchange during fabrication of flat sheet membrane by phase separation process and (b) Solvent/non-solvent exchange during fabrication of hollow fiber membrane by

Figure.2.2. Schematic representation of cross-section of symmetric and asymmetric membrane

Figure.2.3. Hollow fiber membrane module

Figure.2.4. (a) Inside-out filtration, (b) outside-in filtration

Figure.2.5. Spiral-wound membrane module assembly

Figure.2.6. Schematic diagram of a dead-end flow filtration

Figure.2.7. Schematic diagram of a crossflow filtration

Figure.2.8. Step by step formation of biofilm (attachment, colonization and growth)

Figure.2.9. State of membrane development for desalination and their commercial viabilities (adapted and modified from *Mary Theresa M. et al., Energy Environ. Sci.*, 2011, 4, 1946-1971)

Figure.2.10. Chemical structure of PES polymer

Figure.2.11. Chemical structure of sulfonated PES

Figure.2.12. Degradation of PES during sulphonation (reaction with strong sulphuric acid)

Figure.2.13. Process of fabrication of carboxylic polyethersulfone (CPES)

Figure.2.14. PES modification by grafting different functional groups

Figure.2.15. Layer by layer deposition by alternating spray coating of polyanions and polycations

Figure.2.16. Preparation of grafted PES membrane by gamma-ray irradiation

Figure.2.17. O₂ plasma treatment of the membrane

Figure.2.18. Reaction schemes of hydrophilic polymers grafting on to the PES membrane activated by UV/ozone treatment (a) PVA, (b) PEG and (c) chitosan

Figure.2.19. Dual layer hollow fiber spinning unit

Figure.2.20. (a) Cationic polymerization of styrene (b) polystyrene grafts in the membrane pore

Figure.2.21. Thermal induced surface cross-linking on PES membrane

Figure.2.22. Reaction scheme of PES modification

Figure.2.23. Cleaning process by SDS solution

Figure.2.24. Synthesis of SMA-g-MPEG

Figure.2.25. Effect of AA and HEMA on flux stability of PES membranes

Figure.2.26. Synthesis of SMA-g-MPEG

Figure.2.27. Effect of AA and HEMA on flux stability of PES membranes

Figure.2.28. MWCOs of unmodified and modified membranes

Figure.2.29. Chemical modification of zeolite surface

CHAPTER: 4

Figure.4.1. SurPASS electro kinetic analyzer (Anton Paar Corporation)

Figure.4.2. Fourier transforms infrared spectroscopy used in this study

Figure.4.3. Thermo Gravimetric Analyzer (TGA5000, TA instrument) used in this study

Figure.4.4. Capillary flow porometer for measuring pore size of the membranes

Figure.4.5. Transmission electron microscopy (TEM) used in this study

Figure.4.6. Scanning electron microscope (SEM) (Jeol Jsm-7600F) coupled to an XmaxN detector for energy-dispersive X-ray (EDX) analysis used in this study

Figure.4.7. Gel permeation chromatography (GPC)

Figure.4.8. Contact angle analyzer (Sigma 701 Tensiometer)

Figure 4.9. Confocal instrument used for this study

Figure 4.10. Raman spectroscopy used for this study

Figure.4.11. Filtration set up used to study the clean water flux

CHAPTER: 5

Figure.5.1. Phase diagram for the dope composition

Figure.5.2. Schematic representation of stepwise modification of hollow fiber

Figure.5.3. FTIR spectra of S1) PES S2) PES/PANCMA (2.5 wt%)/PEG/Ag S3) PES/PANCMA (5wt%)/PEG/Ag S4) PES/PANCMA (7.5wt%)/PEG/Ag

Figure.5.4. Schematic representation of possible grafting of PEG/Ag to PANCMA

Figure.5.5. SEM pictures of unmodified and modified hollow fiber membranes

Figure.5.6. Cross section morphology of unmodified and modified hollow fiber membranes

Figure.5.7. EDX results of unmodified and modified hollow fiber membranes

Figure.5.8. Zone of inhibition of modified and unmodified membranes

Figure.5.9. Pure water flux (a) and Flux drop (b) for the control and the best performing membrane in long time run

Figure.5.10. Contaminant removal efficiency for the control and the best performing membrane in long time run with wastewater: TOC rejection (a) Turbidity rejection (b)

CHAPTER: 6

Figure.6.1. Schematic representation of the self-cleaning property of the membrane

Figure.6.2. Synthesis of Synthesis of poly (acrylonitrile co maleic anhydride) (PANCMA)

Figure.6.3. Synthesis of Ag capped PEI

Figure.6.4. Synthesis of Ag capped PEI attached PANCMA

Figure.6.5. (a) TEM image of silver attached PEI (b) Chemical model of silver attached PEI

Figure.6.6. FTIR Spectrum of the PANCMA and Silver-PEI attached PANCMA

Figure.6.7. FTIR spectra of S1) PES S2) PES-PANCMA (5 wt%) S3) PES-PANCMA-PEI-Ag (5wt %)

Figure.6.8. SEM images of membrane samples S1-PES, S2-PES-PANCMA and S3-PES-PANCMA-PEI-Ag (a) Cross section (b) Outer surface

Figure.6.9. Cross section (a) and the distribution of silver (Ag) element (points measured by EDX mapping analysis) on the membrane cross-section (b) of the sample S3-PES-PANCMA-PEI-Ag

Figure.6.10. Zone of inhibition of modified and unmodified membranes before filtration with sodium alginate solution (a) and after filtration with sodium alginate solution (b)

Figure.6.11. Pure water flux (a), Flux drop (b) and sodium alginate (TOC) removal efficiency (c) for the membrane samples S1 to S3 in long time run with 10ppm sodium alginate solution

CHAPTER: 7

Figure.7.1. Schematic representation of the silver modified membrane and the proposed self-cleaning biofouling resistant membrane.

Figure.7.2. Synthesis of PANCMACDAMN and attachment of PEG and Ag with PANCMACDAMN

Figure.7.3. Phase diagram of the dope composition with optimization direction

Figure.7.4. FTIR spectrum of the new additive PANCMACDAMN and presence of the new additive in the modified PES membranes

Figure.7.5. Gel permeation chromatography analysis of PANCMACDAMN

Figure.7.6. SEM image (cross section) of control membrane M1 (a) and modified (best performing) hollow fiber membranes sample M4 (b)

Figure.7.7. SEM image (cross section) (a) and Elemental mapping (b) of modified (best performing) hollow fiber membranes sample M4

Figure.7.8. Zone of inhibition of control S1 and modified best performing membrane M4 (a) before protein filtration, (b) after protein filtration

Figure.7.9. Pure water flux for the control membrane sample M1 and the best performing membrane sample M4 at 1bar feed pressure (a), water permeability during long time run with 10ppm BSA solution at 1bar feed pressure for the same samples (b), normalized water permeability for the BSA solution separation during long time run (c) and BSA protein (TOC) removal efficiency / selectivity of the membranes in % (d)

Figure.7.10. Confocal laser scanning (CLSM) image of control sample M1 and the best performing membrane sample M4

CHAPTER: 8

Figure.8.1. Synthesis of functionalized xGnP (a) Synthesis of G-PANCMI (b)

Figure.8.2. Phase diagram for the G-PANCMI dope compositions

Figure.8.3. Phase diagram for the PES-G-PANCMI dope compositions

Figure.8.4. FTIR spectrum of xGnP, amine modified xGnP, PANCMA (anhydride) and G-PANCMI

Figure.8.5. Raman spectroscopy analysis of unmodified graphene, amine and carboxylated graphene and G-PANCMi

Figure.8.6. Zeta potential analysis of PANCMa and G-PANCMi membranes

Figure.8.7. TGA analysis of PANCMa and G-PANCMi membranes (d)

Figure.8.8. Average water contact angle (a), water contact angle reduction of the **PANCMa** and **G-PANCMi** membranes with time (b) and the dispersibility or stability of the unmodified (xGnP) and modified graphene (G-PANCMi) in solution with time.

Figure.8.9. SEM images of PANCMa and G-PANCMi membranes (a) Cross section (b) Outer surface (c) Actual image of synthesized PANCMa and G-PANCMi membranes

Figure.8.10. Pure water flux at 1bar feed pressure (a), water permeability during long time run with 10ppm BSA solution at 1bar feed pressure (b), normalized water permeability for the BSA solution separation during long time run (c) and BSA protein (TOC) removal efficiency in % (d)

Figure.8.11. Schematic representation of hydrogen bonding and protein repulsion of the novel membrane (a) and confocal laser analysis of the membrane after protein filtration (b)

Figure.8.12. Comparison of the performance of the ultra-wetting graphene based membrane against different current state of art polymer-graphene oxide (GO) composite ultrafiltration membranes in terms of permeability and BSA selectivity

Figure.8.13. SEM images of PES and PES-G-PANCMi membranes (a) Cross section (b) Outer surface (c) Actual image of synthesized PES and PES-G-PANCMa membranes

Figure.8.14. (a) Liquid entry pressure of oil (LEP_{oil}) analysis, (g) Water and oil contact angle and (c) Clean water flux of the PES and PES-G-PANCMi membrane samples

Figure.8.15. Permeability (flux drop) (a) and oil removal efficiency (b) of the membrane samples PANCMa & G-PANCMi in a long time study of 8 hrs

CHAPTER: 9

Figure.9.1. Schematic representation of self-cleaning mechanism of the new membrane

Figure.9.2. Comparison of various membranes prepared in this thesis

Figure.9.3. Schematic representation of water transportation through membrane surface by intermolecular hydrogen bonding between hydrophilic functional groups and water.

List of tables

CHAPTER: 2

Table.2.1. Different configurations of ultrafiltration membrane modules

Table.2.2. Advantages and disadvantages of different membrane module configurations

CHAPTER: 5

Table.5.1. Composition of the dope solutions for the hollow fiber membrane fabrications

Table.5.2. Pore size, contact angle and the clean water flux of the control PES membrane and the modified PES-PANCMMA membrane samples.

CHAPTER: 6

Table.6.1. Composition of the dope solutions for the hollow fiber membrane fabrications

CHAPTER: 7

Table.7.1. Pore size, contact angle and the clean water flux of the control PES membrane and the PEG-Ag grafted PANCMACDAMN modified PES membrane samples.

CHAPTER: 9

Table.9.1. Performance of various membrane prepared in this thesis in terms of hydrophilicity, permeability, selectivity and Flux drop

1. Introduction

1.1 INCREASING GLOBAL DEMAND FOR CLEAN FRESHWATER

Water is a valuable resource for mankind. Over 3.6 million people around the world die each year from drinking unsafe water¹. Waterborne pathogens have a negative effect on public health in the developing countries. These problems are expected to grow in the coming decades. Based on the projected global water scarcity in 2025, as shown in Figure 1.1, it has been estimated that the number of people affected by severe water shortages in 2025 is expected to increase from the current (2014) fourfold to six fold². Besides a shortage of fresh water problem, there is also an increasing need for extensive treatment of the existing fresh water resources. In both developing and developed nations, growing tendencies of (micro) pollutants such as heavy metals, pesticides, pharmaceutical derivatives, disinfection by-products, and endocrine disruptors are discharged into water supplies. The amount of these harmful contaminants is growing rapidly and the fact that many of these compounds are already toxic in trace quantities³, is nowadays, resulting in the regulations on drinking water quality becoming more stringent.

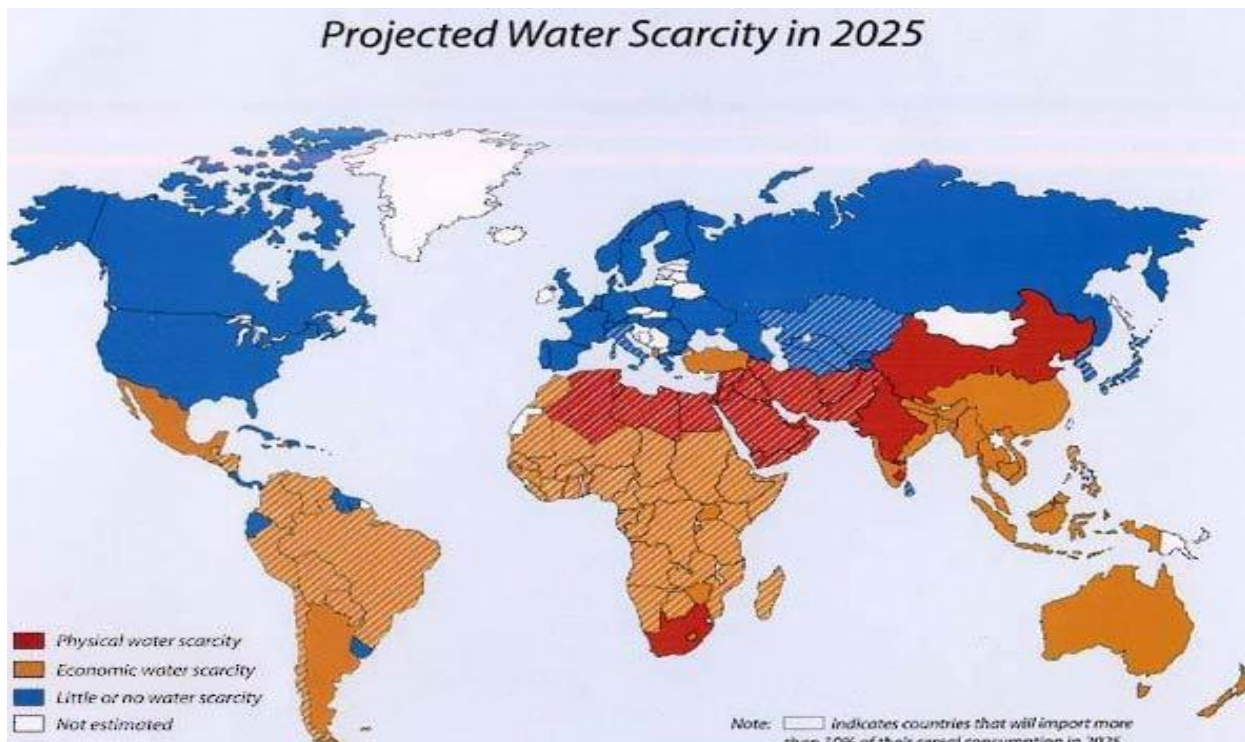


Figure.1.1. Projected global water scarcity in 2025 (International Water Management Institute)².

With the growing demand for high quality water, many new technologies of water purification are being developed to cater for potable and palatable water to humans. Wastewater treatment facilities are also becoming popular in chemical and manufacturing industries to reduce pollution and to protect the marine environment. Among these technologies are membrane-based processes that are inherently advantageous because of their high efficiency, ease of implementation, declining costs⁴ and low environmental impact. Their versatility to purify and recycle water renders them highly competitive candidates for use in water purification and water reclamation plants.

1.2 MEMBRANE TECHNOLOGY FOR WATER FILTRATION

In membrane based filtration process, membrane is used as a selective physical barrier to separate compounds (contaminants) from pure water by applying a driving force across the membrane. In membrane based filtration system a feed water stream is separated in two different streams, a) the product/filtrate/ permeates, containing solutes that pass through the membrane and b) the concentrate containing solutes and particles rejected by the membrane⁶. Figure 1.2 shows the schematic of membrane filtration process.

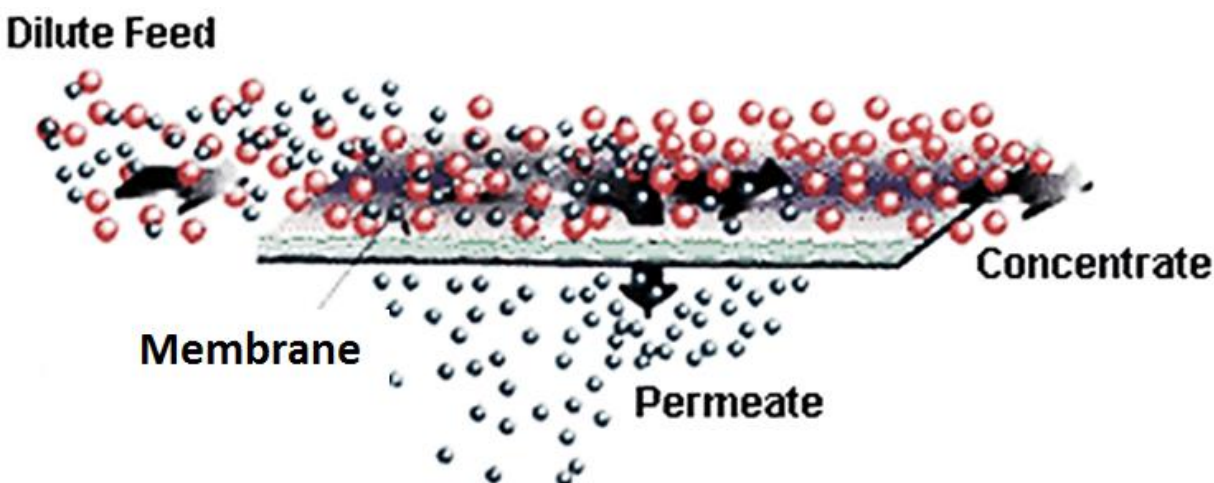


Figure 1.2: Schematic of membrane filtration process.

Membrane operation methods can be classified considering the parameters of driving force, separation mechanism and the rejection properties of the membrane. In case of pressure driven membrane processes, the driving force is a pressure difference (ΔP) across the membrane. Four pressure driven water filtration membrane processes can be discriminated based on differences in feed pressures and membrane rejection capacities: (1) micro filtration, (2) ultrafiltration, (3)

nanofiltration and (4) reverse osmosis, ranked by increasing pressure. Figure.1.3. shows the scheme of different pressure-driven membrane filtration processes and rejection.

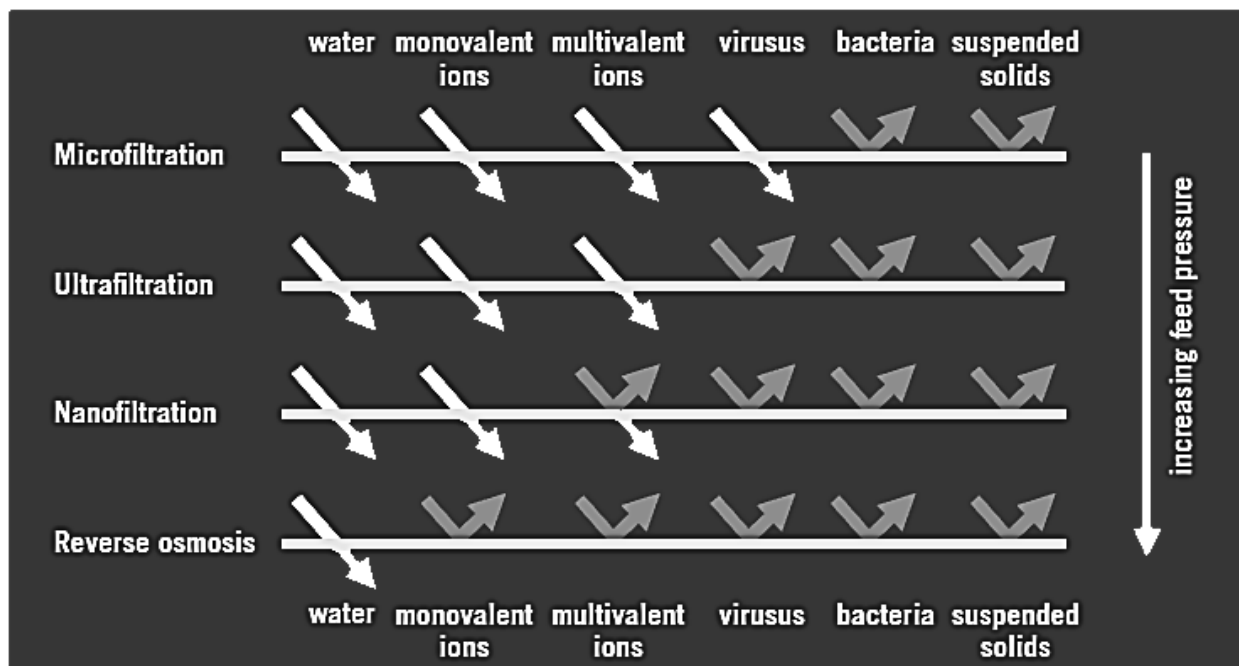


Figure.1.3. Scheme of different pressure-driven membrane filtration processes and rejection capacities

A classification generally made is low pressure membranes for microfiltration and ultrafiltration and high pressure membranes for nanofiltration and reverse osmosis. Microfiltration screens particles from 0.1 to 10 microns and ultrafiltration screens particles from 0.1 to 0.01 microns. Nanofiltration is applied for removal of divalent ions to reduce the hardness of the water and Reverse osmosis membranes are able to remove monovalent ions for more than 99%. The pores in NF and RO membranes are smaller than 2 nm. Low pressure microfiltration (MF) and ultrafiltration (UF) membranes are the research focus of this thesis. Each of these will be discussed in more detail in the literature review chapter.

1.3. HISTORY OF MEMBRANE PROCESS

The history of membrane technology based filtration was started over 250 year ago with the French cleric Abbe Nollet when he observed water transport across a pig bladder covering the mouth of a jar containing wine⁷⁻⁹. Moritz Traube, prepared the first artificial membrane in 1867¹⁰. Hassler introduced the first concept of membrane desalination in 1950, by describing “salt repelling

osmotic membranes” and “perm selective films”^{11,12}. In the early 1960s, Loeb and Sourirajan (1960, 1963) introduced the basis for modern-day reverse osmosis by research with cellulose acetate membranes with improved salt rejection and water flux, making membrane desalination practical^{13,14}. In 1963, the first spiral-wound element was developed by General Atomics. The first patent for reverse osmosis was dated 1964 by Loeb and Sourirajan¹⁵. Thin film composite membranes were introduced in the 1970s, and improvements were made to enhance water permeability and rejection (selectivity) properties and reduce the feed pressure. The history of membrane science is well described in several reviews^{9,12,16-18}. Figure 1.4 shows the historical development of pressure driven membrane process and the future direction

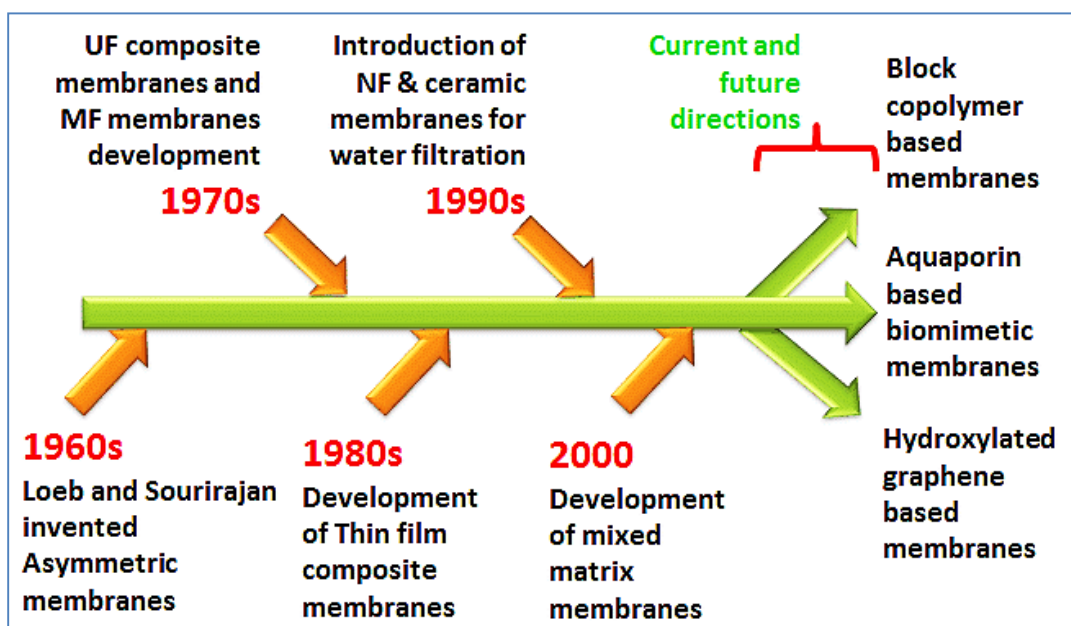


Figure.1.4. Historical development of pressure driven membrane process and the future direction

Recently, biologically inspired materials (block-copolymer/copolymer with desired functional groups, hydroxylated graphene, carbon nanotubes and aquaporin-protein water channel) based biomimetic membranes have been getting much attention in developing new membranes for water filtration¹⁹. Research on biomimetic membrane has developed rapidly during the last decade and these biomimetic and bio-inspired materials based membranes are considered as the next generation of advanced membranes. Some of the areas which are being considered for these biomimetic membranes are block copolymers^{19,20}. Ultrafiltration (UF) membrane process are well being used for the pretreatment to RO process. Hence, in this research, carboxylic (-COOH),

hydroxyl (-OH) and amine (-NH₂) functionalized copolymers and graphene (which are previously studied for RO) will be used to modify the polyethersulfone (PES) ultrafiltration (UF) membranes to improve the permeability, selectivity and antifouling properties (flux drop).

1.4. DISSERTATION OUTLINE

The thesis consists of 10 chapters, the structures of which are outlined as follows:

Chapter 2 consists of 3 major sections and several sub sections which provide sufficient background and theories on low pressure membrane (ultrafiltration and microfiltration) processes, membrane modules, operation of low pressure membrane systems and different fouling types with current fouling mitigation strategies. This chapter also gives information about different type of materials used in the development of ultrafiltration membrane and the principles of membrane surface modification. A comprehensive review in the present chapter covers the latest works and gaps on the PES ultrafiltration membrane surface modifications. PES bulk modification including sulfonation, grafting and hydroxylation chemistry and their limitations were also discussed. Blending of additives and nanoparticles to PES dope solution and their effect on hydrophilicity, permeability and antifouling properties are also discussed. The current limitations and practical challenges in blending of hydrophilic additives are finally addressed.

Chapter 3 summarizes the literature review and the research gap in a short form. The novelty and the detailed scope and objectives of the current work are also discussed in this chapter.

Chapter 4 provides information on the materials used, general membrane preparation procedures, experimental set-ups for membrane performance evaluation, protocols and characterization techniques involved throughout this research.

Chapter 5 presents the synthesis of highly hydrophilic, acid functionalized water insoluble copolymer additive poly acrylonitrile co maleic acid (PANCMA). This chapter also covers the development of PES membrane by dry wet spinning method and the modification of PES membrane by highly hydrophilic hydroxyl (-OH) rich polyethylene glycol (PEG) and silver nanoparticle (Ag). Finally, the membrane characterization and performance results are also discussed and compared against the control PES membrane.

CHAPTER: 1

Chapter 6 introduces a novel concept to develop self-cleaning membrane surface with negatively charged acid functionalized (-COOH) hydrophilic water insoluble PANcMA with thermally grafted amine (-NH₂) functionalized PEI and positively charged antimicrobial silver (Ag⁺). The effect of this novel surface chemistry on the hydrophilicity, water permeability and selectivity of the membrane is also discussed. Moreover, the antibacterial properties of the membrane are also evaluated before and after long time filtration and the results are discussed.

Chapter 7 presents the synthetic route to another the self-cleaning membrane prepared using a new polymeric additive poly (acrylonitrile co maleic acid co di-amino melionitrile) (PANcMACDAMN). This chapter also discusses the synthesis of a novel biologically inspired copolymer PANcMACDAMN with carboxylic (-COOH) and amine (-NH₂) functional groups. In addition, this chapter reveals the method of covalently attaching the positively charged antimicrobial silver (Ag⁺) and hydroxyl (-OH) rich PEG to PANcMACDAMN. The effect of this new additive on the performance of the PES ultrafiltration membrane in terms of permeability, selectivity and antifouling properties is also discussed.

Chapter 8 discusses the synthesis of a novel ultra-wetting graphene based ultrafiltration membrane using carboxylic, hydroxyl and amine functionalized graphene. It also reveals the effect of incorporation modified ultra-wetting graphene into the PES ultrafiltration membrane matrix. The synthesis of ultra-wetting graphene / graphene modified poly acrylonitrile co melimide (G-PANcMI), PES-Graphene dope formulation and the ultra-wetting graphene based composite UF membrane development are also discussed in details. Finally, the effect of ultra-wetting graphene on the PES membrane's surface hydrophilicity, permeability and selectivity with oil-water emulsion were analyzed and the results are discussed.

Chapter 9 outlines the summary of result and discussion / the effect of different (4 different additives) additives on the hydrophilicity, water permeability, selectivity and the antifouling properties of the PES ultrafiltration membrane.

Chapter 10 summarizes the conclusions of this research and provides recommendations for future work.

2. Literature review

2.1. LOW PRESSURE MEMBRANE PROCESS

Low pressure membrane process, microfiltration and ultrafiltration are typically used for the removal of particulate, suspended solids and microbial contaminants, and can be operated under positive pressure or negative pressure (i.e., vacuum pressure). Positive pressure systems typically operate between 0.2 bar and 2.76 bar, whereas, vacuum systems operate between -0.2 bar to -0.83 bar. There is no significant pressure difference between microfiltration and ultrafiltration system operation. In the membrane process, the distinction between microfiltration and ultrafiltration is typically based upon the pore size or molecular weight cut-off (MWCO). MWCO is a specification that refers to molecular mass of macro solute (e.g. protein/glycol and or water soluble polymers) for which a membrane has a retention of greater than 90 percent²¹.

2.1.1. MICROFILTRATION

Microfiltration refers to the separation of contaminants/particles in the range 0.1 μm – 10 μm . Pressure difference across the membrane is the driving force for microfiltration, which forces filtrate through the membrane. The necessary pressure difference is achieved either by a compressed gas or pump on the upstream side of the membrane, or by applying a vacuum to the filtrate/permeate side of the membrane. Microfiltration is characterized by high permeation fluxes and by operation at low pressures. Microfiltration process can be performed in two major configurations: dead-end flow and crossflow for various applications such as, wastewater treatments^{22,23}, clarification fruit juices²⁴, wine and beer²⁵⁻²⁷, continuous product elimination and cell recycle during fermentation and downstream processing of fermentation broths²⁸ and continuous separation of blood from plasma cells²⁹.

2.1.2. ULTRAFILTRATION

Ultrafiltration (UF) is one of the membrane based process which operates by pressure difference as its driving force and constitutes the research focus of this project. Cheryan (1986) has defined ultrafiltration as a fractionation technique that can simultaneously concentrate colloidal substances

or macromolecules in process stream. Ultrafiltration is a low-pressure operation at transmembrane pressures (TMP) of, typically, 0.5 to 5 bars. Ultrafiltration can be considered as a method for simultaneously concentrating, purifying, and fractionating macromolecules or fine colloidal suspensions. Molecular weight cut-off (MWCO) is a specification used by membrane suppliers/manufacturers to describe the retention capabilities of UF membrane. Ultrafiltration covers particles, contaminants and molecules that range molecular weight from about 1000 Daltons to about 500,000 Daltons³⁰. Numerous researches around the world have proven that ultrafiltration provides most favorable pretreatment for seawater desalination based on reverse osmosis membranes (SWRO)³¹⁻³⁵, treatment of municipal wastewater^{36,37}, treatment of oily wastewater from petroleum industries³⁸⁻⁴⁰, textile industry (dye) waste water treatment⁴¹⁻⁴³ and demineralization of animal blood plasma⁴⁴.

2.1.2.1. ULTRAFILTRATION MEMBRANES

Membranes with the pore size between 10 nm to 100 nm and are called ultrafiltration membranes. These membranes are porous and asymmetric in structure with a wall thickness around 150 μm ⁴⁵. Ultrafiltration membranes are manufactured using either organic (polymeric) materials or inorganic (ceramic) materials. Generally, ceramic membranes are prepared from metal oxides like, alumina⁴⁶, zirconia⁴⁷, titania⁴⁸ and zeolite⁴⁹. Similarly, the polymeric membranes are made up of polymer with high mechanical strength and chemical stability in addition to high molecular weight, chain flexibility, chain interaction, *etc.* Some of the commonly used polymeric membrane materials are polysulfone³⁸, polyethersulfone⁵⁰, sulfonated polysulfone⁵¹, polyvinylidene fluoride⁵², polyacrylonitrile⁵³, cellulose acetate⁵⁴, polyimide⁵⁵, polyetherimide⁵⁶, aliphatic polyamides⁵⁷, and polyetherketone⁵⁸. Compared to polymeric membrane, ceramic membranes have high mechanical, chemical, microbiological and thermal stability. However, ceramic membranes are generally much more expensive with respect to membrane area compared to polymeric membranes⁵⁹. Thus polymeric membranes are more commonly used for large scale ultrafiltration applications. Polymeric ultrafiltration membranes are the focus of this thesis.

Generally, polymeric membranes are fabricated in two different configurations: flat sheet or cylinder (tubular / hollow fiber). Polymeric flat sheet membranes are fabricated by using thermodynamically stable polymer solution through phase inversion technique via immersion

precipitation⁶⁰. Polymeric membrane technology obtained much attention from both academia and industry for its potential application in separation processes after 1966 when Mahon made the first hollow fiber membranes^{61,62}. The principle of membrane formation by phase separation process is independent of the membrane configuration. Figure.2.1 (a) and (b) show the principle of membrane formation by phase separation process.

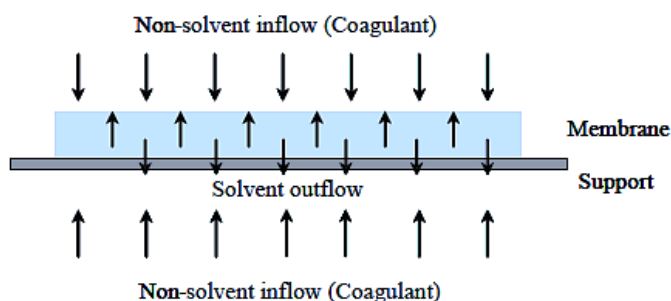


Figure.2.1. (a) Solvent/non-solvent exchange during fabrication of flat sheet membrane by phase separation process.

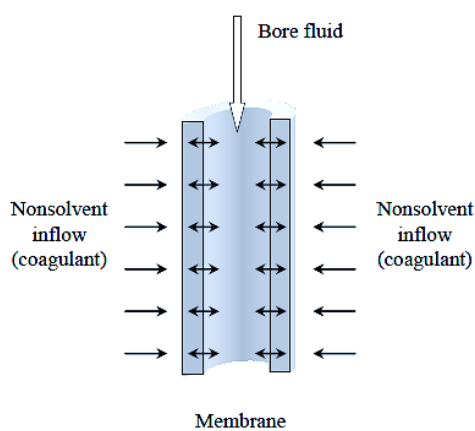


Figure.2.1. (b) Solvent/non-solvent exchange during fabrication of hollow fiber membrane by dry wet spinning process (by phase separation process)

However, hollow fiber spinning process is slightly complex than the casting process of flat sheet membranes because in hollow fiber spinning process, a pressurized viscous polymer solution is extruded through a spinneret. Several other parameters play important roles on the membrane morphology and separation performance of the hollow fiber membrane (eg., structure and dimensions of the spinneret, viscosity of the dope, polymer flow rate, dope temperature and

composition, internal and external coagulants, bore fluid flow rate, air gap, humidity and fiber take-up speed). Ultrafiltration membranes can be fabricated in two different morphologies (1) Symmetric or homogeneous (cross section shows a uniform porous structure) and (2) Asymmetric (cross section shows two different structure – thin dense layer with a porous support layer). Figure.2.2.shows the schematic representation of symmetric and asymmetric membrane

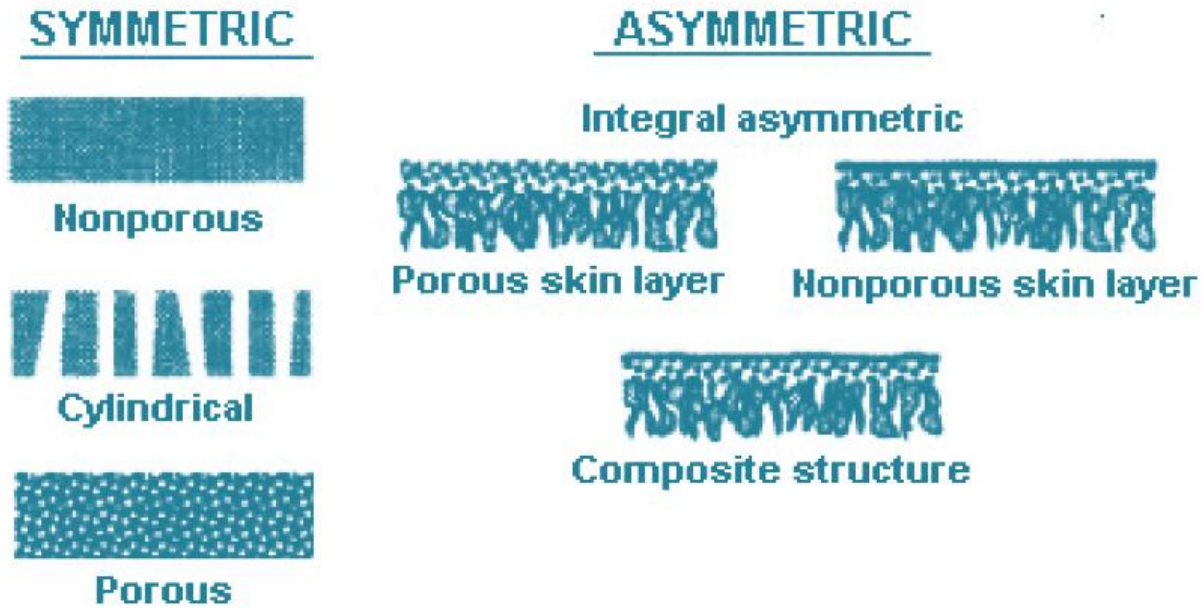


Figure.2.2. Schematic representation of cross-section of symmetric and asymmetric membrane⁶³

In comparison, hollow fiber configuration is a favorite choice for modules in membrane separation process compared to flat sheet membranes because of the larger membrane area per unit volume, self-mechanical support which can be back flushed for liquid separation and good flexibility and easy handling⁶⁴. Hollow fiber membranes are widely used for ultrafiltration and these membranes can also be applied as porous support to make nanofiltration and reverse osmosis membranes through coating the surface with polymeric materials

2.1.3. MEMBRANE MODULES

As indicated above, ultrafiltration membranes can be fabricated in two major geometries: tubular and flat sheet forms. These two geometries are the basis for five principal configurations of membrane modules. Table.2.1 shows the five different configurations of ultrafiltration membrane modules⁶⁵.

Table.2.1. Different configurations of ultrafiltration membrane modules

SI NO	Module Configurations
1	Hollow fiber
2	Tubular
3	Flat plate
4	Spiral wound
5	Rotating

Ultrafiltration membrane module configuration refers to the membrane geometry and the way it is mounted in the module and oriented with respect to the feed solution flow. The configuration is the basis to determine the process performance and the applicability to feed solutions with certain characteristics. An ideal membrane module configuration would provide a high membrane area per volume ratio, low energy expenditure, high turbulence, easy to clean and low maintenance. Table.2.2. shows the advantages and disadvantages of the above five different membrane module configurations.

Table.2.2. Advantages and disadvantages of different membrane module configurations^{18,65,66}

Module configuration	Channel spacing (cm)	Packing density (m ² /m ³)	Energy costs (pumping)	Particulate plugging	Ease of cleaning
Hollow fiber	0.02-0.25	1200	Low	High	Fair
Tubular	1.0-2.5	60	High	Low	Excellent
Flat plate	0.03-0.25	300	Moderate	Moderate	Good
Spiral wound	0.03-0.1	600	Low	Very high	Poor-fair
Rotating	0.05-0.1	10	a	Moderate	Fair

a: Energy costs are determined by the rotation speed instead of the pumping.

Each type of membrane module configurations has its specific characteristics based on its packing density, hold up volume, ease of cleaning, cost of module, pressure drop and quality of pre-treatment required. As shown in the above table, the hollow fiber and spiral wound modules have the highest packing density compared to other types of membrane module configurations. Hence, the hollow fibers (capillary), and spiral wound ultrafiltration membrane modules are the two major

types of membrane modules used for most of the ultrafiltration applications⁶⁷. Hollow fibers, tubular and capillary involve the hollow fiber configuration, whereas the modules of flat sheet membranes are usually contained in the plate-and-frame devices and spiral wound elements. Two most commonly used ultrafiltration membrane modules configurations in industrial membranes separation processes are discussed below.

2.1.3.1. HOLLOW FIBER MEMBRANE MODULES

The hollow fiber membranes are in the shape of thin hollow tubes with a very small diameter. In hollow fiber module, a large number of hollow fibers are assembled together into a pressure vessel. The geometric arrangement of hollow fiber membrane module is similar to conventional tubular heat-exchanger assembly. Figure.2.3. shows a cutting view of a hollow fiber membrane module. Hollow fiber membrane module has the highest packing density compared to other types of modules and it has a maximum membrane surface area per unit volume as high as $10,000\text{m}^2/\text{m}^3$ ^{68,69}.

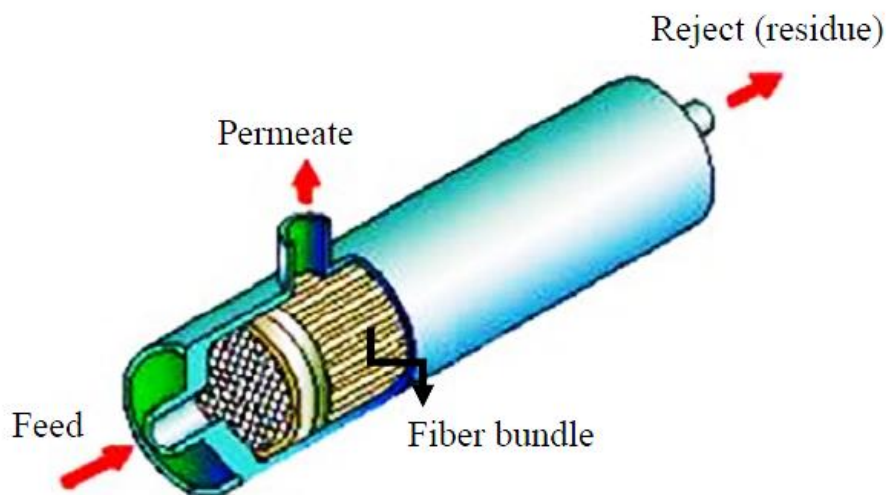


Figure.2.3. Hollow fiber membrane module ⁶⁹

Ultrafiltration hollow fiber membrane module can be operated in two different configurations a) inside-out filtration and b) outside-in filtration. In inside-out operation the high pressure feed solution enters into bore side of the membrane and permeate is collected in the shell side⁷⁰. Whereas, in outside-in filtration process the high pressure feed solution enters into shell side and permeate is collected in the bore side⁷¹. Figure.2.4.shows the two different configurations based on the feed flow.



Figure.2.4. (a) Inside-out filtration, (b) outside-in filtration

In general, the hollow fiber membrane module can achieve high packing density in a cost-effective manner which is the most critical criteria to be considered in a membrane system. This results in higher productivity, mechanically self-support, easy backwash for liquid separation and easy handling during module fabrication and in the operation⁶⁴. From many of the previously conducted studies, it was found that the common filtration behavior of hollow fiber membranes is characterized by treatment operational parameters such as time-dependent non-uniform distribution of trans membrane pressure (TMP), flux, and filtration resistance along the fiber due to lumen-side pressure drop induced by permeate flow⁷². In choosing the right membrane module configuration for a water treatment system, the module may be tested and evaluated first for the specific waste water⁷³. In this work, the hollow fiber membrane module is used in outside-in configuration.

2.1.3.2. SPIRALWOUND MEMBRANE MODULE

Membrane modules, such as tubular and plate frame operate at low quantity of feed volume and consist of small membrane area with low permeate flux. As a spiral wound module has a large membrane surface area and membrane packing density ($300\text{-}1000\text{ m}^2/\text{m}^3$) compared to tubular and plate frame membrane modules, it is used to treat large feed volume application⁷⁴. In addition, spiral wound module can operate at high trans-membrane pressure drop and turbulent flow regimes, due to the presence of spacer. Figure.2.5.shows the assembly of spiral wound module, consisting of a sandwich of flat sheet membranes and a separator/spacer to form an envelope enclosing them to provide mechanical strength and permeate flow space.

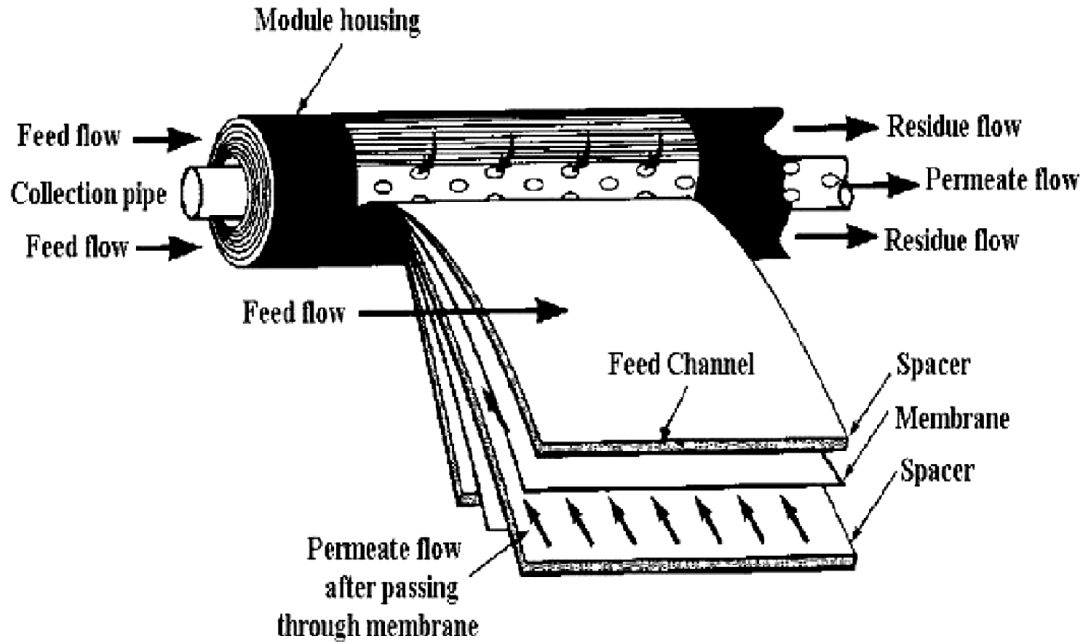


Figure.2.5. Spiral-wound membrane module assembly⁷⁴

In spiral wound modules, the spacer enhances mass transport in the feed channel and also it develops the turbulence at the membrane surface and reduces the concentration polarization across the membrane module and hence, it enhances the pure water flux and minimizes the pressure drop⁷⁵. The spacer also directly reduces the pumping power consumption⁷⁶. However, the spacer increases the flow resistance and the suspended materials can easily block the spacer and also partially block the feed channel⁷⁷.

2.1.4. ULTRAFILTRATION OPERATION METHODS

Ultrafiltration operation methods are generally classified into two main categories, either dead-end filtration or crossflow filtration, based on direction of the flow of the processed feed solution and the nature of the latter. In theory, all contaminants/particles in a feed solution that are smaller than the pore size of the membrane will pass through the membrane, and contaminants or particles larger than the pores of the membrane will be retained on the upstream/rejection side of the membrane. Compared to crossflow system, dead-end filtration systems usually involve simpler configurations and require less capital outlay and maintenance costs. However, filtration performance is often poor in dead-end mode compared to crossflow system due to the high

resistance to filtrate flow by rejected material (particles bigger than the pore size of the membrane). Thus the dead-end configuration is more suitable option only when the particle loading in the feed is low, for example in clarification of filtration media or purification of gases. Crossflow filtration mode can be used even for higher solids loading.

2.1.4.1. DEAD-END FLOW FILTRATION

In dead-end ultrafiltration operations the flow is perpendicular to the membrane and the entire filtration volume is passed through the membrane. Any particles/contaminants in the feed solutions that are larger than the pore size of the membranes are deposited on the membrane surface, forming a cake layer of solids on the membrane surface. The liquid that passes through the membrane is known as the filtrate/permeate. Figure.2.6. shows the schematic diagram of a dead-end flow filtration system, where the thickness of the cake layer grows until further filtration is not possible. The filtration rate also decrease with filtration time due to the hydraulic resistance of the cake layer.

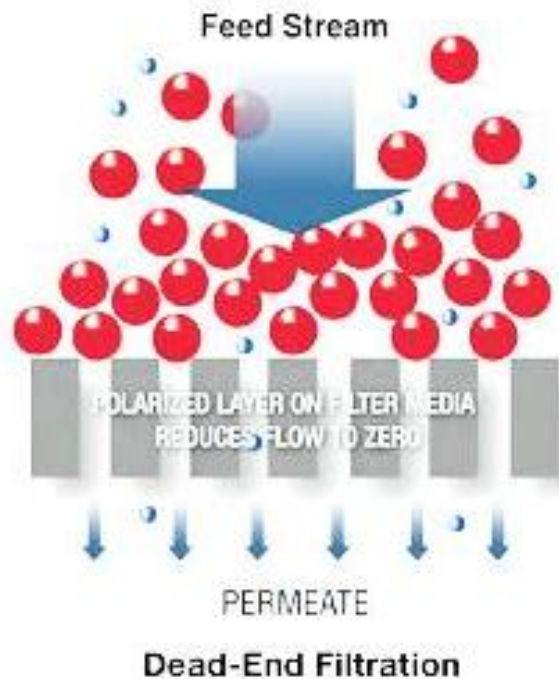


Figure.2.6. Schematic diagram of a dead-end flow filtration

2.1.4.2. CROSSFLOW FILTRATION

In crossflow ultrafiltration, the feed solution flows tangentially to the membrane surface. Crossflow ultrafiltration is operated with two effluent streams: a permeate/filtrate stream and a retentate/rejection stream. Only a portion of the feed solution passes through the membrane as product/permeates, and the other portion flows tangentially along the membrane surface as rejection. Figure 2.7. shows the schematic diagram of a crossflow filtration system. In dead-end operations all the transported materials accumulate on the membrane surface, whereas during crossflow ultrafiltration most of the particles/contaminants are carried away in the retentate. Crossflow configuration is more suitable for treating wastewater with high solids content and higher permeation fluxes can be achieved compared to the dead-end filtration method.

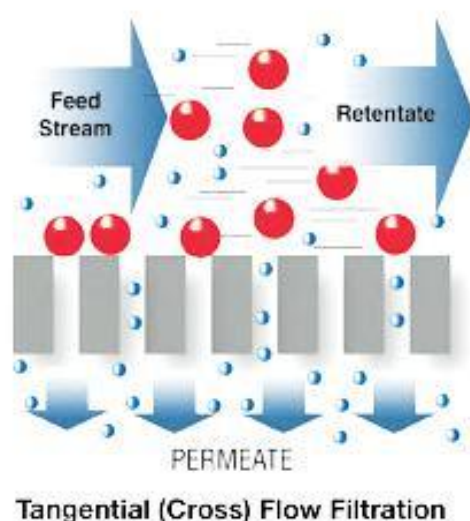


Figure.2.7. Schematic diagram of a crossflow filtration

2.2. MEMBRANE FOULING

One major drawback of membrane technology is its depleting performance over time such as flux reduction, rejection impairment and membrane breakage, leading to high operational costs and short service life⁷⁸⁻⁸⁰. According to the Union of Pure and Applied Chemistry (UPAC), fouling is the loss of performance of a membrane due to deposition of suspended or dissolved substances on

its external surfaces, at its pore openings, or within its pores⁸¹. The three main consequences of fouling are as below:

- (i) Increase of required feed pressure and consequently higher operating cost
- (ii) Frequent chemical cleaning of the membranes to maintain the permeate flow or TMP
- (iii) Shortening membranes lifetime

The major fouling mechanisms of ultrafiltration (UF) membranes are scaling of inorganic deposits, particulate and colloidal matter, organic fouling and bio-fouling. Different types of fouling may occur simultaneously and can influence one another⁸². Scaling by inorganic compounds is usually controlled by an anti-scalant and/or acid cleaning. Particulate fouling can be controlled by pretreatment like coagulation and flocculation process. Therefore, organic and bio-fouling are the critical types of fouling.

Bio-fouling problems originate from organic fouling. The accumulation of the organics (organic fouling) favors the attachment and growth of microorganisms (bio-fouling) onto the surface of the membrane. Numerous previously reported researches indicate that the electrostatic interactions and hydrophobic interactions enhance the natural organic matters (NOMs) attachment on the membrane surface, which was reported as the initial step in membrane fouling⁸³⁻⁸⁶. Low pressure UF membrane systems are more suitable for rejection of pathogens and (in) organic micro pollutants and numerous reports indicate that organic fouling and followed by bio-fouling (bio-fouling is the final stage of organic fouling) are the most serious problems in these membrane systems^{87,88}. Principle and consequences of bio-fouling are discussed further below.

2.2.1. BIO-FOULING

Generally bacteria grow on an available surface exposed to an aqueous environment rather than in the aqueous phase and form biofilm on the surface^{89,90}. According to Characklis and Marshall, biofouling is the extent of biofilm formation which causes unacceptable operational problems⁹¹. The beginning of biofilm formation is influenced by a several factors, such as conditioning film⁹², electrostatic, hydrophobic and van der Waals interactions⁹³, surface characteristics of substratum and microorganisms⁹⁴ and quorum sensing⁹⁵. Bio-fouling originate from the accumulation of the

organics (protein, humic substance, natural organic matters etc.,) called conditioning film that favors the attachment and growth of microorganisms onto the surface of the membrane^{94,96}. The conditioning film contains a higher concentration of nutrients compared with the liquid phase. Formation of biofilm is initiated by the attachment of microorganisms to the conditioning film. When the attached microorganisms grow, the biofilm starts to develop⁹⁷. The matured biofilm formation is due to early surface colonization by some microorganisms and these deposited bacteria then produce extracellular polymeric substances (EPS) that facilitate the attachment and growth of other microorganisms⁹⁸. EPS are mainly carbohydrates, lipids, proteins, variety of humic substances and a small quantity of nucleic acids. According to Dang & Lovel, the initial adhesion of microorganisms is critical for biofilm formation⁹⁹. Generally, EPS are responsible for membrane fouling by irreversibly binding to the membrane surface and they enhance the bacteria survival of the biofilm by forming a chemically reactive diffusion transport barrier with bacterial cells¹⁰⁰. Figure.2.8. shows the stepwise process of biofilm formation.

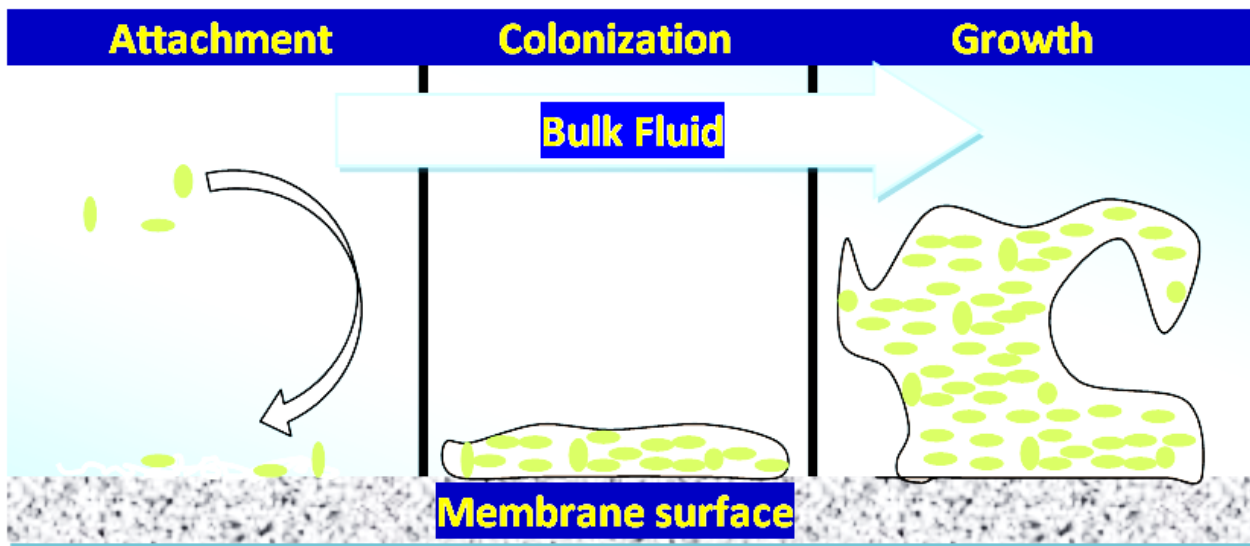


Figure.2.8. Step by step formation of biofilm (attachment, colonization and growth)

The formation of a biofilm on a membrane surface will result in increased operating pressures, loss of product water quality, increased chemical cleaning frequency, and reduced membrane life time¹⁰¹. Moreover, it is extremely difficult to clean the membrane that has been fouled by biofilms because the micro-organisms are protected by the matrix of EPS which are chemically bound to the membrane surface¹⁰².

2.2.2. BIOFILM CONTROL ON MEMBRANES

In general, biofilm on membrane surface can be treated by physical, chemical and biological treatment methods. There are number of physical methods such as backwashing the membrane module, reducing the concentration of solids in the liquid by pretreatment method before flow in to the membrane module and applying a tangential surface shear force¹⁰³. However, Percival et al., suggested that structurally strong biofilm may form due to high feed flow¹⁰⁴.

In biological method, enzyme based cleaning agents can be used to treat membrane fouling and compared to many chemical cleaning, enzymes based cleaning agents are less aggressive to the membrane¹⁰⁵. Compared to traditional alkali cleaning, enzymatic cleaning was found to be much better in removing biofilm from ultrafiltration membrane¹⁰⁶. It has been reported that bacteriophage can be used to infect the host bacteria by rapid replication of virions to lyse the host cells¹⁰⁷. According to Goldman et al., bacteriophage can be used to reduce microbial attachment on ultrafiltration membrane surface by an average of 40%. However, bacteriophage tends to be rather host-specific and so cocktails of phages would be required for microbial control¹⁰⁰.

The dosing of biocides may decrease bacterial levels in the bulk liquid by killing the free floating cells but may be less efficient on the biofilm¹⁰⁸. Simoes et al., also highlight that the food debris residues may contain microorganisms which may behave as a surface for colonization¹⁰⁸. Hydrogen peroxide and hypochlorites have been used as effective disinfectants¹⁰⁵. In addition, hypochlorites are also used as membrane-swelling agents and may flush out the material lodged within the membrane pores. However hypochlorites may decrease membrane life¹⁰⁹. Quaternary ammonium compounds based products are not suitable to be used on membranes because they may adsorb onto the membrane surface, resulting in flux decline and damage the membranes¹¹⁰.

Moreover, EPS matrixes protect the biofilms which tend to be very resistant to biocides, thus it is very difficult to clean the membrane that has been fouled by biofilm¹⁰². Disinfectants are not always successful in controlling biofilm since it is impossible to inactivate all microorganisms in the feed water (small number of microorganisms is enough to form a biofilm)¹⁰². Furthermore, the extended exposure of membranes to disinfectants may damage the membrane structures, which may lead to the loss of ability to reject contaminants. The use of disinfectants can also lead to the generation of carcinogenic disinfection by products¹¹¹⁻¹¹³. Since prevention is better than cure, it

is more effective to prevent the attachment of bacteria on the membrane in the first place than killing the bacteria already formed in the biofilm. This leads to the concept of membrane engineering to modify the membrane surface in order to reduce / prevent bacterial adhesion¹¹¹.

2.3. MEMBRANE SURFACE MODIFICATION

2.3.1. MEMBRANE MATERIALS

Membrane material is the key parameter to be understood before modification of the membrane surface to prevent biofilm. Polymeric membranes are most widely used for wastewater treatment. This is due to their increased separation efficiency and decreased maintenance costs when compared to inorganic materials based membranes. Long term liquid based pressure driven separation processes ultrafiltration requires polymeric membrane materials that possess properties such as good mechanical strength, thermal stability and excellent chemical resistance to have a sustained reduced maintenance cost^{63,114}. The well-known polymeric materials include polysulphone (PS), cellulose acetate (CA), polyvinyl alcohol (PVA), polyvinyl chloride (PVC), polyvinylidene fluoride (PVDF), cellulose nitrate (CN), polyethersulphone (PES), polyacrylonitrile (PAN) etc¹¹⁵⁻¹²¹. Among these materials PES and PVDF are the most popular membrane materials and have been studied for many years for the synthesis of ultrafiltration (UF) membranes due to their excellent chemical and mechanical properties¹²²⁻¹²⁵. In general, hydrophilic materials have a tendency to swell in water, which results in loss of mechanical strength and lower rejection is attained. To overcome this problem, hydrophobic stable polymer based membranes are used and are imparted with improved hydrophilicity by surface modification for high water permeability, selectivity and antifouling properties. The hydrophobic/hydrophilic properties of the membrane can be studied by measuring the contact angle of the membrane. The membranes having higher contact angle ($>90^\circ$) are said to be hydrophobic and lower contact angle ($<90^\circ$) are said to be hydrophilic. Contact angle of the membranes is generally affected by the membrane surface properties such as roughness, pore size, porosity and the pore size distribution. PES based ultrafiltration membranes are the focus of this thesis.

2.3.1.1. BIOLOGICALLY INSPIRED MATERIALS

Recently, biologically inspired materials (block-copolymer/copolymer with desired functional groups, hydroxylated graphene, carbon nanotubes and aquaporin-protein water channel) based

biomimetic membranes have been getting much attention in desalination¹⁹. Biomimetic membranes are generally developed with natural or natural-like hybrid materials by mimicking the biological approaches to bring in specific properties to the membranes¹²⁶⁻¹²⁸. Research on biomimetic membrane has developed rapidly during the last decade. Even though there are still many challenges to overcome, biomimetic and bio-inspired membranes are still considered as the next generation of advanced membranes. Some of the areas which are being considered for these biomimetic membranes are block copolymers^{19,20} with desired functional groups, hydrogenated/hydroxylated and aminated graphene¹²⁹⁻¹³³ and water channel proteins (aquaporin)¹²⁸ based membranes. Different membranes for desalination and their commercial viabilities are presented in Figure 2.9

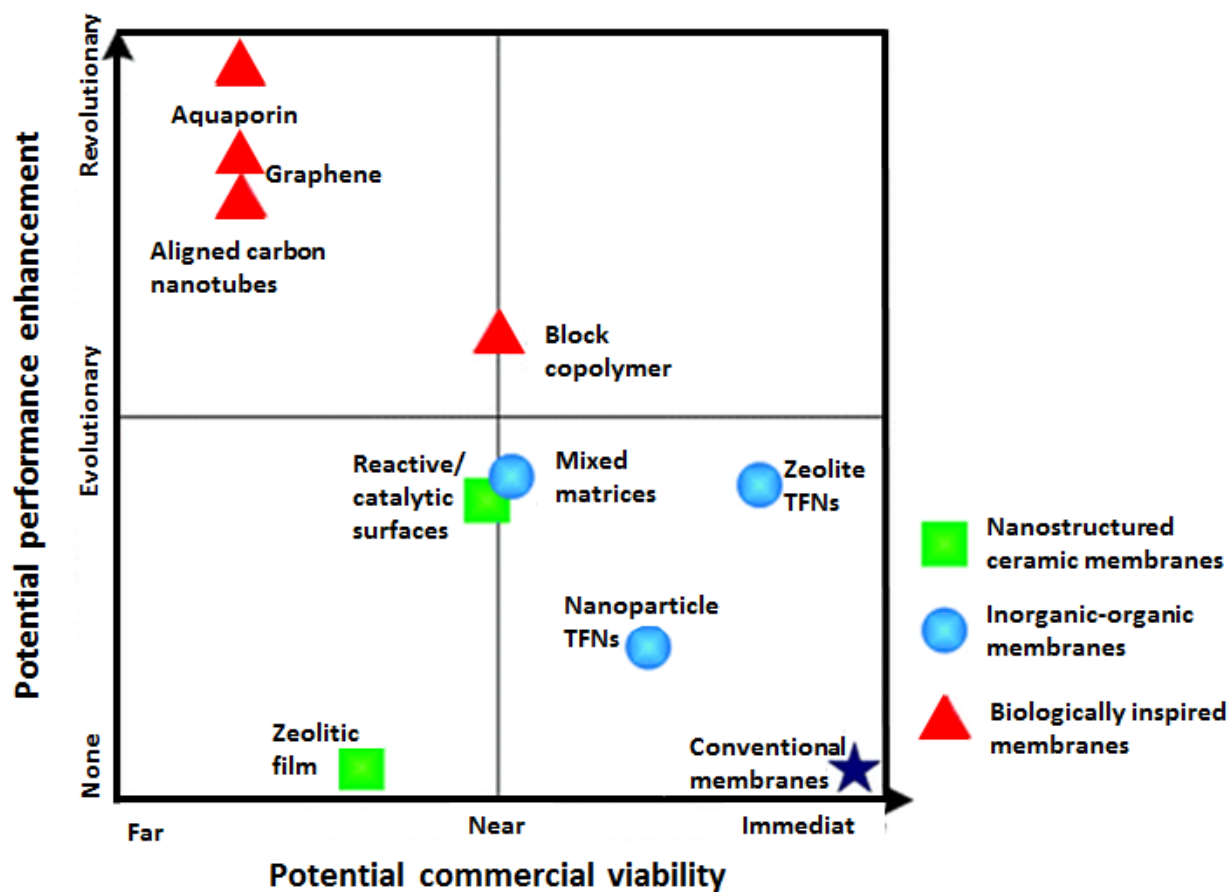


Figure 2.9 Current state of membrane development for desalination and their commercial viabilities (adapted and modified from *Mary Theresa M. et al., Energy Environ. Sci.*, 2011, 4, 1946-1971)¹⁹

2.3.1.1.1 BLOCK COPOLYMER BASED BIOMIMETIC MEMBRANES

The most immediate approach to fabricate biomimetic membranes is to bring in or build the structure of natural cell membrane into the synthetic membranes. One such way is to incorporate the biological proteins into the bilayer lipid membrane (BLM)¹²⁸. However, the inherent drawback of this method is the low stability of the phospholipid bilayer in the cell membrane. To overcome this issue, supported lipid bilayer membranes are developed¹²⁸. Block-copolymer / copolymer with carboxylic (-COOH), hydroxyl (-OH) and amine (-NH₂) functional groups are considered as biologically inspired materials. These functional groups will form inter molecular hydrogen bond with water molecules. In recent studies, these negatively charged functional groups have been shown to give significant improvements in the hydrophilicity of the membranes¹³⁴⁻¹³⁸ due to inter molecular hydrogen bonding¹³⁴.

2.3.1.1.2. AQUAPORIN BASED BIOMIMETIC MEMBRANES

Another approach to develop biomimetic membranes is to incorporate the pore-forming proteins called Aquaporin into the polymer support¹²⁸. These aquaporins are capable of forming water channels under the right conditions¹²⁷. Followed by an interesting paper from Kumar et al¹³⁹ on the possibility of achieving higher permeability and selectivity by bio mimicking the membranes using aquaporin, researchers are scrambling to synthesize this biomimetic aquaporin based desalination membranes in a practically viable scale and method as possible. However, the large scale production of aquaporin, incorporation of aquaporin into the membrane surface in fairly large numbers and the development of proper and suitable support membrane layers for the stable immobilization of these aquaporins are still very challenging¹⁴⁰.

2.3.1.1.3 GRAPHENE BASED BIOMIMETIC MEMBRANES

Graphene is a sp²-hybridized two-dimensional carbon sheet¹⁴¹ which has been used for several promising applications such as energy storage¹⁴², surface coating¹⁴³⁻¹⁴⁶, nanopore sequencing¹⁴⁷ and filtration¹⁴⁸. The wetting behavior of graphene plays an important role in these applications in addition to its energy storage efficiency and heat transfer capacity.^{149,150}. Recently, graphene gained much attention in the field of membrane science and engineering due to its high surface area¹⁵¹, high mechanical strength¹⁵² and chemical stability¹⁵³. Theoretical analysis have also predicted that graphene based membranes may exhibit orders of magnitude greater permeability than the current state of the art membranes^{154,155}. However, most of these studies are based on a

single layer of graphene sheet¹⁵⁶. Experimental studies also show that it is difficult to fabricate leak-free porous graphene membranes with large surface area^{147,157}. Moreover, it is commonly accepted that supported graphene is hydrophobic in nature and its water contact angle is, to some extent, higher than that of graphite^{150,158,159}.

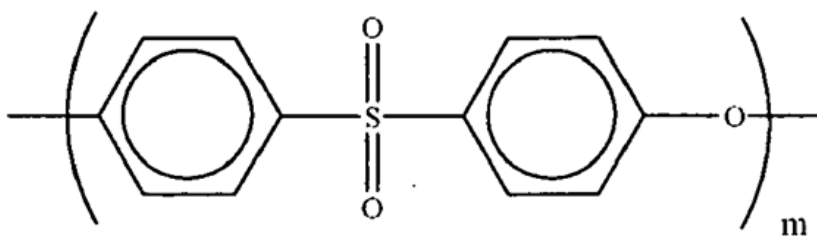
Graphene oxide (GO) is an amphiphilic graphene derivative (a single-atom layer of graphene) with oxygen containing functional groups (-OH, -COOH) attached to both sides of the graphene flake¹⁶⁰⁻¹⁶³. There are important beneficial aspects to having these oxygen containing functional groups attached to the graphene structure. Firstly, they impart polarity to the flake so that the graphene oxide is able to be more uniformly dispersed in solvents and eventually in the polymer matrix it is blended into^{160,164}. Further, these oxygen containing hydrophilic functional groups improve the wetting properties (hydrophilic properties) of the normally hydrophobic polymeric membranes through hydrogen bonding¹³⁴. Indeed, literature reports that the contact angle of water on pristine graphene oxide films can vary from 0 to 60 degrees^{165,166}.

Graphene oxide-polymer hybrid material based membranes exhibit excellent antifouling property¹²⁹ due to the interaction of contaminants with the delocalized p-electrons of the nanocarbons¹³⁰⁻¹³². Thermal stability and mechanical strength of the polymeric membranes is also increased by the addition of graphene¹⁶⁷. Graphene oxide-based membranes exhibit promising qualities in the field of desalination¹³³ and selective ion penetration¹⁶⁸.

In this research, carboxyl (-COOH), hydroxyl (-OH) and amine (-NH₂) functionalized copolymers and graphene have been used to modify the PES membrane

2.3.1.2. POLYETHERSULFONE (PES) MEMBRANE

PES possesses very high mechanical, chemical and thermal resistances with a glass transition temperature of 225°C. It also has outstanding oxidative and hydrolytic stability, which makes it an ideal material to prepare membranes to be used in the water treatment processes^{169,170}. Figure.2.10. shows the structure of PES polymer.



polyethersulfone

Figure.2.10. Chemical structure of PES polymer

Although PES and PES modified membranes have been widely used in water treatment, they inherently possess hydrophobic surface property, which is the main disadvantage for their function as an effective filtration membrane. Many studies have shown that membrane fouling is the major problem in membrane filtration, is directly related to hydrophobic nature of the membranes^{138,171}. Membrane fouling is mainly caused by adsorption of non-polar solutes as well as hydrophobic and electrostatic interactions of particles or bacteria with membrane surface. The operational drawbacks of such fouling problems include higher energy consumption, shorter membrane lifetime and unstable separation performance^{172,173}.

Since PES is hydrophobic in nature, various significant studies focusing on approaches adopted to impart more hydrophilicity via surface modifications have been reported¹⁷⁴⁻¹⁷⁶. There are several methods reported for the hydrophilic modification of PES polymers or membranes to increase the antifouling property, water flux, biocompatibility and other specialized functions in membrane filtration.

2.3.1.3. POLYETHERSULFONE (PES) MEMBRANE MODIFICATION

There are three main ways to modify the PES polymer and membranes to obtain long-lasting antifouling, hydrophilic properties for water filtration. They are (1) bulk modification of PES, (2) surface modification of PES membranes and (3) blending method. The various PES membrane modification approaches are described in detail below.

2.3.2. BULK MODIFICATION OF POLYETHERSULFONE (PES)

Bulk modification is a method of incorporating different functionality/functional groups into the polymer back bone (molecular structure). Various types of modification of PES polymer are discussed below

2.3.2.1. SULFONATION OF POLYETHERSULFONE (PES)

Sulfonation is an electrophilic aromatic substitution reaction, in which sulfonic acid groups ($-\text{SO}_3\text{H}$) are introduced into the structure of PES molecule in place of a hydrogen atom¹⁷⁷ as shown in Figure 2.11 below. The sulfonic acid groups introduced by this method are usually localized in the ortho positions on the aromatic rings of the PES, which are activated by the electron donating oxygen atom of the main chain^{174,175}. The sulfonic acid group repulses the electron and deactivates the aromatic rings for substitution, which makes sulfonation a difficult process.

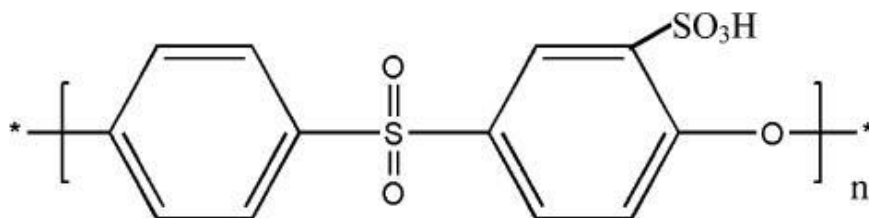


Figure.2.11. Chemical structure of sulfonated PES

The sulfonation of the PES polymer is normally carried out using sulfonating agents such as sulfuric acid H_2SO_4 , sulfur trioxide SO_3 , chlorosulfonic acid ClSO_3H , trimethylsilylchlorosulfate $(\text{CH}_3)_3\text{SiSO}_3\text{Cl}$ etc.,^{178,179}. The chosen reagent is added dropwise to the polymer solution at a constant temperature after which the polymer is precipitated in ice cold water, filtered, separated, washed with deionized water and then dried. Of all the sulfonating agents, sulfuric acid is the cheapest but its disadvantage is that it can cause the polymer chain to degrade as a result of high temperature or long reaction time. This may possibly bring down the mechanical resistance of the membrane, limiting its use in industrial applications. Figure.2.12. shows the possible chemical degradation of PES during sulfonation.

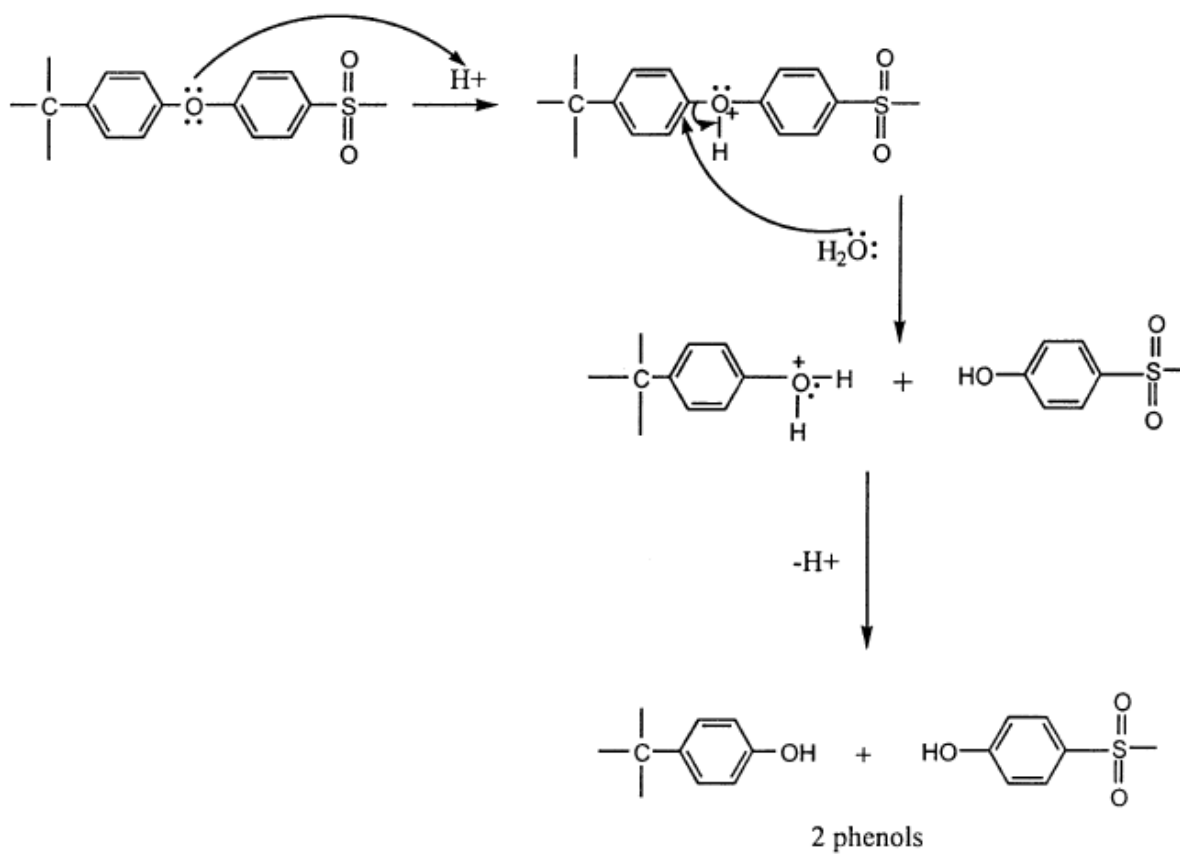


Figure.2.12. Degradation of PES during sulphonation (reaction with strong sulphuric acid)¹⁸⁰.

Therefore, control of temperature and reaction time is critically important when employing sulfuric acid. Sulfonation of PES using chlorosulfonic acid also causes degradation, crosslinking and branching in the polymer. However, its main advantage is that a homogeneous solution is formed which can be effective in controlling the degree of sulfonation (DS)¹⁸¹. The latter is an important factor representing the rate and level of sulfonation, which has a direct impact on the mechanical properties as well as the hydrophilicity of the membrane material. For instance, it is known that as the DS decreases, the tensile strength of the membrane decreases whilst its hydrophilicity increases¹⁸¹. DS is affected by reaction parameters such as the reaction time, temperature, sulfonating agents, and ratio of sulfonating agents, PES and solvents. It is typically determined using the ion exchange capacity of the sulfonated PES (SPES)^{171,182} or through proton NMR¹⁸³ or infrared spectroscopy. The presence of sulfonic acid groups was confirmed by the FTIR and NMR spectroscopy. However, the possibility of polymer chain degradation may affect the physical and

chemical property of the material, thus limiting its use in industrial applications¹⁸⁰ more particularly in membrane application.

2.3.2.2. GRAFTING FUNCTIONAL GROUPS TO POLYETHERSULFONE (PES)

Grafting is the process of adding functional groups to the polymer to enhance its properties. Carboxylic group is the most commonly used functional group to graft on to the PES surface. The presence of carboxylic groups has been shown to increase the hydrophilicity of the PES polymer, as measured by water contact angle measurements¹⁷¹. This grafting requires more energy than simultaneous gamma-ray irradiation. Briefly, PES polymer, aqueous acrylic acid and measured amount of additives are added and treated with nitrogen and sealed. Further, the mixture was irradiated with gamma ray source at room temperature followed by filtration and washing. The powder was then extracted and dried in oven at vacuum¹⁸⁴. The higher the absorbed dose of radiation, the more free radicals formed for grafting, resulting in increased degree of grafting (DG). However, this method also causes degradation of the PES polymeric materials and to avoid extensive degradation, it is necessary to control acetylation and oxidation reactions in the process¹⁸⁵. Figure.2.13 shows the process of fabrication of carboxylic polyethersulfone (CPES)

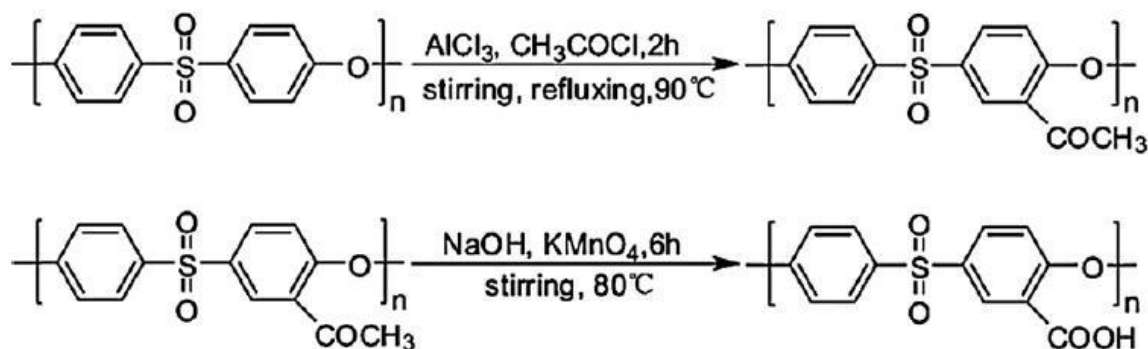
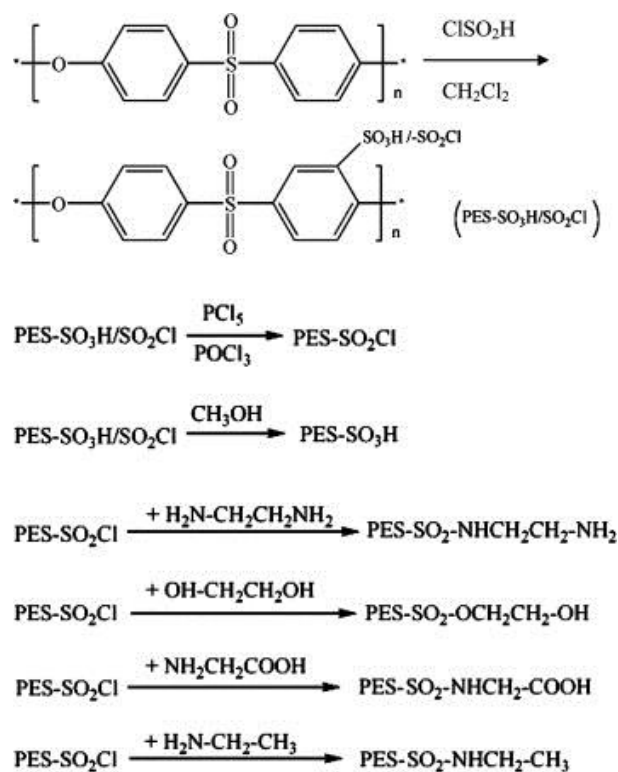


Figure.2.13.Process of fabrication of carboxylic polyethersulfone (CPES)¹⁸⁵.

Recently, membranes grafted with various other functional groups have also been synthesized by chlorosulfonation first and then chlorinated by phosphorous pentachloride¹⁸⁶. Hydroxyl, carboxyl and methyl groups have subsequently been grafted onto the PES matrix through different reactions. The synthesis is shown in figure.2.14¹⁸³.

Figure.2.14. PES modification by grafting different functional groups¹⁸³

2.3.3. SURFACE MODIFICATION OF POLYETHERSULFONE (PES) MEMBRANE

As mentioned in the section 2.2.2, bulk modification is a method of incorporating different functionality/functional groups into the polymer backbone (material modification) before the dope formulation. Surface modification is a post modification (post fabrication) process. There are many types of PES membrane surface modification as described below.

2.3.3.1. SURFACE COATING VIA THIN FILM LAYER

Several polymers were coated onto the PES membranes, which showed higher water permeability compared to the uncoated ones¹⁸⁷. In this method, a thin selective layer, referred to as a thin film layer (TFL), is directly deposited as a coating onto the membrane surface. The TFL coating has been proved to improve the anti-fouling properties of PES membranes. For instance, Ma et al. developed a dual layer membrane by coating and cross linking polyvinyl alcohol (PVA) onto the PES membrane. The hydrophilicity was found to increase with increasing antifouling properties of the coated PES membrane¹⁸⁸. Polite et al. coated PES membrane with the surface active agents such as Triton and cationic phenyl trimethyl ammonium bromide (PTAB), which was also found to increase the antifouling properties of the membrane¹⁸⁹. Similar effects have been observed with

PES coated with inorganic compounds such as zeolite, TiO₂, alumina etc. Bae et al dip coated the sulfonated polyethersulfone (SPES) membrane by TiO₂ nanoparticle suspension and formed nanocomposites, which was proved to decrease the amount and rate of fouling¹⁹⁰. Similarly, Kochkodan et al. dip coated their PES membrane by TiO₂ particles using UV irradiation at 365 nm which resulted in improvements in the flux by increasing hydrophilicity and antifouling properties of the membrane¹⁹¹. Recently, layer by layer deposition of polyelectrolytes, as depicted in Figure 2.15, was used to enhance the selectivity and water flux of the PES membranes¹⁹².

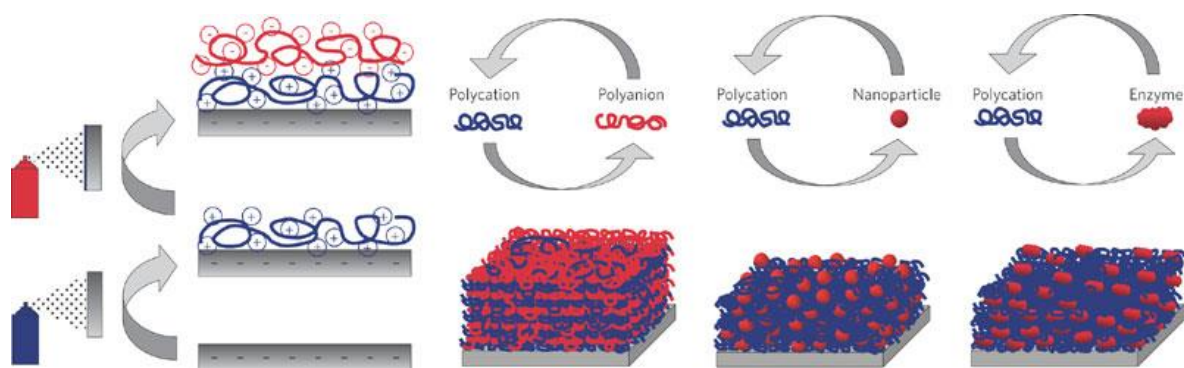


Figure.2.15. Layer by layer deposition by alternating spray coating of polyanions and polycations¹⁹³

Aravind, U. K. et al, reported that protein separation can be enhanced by coating chitosan or polystyrene sulfonate on to the PES membranes which forms a novel composite membrane with high flux and permeability¹⁹⁴. This protein separation is dependent on the thickness of the deposited layers and the solution pH. The coating technique also improves other properties of the PES membranes such as the stimuli responsivity¹⁹⁵, electronic property¹⁹⁶ and biocompatibility¹⁹⁷.

2.3.3.2. SURFACE COATING VIA INTERFACIAL POLYMERIZATION

Unlike the thin film coating, interfacial polymerization involves a chemical reaction which occurs at the interfacial boundary of immiscible solutions such as water and organic solvent or at the membrane surface or at the pore surface. Interfacial polymerization can be used to modify the surface of flat sheet membranes but is difficult to use for hollow fiber membranes, which represents an inherent limitation of this technique¹⁷⁰. It can be considered as the combination of coating and polymerization. This method of coating has been demonstrated to increase the antifouling property due to increased hydrophilicity and the separation performance of PES membranes. By choosing

different monomers, many kinds of functional composite membranes can be prepared for different purposes. Thus, PES membranes have been modified by PVA/PA composite thin layer¹⁹⁸ and PVA, PEG and chitosan¹⁹⁹. As a result, the membranes exhibited no tendency to be irreversibly fouled by humic acid at neutral pH and increased with decreasing the pH to a value of 3.

With the application of interfacial polymerization method, efficient membranes that can perform selective separation of gaseous compounds such as CO₂, CH₄ etc. have been developed. The separation performance of the composite polyaniline (PA) membranes was investigated by Ramachandhran et al. by the in situ interfacial polymerization over polysulfone (PSF) and PES membranes using different amines with aromatic acid chlorides. The PEI based composite membranes showed better salt rejection, permeation performance at the acidic feed and Polydiacetylene (PDA) based membranes showed better performance at the alkaline feed. Carrier composite membranes containing trimethylenetetramine (TETA) and hexane soluble trimesoyl chloride (TMC) were developed on to the PES support by interfacial polymerization which had honey comb like structure²⁰⁰. These membranes with a thickness of 0.2µm were said to have high selectivity for CO₂ and CH₄. Another work involved the preparation of PA layer by applying TMC and piperazine via interfacial polymerization on to the PES membrane²⁰¹. It is found that the salt rejection capability decreases as the irradiation power increases and the membrane is characterized using SEM and AFM studies²⁰². Moreover, the modified membranes showed structural and performance stabilities. Similar work has been done by Buch et al²⁰³ who prepared the composite NF membranes containing aromatic cycloaliphatic polyamide layer on to the PES membranes via interfacial polymerization of 1,3-cyclohexanebis(methylamine) (CHMA) in water with TMC in hexane. The flux and the rejection decrease as the chlorine concentration increase due to the conversion of H₂ bonding amide N-H group to the non-hydrogen bonding N-Cl group.

Man-made polymers with optimized molecular recognition cavities called molecularly imprinted polymers (MIPs) have attracted extensive attention due to their potential applications. These MIPs can also be attached to PES membranes via the interfacial polymerization technique in order to enhance the selective separation properties of the membranes²⁰⁴.

2.3.3.3. PHOTO-INDUCED SURFACE MODIFICATION

Photo-induced chemical surface modification involves mild reaction conditions, low temperature, high selectivity, suitable excitation wavelength and can be incorporated at the end of membrane

manufacturing process²⁰⁵. However, this method is difficult to implement within the internal surface of hollow fiber membranes.

Many studies have been carried out to modify polyolefins using vinyl monomers via UV induced grafting. Initially, photoactive poly(aryl-sulfone) requiring no photo initiators was used to modify the PES membranes by photo-induced grafting and the extent of the modification using different monomers was examined²⁰⁶. Also, 2-hydroxyethyl methacrylate (HEMA) was grafted on to the PES membrane using glow discharge technique. However, this photo-induced surface modification depends highly on the membrane properties such as the pore size, pore distribution, surface charge and interactions²⁰⁷. This type of PES membrane modification always causes degradation of the membranes if the irradiation time is uncontrolled²⁰⁸. Norman et al. used the time of flight ion mass spectroscopy after irradiation and studied the surface chemical changes in the PES UF membranes. They found a number of chemical changes such as addition of oxygen, degradation of benzene rings, carbon depletion, hydroxyl formation etc²⁰⁸.

Modification of PES membranes by using N-vinyl-2-pyrrolidinone (NVP) as the monomer, the hydrophilicity was said to increase by 25% and the fouling decreased by 49%²⁰⁹. However, the dip modified membranes exhibit simultaneous loss of Bovine Serum Albumin (BSA) rejection and permeability, which showed that there is a high degree of polymer chains that block the pores and decrease the permeability²¹⁰, but the immersion modified membranes retained their permeability and rejection. For dip modification, UV lamps and light filters were used to filter out 254 nm wavelength light which caused the protein rejection and thus the membrane fouling was reduced significantly²¹¹. Apart from NVP monomer, various other hydrophilic monomers have been used to modify PES membranes by photo-irradiation technique to improve the antifouling properties²¹²⁻²¹⁴. Also, another work by Abu et al. showed that the acrylic acid (AA) modified PES NF membranes had increased permeability compared to the unmodified membranes²¹⁵. In addition to the use of negatively charged hydrophilic monomers such as AA, several positively charged hydrophilic monomers were also grafted on to the PES membrane to inhibit bacterial growth or to have antibacterial activity along with reducing biofouling and enhance membrane cleaning¹⁸¹. The performances of the modified PES membranes using 6 grafted monomers were investigated by Taniguchi et al. and the surface wettability of the modified PES membranes was increased^{212,214}. Pore size was seen to have a major effect on membrane performance. With pore size of 50 kDa,

the modified PES membranes using NVP, AA and acrylamido-2-methyl-1-propanesulphonic acid (AMPS) monomers, achieved high retention and flux with lower fouling properties. With larger pore size of 70 and 100 kDa, the modified PES membranes using AA and AMPS monomers, showed high rejection and fluxes with greater cleaning capacity. Also, the PES membranes modified with weak acid AA monomer reduced the irreversible fouling properties to zero, whereas the hydrophilic monomers increased the irreversible fouling properties²¹⁴.

Better separation performances of the PES membranes were achieved by modifying the membranes using hydrophilic functional moieties such as AA and acrylamide (AM) by UV induced modification²¹⁶. The separation trend depends on the pH and decreases as the pH increases. For both the modified PES membranes, the water fouling recovery ratio and the antifouling property was found to be greater than for the unmodified PES membranes, even though the permeation and separation performances were different. Using this UV assisted method of modification, the PES membranes were modified using graft polymerization of 3 hydrophilic monomers, NVP, 2-acrylamidoglycolic acid monohydrate (AAG) and 2-acrylamido-2-methyl-1-propanesulfonic acid (AAP), with 300 nm wavelength lamps²¹³. Since BSA was negatively charged, the antifouling performance was better for the modified membranes using the AAP monomer. Wei et al. developed a method for depositing the charged molecules layer by layer by electrophoresis with UV grafting on the PES membrane surfaces with different types of monomers, MA, AA and AAG, which are strong polyelectrolytes, HEMA and N-vinylformamide (NVF), which are weak polyelectrolytes²¹⁷. After modification, the membrane possessed more hydrophilic and negative charges on its surface, which gives lower fouling properties. The strong polyelectrolytes improved the NOM retention and decreased the permeability and molecular weight cut off (MWCO) of the PES membranes, whereas the weak polyelectrolytes increased the permeability, MWCO and the pore size of the membranes.

The commercial PES membrane was modified by photo-induced grafting method to resist biofouling²¹⁸. Also, the PES membrane can be modified by photo graft polymerization of polyethylene glycol monoacrylate (PEGMA) on to the surface controlling the UV irradiation time, monomer composition and the degree of functionalization²¹⁹. However, the recommended best conditions are high monomer concentration (40g/L), average irradiation time (1.5-3 mins) for achieving higher flux and lower fouling. Heterogeneous photo graft copolymerization of 2 water-

soluble monomers PEGMA and N,N-dimethyl-N-(2-methacryloyloxyethyl-N-(3-sulfopropyl)ammonium betaine (SPE), was carried out to modify the PES membranes, which achieved higher fouling resistance²²⁰.

Zhou et al. combined the photo-induced graft polymerization with the high throughput platform and modified commercial poly(aryl sulfone) membranes. They prepared the BSA resisting surfaces using graft polymerization on to PES membranes and were shown to have reduced NOM fouling^{221,222}. Another work involves preparation of the PEGA by esterification of PES with AA and then using this to modify the PES membranes via UV irradiation²²³. The pure water flux and the PES rejection comparison of the control and modified membranes suggested that the permeability and the rejection ratio can be optimized by controlling the PEGA concentration. Also, it was found that the tensile strength and the elongation ratio were decreased for the modified PES membranes. However, they had good stability even after swelling in NaClO solution for a long period of time. To attach active biomolecules and reactive groups on to the surface of the PES membranes, a new heterogeneous UV irradiation method was developed without compromising the membrane selectivity²²⁴. PES membrane was also reported to be modified by the photo induced graft copolymerization of quaternized 2-(dimethylamino)ethyl methacrylate (qDMAEM)²²⁵. This modification showed that the pore size and the pore size distribution was reduced, which was attributed to free radical density for the photo reactive PES.

Even though it is difficult to modify the PES hollow fiber membranes by photo-induced method, as has been highlighted earlier in this section, there are a few studies reported to overcome this drawback. Bequet et al. developed a novel method of preparing NF hollow fiber from the UF membranes by modifying the PSF ultra filtration hollow fibers by grafting AA or MA via photochemical method²²⁶. Goma-Bilongo et al. developed a numerical model to represent this modification method using UV irradiation²²⁷. This method could be adopted to modify the PES hollow fiber membranes as well. Anyhow, the carboxyl groups showed pH sensitivity. Another method involves modifying the inner surface of the PSF hollow fibers by gas initiation under UV that optimizes the pore size in the membranes²²⁸. Here benzophenone was used as a photo initiator, AM as the graft monomer and polyacrylamide (PAM) was grafted on to the membrane surface. This method can also be applied to modify the PES hollow fiber membranes.

2.3.3.4. GAMMA RAY AND ION BEAM INDUCED GRAFTING

Gamma rays have high intensity and energy that can break down the chemical bonds in polymers leading to the formation of free radicals which are highly reactive due to their single unpaired electron and can readily initiate a polymerization reaction. Filho et al. studied the radiation induced grafting of styrene on to casted PES membrane using the gamma ray, whereby polystyrene side chains were grafted onto the membrane which could then be sulfonated to become proton conductive¹⁸⁴. Similarly, PES powder has also been grafted using polymethacrylic acid (PMAA) and poly acrylic acid (PAA) monomers using gamma ray irradiation graft polymerization^{229,230}. Figure.2.16 shows the preparation of grafted PES membrane by gamma-ray irradiation.

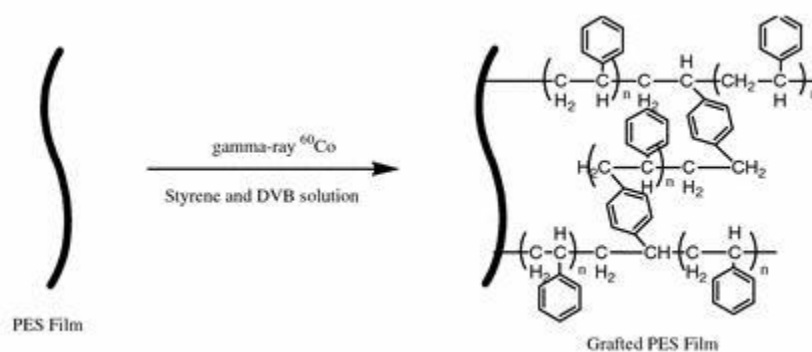


Figure.2.16. Preparation of grafted PES membrane by gamma-ray irradiation²²⁹

Because this gamma irradiation method involves breaking down the chemical bonds of the polymeric membranes, their mechanical strength can be severely affected. For this reason, this method is rarely used for modifying PES membranes. Instead, ion beam irradiation is the preferred method to graft monomers. It works by creating active sites on the membrane surface. AA monomers have been grafted on to PES membrane using such ion beam irradiation technique¹⁷⁰. The grafted PES membrane was seen to have increased water flux and rejection compared to the neat PES membrane with pH response due to the presence of hydroxyl groups. This method can be used to develop cationic and anionic membranes. PES membranes have also been modified using an electron beam irradiation method involving a single step of treating the membranes soaked in aqueous solutions of low molecular weight compounds with hydrophilic functional moieties prior to exposure to the electron beam²³¹. The advantage of this single step method is that it does not require any catalysts, solvents, photo initiators or any additional purifications steps.

2.3.3.5. PLASMA BASED GRAFTING POLYMERIZATION AND TREATMENT

Plasma, generated by the process of ionizing gas or water, is another surface modification technique that has been used to achieve or increase PES membrane hydrophilicity²³² through the formation of functional groups and radicals that are required for graft polymerization. Ionization of a gas can occur via electrical discharge at high frequencies using microwaves and radio frequency waves. Using these waves, the upper surface of polymeric membranes have been modified and activated by introducing functional groups to increase the hydrophilicity without changing the polymer itself²³³. Such plasma treatment can be optimized to impart the modified membrane surface with different properties.

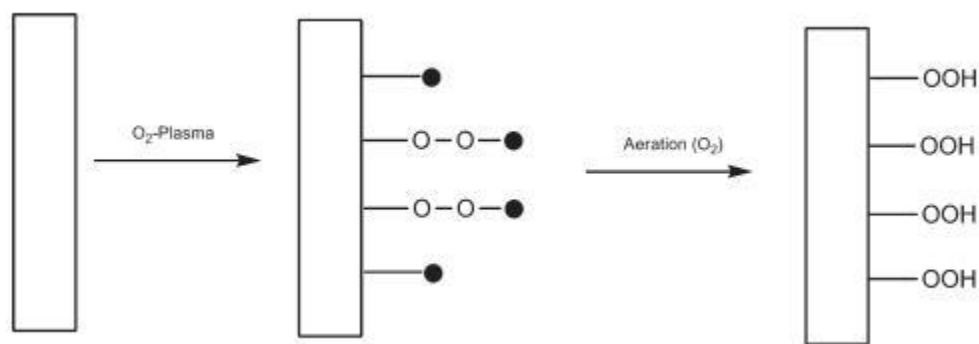


Figure.2.17. O₂ plasma treatment of the membrane²³⁴

Figure 2.17 shows the plasma treatment of the membrane using oxygen gas. Initially, the membrane surface is bombarded with the plasma components which are ionized and thus radical active sites are created. These radicals are capable of photodegrading carbon bonds except the C-H and C-C bonds and thus react with the oxygen molecules²³⁴. For oxygen plasma treatment, the functional groups reported are carboxyl, carbonyl and the hydroxyl groups. Other gases that have been used for PES modification include argon, CO₂, N₂, NH₃, and H₂O²³⁵⁻²³⁸. Plasma treatment using nitrogen gas introduces functional groups such as amine, amide, imine and nitrile on to the PES membrane surface. Similarly, CO₂ plasma treatment introduces oxygen molecule on to the membrane surface in the form of carbonyl, acid and ester groups via surface oxidation, which increases the membrane's hydrophilicity.

The methods of plasma treatment and plasma induced grafting have been applied to modify both flat sheet and the hollow fiber PES membranes. Improvement in performances in terms of

membrane fouling and hydrophilicity have been demonstrated after plasma treatment of these two membrane designs with oxygen gas²³⁹.

2.3.3.6. ATOM TRANSFER RADICAL POLYMERIZATION (ATRP)

ATRP is one of the convenient methods for new graft polymer synthesis under mild conditions and different types of vinyl monomers can be polymerized under controlled conditions. Three grafting methods including grafting-to, grafting-through and grafting-from, have employed ATRP to modify membranes based on the applications of the graft copolymers²⁴⁰. In one reported work, the PES underwent chloromethylation at mild conditions to produce benzyl chloride functional groups at the surfaces. These groups act as the initiators for the surface-initiated ATRP to modify the PES membrane functionality. The ATRP was carried out using the hydrophilic polymer brushes of PES monomethacrylate (PEGMA), sodium-4-styrenesulfonate (NaStS) and their copolymer brushes via chloromethylated PES surfaces. The PEGMA-grafted PES membranes showed higher protein resistance^{240,241}. Other methods which can be used are free radical mediated polymerization (SFRP), iodine-transfer polymerization and reversible addition-fragmentation chain transfer polymerization (RAFT).

2.3.3.7. OZONE-INDUCED GRAFTING

Ozone (O₃) is a triatomic allotrope which is less stable than the O₂ and is present at lower concentration in the earth's atmosphere. Ozone layer in the upper atmosphere efficiently prevents UV light from reaching the earth's surface, whereas the ozone layer in the lower atmosphere behaves as a pollutant that can cause respiratory problems and burn sensitive plants. However, ozone has many industrial and consumer applications and one such application is related to membrane surface modification, as illustrated in Figure 2.18.

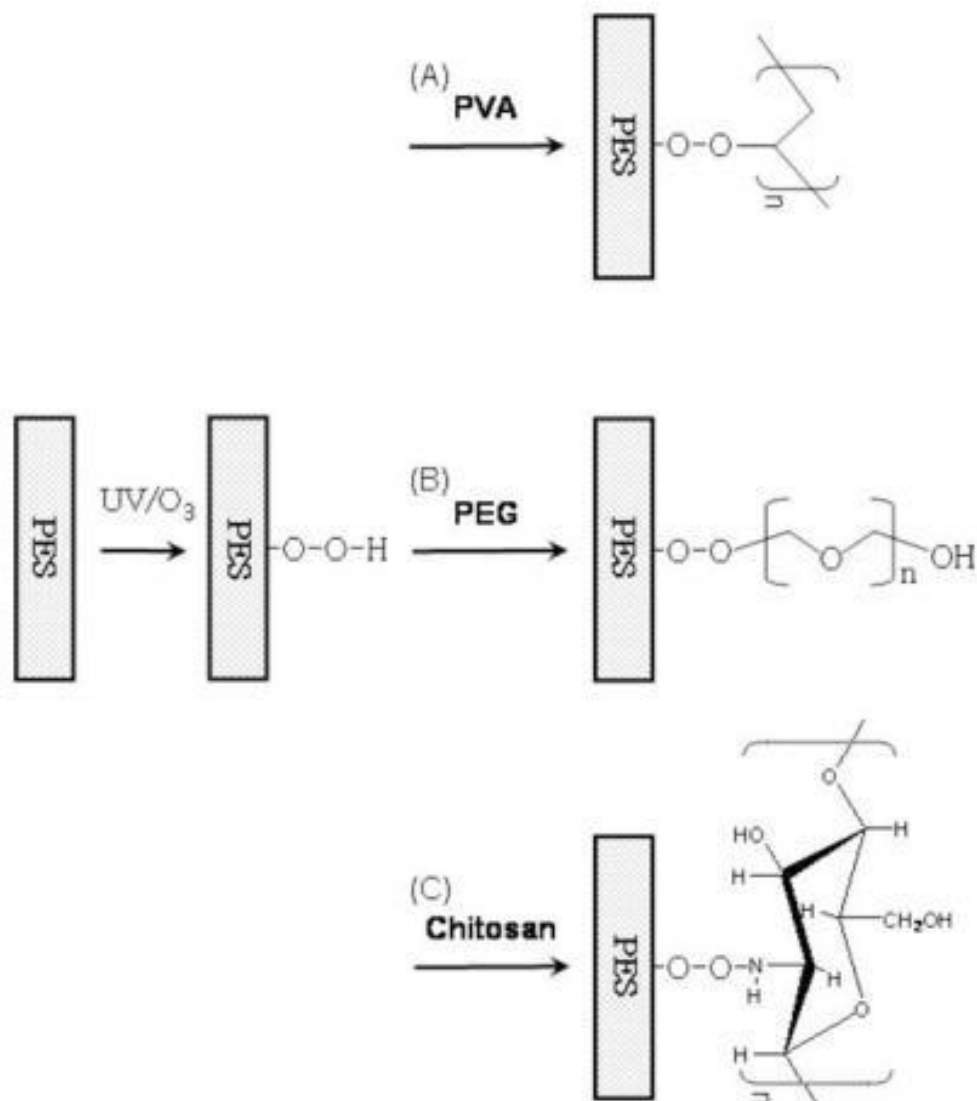


Figure.2.18. Reaction schemes of hydrophilic polymers grafting on to the PES membrane activated by UV/ozone treatment (a) PVA, (b) PEG and (c) chitosan²⁴²

To improve the hydrophilicity of the PES membrane, it is possible to graft hydrophilic polymers such as PEG, PVA and chitosan on to PES membrane via UV/ozone treatment²⁴². It was shown that the modified PES membrane had increased surface roughness, increased hydrophilicity and decreased protein absorption when compared to the unmodified PES membrane. Among all the three polymers used, PEG was shown to be the best polymer to enhance the antifouling properties via lower contact angle and protein absorption.

2.3.3.8. IONIC MODIFICATION METHOD

PES hollow fiber membranes which are delamination-free dual-layer asymmetric composite membranes have been developed for gas separation. These membranes were fabricated using the co-extrusion and dry-jet wet-spinning phase inversion techniques²⁴³. More recently, dual-layer hollow fiber spinning technology and the silver ionic modification method have been combined to increase gas selectivity²⁴⁴. Figure.2.19 shows the dual layer hollow fiber spinning unit. The three main factors that are responsible for the enhanced gas separation performance have been reported to be the steric hindrance, electrostatic cross linking and affinity to specific gases, which have been attributed to the ionic groups incorporated into the PES matrix.

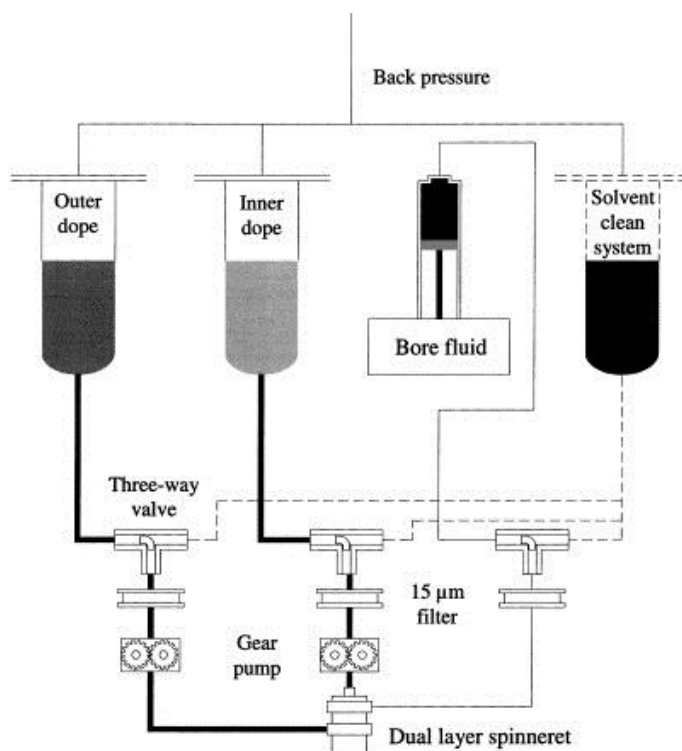


Figure.2.19. Dual layer hollow fiber spinning unit²⁴³

This method can be used to develop PES that possess antibacterial activity for food processing industries. Recently, silver ion modified PES membranes were prepared using the interaction between the sulfonated groups and silver ions²⁴⁵. The silver particles were successfully incorporated on to the sulfonated PES membranes using vitamin C as the reducing agent. The

modified PES membrane can be used to inhibit bacteria such as *Staphylococcus aureus*, *E. coli* and *Staphylococcus albus*.

2.3.3.9. PORE FILLING METHOD

The pore filling method can be used to surface modify the PES membranes. Shah et al. developed functionalized membranes in the pores of a PES porous matrix by cationic polymerization of styrene. The polystyrene is sulfonated using sulfuric acid to provide catalytic sites²⁴⁶. This charged membrane can also be used for separating whey protein, where a much higher selectivity (a five-fold increase) has been achieved compared to the unmodified membrane at pH 7.2²⁴⁷. Figure.2.20 shows cationic polymerization of styrene (a) and polystyrene grafts in the membrane pore (b).

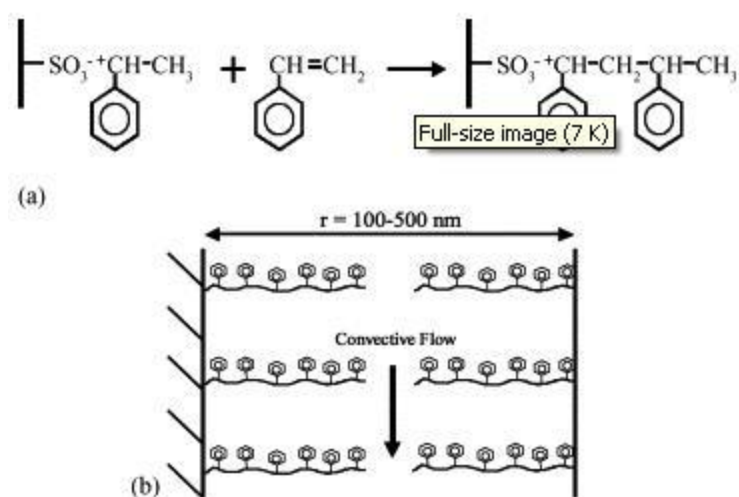


Figure.2.20. (a) Cationic polymerization of styrene (b) polystyrene grafts in the membrane pore²⁴⁶

2.3.3.10. REDOX GRAFTING METHOD

Redox reactions are those that involve the transfer of electrons between two chemical species via oxidation and reduction. The most widely used redox system consists of potassium persulfate and sodium meta bisulfite that can generate radicals on the membrane surface for grafting. This method of grafting is used for initiating polymerization reactions whereby the redox initiators are used to produce radicals under controlled conditions. The initiation takes place when an oxidant and a reductant are present in the reaction mixture and not limited by temperature, such that the membrane can be modified in aqueous environment at room temperature without removing oxygen.

Low molecular weight PES NF membranes and thin film composite membranes have been developed using the redox grafting method whereby negatively charged and neutral hydrophilic functional groups were inserted on the membrane surface via in situ redox polymerization of acrylate monomers²⁴⁸. The modified NF membranes have been used to treat dye effluent solutions and the composite membranes used for brackish water desalination with good fouling resistance. Similarly, Belfer et al. modified the PES UF membranes using redox initiators to produce radicals and the methacrylate based monomers for polymerization²⁴⁹.

2.3.3.11. MOLECULAR IMPRINTING

Molecular imprinting is a method of incorporating molecular recognition sites in polymeric membranes in the presence of a template molecule resulting in sites similar in shape and functionality to the template molecule²⁵⁰. The template molecule is also called the imprinting molecule and the imprinted polymers are called the molecularly imprinted polymers (MIPs).

Recently, Bisphenol A (BPA) imprinted PES hollow fiber membrane was developed using dry-wet spinning method and this was used for advanced separation processes made possible by the increase in the binding sites in the polymer²⁵¹. The separation process may be affected by pH conditions that cause the concentration driving force required for rapid and efficient separations. MIPs have high selectivity and sensitivity for compounds with low molecular mass in medical field. The BPA-imprinted PES membranes also have the capability for whole extraction devices²⁵².

2.3.3.12. THERMAL INDUCED GRAFTING AND IMMOBILIZATION METHOD

This method is used to covalently immobilize biomolecules such as protein, amino acids, enzymes etc. on to PES membranes via chemical reactions involving thermal activation of the chemical initiator or the cleavage agent. The thermal grafting method can be used to prepare modified PES membranes that help to improve their antifouling and their pH properties. Recently, the stable PES membranes were modified by the thermal crosslinking method using poly(ethylene glycol) diacrylate as the crosslinking modifier in the presence of catalyst (accelerator)²⁵³. Figure.2.21 shows the method of thermal induced surface cross-linking on PES membrane. These modified membranes was said to increase in mass with improved permeability and antifouling property.

However, excessive increase in mass will cause decreased performance. Another study involved modifying the PES membranes to increase the antifouling property and self-cleaning capability of the membranes²⁵⁴. PES membranes were first grafted using poly (methacrylic acid) to form PMAA-g-PES which introduces acid functional groups on the membrane surface. These acid groups were activated by N-hydroxysuccinimide for trypsin to attach covalently to the membrane. The modified membranes can be recovered by simple flushing showing self-cleaning property.

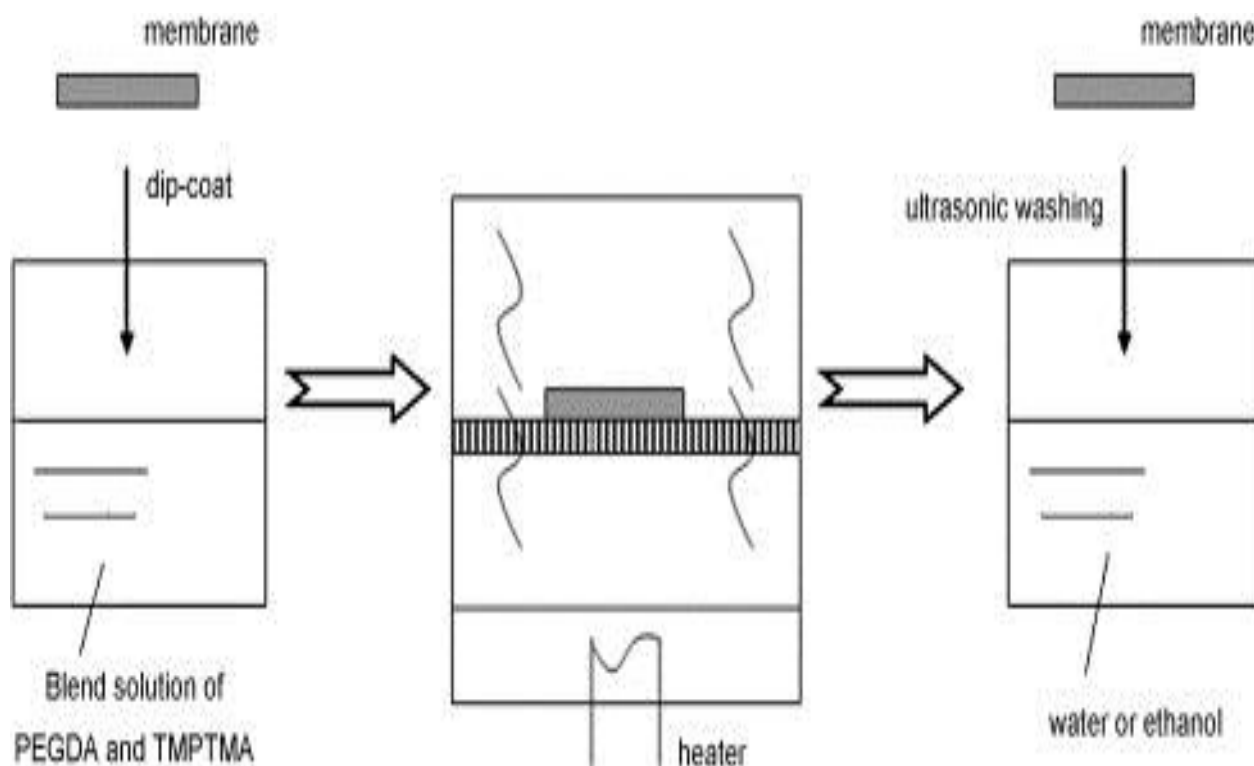
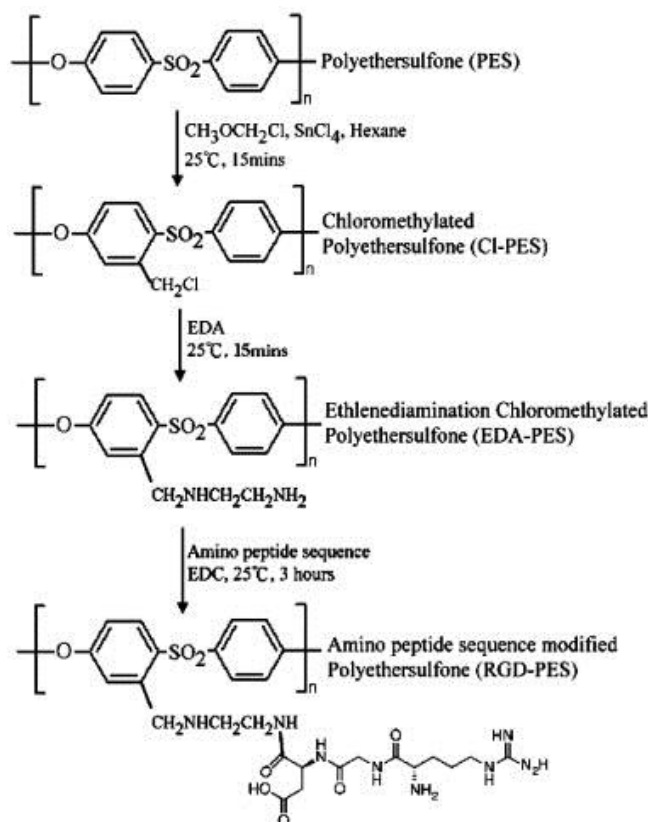


Figure.2.21. Thermal induced surface cross-linking on PES membrane²⁵³

Various PES membrane modifications using thermal induced method have been reported. Methacrylic acid grafted PES membranes were prepared using benzoyl peroxide (BPO) as the initiator²⁵⁵. Two or more amino acids linked via peptide bonds were used to modify the PES membrane. The amino acid sequence was covalently linked to the amine modified PES membrane using ethyl dimethyl aminopropylcarbodiimide (EDC)²⁵⁶. Figure.2.22 shows the reaction scheme of PES modification.

Figure.2.22. Reaction scheme of PES modification²⁵⁶

2.3.4. BLENDING METHOD

2.3.4.1. BLENDING OF HYDROPHILIC ADDITIVES WITH PES DOPE SOLUTION

The pure PES membrane does not have antifouling property due to its hydrophobicity and thus need to be modified via blending to increase its hydrophilicity and antifouling property. This method involves blending of PES with surface modifying macromolecules (SMMs), amphiphilic copolymers, hydrophilic monomers, biocompatible compounds etc. In the amphiphilic copolymers, the hydrophilic group allows increasing hydrophilicity and hydrophobic group allows it to be miscible with membrane materials. During blending and membrane formation, the copolymers accumulate on the membrane surface that was controlled by kinetics of the membrane forming systems. Based on this, the amphiphilic copolymers can have hydrophilic and biocompatible functional groups on the surface to increase the hydrophilicity and biocompatibility of the membranes respectively.

Blending is one of the simplest methods widely used for PES membrane modification. This method involves direct blending of the pore forming hydrophilic polymers such as PVP and PEG with PES dope solution to increase membrane hydrophilicity and antifouling properties^{257,258}. Amphiphilic polymers have also been synthesized and blended with PES membranes^{259,260}. The most serious problem in water treatment using membranes is the ‘fouling effect’ of membranes that makes the membrane impermeable to the water as time increases. Many studies have been reported to improve the antifouling property of the PES membranes using the blending method. The antifouling properties of PES ultrafiltration membranes were studied using the natural organic matter (NOM) that showed decrease in flux due to NOM fouling on the membrane. The water flux and the milk permeation flux of the PES membrane decreased with increase in protein rejection and enhanced antifouling property due to smaller surface pore size when treated with hot water²⁶¹. Another study reported that the membrane flux of PES was not much affected by the fouling layer formation²⁶². Having rough surfaces, PES formed a thick fouling layer during apple juice clarification that was found to have more openings when compared to other smoother membranes made of nylon. Amphiphilic pluronic copolymer with PEO and other contents was synthesized and blended with PES by Jiang et al²⁶³. They were able to modify the length of the PEO chain and the pluronic content in the membrane to increase the antifouling property and flux recovery. Later, pluronic F127 was used to modify the surface and to form pores²⁵⁹.

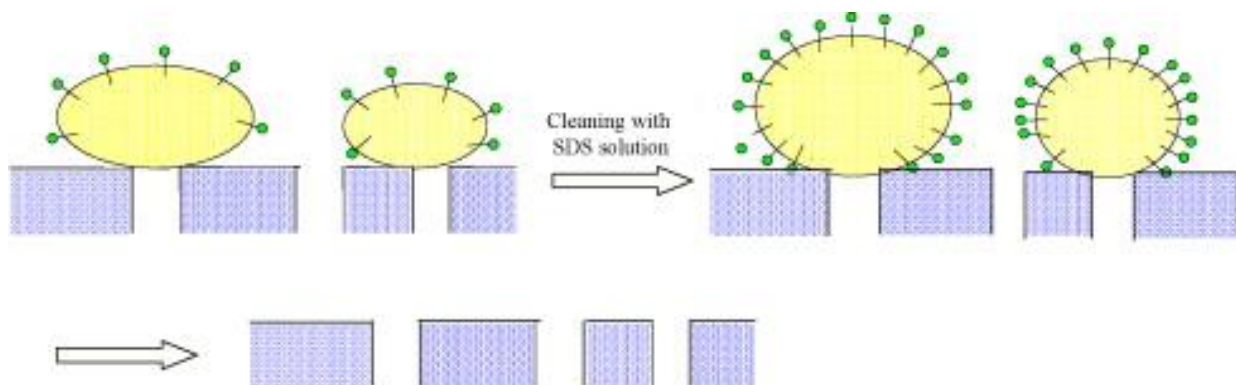


Figure.2.23. Cleaning process by SDS solution²⁶⁴

Increasing the pluronic F127 content was shown to increase the surface pore size and antifouling property of the membrane. However, when blended with PES, the flux recovery remained the same when washed with water. When washed with sodium dodecyl sulfate (SDS) solution, the flux

recovery increased to 93.33% due to prevention of oil droplets accumulating on membrane surface and thus can be used for oil/water separation²⁶⁴.

An ultrahigh molecular weight copolymer styrene maleic anhydride (SMA) was prepared using super critical carbon dioxide²⁶⁵. This hydrophilic copolymer was blended with PES to form SMA/PES membrane with increased surface hydrophilicity and protein absorption resistance.

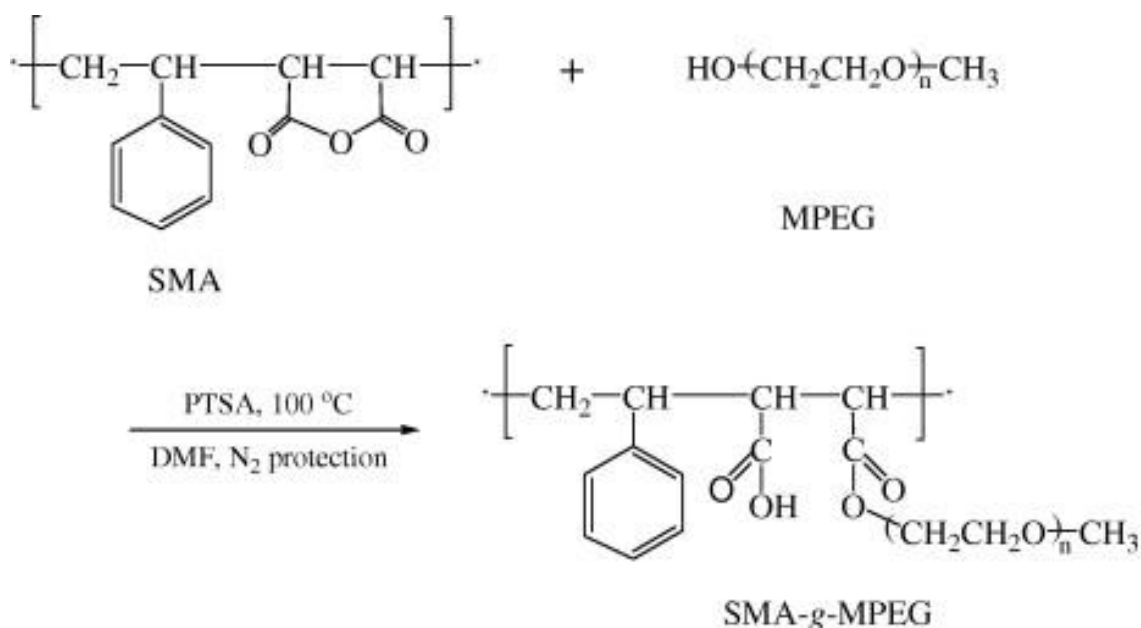


Figure.2.24.Synthesis of SMA-g-MPEG²⁶⁰

They also prepared amphiphilic copolymers with SMA and methoxy PEG grafts that was blended with PES to form membranes with fouling resistance²⁶⁰. Acrylonitrile copolymer with charged functional groups was blended with phenolphthalein-PES compound to form ultrafiltration membranes that are antifouling and used for protein separation depending on the pH of the solution²⁶⁶. PES-PAN membranes were also prepared for ultrafiltration with antifouling properties improved by aqueous alkali treatment at room temperature²⁶⁷. Recently, hydrophilic monomers such as acrylic acid/HEMA and PVP were blended with PES casting solution in DMAC to form the modified PES membrane via phase inversion technique by immersion precipitation²⁶⁸. This membrane was found to be fouling resistant with decreasing water fluxes and increasing milk water permeation.

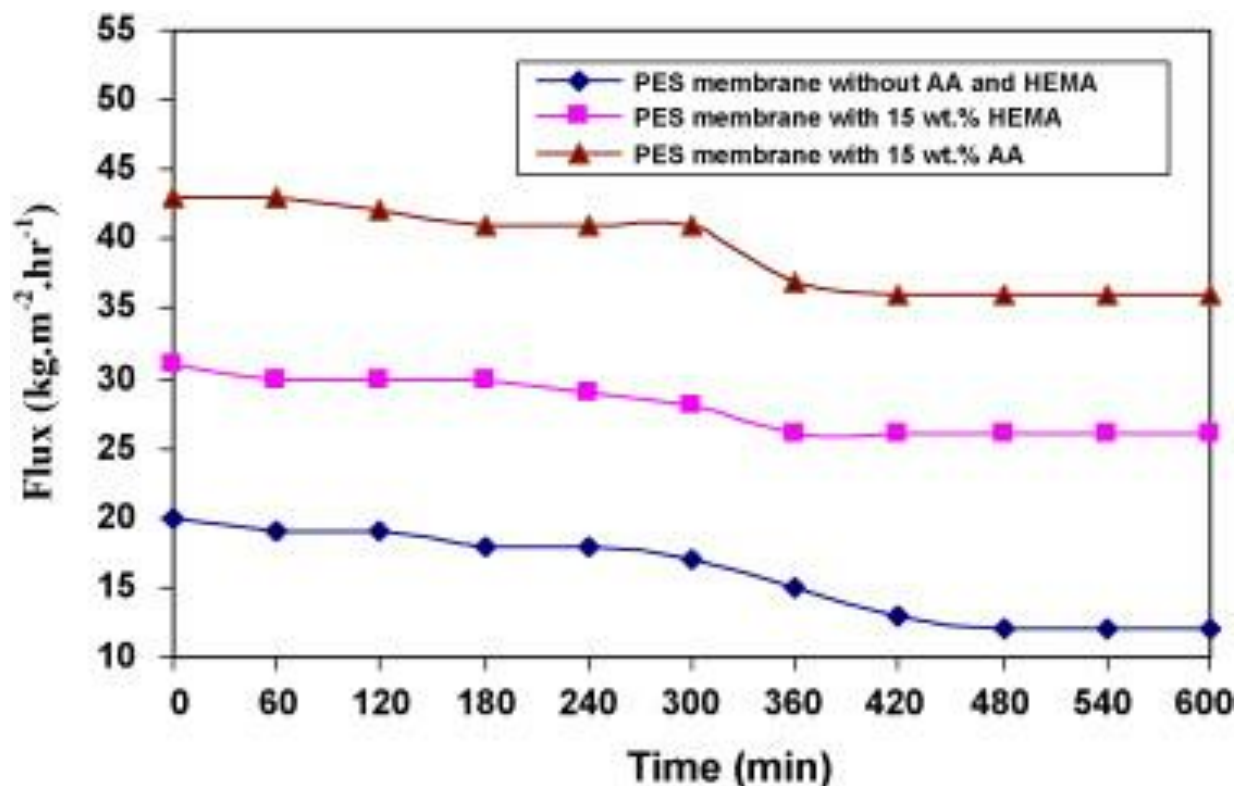


Figure.2.25.Effect of AA and HEMA on flux stability of PES membranes²⁶⁸

The pore size and the performance of modified PES membranes were usually modified using the synthesizing method and conditions that could increase the solvent evaporation time, lower the pore size and permeation rate²⁵⁸. However, the organic compounds removal from river water was not affected much by the modified membrane. Macromolecules that can modify the membrane surfaces were used to PES membrane via blending them together which leads to an increase in membrane performance and stability. This was reported by Susanto et al. using macromolecules like PVP, PES and Pluronic to modify PES membrane, out of which pluronic showed the best performance among all in terms of stability, antifouling property and biocompatibility²⁶⁹.

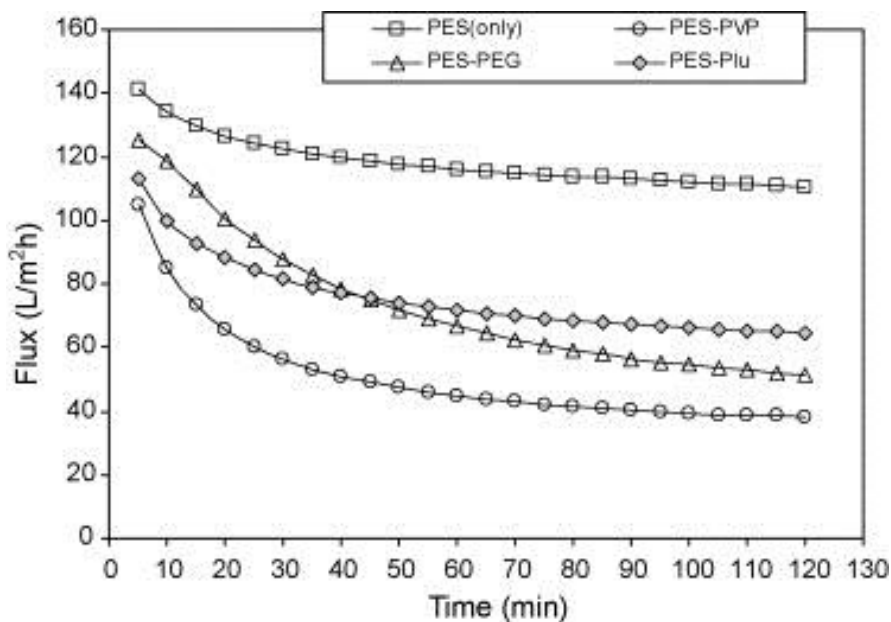
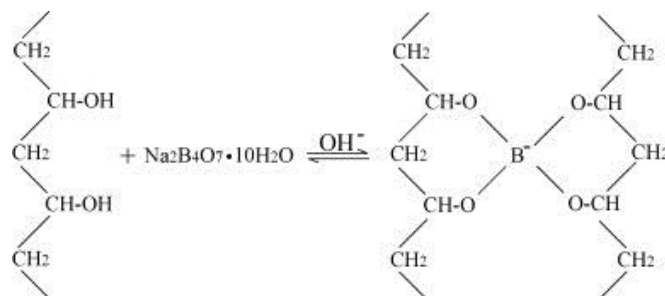


Figure.2.26. Water flux over time at pressure 450 kPa²⁶⁹

Surface modifying macromolecules (SMMs) were developed for modifying the PES membrane surfaces and thus enhance the membrane properties. They can be fluoropolymers with fluorinated end groups²⁷⁰. SMMs on PES UF membranes via blending method was studied by Matsuura et al¹⁷⁵. In this study polypropylene glycol based additive was used to modify PES membranes. The modified membranes with lower MWCO and smaller pore size had high TOC removal, lesser permeate fluxes and hence decreased fouling. An amphiphilic copolymer is synthesized by Wang et al using hydrophilic DMMSA and hydrophobic BMA through radical polymerization and different concentrations of these compounds is then blended with PES to fabricate the UF membrane with antifouling properties²⁷¹.

In another work, PES was modified by PEGylating via chlorosulfonated PES to increase hydrophilicity of the membranes²⁷². Also, it was proved that both the PEGylated PES and SPES membranes could have increased permeation properties. Matsuura et al studied the modified PES membrane using Sodium dodecyl sulfate (SDS) solutions as the gelation media²⁷³. With increasing SDS concentration, it was found that the MWCO and pore size decreases. The membrane pore size increases and the rejection ratio decreases with the addition of hydrophilic additives and solvents in the gelation bath.

Figure.2.27.PVA and Borax cross-linking²⁷⁴

Antifouling property of the PES membrane can be enhanced by blending other copolymers such as hydrophilic additive of silica-PVP nanocomposites²⁷⁴. The elution of PVP was prevented by preparing terpolymer, PAN-AA-VP using NMP solvent via free radical polymerization²⁷⁵. However, the acrylonitrile chains in the terpolymer make it insoluble. The acrylic acid chain imposes negative charge and vinyl pyrrolidone imposed miscibility with PES. The terpolymer blended PES membrane has reduced protein adsorption with increasing antifouling property. Su et al prepared a copolymer with 2-methacryloyloxyethylphosphorylcholine (MPC) and butyl methacrylate (BMA) and then blended with PES to prepare antifouling UF membranes²⁷⁶. It was reported that the BSA rejection was decreased with increase in flux recovery ratio and thus a decrease in irreversible fouling was shown. Another polymer, polyimide, being chemically and thermally resistant, was used to enhance the antifouling properties of the PES membrane by blending it together in DMF solvent²⁷⁷. Another polymer, poly(amide-imide) was synthesized and blended with PES to prepare membranes by phase inversion method, which had improved protein rejection and antifouling properties²⁷⁸. Blending PES with various other polymers such as polypropylene glycol and poly (acrylonitrile-co-acrylic acid co vinyl pyrrolidone P(AN-AA-VP) showed good antifouling property due to increased hydrophilicity with increased flux recovery^{275,279}. Moreover, addition of surfactants to the casting solution of PES improves the permeation performance and antifouling properties of the membrane²⁸⁰.

2.3.4.2. BLENDING NANOPARTICLES WITH PES DOPE SOLUTION

Recently, different nanoparticles were blended with PES dope solution to improve the hydrophilic and the antibacterial properties of the PES membrane^{281,282}. It was reported that the concentrations

of TiO₂ nanoparticles influences the pore size, porosity, rejection rates and permeation rates of the TiO₂-PES composite membranes with improved fouling resistance²⁸¹.

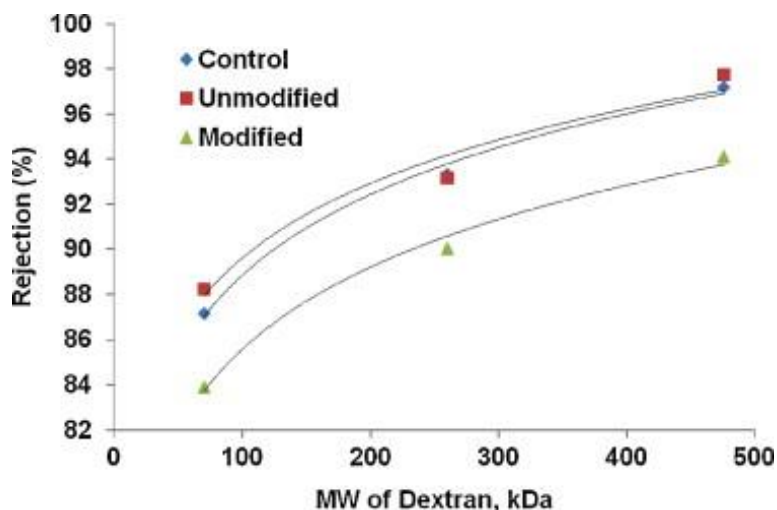


Figure.2.28.MWCOs of unmodified and modified membranes²⁸¹

Also, the mechanical and chemical modification of the nanoparticles on the surface of the membrane was studied¹²². This was found to improve the dispersion properties of the nanoparticles with less agglomeration. TiO₂ nanoparticles were also used to blend with PES-polyimide and prepare nanofiltration membranes²⁸². Here, the PES-polyimide was modified for OH groups for attachment of nanoparticles on to it. The -OH groups on the membrane surface helps uniform attachment of the nanoparticles. The sulfonated PES (SPES) ultrafiltration membrane was modified by TiO₂ nanoparticles and was found to have improved electronegativity and antifouling performance exhibiting good adhesion between the nanoparticles and the PES polymer. It was also reported that the TiO₂ nanoparticle decorated SPES were homogenous with increased proton conductivity and water swelling²⁸³. In addition to the inorganic nanoparticles, polymeric nanoparticles were also blended with PES membrane to have increased membrane performance. The polymeric nanoparticles used are biodegradable and non-biodegradable depending on the membrane applications. Recently, pH specialized membranes were prepared by blending PAA gels of size 250 to 3000 nm with PES²⁸⁴. These membranes were also used for ion exchange and were found to be stable. Semi-interpenetrating nanoparticles were also used to prepare PES membranes via blending method¹²¹. Here, PES was blended with cross-linked PVP semi-IPN

nanoparticles and the resulting modified membrane was reported to have increased hydrophilicity and blood compatibility.

Apart from nanoparticles, the inorganic compounds such as zeolite and alumina were also blended with PES to have increased antifouling property. Zeolites, being microporous aluminosilicate minerals, were blended with PES to form mixed matrix membranes of 3, 4 and 5 angstrom at high temperature close to glass transition temperature that has high gas selectivity²⁸⁵. The separation properties of the mixed matrix membranes were affected by the pore blockage of zeolites by the polymer. A novel silane coupling agent was used to modify the zeolite giving higher permeability and selectivity than the unmodified one, when made into mixed matrix membranes²⁸⁶.

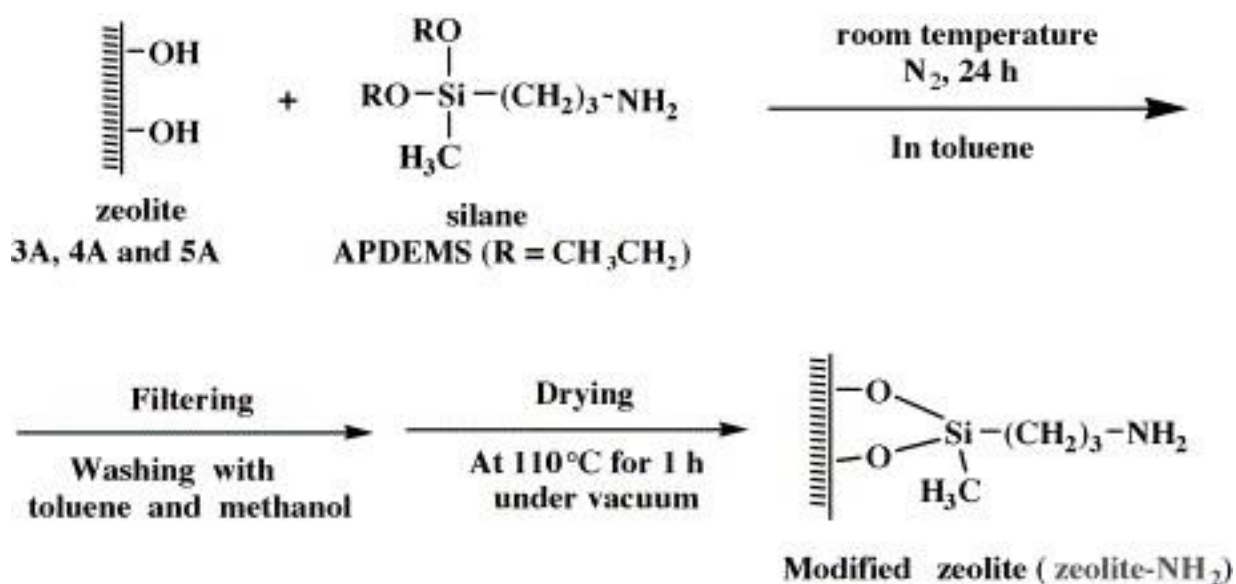


Figure.2.29. Chemical modification of zeolite surface²⁸⁶

To improve the gas separation performance, Kusworo et al synthesized 4 angstrom flat sheet polyimide PES-zeolite membranes. It was reported that the O_2 and N_2 permeation decreased and their selectivity increased²⁸⁷. Another important inorganic compound that has been used for PES modification is alumina²⁸⁸. This modified membrane was shown to reduce the flux decline, fouling rate and increase the membrane permeability. Similarly, ZrO_2 was blended with PES was prepared and studied²⁸⁹. Sulfonated PES could also be blended with PES, PVP and PEG to prepare the casting solution and then prepared into membranes with permanent hydrophilicity due to macromolecular compounds²⁹⁰. By increasing the concentration of SPES in the membrane, the

contact angle was shown to decrease, indicating an increase in the hydrophilicity of the membrane²⁹¹. Also, the surface pore size, pure water flux, milk water permeation and the sub-layer porosity were all increased. Hydroxyl, carboxyl, amino and methyl groups can be grafted to PES membrane matrix by reacting with the chlorosulfonic groups to increase the membrane biocompatibility¹⁸³.

2.3.4.3. BLENDING OF NANOBIOCIDES WITH PES DOPE SOLUTION

In general, noble metals are toxic to microorganisms and the effectiveness of these metals are in the following order: Ag > Hg > Cu > Cd > Cr > Pb > Co > Au > Zn > Fe > Mn > Mo > Sn²⁹². Silver is the best biocide among all the noble metals. The anti-microbial activity of silver has been studied in a broad spectrum against Gram-negative and Gram-positive bacteria, including drug resistant strains, viruses, fungi and protozoa has been well studied and proven²⁹³⁻²⁹⁵. As the size of a silver particle decreases to nano-scale, the anti-microbial efficacy increases due to the larger surface area per unit volume²⁹⁶. Hence, silver nanoparticles are being considered as an effective anti-microbial additive to prevent bacterial growth on the membrane compared to other antimicrobial agents. In the recent years, several research reports indicate that those polymeric membranes fabricated with silver nanoparticles show high antibacterial activity^{112,242,297}. However, the main disadvantage of this method is the leaching of these particles from the membrane matrix due to the harsh operation conditions. The leached Ag particles exhibit toxicity in drinking water application. Because of leaching problems, it is difficult to use these materials for drinking water applications.

3. Scope and Objectives of Present Work

As highlighted in Chapter 2, Polyether sulfone (PES), a popular membrane material, has been studied for many years for the synthesis of microfiltration (MF), ultrafiltration (UF) and nanofiltration (NF) membranes due to its excellent chemical and mechanical properties. However, its hydrophobic nature has limited its applications especially in membrane separation processes involving water treatment. Thus, several techniques have been proposed and developed in order to overcome this major disadvantage of PES. These techniques, which have been extensively reviewed in Chapter 2, include hydrophilic modifications of the PES/PES based membrane surface to increase its permeability and reduce membrane fouling. As highlighted earlier, one of the most effective modifications involves sulphonation reaction to bring the highly hydrophilic, negatively charged sulphonic functional group in to PES matrix. Several studies have shown that that PES membranes generated by sulphonation are more hydrophilic, more selective and more resistant to fouling than normal unmodified PES membranes. However, during sulphonation especially involving reaction with concentrated sulphuric acid, the physical and chemical property of the material could change or PES may degrade as phenol.

In addition, methods such as coating, nitration, carboxylation, plasma treatment, blending etc, have been reported to enhance hydrophilicity and reduce the fouling (deposition of hydrophobic organics on the surface) on the membrane. Most of these methods are post fabrication process/methods and hence, these methods required additional setup / process. The post modification process will also compress or reduce the pore size of the membrane which may increase the selectivity at the expense, however, of reduced permeability. Among all these methods, blending method has been widely used since it is by far the simplest method. Poly (N-vinyl pyrrolidinone) (PVP), a hydrophilic polymer having no hydroxide group or ionic charged group, has been widely used as a good additive for the modification of PES membrane through the blending method. Hydrophilicity and the anti-fouling property of the PES membranes blended with PVP were significantly increased. Similarly, polyethylene glycol (PEG) can also increase the membrane hydrophilicity and water permeability. However, it is well known that PVP and PEG

are water soluble additives, and the elution of PVP and PEG from the blended membrane is unavoidable due to the harsh operating condition.

Incorporation of nanomaterials into polymeric matrices could also alter the hydrophilicity and the antimicrobial (anti-bio-fouling) properties of polymeric membranes. The nanoparticles such as silica, titanium dioxide, silver, zirconium dioxide, selenium and copper were used to modify the PES membrane surface. As it is physically attached to the membrane matrix, blending of these nanomaterials may also leach during the harsh operating condition and the addition of a photo catalyst like titanium dioxide may degrade the polymeric membranes. Still, research has been geared up again in search of a better membrane modification method to improve the PES-based membranes in the past few years.

3.1 SCOPE AND OBJECTIVES OF THE PRESENT WORK

As mentioned above, it is well known that PVP and PEG are water soluble additives, and the elution of these additives from the membrane matrix is unavoidable due to the harsh operating condition. In order to overcome the above issues, the present work highlights the development of PES ultrafiltration hollow fiber membranes with long lasting antifouling properties by blending water insoluble highly hydrophilic copolymer additives with immobilized silver nanoparticles. In order to achieve this objective, highly hydrophilic negatively charged carboxyl (-COOH) and positively charged amine (-NH₂) functional group containing monomers such as, maleic acid and diaminomaleonitrile will be polymerized with water insoluble monomer acrylonitrile to obtain a final highly hydrophilic water insoluble copolymer additive. In addition to this, highly hydrophilic hydroxyl group (-OH) containing polyethylene glycol (PEG) or amine functionalized polyethylene imine (PEI) will be grafted to the prepared copolymer to get the final additives. The final additive will have these highly hydrophilic electronegative carboxyl, hydroxyl and positively charged amine functional groups, which have been shown to give significant improvements in the hydrophilicity of the membranes¹³⁴⁻¹³⁸ by inter molecular hydrogen bonding^{134,135,298,299} and antifouling properties by zwitterionic functionality. In addition, antibacterial compound, silver (Ag) nanoparticles, will be covalently attached to some of these functional groups to have a self-cleaning surface. It is generally accepted that silver kills bacteria by rupturing the cell wall³⁰⁰ and negatively charged protoplasm compounds will deposit on the positively charged silver containing surface by electrostatic attraction^{135,301}. Similarly, it has been proven that the electro negative

hydroxyl, carboxyl and amine functional groups repel the protoplasm compound by electrostatic repulsion^{101,135,302}. In the proposed membrane, when the bacteria approaches the membrane surface, the positively charged antimicrobial silver will kill them by rupturing their negatively charged plasma wall (which leads to the leakage of negatively charged protein molecules through the ruptured bacterial cell wall), whereas the highly hydrophilic, negatively charged acid and hydroxyl functionalities will prevent the deposition of these protein molecules onto the membrane surface by electrostatic repulsion. Thereby, the membrane can exhibit the self-cleaning property. In addition, since the silver nanoparticles (AgNPs) are embedded by covalently attachment in the copolymer matrix, the leaching of AgNPs will be completely prevented.

Thus four different membrane modifications will be implemented as follows:

- (1) As an initial step, highly hydrophilic –COOH functional groups containing maleic acid will be polymerized with acrylonitrile to obtain a final water insoluble copolymer additive poly acrylonitrile co maleic acid (PANCMA) (PANCMA will be used as a base additive/linker for all the work in this thesis). This new additive will be blended with PES dope solution to increase the hydrophilicity, water permeability and the antifouling properties of the PES membrane. Highly hydrophilic –OH containing polyethylene glycol (PEG) and silver nanoparticle (Ag) will be covalently attached to the PANCMA in the membrane matrix to evaluate the effect of these functional groups on the performance of PES membrane.
- (2) In the second step, a novel self-cleaning membrane surface will be developed. In order to develop a self-cleaning surface, negatively charged carboxyl (-COOH) rich, hydrophilic water insoluble PANCMA will be used as a base additive. Hyper branched Polyethyleneimine (PEI) will be thermally grafted to PANCMA to obtain the final additive and positively charged antimicrobial silver (Ag⁺) will be chemically attached to the final additive by thermal grafting. This Ag attached PEI will attach to the base PANCMA additive to get the final additive PANCMA-PEI-Ag. The modified PANCMA-PEI-Ag will be then blended with PES dope solution to prepare the hollow fiber ultrafiltration

CHAPTER: 3

membranes by dry wet spinning process to evaluate the effect of this novel additive on the performance of the membrane.

- (3) Third step will involve the formation of another self-cleaning membrane surface via a new polymeric additive poly (acrylonitrile co maleic acid co di-amino maleionitrile) (PANCMACDAMN). Negatively charged carboxylic (-COOH) acid functionalised maleic acid and amine positively charged (-NH₂) rich diaminomaleionitrile and acrylonitrile (alkenes monomers) will be polymerized to obtain PANCMACDAMN. Positively charged antimicrobial silver (Ag⁺) and hydroxyl (-OH) rich PEG will be chemically attached to the new additive by thermal grafting. The modified PEG-Ag attached PANCMADAMN will then be blended with PES dope solution to prepare the hollow fiber ultrafiltration membranes by dry wet spinning process to evaluate the effect of this novel additive on the performance of the membrane.

- (4) In the final step, a novel ultra-wetting graphene based ultrafiltration membrane will be synthesized with carboxylic, hydroxyl and amine functional groups. In order to develop the membrane, initially, the wettability of graphene will be increased by amine and carboxyl functional groups. Initially, Graphene will be t acid functionalized with highly concentrated hydrochloric acid and sulphuric acid. The carboxylic group will then be modified to acid chloride. Finally the acid chloride modified graphene will be aminated by using diethylene amine. The amine and carboxylated graphene will be attached to a highly hydrophilic water insoluble poly acrylonitrile co maleic acid (PANCMA) and imidized by thermal imidization process. The graphene modified poly acrylonitrile co maleimide (G-PANCMI) will be used to prepare/blended with PES dope solution. The hollow fiber ultrafiltration membranes will be prepared by dry wet spinning to evaluate the effect of this novel additive on the performance of the membrane.

- (5) All the prepared membranes will be characterized using nuclear magnetic resonance spectroscopy (NMR), Fourier transform infrared (FTIR) spectroscopy, Raman spectroscopy, energy-dispersive x-ray (EDX) spectroscopy, contact angle (CA), tensile testing, zeta potential (surface charge analyzer), scanning electron microscopy (SEM), zone of inhibition and the porometer. Finally, all the prepared membranes will be tested for their permeability, selectivity and antifouling property in long term experiments.

4. Materials and Characterization Methods

Only common materials used for modification and fabrication of membranes and the general characterization methods of these membranes will be discussed here. The procedures involved for fabricating the membranes themselves will be covered in the individual chapters 5, 6, 7 and 8.

4.1. MATERIALS

Polyethersulphone (PES) powder was purchased from Sumitomo chemicals pte ltd, Japan. Acrylonitrile, maleic anhydride, potassium persulphate ($K_2S_2O_8$), anhydrous sodium sulfite (Na_2SO_3), silver nitrate ($AgNO_3$), azoisobisbutyronitrile (AIBIN), sodium borohydride ($NaBH_4$) and polyethylene glycol (PEG) of molecular weight 400 were purchased from sigma Aldrich with 99% purity. High purity ethanol, N-methyl-2- pyrrolidone (NMP), polyvinyl pyrrolidone (PVP) and diethylene glycol (DEG) were also purchased from Sigma Aldrich and used as received. Exfoliated graphite nano platelets xGnP was purchased from xGnP Sciences Pte Ltd. The water used for the reaction was distilled and de-ionized (DI) with a Milli-Q plus system from Millipore, Bedford, MA, USA.

4.2. CHARACTERIZATION METHODS

All prepared polymeric additives and the membranes were characterized thoroughly using Fourier transform infrared (FTIR) spectroscopy, Raman spectroscopy, gel permeable chromatography (GPC), thermo gravimetric analysis (TGA), energy-dispersive x-ray (EDX), transmission electron microscopy (TEM), contact angle (CA), scanning electron microscopy (SEM), porometer, zone of inhibition test and clean water permeability test. Finally, the membranes will be tested for their permeability, selectivity and antifouling property in long term experiments using different feed water.

4.2.1. STREAMING POTENTIAL MEASUREMENTS

The surface zeta potential of membranes was measured by the SurPASS electro kinetic analyzer (Anton Paar Corporation). The measurements were based on the streaming potential and streaming current and are related to the surface charge at a solid/liquid interface. The zeta potential measurements also indicate the surface chemistry (pH titration) and liquid phase adsorption processes. The membrane was cut to 2cm by 5cm dimension and placed in the clamping cell with two spacers (Figure.4.1.). Here, 500mL of 1mM aqueous potassium chloride solution was supplied to cell as the background electrolyte and 0.25M HCl (acid) and 0.1M KOH were chosen for titration. The acid and the base volume increments were set to 0.1mL. The zeta potential was measured each time starting from pH of around 5 up to 9.5 (for basic range) and then after two times rinsing with MQ water from pH down to 2 (for acidic range). For each pH, the zeta potential measurement was repeated 4 times (2 measurements from left to right and another 2 from right to left) and average was taken.

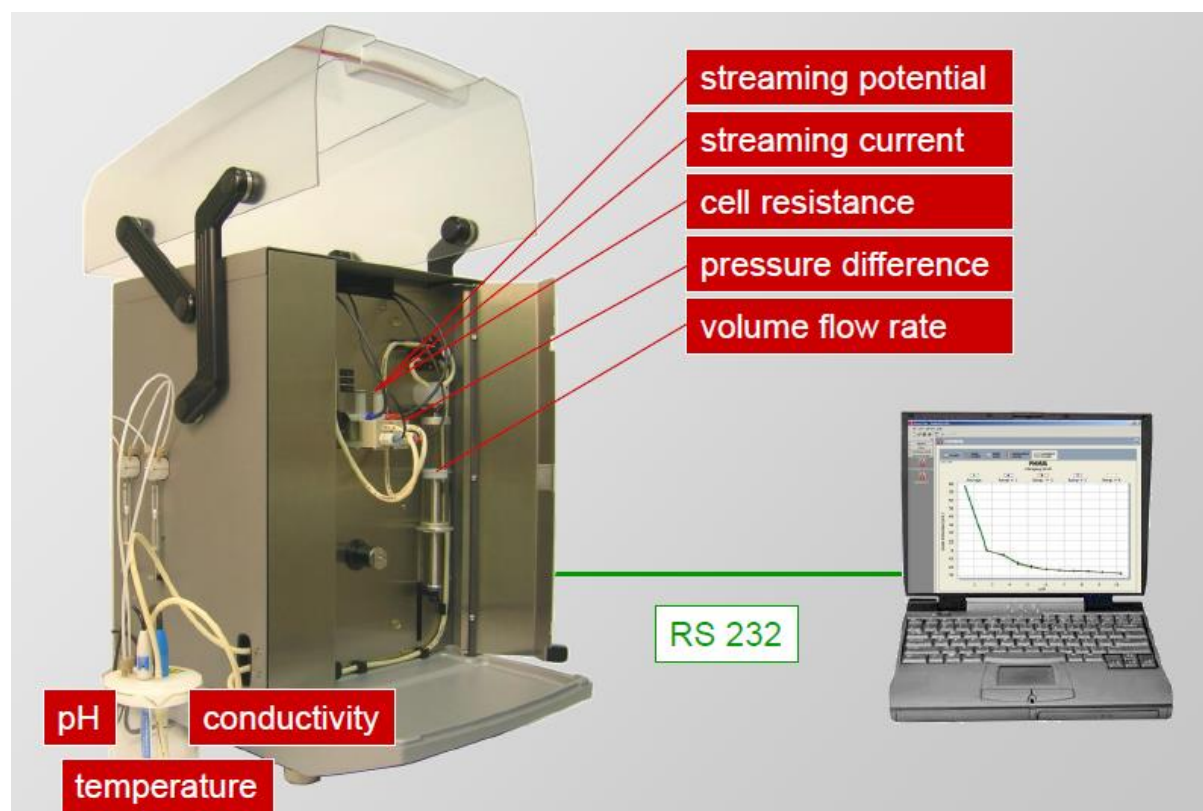


Figure 4.1. SurPASS electro kinetic analyzer (Anton Paar Corporation)

4.2.2. FOURIER TRANSFORM INFRARED SPECTROSCOPY (FTIR)

The surface functional groups and the chemical structures of modified polymer samples and membranes were investigated by using Fourier Transform Infrared (FTIR) Spectroscopy shown in Figure.4.2. (FTIR8400, Shimadzu, Japan). To examine the modified polymer samples, dried 99% KBr was mixed with 1% sample and then pressed into a transparent pellet which was mounted onto the instrument using the pellet holder. On the other hand, to investigate the hollow fiber membranes, single reflected attenuated total reflection (ATR) plate was used and the film sample holder was used to study the flat sheet membranes. All the spectra were measured in the transmittance mode from the wave number range $4000\text{--}450\text{cm}^{-1}$ with 45 scans.

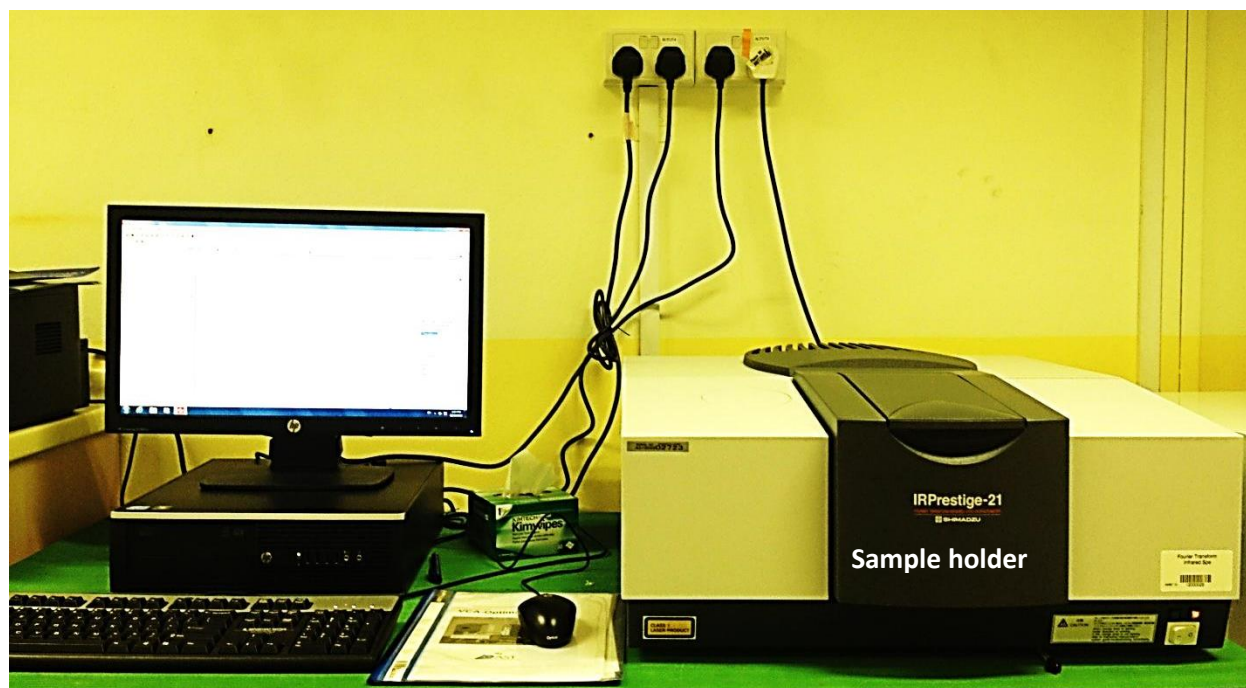


Figure 4.2. Fourier Transform Infrared Spectroscopy used in this study

4.2.3. THERMAL ANALYSIS (TGA)

To investigate thermal properties of the membrane materials thermo gravimetric analysis (TGA5000, TA instrument) was used. TGA was used at a heating rate of $20^{\circ}\text{C}/\text{min}$ up to 800°C

under nitrogen atmosphere was used. Membrane samples were cut into small pieces and were placed in a high thermal resistance tray (Figure.4.3.).



Figure.4.3. Thermo Gravimetric Analyzer (TGA5000, TA instrument) used in this study

4.2.4. PORE SIZE ANALYSIS – CAPILLARY FLOW POROMETRY

To study the mean flow pore size, the bubble pressure point and porosity of the membranes, a capillary flow porometer (model no: CFP-1200-AEXL) from PMI Porous Materials Inc., shown in Figure 4.4, was used. Wet-up/dry-down mode was used for the test on flat sheet membranes with the diameter of about 22 mm. In order to wet the samples, before running the experiments, one side of the membranes was filled with GalWick liquid with surface tension of 15.9mN/m. Hollow fiber membranes with one side potted with a sample holder (using epoxy resin) and wetted with GalWick liquid was used for the test. Each experiment was repeated at least 3 times and the average was calculated.



Figure.4.4. Capillary flow porometer for measuring pore size of the membranes

4.2.5. TRANSMISSION ELECTRON MICROSCOPY (TEM)

To study the structure of the polymer encapsulated nanomaterials, the transmission electron microscopy (TEM) was used (Figure.4.5). The transmission electron micrographs were taken using a Hitachi H-8100 electron microscope operating at 200 kV and a JEOL 3010 UHR transmission electron microscope (TEM) operating at 300 kV. For TEM imaging, the polymer encapsulated nanomaterials were first dispersed in ethanol by sonication for a few minutes and then a droplet of the prepared solution was dropped on the carbon coated copper grid and was

allowed to evaporate under ambient conditions. The grid was then subjected to vacuum overnight and used for TEM measurements.

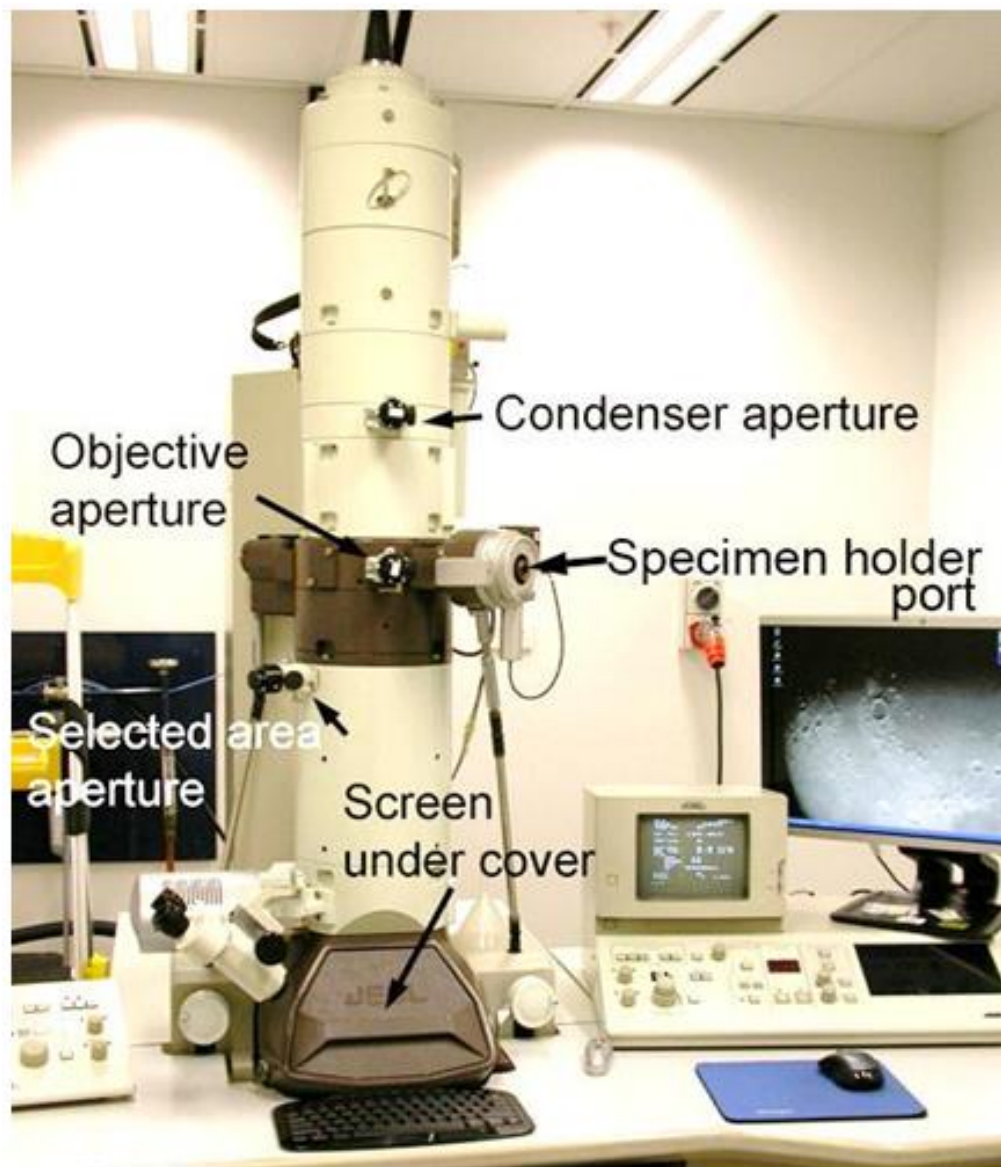


Figure.4.5. Transmission electron microscopy (TEM)

4.2.6. SCANNING ELECTRON MICROSCOPY (SEM)

A scanning electron microscope (SEM) Jeol Jsm-7600F coupled to an XmaxN detector for energy-dispersive X-ray (EDX) analysis was used (Figure.4.6.) to study the morphological appearance, the overall chemical composition and the distribution of the chemical elements of interest in the

membrane. To obtain clear images, the samples were sputter coated with platinum, using a JFC-1600 auto fine coater (JOEL, Tokyo, Japan) and then observed by using scanning electron microscopy. To obtain the cross-section images, membranes were immersed in liquid nitrogen and fractured before measurement.



Figure.4.6. Scanning electron microscope (SEM) (Jeol Jsm-7600F) coupled to an XmaxN detector for energy-dispersive X-ray (EDX) analysis used in this study

4.2.7. GPC

Gel permeation chromatography (GPC) (Figure.4.7.) was performed at National University of Singapore (NUS) using a Waters GPC system, equipped with a Waters 1515 isocratic HPLC pump, a Waters 717 plus Autosampler injector, a Waters 2414 refractive index detector, and a series of three linear Jordi columns (Jordi Gel DVB 1000A, packed with 5 mm PDVB particles), using DMF as the eluent at a flow rate of 1.0 mL/min. The samples were submitted to NUS and the analysis procedures and the results provided by NUS was used as such to report the molecular weight of the polymer. The analysis procedure was as described below. The calibration curve was

generated using polystyrene standards and a Shimadzu RID-10A refractive index detector. Tetrahydrofuran (THF) was selected as the mobile phase and the system was calibrated with mono dispersed poly(ethylene glycol) standards.



Figure.4.7. Gel permeation chromatography (GPC)

4.2.8. CONTACT ANGLE (CA) ANALYSIS

The contact angles of water / oils (CA_{water} / CA_{oil}) of the unmodified and modified membranes were determined using the Sigma 701 Tensiometer (Figure.4.8.) from KSV Instruments Limited to investigate the effect of surface modification on the hydrophilicity and the oleophobicity of the membranes. The liquid bowl was filled with DI water or toluene. The membrane samples were cut into 15mm pieces and clamped to the sample holder. The membranes were immersed into the liquid in the bowl and the advancing contact angle was calculated with the aid of computer software. An average of five readings was recorded for each sample.



Figure.4.8. Contact angle analyzer (Sigma 701 Tensiometer)

4.2.9. ANTIBACTERIAL ACTIVITY BY ZONE OF INHIBITION TEST

The material with antibacterial property will have resistance towards bacterial growth and hence the membranes made from these materials are expected to have bio-fouling resistance. The antibacterial activity of the control and the modified membranes were determined qualitatively using the zone of inhibition test. First, the nutrient agar is poured onto the disposable sterilized petri dishes and was allowed to solidify. 100 ml of 5×10^5 CFU/ml *E.coli* concentrations was streaked over the culture plate and was spread uniformly. The membrane samples were cut into small pieces (10mm in length) and were placed gently over the solidified agar plate. The plate was incubated at 37°C for overnight and was observed. The antibacterial activity was identified and estimated by a clear zone of inhibition.

4.2.10. CONFOCAL MICROSCOPE ANALYSIS

To visually evaluate the antifouling efficiency of the membrane, filtration test was conducted using 10 ppm fluorescein isothiocyanate (FITC) loaded bovine serum albumin (BSA) in DI water as a feed solution. The membrane samples before and after filtration was analyzed using the confocal laser scanning microscopy (CLSM) (Olympus FV 1000 with TIRF microscopy -Figure 4.9) to see the protein absorption on the membrane surface. The membrane samples were mounted on to the

instrument by using coverslip facing down to the objective lens on the stage. Then, the fluorescence of FITC loaded BSA was observed at $\lambda_{\text{ex}} = 495 \text{ nm}$, $\lambda_{\text{em}} = 520 \text{ nm}$ to visualize the presence and amount of BSA protein present on the membrane surface before and after filtration.



Figure 4.9. Confocal instrument

4.2.11. RAMAN SCPECTROSCOPY ANALYSIS

Raman spectroscopy is a vibrational technique that is extremely sensitive to geometric structure and bonding within molecules. Even small differences in geometric structure lead to significant differences in the observed Raman spectrum of a molecule. Raman spectroscopy is a relatively easy, non-destructive, non-contacting and quick measurement method to probe the inelastic scattering of light from a sample surface at room temperature at ambient pressure. A single frequency of radiation is used to irradiate the sample. The spectrometer detects scattered light with respect to its energy difference from the incident beam. The spectrum measured is used mainly to detect vibration states in the molecules to provide information on the chemical structure of substances. Raman spectroscopy was carried out using a Micro-Raman spectrometer - Figure 4.10 (ANDOR-DU420A-OE-152, EU) in the range of 2000 to 500 cm^{-1} . The laser spot size was 0 to

250 μm and the excitation was 532 nm. An integration time of 30 s was chosen for each measurement to achieve spectra with good counting rates. The laser power was kept at 28.2 mW to prevent irreversible thermal damages of the specimen surfaces



Figure 4.10. Raman spectroscopy used for this study

4.2.12. NANOMATERIAL LEACHING TEST

The leaching test was conducted by subjecting the membranes to ultrasonication which is actually the worst condition that a membrane can experience than the normal operating conditions (e.g. 3 months operation at 50 L/m²/h). If the Ag leakage under such harsh condition is low, then it can be concluded that Ag will not leach from the membrane at the normal operating conditions. The detailed analysis methodology is as below.

The leaching test for the nanoparticle incorporated membrane was carried out using the Inductively Coupled Plasma Optical Emission Spectrometry (ICP-OES) instrument to detect the concentration of silver that has been leached out. The silver attached membrane samples were immersed in DI water and ultrasonicated at 37 kW for 60 mins. After ultrasonication, the water was analyzed using ICP-OES to detect the concentration of silver in the water.

4.3. MEMBRANE PERFORMANCE EVALUATION

4.3.1. CLEAN WATER FLUX TEST

The clean water fluxes for the all prepared membranes were measured by using the filtration system shown in Figure.4.11. The hollow fiber membranes with the total effective membrane area of 0.03 m^2 were used to fabricate the membrane module. The two edges of the membrane module were sealed by using epoxy glue while keeping the lumen open on one side to collect the permeate water. The developed membrane module was mounted into the filtration system. Cross-flow ultrafiltration experiments were carried out at 1bar feed pressure.

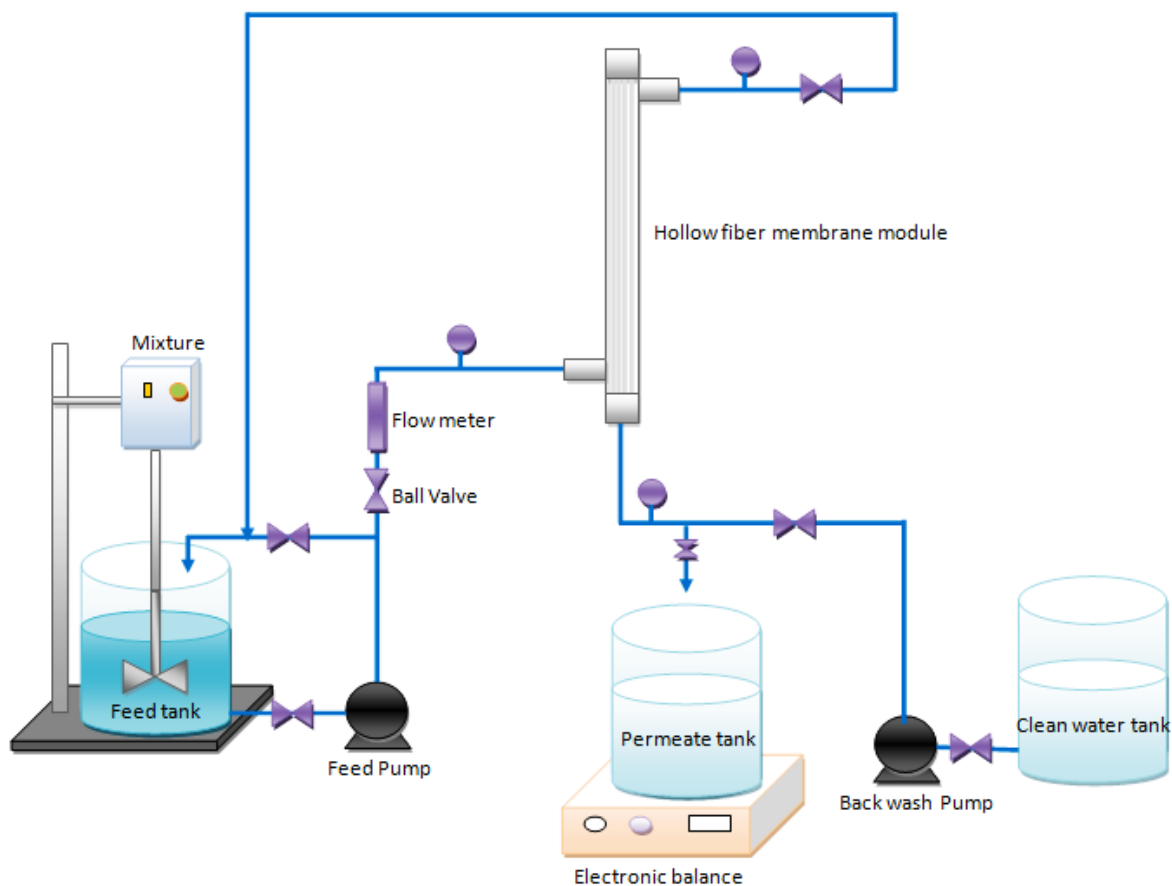


Figure.4.11. Filtration set up used to study the clean water flux

Filtration occurred from the outside to the inside of the hollow fiber membrane. The permeation was collected in a beaker mounted on an electronic balance. After compaction, the pure water flux (J_w) was determined. The pure water weight at four different time intervals (interval between each

sampling point was 15 min) was measured to get the average water flux for each sample. The pure water flux / permeability were calculated by the following equations:

$$\text{Water flux } (J_w) = \frac{\text{Permeate volume (L)}}{\text{Area (m}^2\text{)} \times \text{Time (h)}} \quad (\text{Eq. 4.1})$$

$$\text{Pure water permeability} = J_w / \Delta P$$

ΔP is the pressure drop through the membrane (bar).

4.3.2. LONG TERM EXPERIMENT WITH POLLUTED WASTEWATER

A long term (4200 min) filtration test was carried out by using different waste water feed. Cross-flow ultrafiltration experiments under constant pressure mode were carried out for all prepared membrane by using the same filtration apparatus shown in Figure.4.11. The feed waste water was stirred using an electrical stirrer to get homogenous feed water and was then pumped through the membrane at 0.4 bar pressure. The permeation was collected in a vessel mounted on an electronic balance. Flux drop was calculated by using the following equation:

$$\text{Flux drop } (\Delta J_w, \%) = 100 - \left(\frac{J_{wx}}{J_w} \times 100 \right) \quad (\text{Eq.4.2})$$

Where J_w is the initial flux and J_{wx} is flux at time x

The antifouling properties of the membranes were measured from permeability drop or flux drop (in %) of the membranes over time using various feed water (reservoir water, protein solution, polysaccharide solution and oil-water emulsion). In order to study the filtration efficiency of the membrane, Total organic carbon (TOC) and turbidity of the feed and permeate were measured and the rejection percentage was calculated according to following equation:

$$\text{Rejection (R, \%)} = \left(1 - \frac{C_p}{C_f} \right) \times 100 \quad (\text{Eq.4.3})$$

Where C_p and C_f are permeate and feed concentrations of TOC and turbidity respectively

5. Effect of hydroxyl (-OH) carboxyl (-COOH) and silver (Ag) functionalization on the antifouling properties of the prepared membranes

5.1. INTRODUCTION

As discussed in literature review Chapter 2, PES material may degrade or its physical/chemical properties may change during sulfonation. Hydrophilic additives blended in the membrane material may leach with time due to harsh operating conditions. In an attempt to circumvent these potential problems, it is proposed in this chapter, to blend highly hydrophilic, water insoluble poly(acrylonitrile-co-maleic acid) (PANCMA) as a co-polymer to the PES dope solution in order to introduce the carboxyl functionality in the membrane, which can be used as a linker to attach the highly hydrophilic polyethylene glycol (PEG) and silver to the membrane without affecting the PES structure. The combination of negatively charged hydroxyl (OH^-) groups and the positively charged (Ag^+) may lead to a neutral surface which can prevent the electrostatic attraction of natural organic matter to the membrane surface. The membranes were characterized using Fourier transform infrared (FTIR) spectroscopy, Energy-Dispersive X-ray (EDX), Contact angle (CA), Scanning electron microscopy (SEM), and the porometer. Both control and modified PES-PANCMA membranes were tested by zone of inhibition test and clean water flux test. Finally, the membranes were tested for their permeability and antifouling activity.

This chapter is based on: “*Synthesis and characterization of PEG-Ag immobilized PES hollow fiber ultrafiltration membranes with long lasting antifouling properties*” by Prince J.A., Bhuvana S., Boodhoo K.V.K., Anbharasi V., Singh G., (2014), published in *Journal of Membrane Science*. 454, 538–548

5.2. EXPERIMENTAL METHODS

General characterization and experimental methods are described in Chapter 4. Specific experimental procedures with conditions particular to this chapter are highlighted below.

5.2.1. MATERIALS

Polyethersulphone (PES) powder was purchased from Sumitomo chemicals pte ltd, Japan. Acrylonitrile, maleic anhydride, potassium persulphate ($K_2S_2O_8$), anhydrous sodium sulfite (Na_2SO_3), silver nitrate ($AgNO_3$) and polyethylene glycol (PEG) of molecular weight 400 were purchased from Sigma Aldrich with 99% purity. High purity ethanol, N-methyl-2- pyrrolidone (NMP), polyvinyl pyrrolidone (PVP) and diethylene glycol (DEG) were also purchased from Sigma Aldrich and used as received. The waste water used for the long time filtration was collected from a local reservoir with a TOC (81.59 ppm) and Turbidity (138 NTU) content. The water used for the reaction was distilled and de-ionized (DI) with a Milli-Q plus system from Millipore, Bedford, MA, USA.

5.2.2. SYNTHESIS OF POYL (ACRYLONITRILE CO MALEIC ACID) (PANCMA)

Copolymerization of acrylonitrile and maleic anhydride was performed according to the previously reported precipitation polymerization process using $K_2S_2O_8$ and Na_2SO_3 as initiator³⁰³. Typically, to 250 ml DI water at 90°C, 98 g maleic anhydride and 53 g acrylonitrile were added into the reactor equipped with a mechanical stirrer, thermometer, and nitrogen inlet tube. After complete dissolution, 4g $K_2S_2O_8$ and 1.85 g Na_2SO_3 were added into the stirring solution while maintaining the reaction temperature at 90°C under a nitrogen atmosphere. The pH value of the mixture was adjusted to around 3 using 0.1N H_2SO_4 . After 5 hours of copolymerization, the precipitated copolymer was filtered and washed with excess de-ionized water and ethanol to remove residual monomers. After thorough drying, the synthesized PANCMA was used to prepare the dope solution.

5.2.3. PREPARATION OF MEMBRANES BY DRY WET SPINNING

The PES hollow fiber membranes were prepared by dry wet spinning method. PES was used as the base polymer, NMP was the base solvent, DI water was used as a non-solvent and two additives, poly vinyl pyrolidone (PVP) (pore forming agent) and hydrophilic PANcMA were used to improve the surface property of the membrane. The composition of the casting solution consisted of 21 wt% PES, 5 wt% PVP-K-30, 5 wt% DEG, 59~69 wt% NMP and 0-10 wt% PANcMA, respectively. The composition of the dope solutions is shown in Table.5.1. The schematic representation of the dope solutions are presented in the phase diagram as shown in Figure.5.1. In general polymeric membranes can be formulated in 3 different directions they are 1) adjusting the polymer concentration to adjust the dope viscosity and coagulation value with respect to solvent; 2) adjusting the non-solvent concentration with respect to solvent to adjust the coagulation value; 3) adjusting polymer and non-solvent concentrations at the same time with respect to solvent to adjust viscosity and coagulation value. In this thesis the polymeric additive concentrations were adjusted with respect to the solvent concentration to optimize the polymeric additives concentration in order to achieve higher permeability, selectivity and antifouling properties.

PVP powder was first added into the NMP /DEG mixture in a round bottom flask and the solution was stirred by a mechanical stirrer for at least 1 hour. After complete dissolution of PVP, desired quantities of PANcMA and PES were added and allowed to stir at a constant speed of 250~350 rpm for at least 24 h at 80°C to obtain a completely dissolved homogeneous polymeric solution. The solution (S5) with 10% PANcMA concentration was found to be heterogeneous. All other dope solutions from S0-S4 were used to fabricate the membranes. The dope solution was poured into the polymer tank and degassed at a vacuum pressure of -0.6bar for 20min. Nitrogen gas was purged into the dope tank to create an inert atmosphere and to push the polymer to the polymer pump. NMP and water were mixed in 80:20 volume ratios and poured into the bore liquid tank. The polymer solution and the bore liquid were pumped to the spinneret (OD 1.2mm, ID 0.6mm). The air gap was fixed at 10mm. The hollow fiber membranes were fabricated at around 25° C and at around 65% relative humidity with a take up speed of 0.25 m/s. The membrane turned opaque soon after coming into contact with water which indicates that the coagulation and precipitation of PES from the solution and finally a translucent, white hollow fiber membrane was formed. The membrane was then collected from the winder and left inside a post coagulation water tank for a

minimum of 24 h to washout the residual NMP, DEG and PVP that was not removed from the solution at the point of coagulation.

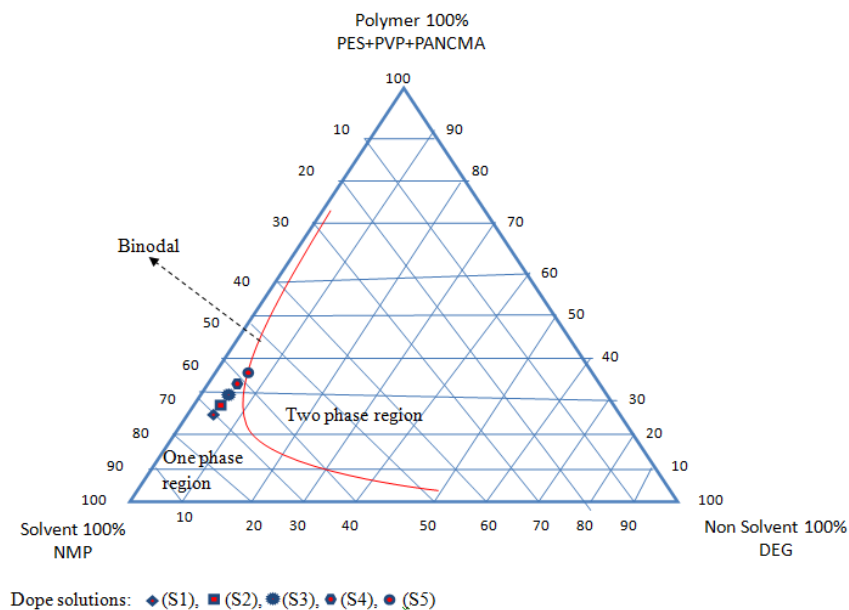


Figure.5.1. Phase diagram for the dope composition

Table.5.1. Composition of the dope solutions for the hollow fiber membrane fabrications

Sample ID	PES (wt%)	PVP- K30 (wt%)	DEG (wt%)	NMP (wt%)	PANCMA (wt%)
S1	21	5	5	69	0
S2	21	5	5	66.5	2.5
S3	21	5	5	64	5
S4	21	5	5	61.5	7.5
S5	21	5	5	59	10

5.2.4. MEMBRANE SURFACE MODIFICATION

Before surface modification, the prepared hollow fiber membranes were washed with water and ethanol to clean the surface of the membrane for about 15 min. The cleaned membranes were then immersed in 500 ml of 2:1 PEG: AgNO₃ aqueous solution at 80° C for 2 h for thermal grafting. Figure.5.2 shows the surface modification of PES-PANCMA membrane. The surface grafted membranes were then washed with excess water and dried at room temperature before characterization. To keep the surface modified membranes wet, they were immersed into a post treatment solution of 40% ethanol and 60% glycerin before testing the clean water flux.

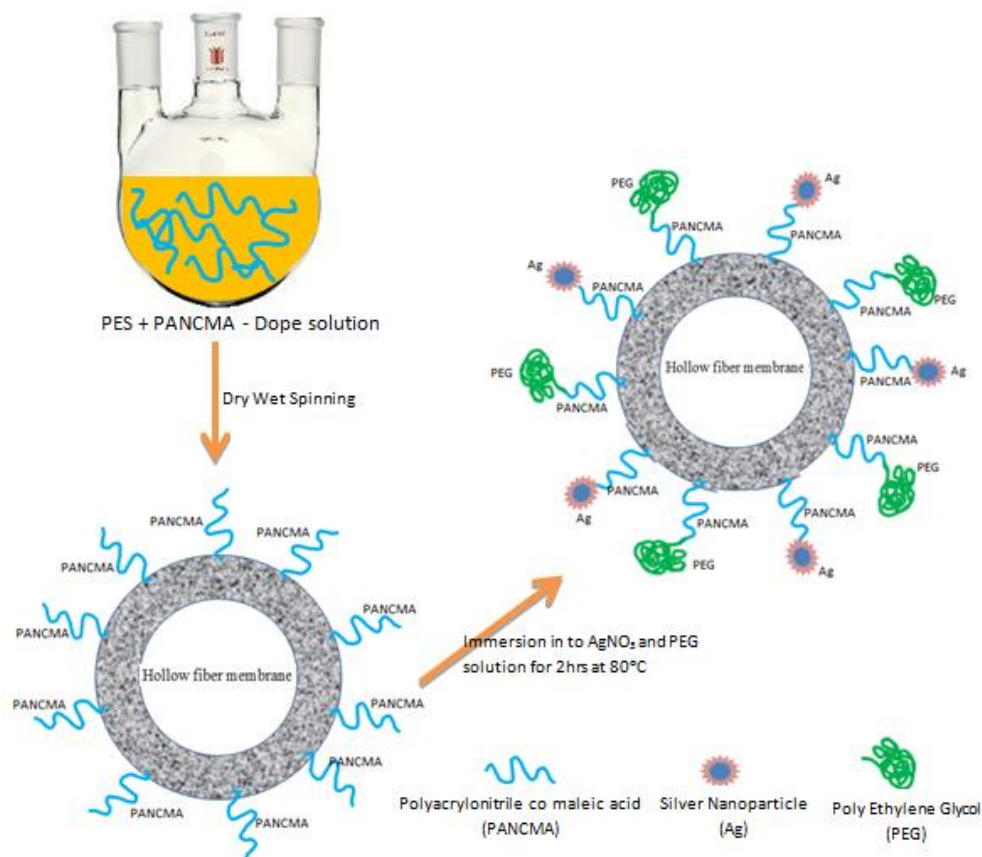


Figure.5.2. Schematic representation of stepwise modification of hollow fiber

5.2.5. MEMBRANE CHARACTERIZATION

General membrane characterization methods are presented in Chapter 4 under Materials and Characterization Methods.

5.3. RESULTS AND DISCUSSION

5.3.1. FOURIER TRANSFORM INFRA-RED ANALYSIS

FTIR analysis was used to investigate the interaction of PEG and Ag to the PANcMA/PES hollow fiber membrane. Figure.5.3. represents the FTIR spectra for neat PES membrane S1 as well as for PES/PANcMA membranes S2, S3 and S4 (blended with 2.5 wt %, 5 wt % and 7.5 wt% of PANcMA respectively) and grafted with PEG and silver. It is confirmed from the spectra that the PEG and silver is successfully grafted to the PES/PANcMA membrane. The band at 2247cm^{-1} is

due to the C-N stretching of the nitrile group and the band at 1710cm^{-1} is the C = O stretching vibration of the acid carbonyl group present in the PANCMA. The absorption band at 1169cm^{-1} is attributed to the C-O-C stretching vibration of repeated $-\text{O}-\text{CH}_2-\text{CH}_2-$ units of polyethylene glycol. The broad band at 3558cm^{-1} is due to the stretching vibration of hydroxyl group present in the PEG. It is also observed that, as the PANCMA concentration increases, the intensity of the PANCMA and PEG vibrational bands increases.

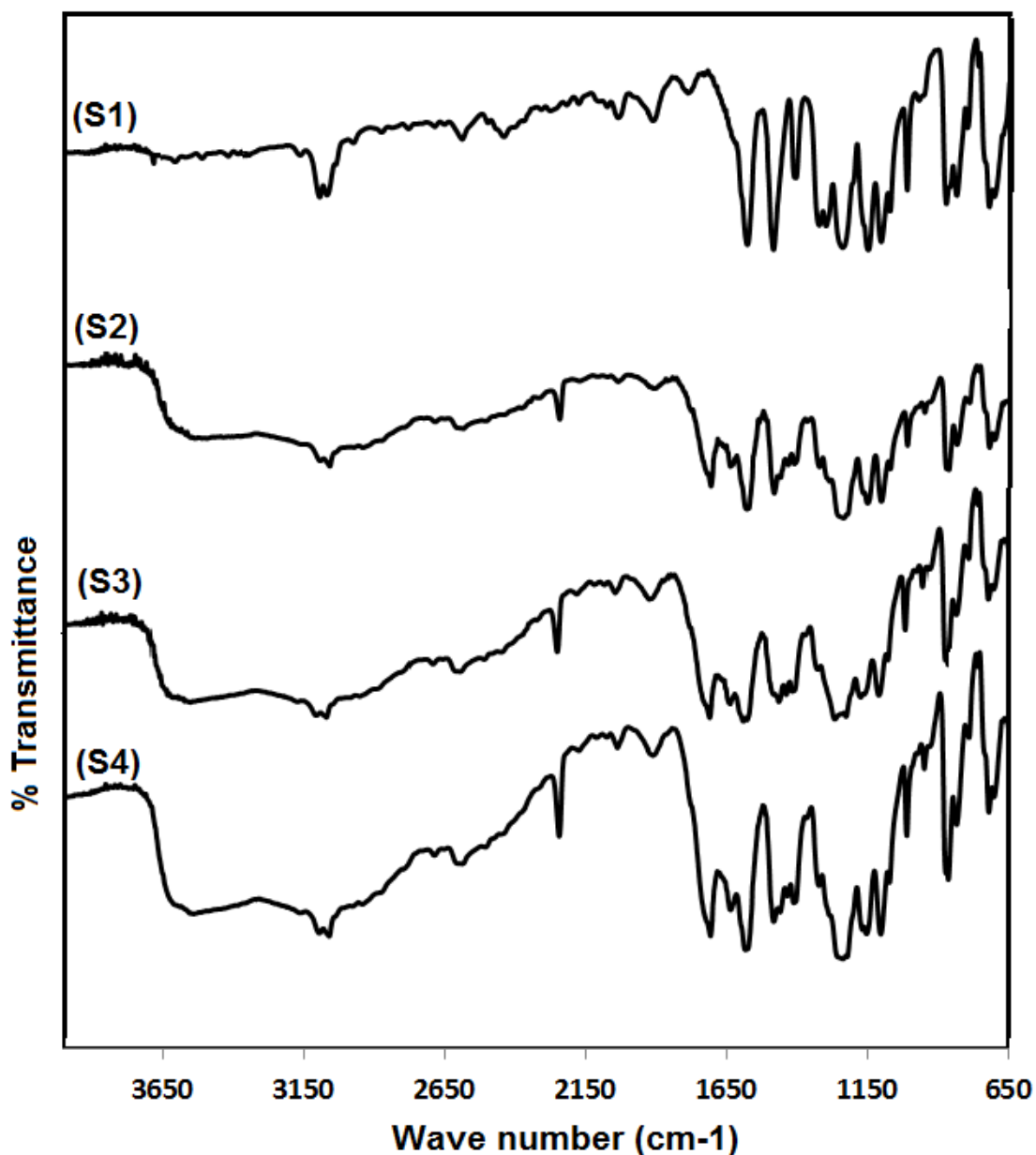
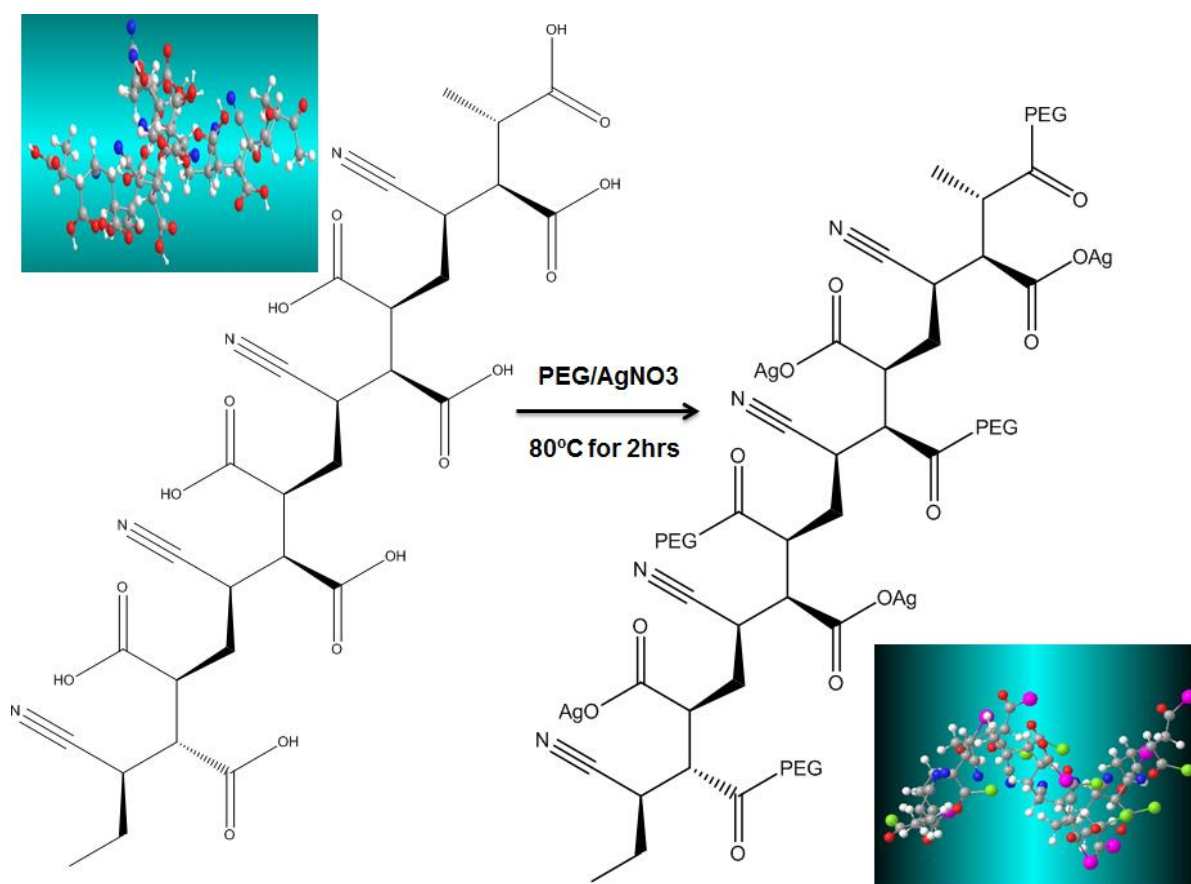


Figure.5.3. FTIR spectra of S1) PES S2) PES/PANCMA (2.5 wt%)/PEG/Ag S3) PES/PANCMA (5wt%)/PEG/Ag S4) PES/PANCMA (7.5wt%)/PEG/Ag

Apart from this, it is also observed that, as the interaction between the OH and Ag increases, the peak shifts to lower wavenumber. The OH stretching vibration for neat PANCMA was observed at 3391cm^{-1} , as the Ag gets attached to OH of PANCMA, the peak shifts to 3568cm^{-1} for S2, 3551cm^{-1} for S3 and 3548cm^{-1} for S4.

A schematic representation of the grafting of PEG/Ag to PANCMA and their bonding interaction is shown in Figure.5.4.



Figur.5.4.Proposed schematic representation of grafting of PEG/Ag to PANCMA

5.3.2. MORPHOLOGY OF HOLLOW FIBERS

The hollow fiber membranes fabricated through dry-wet spinning process had an average inner diameter of 0.6mm and an outer diameter of 1.0mm. The surface morphology and cross section of the hollow fiber membranes were examined using SEM and the micrographs are shown in Figure.5.5 and Figure.5.6 The micrographs of the modified hollow fibers show a smooth PEG surface together with uniform distribution of silver.

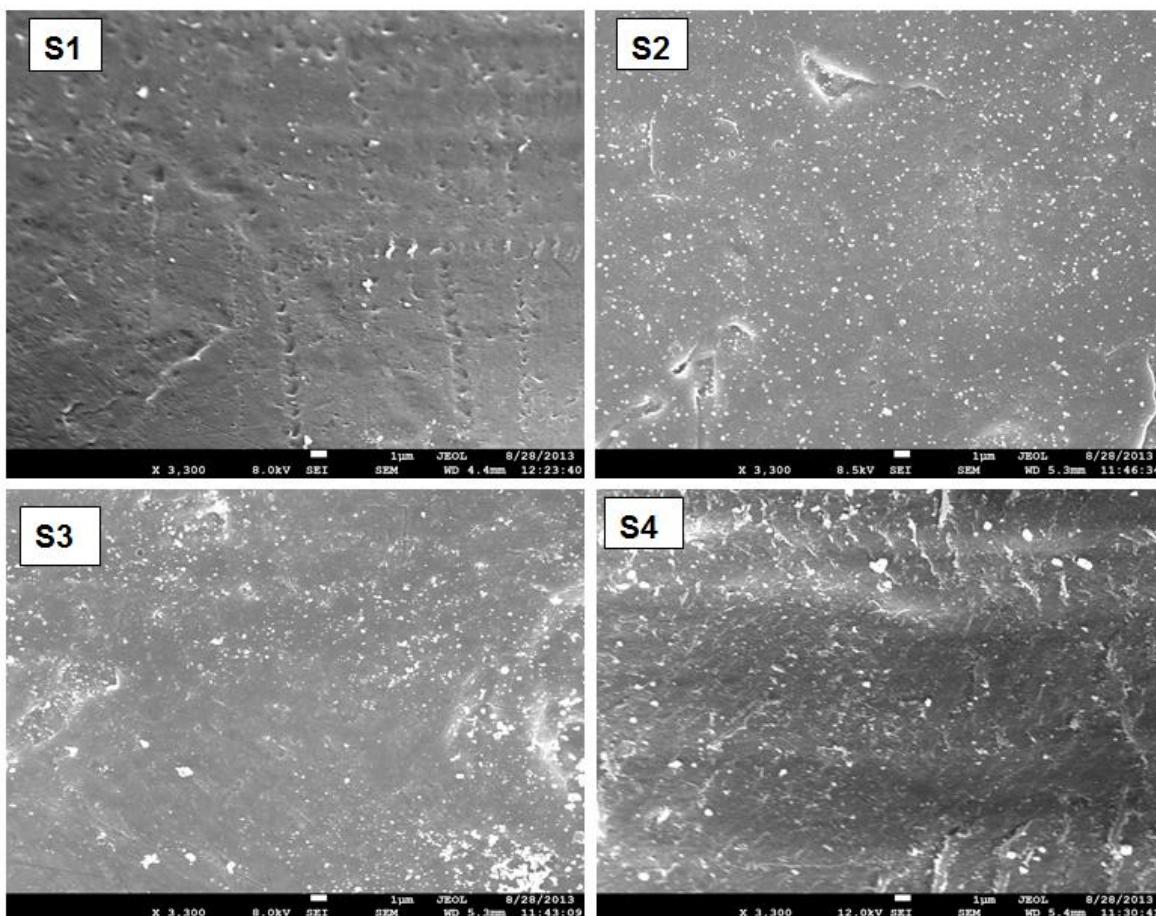


Figure.5.5. SEM pictures of unmodified (S1) and modified (S2, S3 and S4) hollow fiber membranes

As seen in Figure.5.6, the hollow fibers exhibit different internal structures depending on their composition. S1 is the neat PES membrane which shows the presence of a large number of macrovoids in its internal structure. On the other hand, as the PANcMA concentration increases from 2.5 wt% to 7.5wt%, the void structure diminishes gradually and formation of uniform sponge like structures over the entire membrane cross section is observed. According to Khayet et al³⁰⁴, macrovoids and cavity structures are formed when the rate of coagulation is fast and sponge like structures are formed when the coagulation process is slow. From the micrographs, it is observed that, the addition of PANcMA reduced the macro voids in the membrane. This can be explained by the increase in viscosity of the polymer solution with increase in polymer concentration. The

increase in solution viscosity slows down the diffusion of non-solvent into the membrane which in turn decreases the rate of coagulation.

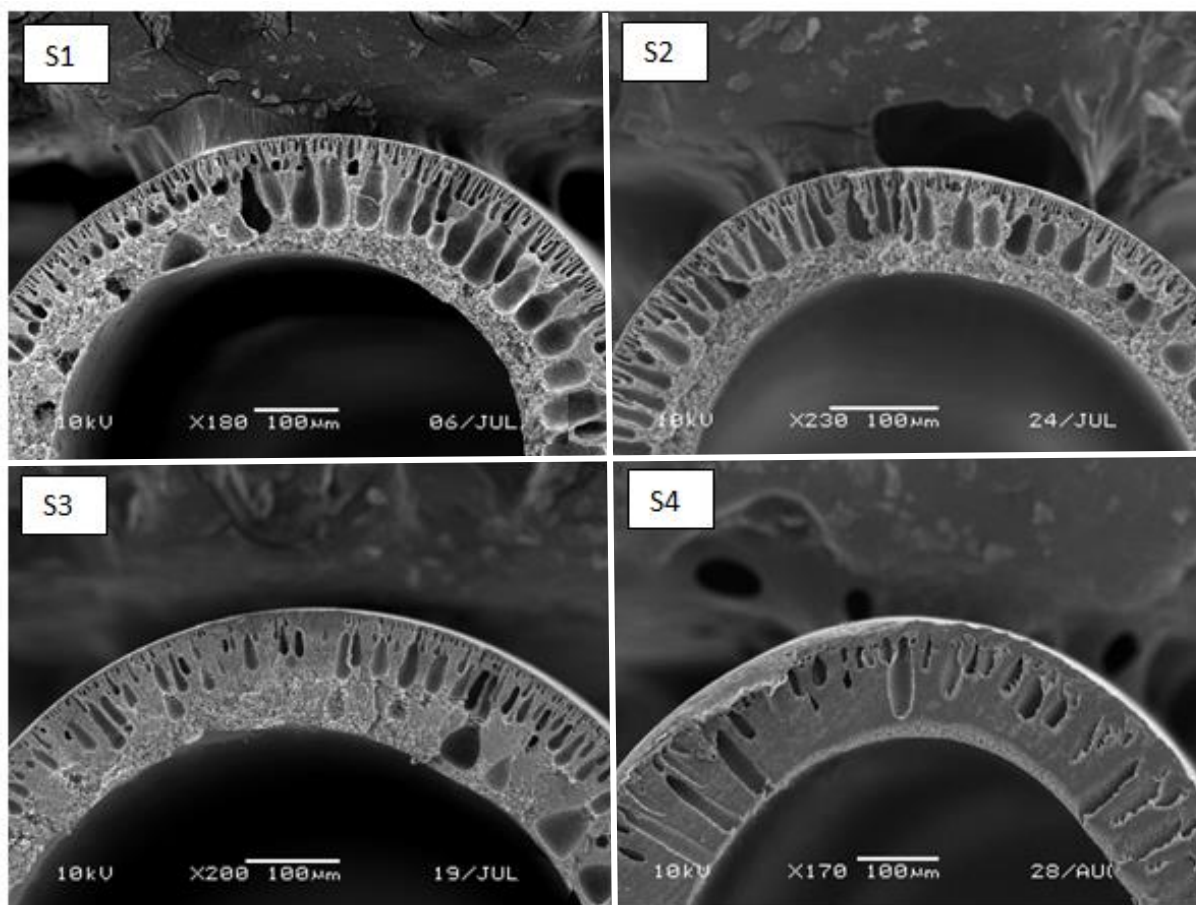


Figure.5.6. Cross section morphology of unmodified (S1) and modified (S2, S3 and S4) hollow fiber membranes

5.3.3. EDX ANALYSIS

The presence of silver was further confirmed by EDX analysis and the spectra are shown in Figure.5.7. The EDX spectra show a peak at 3KeV which corresponds to the silver and the peak around 2.5 KeV belongs to sulphur which comes from PES. It is also observed that the grafted silver concentration increases with the increase in PANCMA concentration (increase in PANCMA concentration will give more active site (acid functional groups) for grafting). This fact is further evidenced from the elemental mapping shown as an inset in Figure.5.7. The EDX mapping also confirms the uniform distribution of silver all over the membrane surface.

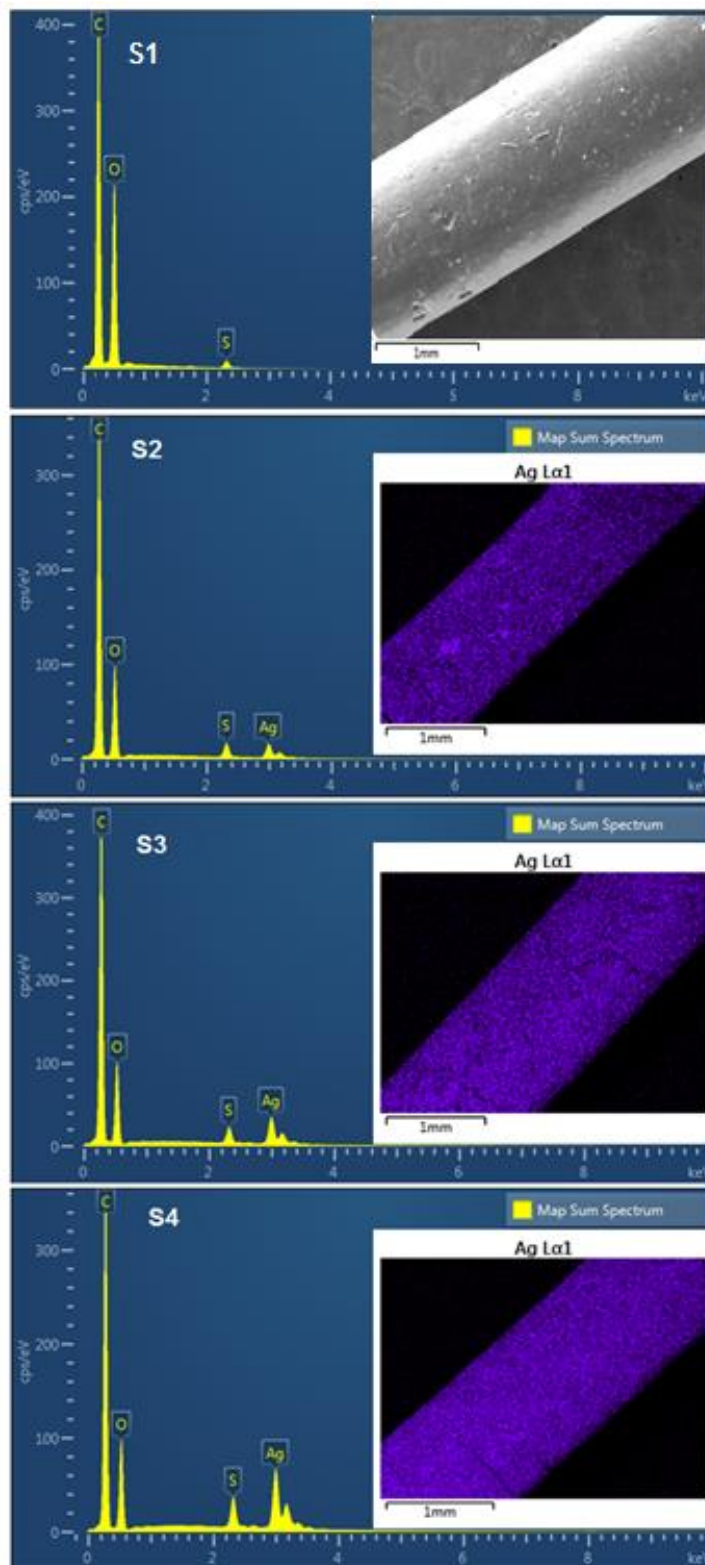


Figure.5.7. EDX results of unmodified and modified hollow fiber membranes

5.3.4. LEACHING TEST FOR SILVER

The surface grafted membranes (after thermal grafting) were then washed with excess DI water for 2 hours and dried at room temperature before testing. The dried samples S2, S3 and S4 were immersed in DI water and ultrasonicated at 37 kW for 60 mins. After ultrasonication, the water is analyzed using ICP-OES. The leached silver is found to be less than 2ppm for all the samples. This confirms that the silver is in strong covalent bonding with the hydroxyl groups of the PANCMA, which prevents the leaching of silver.

5.3.5. CONTACT ANGLE

The hydrophilicity of the PES-PANCMA membranes was measured by their contact angle and the results are tabulated in Table 5.2. With S1 being the control, the rest of the samples shows a decrease in water contact angle with an increase in PANCMA concentration and reached the lowest at S4 with $15.3 \pm 1.2^\circ$. This test has proven the effectiveness of PEG grafting with PANCMA in generating a more hydrophilic membrane with S4 having at least a 75.5% decrease in the contact angle from the control membrane. From the analytical data it is identified that the hydrophilic PEG grafting with PANCMA can be used to reduce the surface CAw of the PES membrane.

5.3.6. PORE SIZE ANALYSIS

The average pore sizes of the control PES membrane (S1) and the modified PES-PANCMA membrane samples S2, S3 and S4 are presented in Table 5.2. The experimental data indicate that the mean pore size of the membranes slightly decrease with the PANCMA concentration. This may be due to the increase in viscosity of the dope solution. Generally, pores in the membranes are formed by diffusion of non-solvent from coagulation bath into the membrane matrix and the de-solvation of casting solvent. If the solution viscosity increases, the diffusion of coagulant into the casting solution will be reduced and hence the macro voids can be reduced. The dense surface generally forms when a high ratio of the solvent out flow occurs compared to the non-solvent inflow³⁰⁵. The lowest average pore size achieved is $0.05 \pm 0.02 \mu\text{m}$ for membrane sample S4 whereas the control membrane exhibited a mean pore size of $0.09 \pm 0.025 \mu\text{m}$.

Table.5.2.Pore size, contact angle and the clean water flux of the control PES membrane (S1) and the modified PES-PANCMA membrane samples.

Sample ID	Pore size (μm)	CAw ($^\circ$)	Clean water flux (LMH)
S1	0.09 ± 0.025	62.6 ± 3.7	513 ± 21
S2	0.08 ± 0.03	48.1 ± 1.8	567 ± 18
S3	0.07 ± 0.015	24.7 ± 2.3	702 ± 27
S4	0.05 ± 0.02	15.3 ± 1.5	581 ± 14

5.3.7. ZONE INHIBITION TEST

The antibacterial activity of the control (S1) and the modified PES-PANCMA membranes S2, S3 and S4 were determined qualitatively using the zone inhibition test. Figure.5.8. shows the zone of inhibition for all different samples from S1 to S4. It is observed that all the membranes with silver (i.e S2, S3 and S4) cleared the *E.coli* bacteria around them giving distinct zones of inhibition (defined as clear areas with no bacterial growth) around the membranes. The width of the zone around the S1, S2, S3 and S4 was about 0 mm, 1 mm, 2 mm and 2.5 mm respectively. This is attributed to the bactericidal property of silver in the composite membranes. It was found that, as the concentration of PANCMA in the membrane increases, the zone of inhibition increases gradually, which is due to the increased attachment of the silver onto the membrane via chemical bonding with the acid functional group in PANCMA. In contrast, the control exhibits no zone of inhibition under the same conditions and high bacterial growth near the membrane was detected. These results indicate that the hollow fiber membranes with silver have very good anti-bacterial property.

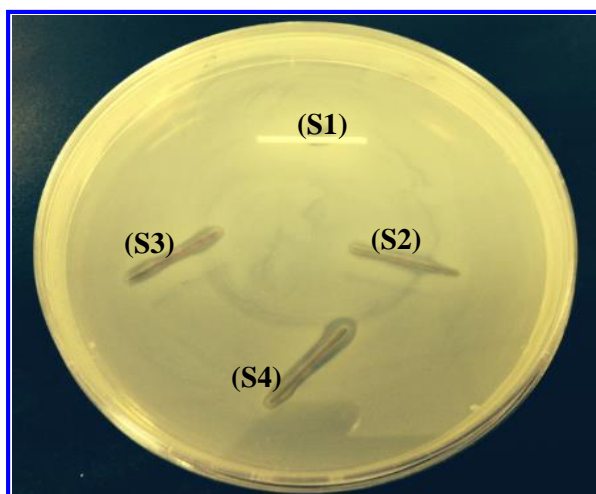


Figure.5.8. Zone of inhibition of modified and unmodified membranes

5.3.8. CLEAN WATER FLUX

The membranes S1-S4 were tested to evaluate the clean water flux of the membrane by using a cross flow filtration setup. Table 5.2 shows the clean water flux for all the four membranes at a constant feed water pressure of 1bar. All membranes were tested in the system under similar conditions with S1 as the control. Even though the pore size is smaller than S1 and S2, samples S3 and S4 gave higher flux, which may be due to the increase in hydrophilicity (decrease in contact angle) of the membrane. However, when compared to S3, sample S4 gives lower flux which could be due to the reduction in membrane pore size. The reduction in pore size may create some resistance to the flow of water and hence, the flux gets reduced. A similar observation was made in a previously reported work using hydrophilic membranes, whereby the flux was reduced as the pore size decreased³⁰⁶.

5.3.9. LONG TIME PERFORMANCE AND THE FOULING EVALUATION

A long time (4200min/72hrs) separation test was carried out for the control membrane (S1) and the best performing membrane (S3), and the results are summarized in Figure.5.9. The flux drop for the control membrane is much higher (45.3% of the initial flux) compared to the PES-PANCMA membrane (19.4% of the initial flux). It is also observed that the surface modified PES-PANCMA membrane (S3) gives comparatively more stable flux than the unmodified PES membrane, which suggests that the PEG-Ag grafted PES-PANCMA membrane repel the organic matters from the surface of the membrane more effectively, thereby establishing a more antifouling surface.

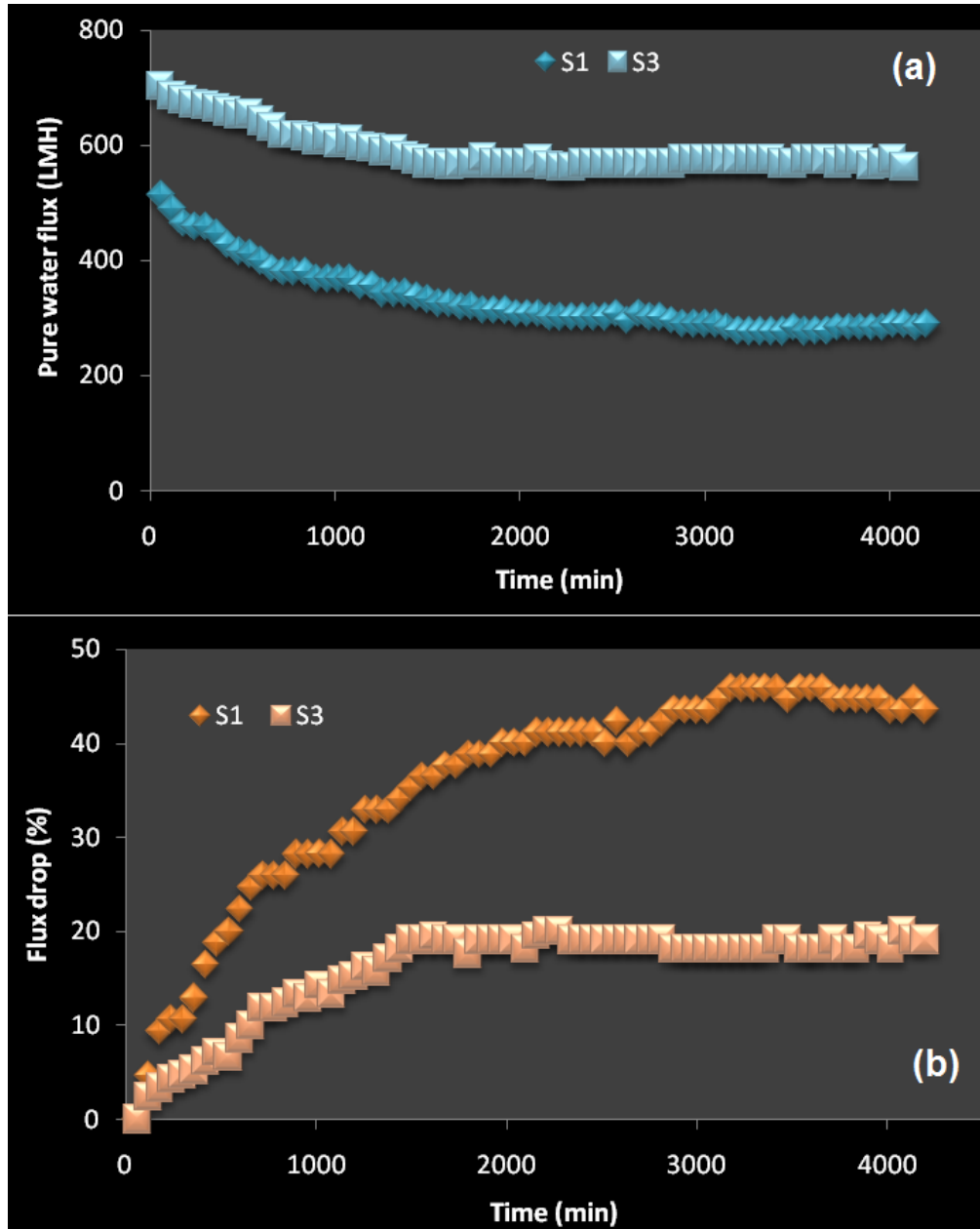


Figure.5.9. Pure water flux (a) and Flux drop (b) for the control (S1) and the best performing membrane (S3) in long time run

In order to study the filtration efficiency of the membrane, the total organic carbon (TOC) and turbidity of the feed water (reservoir water) and permeate water were measured (6 samples were collected every 60mins once and TOC and Turbidity were measured for each sample in order to get the average TOC and Turbidity removal efficiency). Percentage of rejection was calculated and plotted in Figure.5.10. From the experimental data, it was found that the TOC removal of the

CHAPTER: 5

control (S1) and the modified membrane (S3) were almost same for the first 1000min. However, after 1000min the TOC and turbidity removal efficiency of modified sample S3 is slightly better than the control sample S1. This is due to the smaller pore size of the membrane sample S3 ($07 \pm 0.015\mu\text{m}$) compared to the membrane sample S1 ($0.09 \pm 0.025\mu\text{m}$). The membrane surface properties may also play a role on the selectivity because, the modified membrane surface contain highly hydrophilic negatively charged acid and hydroxyl functional groups.

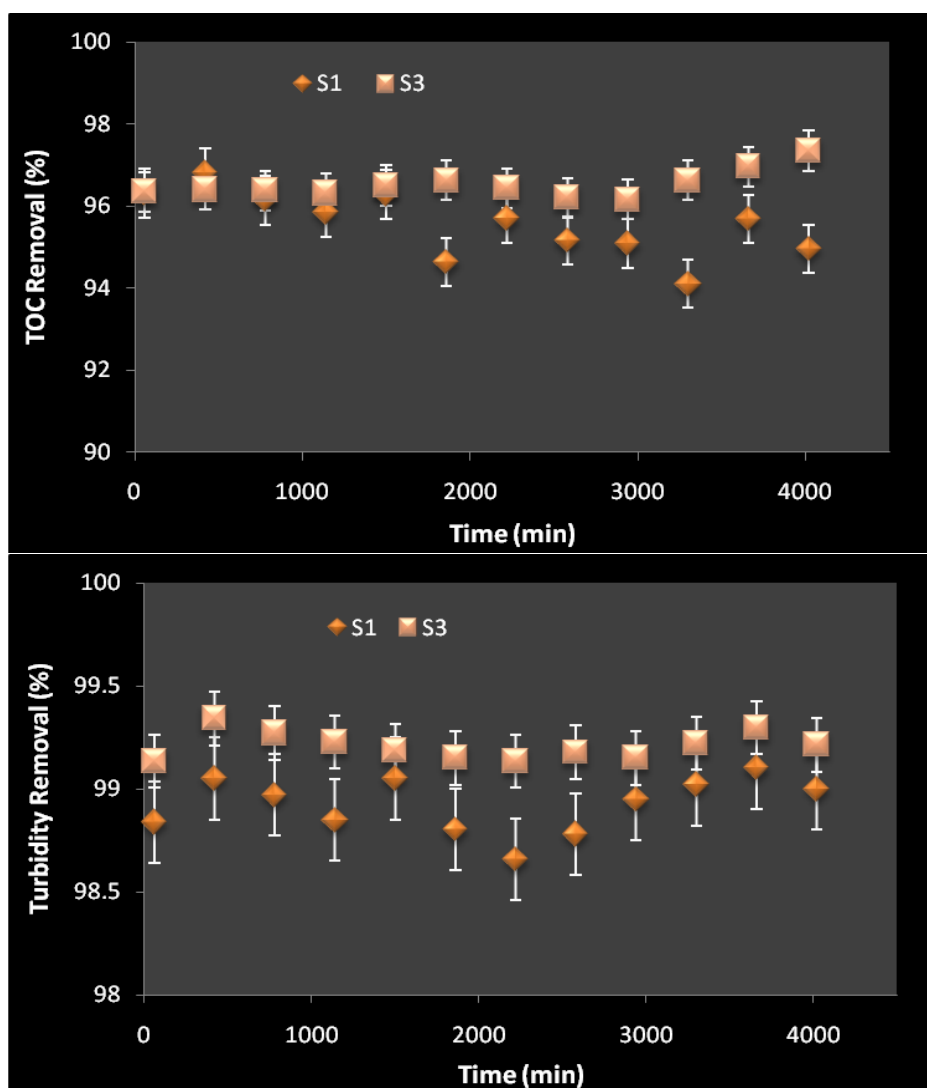


Figure.5.10. Contaminant removal efficiency for the control and the best performing membrane in long time run with wastewater: TOC rejection (a) Turbidity rejection (b)

5.4. SUMMARY

In the current work, PES-PANCMA hollow fiber membranes were fabricated by dry wet spinning. Highly hydrophilic polyethylene glycol (PEG) and silver nanoparticles (Ag) were covalently attached to the acid group in the poly (acrylonitrile-co-maleic acid) (PANCMA). The prepared membranes were characterized thoroughly. The EDX data confirmed the presence of silver (Ag) and the FTIR data confirmed the covalent attachment of polyethylene glycol (PEG) with PANCMA. From the contact angle data, it was identified that the new surface modification can increase the membrane hydrophilicity. The water contact angle of the PES UF membrane can be reduced by around 75.5% from 62.6 ± 3.7 to $15.3 \pm 1.2^\circ$ and the pure water flux increased by about 36% from 513LMH to 702LMH for the modified membrane. Antibacterial study was performed for the prepared membrane using the zone of inhibition test and the clear zone for the modified membranes indicate the antibacterial properties of the membrane. During long time test with reservoir water, it was found that the modified membrane exhibited a lower flux drop giving a stable flux compared to the control membrane. Similarly, the selectivity of the modified membrane (S3) is also better compared to the control membrane sample S1.

6. Effect of amine (-NH₂) carboxyl (-COOH) and silver (Ag) functionalization on the antifouling properties of the prepared membranes

6.1. INTRODUCTION

In the previous chapter the effects of a combination of hydroxyl (-OH), carboxylic (-COOH) and silver on the antifouling properties of the prepared membrane were determined. Here, amine (-NH₂) functional groups were incorporated in the membrane in the place of hydroxyl group to investigate its ability to maintain the antifouling property of the membrane. In this chapter, a novel concept to prevent bio-fouling by developing a killing and self-cleaning membrane surface was proposed and developed.

As mentioned earlier in the literature review (Chapter 2) and scope of this thesis (Chapter 3), the current state of the art membranes are modified either with a hydrophilic additive or with antibacterial compounds, most commonly silver -Ag/ Ag⁺. It has been proven that positively charged silver can kill the bacteria by rupturing their plasma membrane. Once the plasma membrane breaks, the negatively charged compounds rich protoplasm deposits onto the surface of the membrane. The presence of negatively charged -NH₂, -COOH and -OH functional groups on the membrane surface has been shown to be effective in combatting the build-up of the negatively charged colloidal particles, proteins, lipids and amino acids etc. via an electrostatic repulsion mechanism, thereby increasing the hydrophilicity of the membrane,

In order to develop a self-cleaning surface in the present work, the functional groups to be attached onto the membrane surface were carefully chosen. Negatively charged carboxylic acid (-COOH) rich, hydrophilic, water-insoluble PANCMMA was chosen as a base additive. Amine (-NH₂) rich PEI was chosen as another additive and positively charged antimicrobial silver (Ag⁺) was chemically attached to it by thermal grafting. This Ag attached PEI was attached to the base PANCMMA additive to get the final additive PANCMMA-PEI-Ag. The modified PANCMMA-PEI-Ag

was then blended with PES dope solution to prepare the hollow fiber ultrafiltration membranes by dry wet spinning process.

The anti-bio-fouling mechanism of the novel membrane is illustrated in Figure.6.1. From the figure, it can be easily understood that the positively charged Ag^+ attracts bacteria by electrostatic attraction and kills them by rupturing their negatively charged plasma wall. When the protoplasm rich in negatively charged compounds including proteins, lipids and amino acids etc., spill out on the surface of the membrane, the highly negatively charged $-\text{COOH}$, $-\text{N}$, $-\text{NH}$ and $-\text{NH}_2$ functional groups will repel them by electrostatic repulsion, thereby allowing the surface to remain free of the protoplasm deposits.

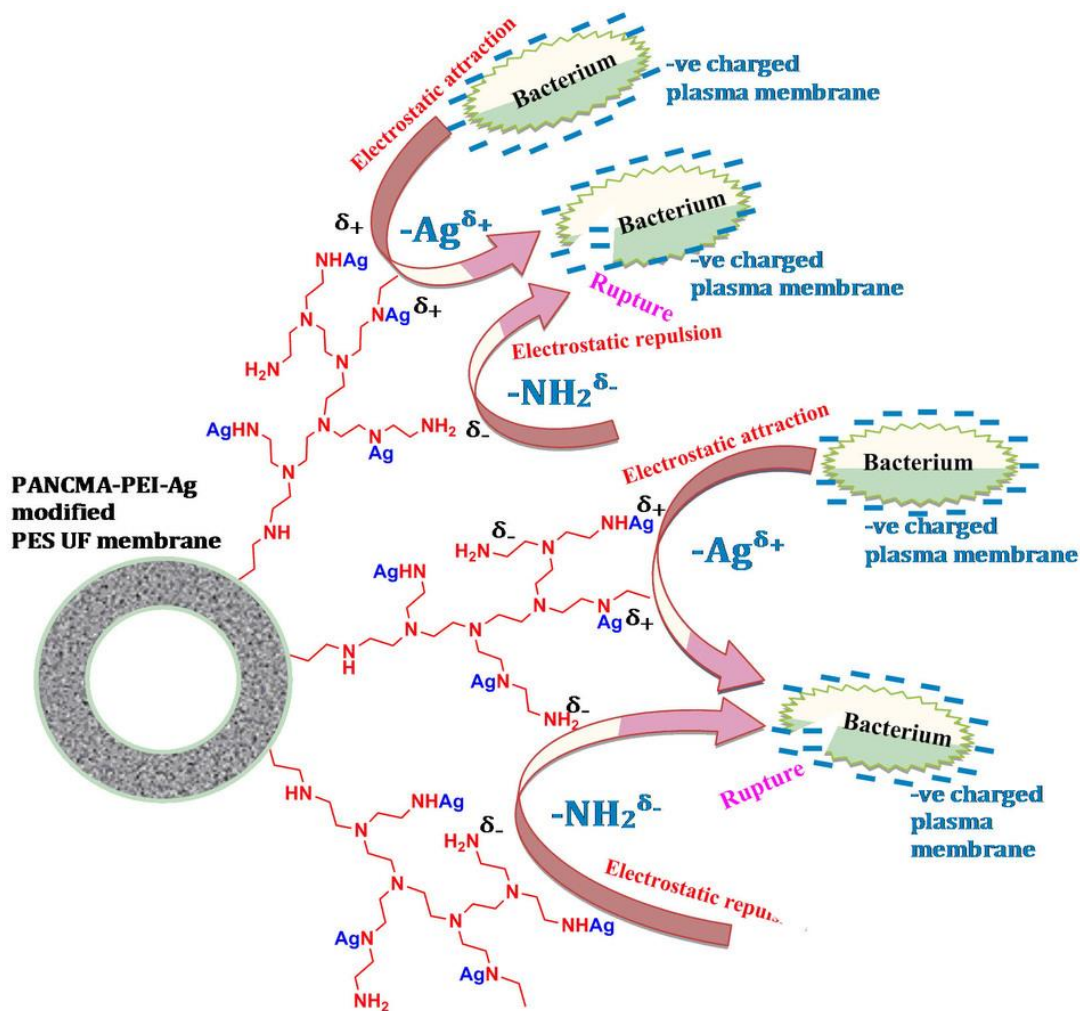


Figure.6.1. Schematic representation of the self-cleaning property of the membrane

The prepared membranes were characterized using Fourier transform infrared (FTIR) spectroscopy, Energy-Dispersive X-ray (EDX), Contact angle (CA), scanning electron microscopy (SEM), and the Porometer. Both control PES and modified PES-PANCMA-PEI-Ag membranes were subjected to zone of inhibition test and measurements of clean water flux. Finally, the membranes were tested for their permeability, selectivity and antifouling property in long term experiments.

This chapter is based on: *“Self-cleaning MOF based PES-PANCMA-PEI-Ag ultrafiltration membranes–A solution to bio-fouling issue in membrane separation process”* by Prince J.A., Bhuvana S., Anbharasi V., Ayyanar N., Boodhoo K.V.K., Singh G., (2014), published in *Nature, Scientific Report 4, 6555; DOI:10.1038/srep06555*

6.2. EXPERIMENTAL METHODS

General characterization and experimental methods are described in Chapter 4. Specific experimental procedures with conditions particular to this chapter are highlighted below.

6.2.1. MATERIALS

Polyethersulphone (PES) k-3010 powder was purchased from Sumitomo Chemicals Pte Ltd, Japan. Acrylonitrile, maleic anhydride, azoisobutyronitrile (AIBN), silver nitrate (AgNO_3) sodium borohydride (NaBH_4) and polyethylenimine (PEI) were purchased from Sigma Aldrich with 99% purity. High purity ethanol, N-methyl-2- pyrrolidone (NMP), N,N-Dimethyl acetamide (DMAc), Polyvinyl pyrrolidone(PVP) and diethylene glycol (DEG) were also purchased from Sigma Aldrich and used as received. The water used for the reaction was distilled and de-ionized (DI) with a Milli-Q plus system from Millipore, Bedford, MA, USA.

6.2.2. SYNTHESIS OF POLY (ACRYLONITRILE CO MALEIC ANHYDRIDE) (PANCMA)

Poly (acrylonitrile-co-maleic anhydride) was synthesized by a free radical polymerization in solution-suspension method using DMAc according to the reaction scheme shown in Figure 6.2

The procedure involved adding 9.89 grams of maleic anhydride and 5.31 grams of acrylonitrile to about 150 ml DMAc and stirring the mixture at room temperature for about 30 minutes. After complete dissolution, 1.25 grams of AIBN was added to the solution and the mixture was stirred at 60°C for about five hours. The polymer obtained as a suspension was separated out by filtration and washed thoroughly with diethyl ether and dried overnight in vacuum at 40°C.

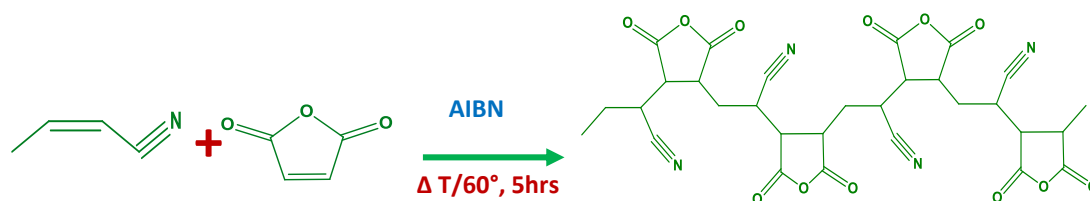


Figure.6.2. Synthesis of poly (acrylonitrile co maleic anhydride) (PANCMA)

6.2.3. SYNTHESIS OF Ag CAPPED PEI

Silver grafted PEI was prepared according to the reaction scheme shown in Figure 6.3. To a 50ml of aqueous PEI (50%) solution, 0.5grams of AgNO₃ was added and allowed to stir at room temperature for 1 hour. About 10ml of freshly prepared NaBH₄ was then added drop wise to the above solution over a period of 30 mins with stirring continued overnight at 80°C. The final dark green solution obtained was then subjected to dialysis for 2 days to remove excess reactants.

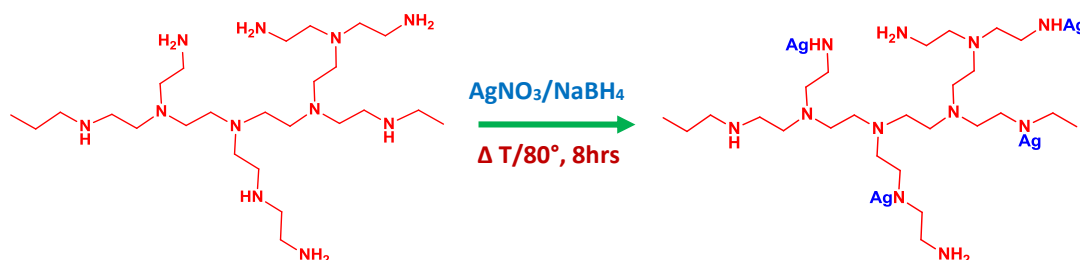


Figure.6.3. Synthesis of Ag capped PEI

6.2.4. SYNTHESIS OF Ag CAPPED PEI ATTACHED PANCMA

Silver capped PEI was attached to PANCMA by a simple nucleophilic addition reaction according to the reaction scheme shown in Figure 6.4. About 10 grams of PANCMA was added to a 250ml flask with 100ml DMAc. The flask was connected to a nitrogen inlet. After complete dissolution,

CHAPTER: 6

25ml of silver capped PEI solution was added drop wise to the polymer solution and allowed to stir at room temperature for 24 hours. The obtained final homogeneous solution was then poured into methanol to separate the Ag capped PEI attached PANCMA. The polymer was filtered, washed with methanol and dried in vacuum at 40°C overnight.

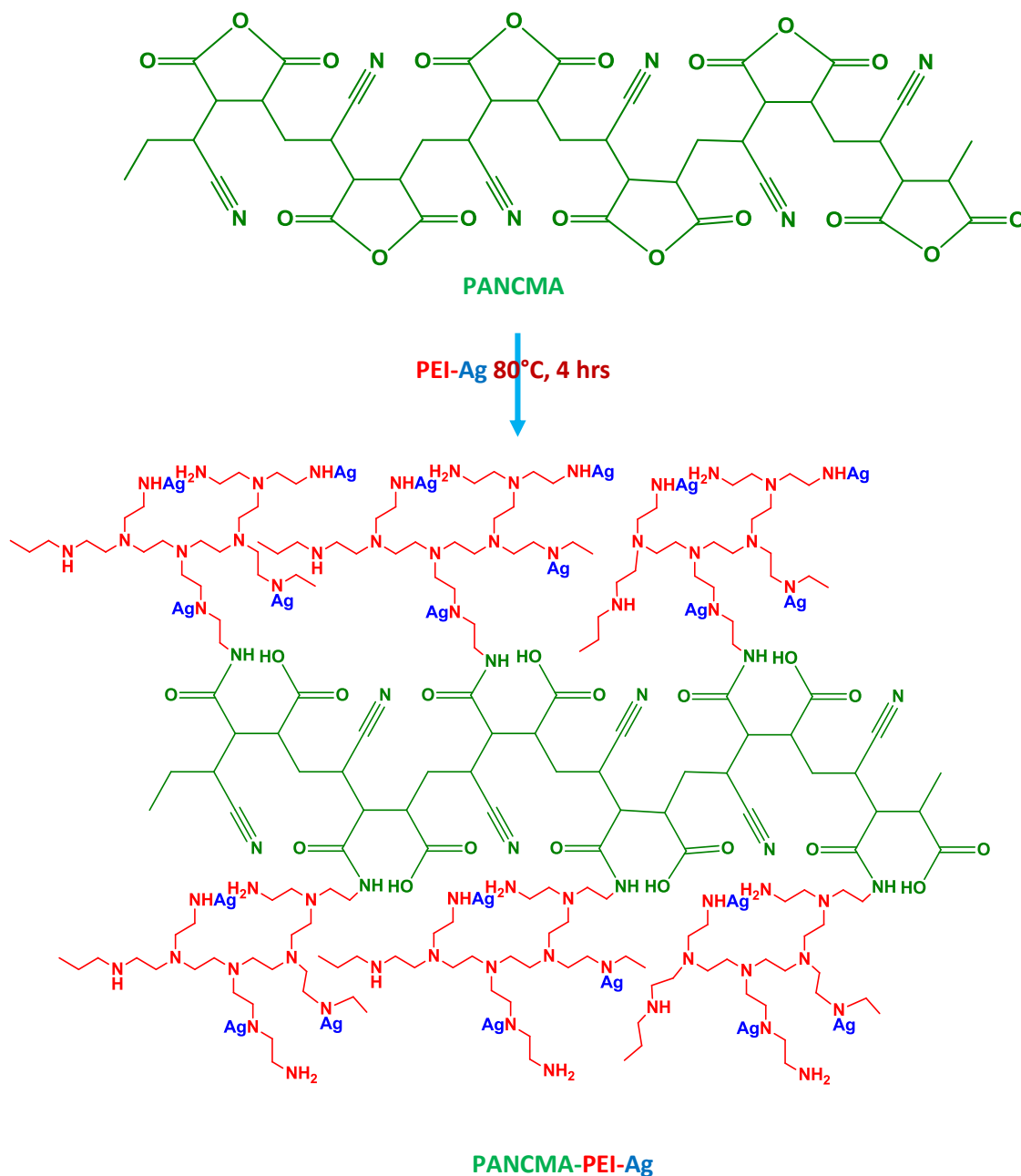


Figure.6.4. Synthesis of Ag capped PEI attached PANCMA

6.2.5. PREPARATION OF MEMBRANES BY DRY WET SPINNING

Polyethersulfone (PES) hollow fiber ultrafiltration membranes were prepared by dry wet spinning method. PES was used as the base polymer, NMP was the base solvent, DEG was used as a non-solvent and two additives, PVP (pore forming agent) and hydrophilic and antimicrobial PANCMA-PEI-Ag polymer composite were used to improve the surface property of the membrane. The casting solution consisted of 21 wt% PES, 5 wt% PVP-K-30, 5 wt% DEG, 64~69 wt% NMP, 0-5 wt% PANCMA and 0-5 wt% PANCMA-PEI-Ag, respectively. PVP powder was first added into the NMP /DEG mixture in a round bottom flask and the solution was mechanically stirred for at least 1-1.5 hours. After complete dissolution of PVP, PANCMA/PANCMA-PEI-Ag and PES were added and allowed to stir at a constant speed of 250~350 rpm for at least 24 h at 80° C to obtain a completely dissolved homogeneous polymeric solution. Table 6.1 shows the composition of the membranes fabricated. The dope solution was poured into the polymer tank and degassed at a negative pressure of -0.6 bar for 15-20 min. Nitrogen gas was purged into the dope tank to create an inert atmosphere and to push the polymer towards the polymer pump. Bore liquid consisting of NMP and water in 80:20 volume ratio was poured into the bore liquid tank. The polymer solution and the bore liquid were pumped to the spinneret (OD 1.2 mm, ID 0.6 mm). The air gap was fixed at 10mm. The hollow fiber membranes were fabricated at around 25° C and at around 65-70% relative humidity with a take up speed of 0.25 m/s. The membranes were then collected from the winder and left inside a post-coagulation water tank for a minimum of 24 hrs to washout the residual NMP, DEG and PVP that were not removed from the solution at the point of fabrication process. To keep the membranes wet, they were immersed into a post treatment solution of 40% ethanol and 60% glycerin before testing the clean water flux.

Table.6.1. Composition of the dope solutions for the hollow fiber membrane fabrications

Sample ID	PES (wt%)	PVP- K30 (wt%)	DEG (wt%)	NMP (wt%)	PANCMA (wt%)	PANCMA-PEI-Ag (wt%)
S1	21	5	5	69	0	0
S2	21	5	5	64	5	0
S3	21	5	5	64	0	5

* All the samples (formulations) are different from the previous chapter (Chapter 5)

6.3. RESULT AND DISCUSSION

6.3.1. TEM ANALYSIS OF Ag CAPPED PEI COLLOID

Figure.6.5.a. shows the TEM picture of the synthesized PEI-Ag. The nanoparticles are spherical in shape with sizes in the range of 3 to 6nm. The nanoparticles also show a more uniform distribution in the PEI matrix. A schematic representation of the silver capped PEI is shown in Figure.6.5.b.

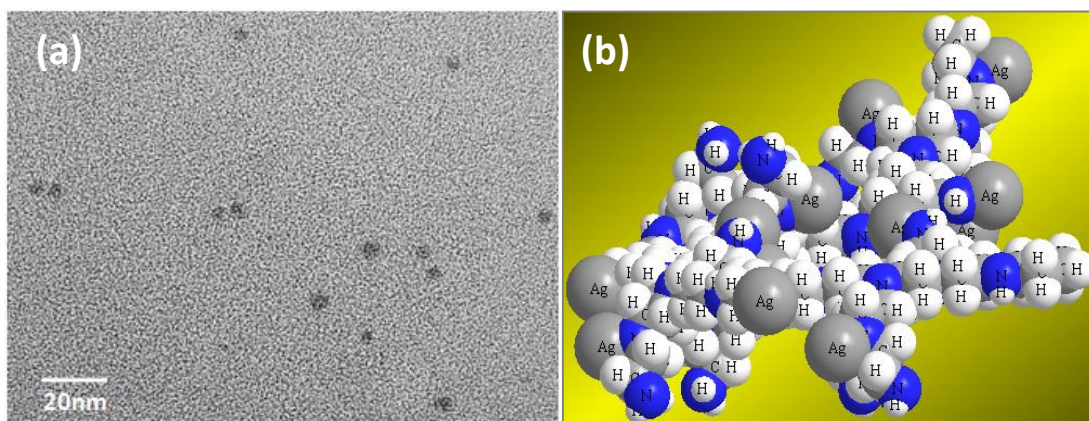


Figure.6.5. (a) TEM image of silver attached PEI (b) Chemical model of silver attached PEI

6.3.2. FTIR ANALYSIS OF PANCMA AND PEI-Ag ATTACHED PANCMA

The structure of the PANCMA polymer, synthesized according to the procedure described in Section 5, was confirmed by FTIR spectrophotometer as shown in Figure.6.6. The presence of CN stretching vibration at 2243cm^{-1} and the imide stretching vibrations at 1784cm^{-1} and 1707cm^{-1} confirms the copolymer formation in anhydride form.

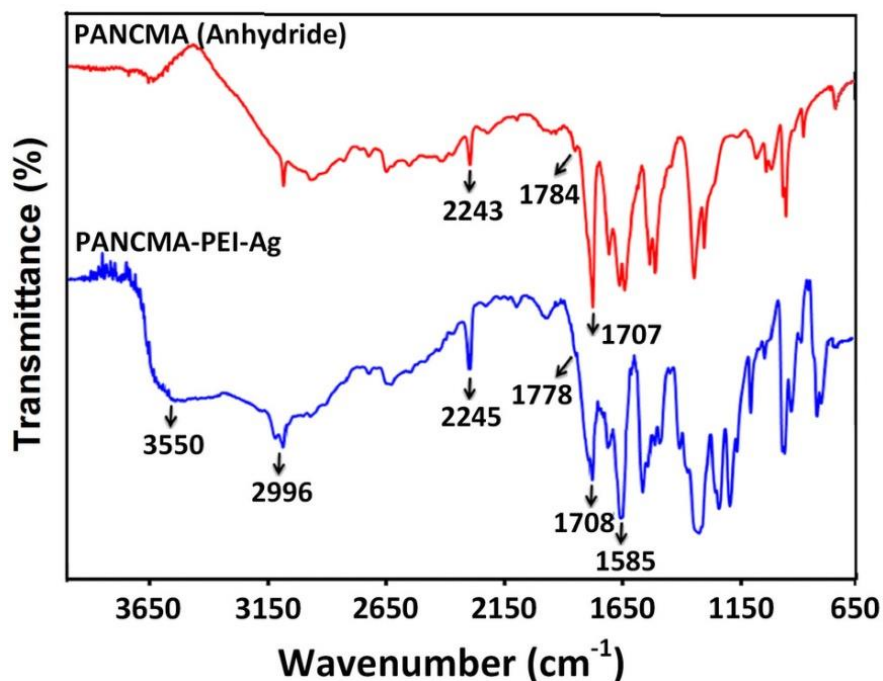


Figure.6.6. FTIR Spectrum of the PANCMA and Silver-PEI attached PANCMA

The attachment of PEI-Ag to the copolymer was also confirmed from the FTIR spectrum in Figure 6.6 by the presence of -OH stretching vibration of the carboxylic acid observed as a broad band at 3550cm^{-1} , nitrile stretching vibration at 2245cm^{-1} and carbonyl stretching vibration observed as a strong band at 1708cm^{-1} . The attachment of PEI to the copolymer was confirmed by the presence of a strong -C-N-C stretching vibration at 1352cm^{-1} and -NH bending vibration at 1585cm^{-1} .

FTIR analysis was used to investigate the chemical composition of fabricated hollow fiber membrane. Figure 6.7 represents the FTIR spectra for neat PES membrane, PES/PANCMA (5 wt %) and PES/PANCMA-PEI-Ag membranes. With the PES/PANCMA membrane, most of the anhydride moiety present in the PANCMA gets hydrolyzed to acid as the blend (dope solution) reaches the coagulation bath containing water; this is confirmed from the broad band at 3560cm^{-1} in the FTIR spectra. The band at 2243cm^{-1} is due to the C-N stretching of the nitrile group whilst the band at 1708cm^{-1} is the C=O stretching vibration of the acid carbonyl group present in the PANCMA. The presence of PANCMA-PEI-Ag in the PES matrix is confirmed from the nitrile, carbonyl, imide and amine vibrations at 2243cm^{-1} , 1716cm^{-1} , 1770cm^{-1} , 1382cm^{-1} and 1625cm^{-1} respectively.

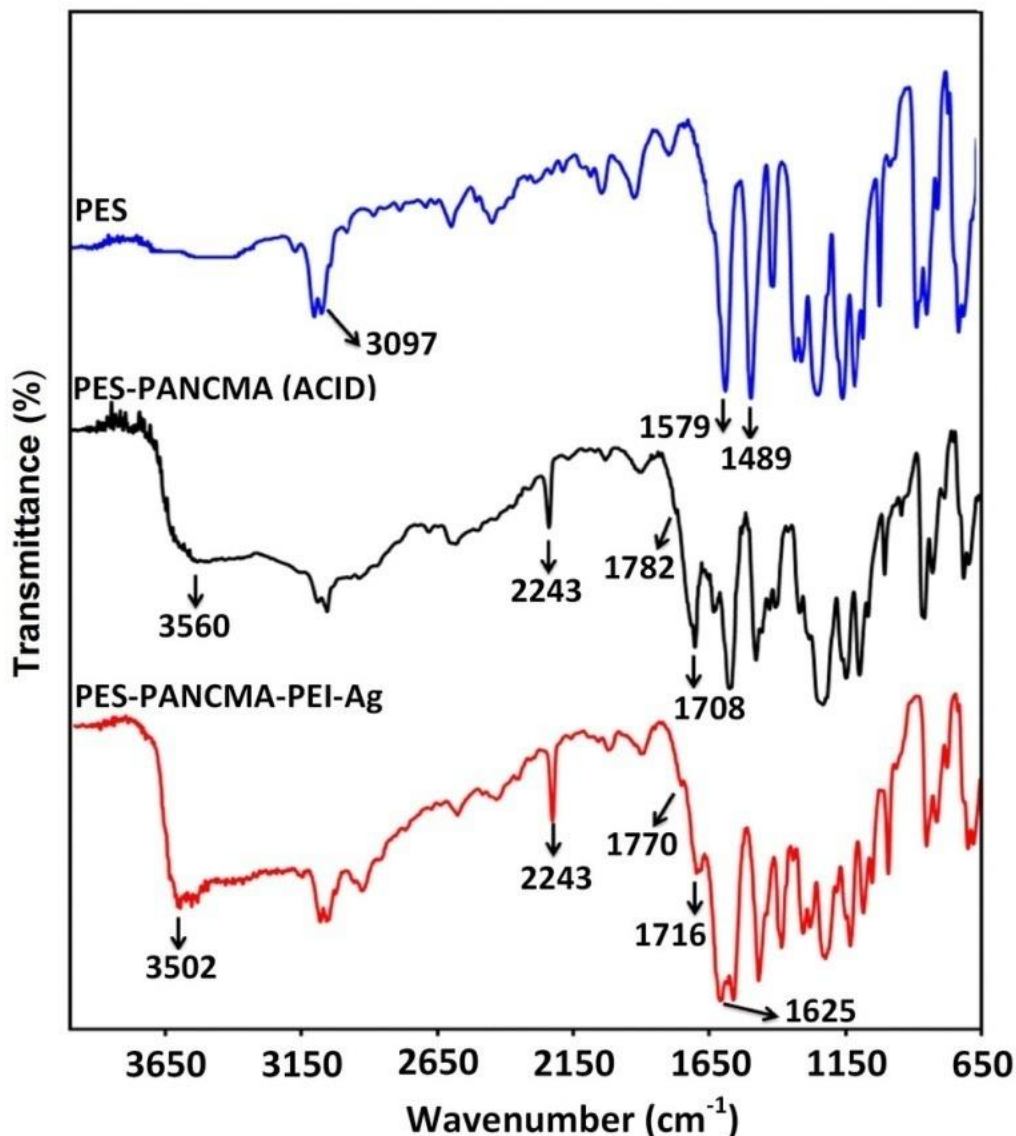


Figure.6.7. FTIR spectra of S1) PES S2) PES-PANcMA (5 wt%) S3) PES-PANcMA-PEI-Ag (5wt %)

6.3.3. MORPHOLOGY OF HOLLOW FIBERS AND EDX ANALYSIS

The hollow fiber membranes fabricated through dry-wet spinning process had an average inner diameter of 0.5mm and an outer diameter of 1.0mm. The surface morphology and cross section of the PES and modified PES hollow fiber membranes were examined using SEM and the micrographs of the Ag modified membranes are shown in Figure.6.8 to consist of a smooth surface together with a uniform distribution of silver particles.

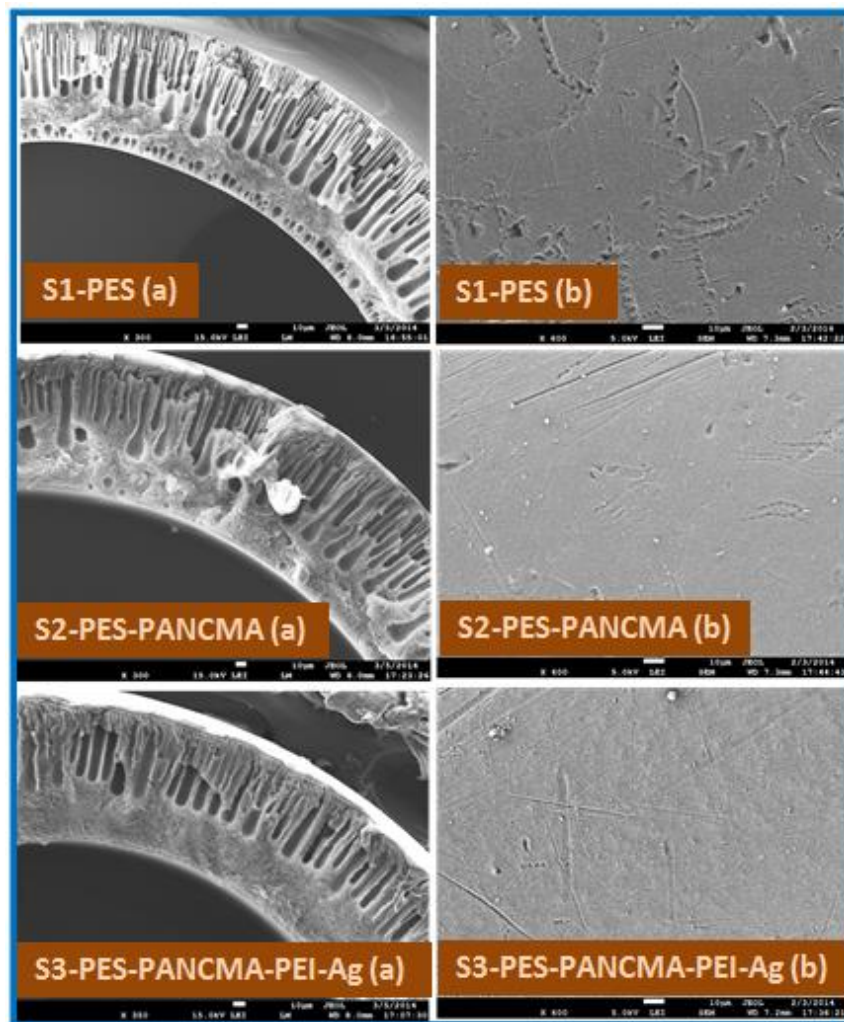


Figure.6.8. SEM images of membrane samples S1-PES, S2-PES-PANcMA and S3-PES-PANcMA-PEI-Ag (a) Cross section (b) Outer surface

Similar to our previous study (Chapter-5)¹³⁶, the hollow fibers exhibit different internal structures depending on their composition. The neat PES membrane shows the presence of a large number of macro voids in its internal structure. The PES membrane with 5wt% PANcMA concentration has fewer macro voids and more sponge like structures. With the PES/PANcMA/PEI-Ag membrane, the sponge like structure predominates the macro voids and correlates well with the increase in dope solution viscosity as described in our previous paper (Chapter-5)¹³⁶. The presence of silver particles was further confirmed by EDX analysis as shown in Figure.6.9. The presence of silver and its uniform distribution all over the membrane is evidenced from the elemental mapping shown in Figure 6.9 b.

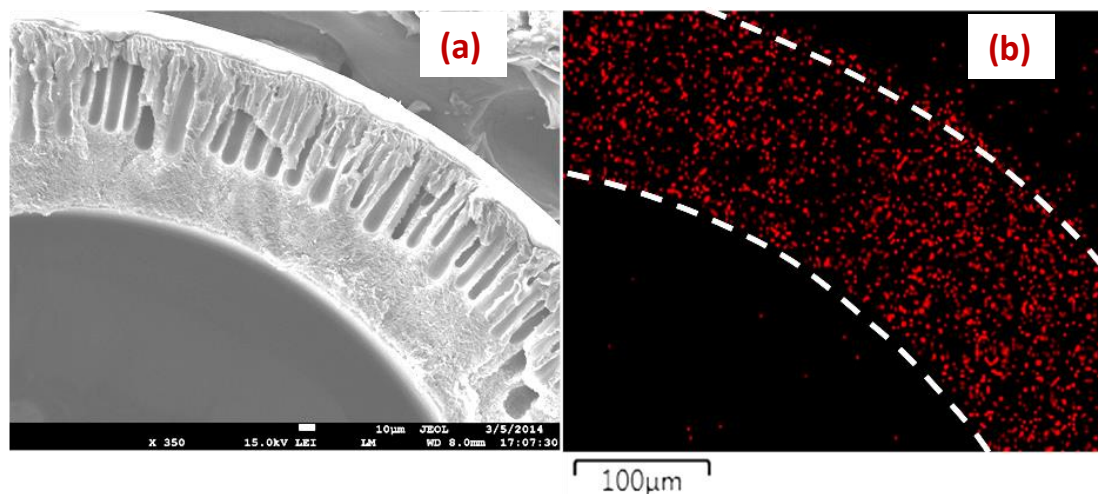


Figure.6.9. Cross section (SEM image) (a) and the distribution of silver (Ag) element (points measured by EDX mapping analysis) on the membrane cross-section (b) of the sample S3-PES-PANCMA-PEI-Ag

6.3.4. LEACHING TEST FOR SILVER

The composite PES-PANCMA-PEI-Ag (S3) membranes were soaked in DI water overnight and dried at ambient temperature before the leaching test. The dried membrane samples were immersed in fresh DI water and ultrasonicated at 37 kW for 120 mins. After ultrasonication, the water was analyzed using Inductively Coupled Plasma Optical Emission Spectroscopy (ICP-OES). The leached silver was found to be less than 2ppm for all the samples. This suggests that the silver has strong interactions with the amine groups of the PEI, which prevents the leaching of silver from the membrane matrix.

The leaching test was conducted by subjecting the membranes to ultrasonication which is actually the worst condition that a membrane can experience than the normal operating conditions (e.g. 3 months operation at 50 L/m²/h). Since the Ag leakage under such harsh condition is only less than 2ppm, Ag will not leach from the membrane at the normal operating conditions.

6.3.5. CONTACT ANGLE

The hydrophilicity of the control PES (S1), PES-PANCMA (S2) and PES-PANCMA-PEI-Ag (S3) membranes were measured by their contact angle. The control PES sample S1 showed a water contact angle of $63.2^\circ \pm 3.9^\circ$. Sample S2 with 5% PANCMA showed a water contact angle of 54.1°

$\pm 2.8^\circ$ which is a 14.4% reduction compared to the control sample. Sample S3, with 5% of Ag capped PEI attached PANCMA, showed the lowest water contact angle of $32.7^\circ \pm 2.1^\circ$, which is about 48.3% reduction on the control sample. The effectiveness of PANCMA-PEI-Ag blending with PES in generating a more hydrophilic membrane is clearly demonstrated by these tests. The increased hydrophilicity is attributed to the presence of the amine ($-\text{NH}_2$) and acid ($-\text{COOH}$) groups attached to the PEI and PANCMA in the PES membrane matrix.

6.3.6. PORE SIZE ANALYSIS

The average pore size of the control PES membrane (S1), PES-PANCMA membrane (S2) and the PES-PANCMA-PEI-Ag membrane (S3) are measured. The experimental data indicate that the addition of the Ag capped PEI attached PANCMA does not have a significant effect on the mean pore size of the PES. The average pore sizes of sample S2 and S3 ($0.08 \pm 0.015\mu\text{m}$) are slightly lower compared to sample S1 ($0.09 \pm 0.02\mu\text{m}$). The reduction in pore size may be due to the increase in the polymer concentration (additional 5% of PANCMA for S2 and 5% PANCMA-PEI-Ag for sample S3 compared to the control membrane) which results in an increase in the viscosity of the dope solution. With the increase in polymer solution concentration, the diffusion of coagulant into the polymer solution is slower leading to the formation of sponge like structures with reduced pore size ⁴⁵.

6.3.7. CLEAN WATER FLUX

The control PES membrane (S1), PES-PANCMA membrane (S2) and the PES-PANCMA-PEI-Ag membrane (S3) were tested to evaluate the clean water flux of the membrane using a cross flow filtration setup. The clean water flux for all the 3 different membranes were measured at a constant feed water pressure of 100 kPa. Even though their pore size is slightly smaller than S1, samples S2 and S3 gave higher pure water flux which may be due to the increase in hydrophilicity (represented by a decrease in contact angle) of the membrane. The highest flux achieved is 687 ± 28 LMH for sample S3 which is about 39.4% higher than that for the control membrane.

6.3.8. ZONE OF INHIBITION TEST

The antibacterial activities of the control PES membrane (S1), PES-PANCMA membrane (S2) and the PES-PANCMA-PEI-Ag membrane (S3) were determined qualitatively using the zone

inhibition test. As shown in Figure.6.10. (a), sample S3 exhibited positive results with a clear inhibition zone of width 2.5-3.0 mm around the membrane in stark contrast to sample S1 and S2 which did not show any inhibition zone. This is due to the bactericidal property of silver nanoparticles in the composite membrane S3.

In order to study the self-cleaning property of the membrane, all 3 membrane samples were filtered with 10 ppm sodium alginate solution (the alginate solution is representative of the negatively charged protoplasm compounds that would be released by lysed bacteria) for 1320 min and then tested for their antibacterial property. The results are presented in Figure.6.10.(b).

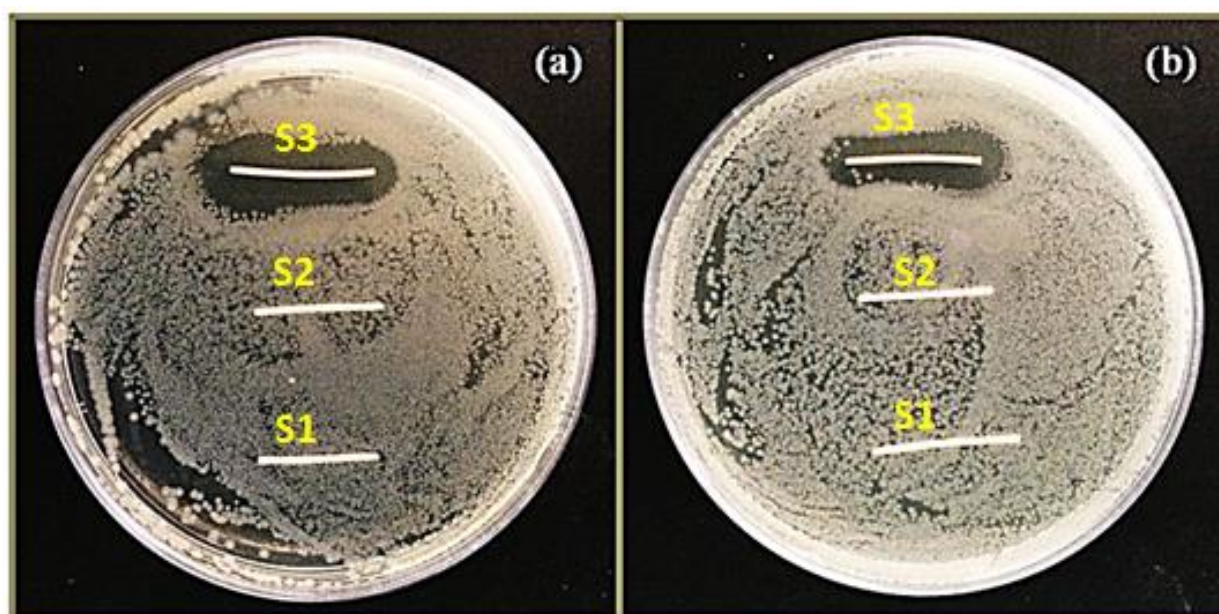
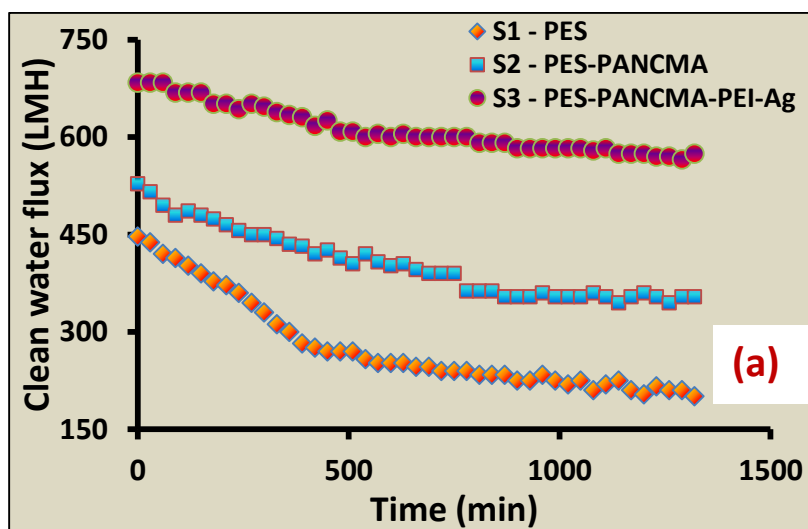


Figure.6.10. Zone of inhibition of modified and unmodified membranes before filtration with sodium alginate solution (a) and after filtration with sodium alginate solution (b)

Sample S3 exhibited positive results with a clear inhibition zone around the membrane even after a long period of continuous filtration of sodium alginate solution. This result confirms that the negatively charged functional groups present in the modified membrane matrix prevent the deposition of sodium alginate on the membrane surface. This finding is in agreement with previously reported work indicating that membranes with hydrophilic negatively charged functional groups on the surface can repel substances which make up extra cellular polymeric substances(EPS)^{101,301,307}.

6.3.9. LONG TIME PERFORMANCE AND FOULING EVALUATION

To evaluate the antifouling efficiency of the membrane, a long time (1320 min) filtration of 10ppm sodium alginate in DI water was carried out for the control PES membrane (S1), PES-PANCMA membrane (S2) and the PES-PANCMA-PEI-Ag membrane (S3) individually, and the results are summarized in Figure.6.11.a. It is observed that the modified PES-PANCMA-PEI-Ag membrane (S3) gives stable flux compared to the other two membrane samples S1 and S2. The flux drop of the membranes is shown in Figure.6.11.b. The flux drop for the modified PES-PANCMA-PEI-Ag membrane (S3) is lower (16.3% of the initial flux) than the control membrane sample S1 (55.3% of the initial flux) and the PES-PANCMA membrane sample S2 (33% of the initial flux). The obtained results indicate that there is not much decrease in the flux with time for the modified PES-PANCMA-PEI-Ag membrane (S3) confirming that the PANCMA-PEI-Ag modified PES membrane can best repel the organic matter in the form of the sodium alginate from the surface of the membrane.



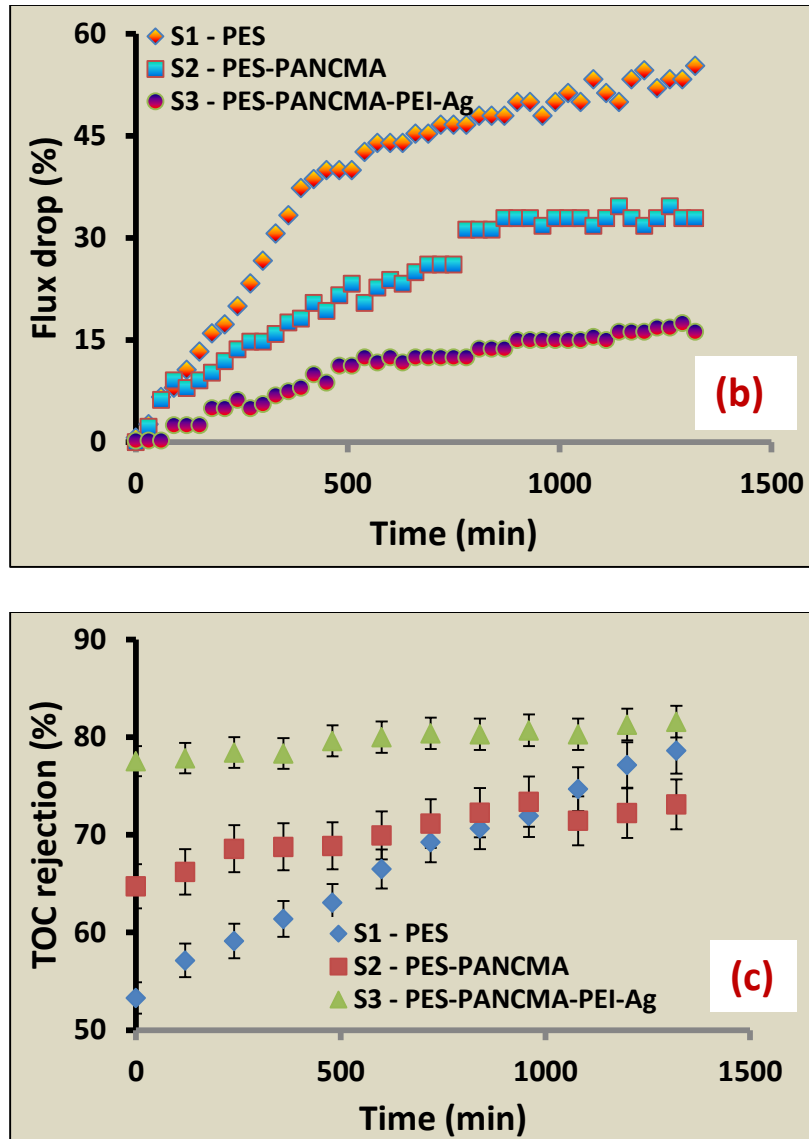


Figure.6.11. Pure water flux (a), Flux drop (b) and sodium alginate (TOC) removal efficiency (c) for the membrane samples S1 to S3 in long time run with 10ppm sodium alginate solution

In order to study the filtration efficiency of the membrane, the total organic carbon (TOC) of the feed water and permeate water were measured (4 samples were collected every 60mins and the TOC was measured in order to get the average TOC removal efficiency over time). Percentage of TOC rejection was calculated and plotted in Figure.6.11.c. From the experimental data, it was found that the TOC removal of the modified PES-PANCMA-PEI-Ag membrane (S3) is highest compared to samples S1 and S2. This may be due to the slight difference in the average pore sizes of the

membrane. The pore size of the membrane sample S2 and S3 ($0.08 \pm 0.015\mu\text{m}$) are slightly lower compared to sample S1 ($0.09 \pm 0.02\mu\text{m}$). It is also found that the modified membrane gives comparatively stable rejection of TOC when compared to the other two samples. This is due to the hydrophilicity and zwitterionic effect by the presence of highly negatively charged $-\text{COOH}$, $-\text{OH}$ and positively charged $-\text{NH}_2$ on the membrane surface. The negative surface charge of the membrane prevents the deposition of the negatively charged colloidal particles (proteins, lipids and amino acids etc.) on the membrane surface by electrostatic repulsion, which can slow down the membrane fouling process³⁰⁵. It is also reported that the membrane fouling can be reduced by increasing the negative surface density of the membrane³⁰⁸. TOC removal efficiency of the control membrane was also increased with time, which may be due to the pore constriction or development of a cake layer (fouling) on the membrane surface¹³⁷.

6.4. SUMMARY

In this chapter, a novel concept was developed to prevent bio-fouling by developing a killing and self-cleaning membrane surface incorporating antibacterial silver nanoparticles and highly hydrophilic negatively charged carboxylic and amine functional groups. The innovative surface chemistry helps to reduce the contact angle of the novel membrane by at least a 48% and increase the pure water flux by 39.4% compared to the control membrane. The flux drop for the novel membrane is also lower (16.3% of the initial flux) than the control membrane (55.3% of the initial flux) during the long term experiments with sodium alginate solution. Moreover, the novel membrane continues to exhibit inhibition to microbes even after 1320 min of sodium alginate filtration.

7. Effect of hydroxyl (-OH), amine (-NH₂), carboxyl (-COOH) and silver (Ag) functionalization on the antifouling properties of the prepared membranes

7.1. INTRODUCTION

In chapter 5, the effect of hydroxyl (-OH) functional group and in chapter 6, the effect of amine (-NH₂) functional groups were tested separately with carboxylic (-COOH) functional groups and antimicrobial silver to evaluate their effect on the performance of the PES membrane in terms of hydrophilicity, water permeability, selectivity and membrane fouling. In this chapter, both hydroxyl (-OH) and amine (-NH₂) functional groups together with carboxylic (-COOH) contain polymeric additive were prepared. In order to prepare the new additive poly (acrylonitrile co maleic acid co diamino maleonitrile) (PANCMACDAMN), alkenes monomers like carboxylic groups rich melic acid, amine groups rich diamino maleonitrile and water insoluble acrylonitrile were chosen carefully and polymerized them by atom transfer radical polymerization method. Hydroxyl rich PEG and antimicrobial silver were chemically attached to the newly synthesized additive PANCMACDAMN to get the final additive PEG-Ag attached PANCMACDAMN. The new highly hydrophilic additive was blended with PES dope solution to evaluate the antifouling properties of the PES membrane.

In this chapter the self-cleaning mechanism was further confirmed and proved experimentally. Silver kills bacteria by rupturing the cell wall³⁰⁰ allowing negatively charged protoplasm compounds to be deposited on the positively charged silver containing surface by electrostatic attraction^{135,301}. Similarly, it has been proven that the electro negative hydroxyl, carboxylic and amine functional groups repel the protoplasm compound by electrostatic repulsion^{101,135,302}. The above Chapters (Chapter 5 & 6) showed that the hydrophilicity and the antifouling property of the

PES UF membrane can be improved by blending the highly hydrophilic, water insoluble poly (acrylonitrile-co-maleic acid) (PANCMA) with covalently attached multi-functional amine containing molecule polyethylene imines-silver (PEI-Ag)¹³⁵ (Chapter-6) and polyethylene glycol-silver (PEG-Ag)¹³⁶ (Chapter-5). The findings proved that these highly hydrophilic electronegative hydroxyl, carboxylic and amine functional groups contain water insoluble additives which not only improve the hydrophilicity of the membrane but, when acting together with silver, also impart long lasting antifouling properties to the membrane via a killing and cleaning mechanism. Figure 7.1 shows a schematic comparison of the anti-fouling mechanism exhibited by the silver modified membrane and the proposed self-cleaning biofouling resistant membrane.

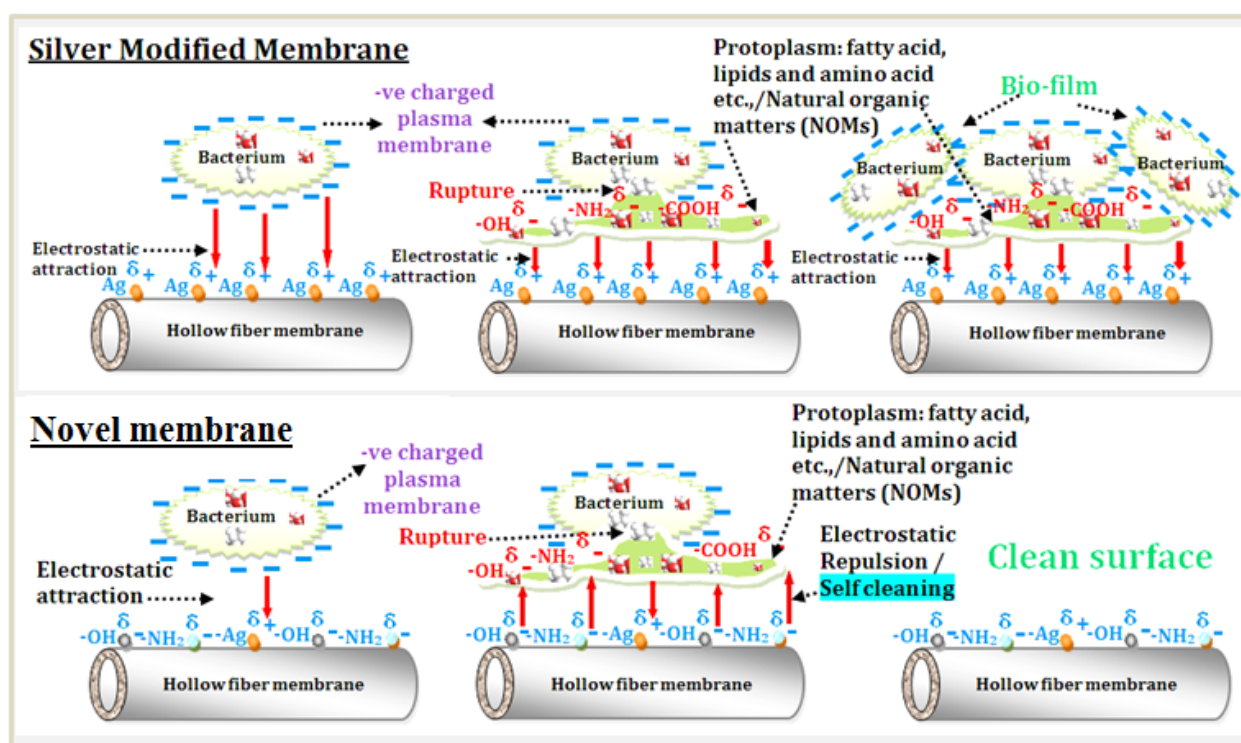


Figure 7.1: Schematic representation of the silver modified membrane and the proposed self-cleaning biofouling resistant membrane.

In this chapter, a novel biofouling resistant self-cleaning membrane will be developed by using a copolymer with electronegative carboxylic and amine group with immobilized PEG and positively charged silver nanoparticle. In order to achieve this objective, monomers with desired functional groups (acrylonitrile, maleic acid and diamino maleionitrile) will be chosen and polymerized to obtain the final polymer poly (acrylonitrile co maleic acid co diamino maleionitrile)

(PANCMACDAMN). PEG and silver nanoparticle will be covalently attached to the prepared copolymer additive by simple thermal grafting method. The final additive will be used to modify the PES ultrafiltration membrane by simple blending method and the membrane will be developed by phase inversion technique.

This chapter is based on: “Highly hydrophilic copolymer modified PES ultrafiltration (UF) membranes with robust antifouling properties.” by *Prince J.A., Bhuvana S., Anbharasi V., Ayyanar N., Boodhoo K.V.K., Singh G.*, Under review in *Desalination (Manuscript ID: DES-D-15-01256)*

7.2. EXPERIMENTAL METHODS

General characterization and experimental methods are described in chapter 4. Specific experiments with conditions particular to this chapter are discussed below.

7.2.1. MATERIALS

Polyethersulphone (PES) powder was purchased from Sumitomo Chemicals pte ltd, Japan. Acrylonitrile, maleic anhydride, azoisobisbutyronitrile (AIBN), silver nitrate (AgNO_3) and polyethylene glycol (PEG) of molecular weight 400 were purchased from Sigma Aldrich with 99% purity. High purity ethanol, N-methyl-2-pyrrolidone (NMP), polyvinyl pyrrolidone (PVP-K30) and diethylene glycol (DEG) were also purchased from Sigma Aldrich and used as received. The water used for the reaction was distilled and de-ionized (DI) with a Milli-Q plus system from Millipore, Bedford, MA, USA.

7.2.2. SYNTHESIS OF POLY (ACRYLONITRILE CO MALEIC ACID CO DIAMINO MELEONITRILE) (PANCMACDAMN)

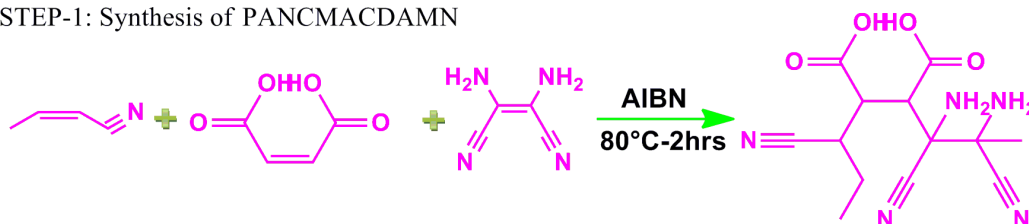
Copolymerization of acrylonitrile, maleic anhydride and diamino maleionitrile was performed using AIBN as initiator. Typically, to a 250 ml DI water at 90°C, 98 g maleic anhydride and 53 g acrylonitrile were added into the reactor equipped with a mechanical stirrer, thermometer, and nitrogen inlet tube. After complete dissolution, 1.85 g AIBIN was added into the stirring solution while maintaining the reaction temperature at 90°C under a nitrogen atmosphere. The

copolymerization was continued for 5 hrs, after which the precipitated copolymer was filtered and washed with excess de-ionized water and ethanol to remove residual monomers. After thorough drying, at 60°C in vacuum oven, the synthesized PANCMACDAMN was further functionalized with PEG and Ag before being used as an additive to prepare the PES dope solution.

7.2.3. ATTACHMENT OF PEG AND Ag WITH PANCMACDAMN

To further functionalize the copolymer, 25 g of PANCMACDAMN is dissolved in 200ml of NMP. After complete dissolution, about 10 g of PEG and 1 g of silver nitrate is added to the solution and allowed to stir at 80°C for about 2 hrs. 10ml of 0.1 M solution of sodium borohydride is slowly added to the above solution and allowed stir at the same temperature for another 3 hours. Finally, the solution is precipitated in methanol and filtered and washed with excess de-ionized water and ethanol to obtain functionalized PANCMACDAMN. Figure 7.2, shows the schematic representation of the synthesis of PANCMACDAMN and attachment of PEG and Ag with PANCMACDAMN

STEP-1: Synthesis of PANCMACDAMN



STEP-2: Attachment of PEG and Ag with PANCMACDAMN

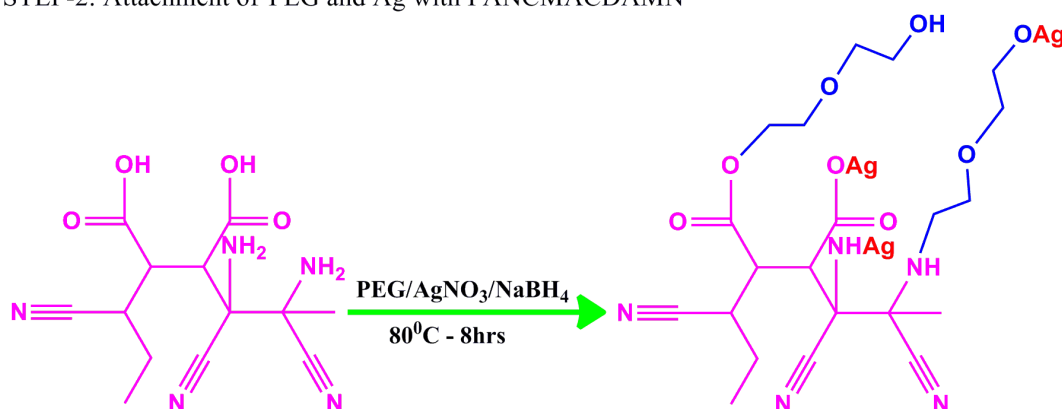


Figure 7.2: Synthesis of PANCMACDAMN and attachment of PEG and Ag with PANCMACDAMN

7.2.4. PREPARATION OF MEMBRANES BY DRY WET SPINNING

The PES hollow fiber membranes were prepared by dry wet spinning method. PES was used as the base polymer, NMP was the base solvent, DI water was used as a non-solvent and two additives, PVP-K-30 as pore forming agent and hydrophilic PEG and silver grafted PANCMACDAMN were used to improve the surface property of the membrane. The composition of the casting solution consists of 21 wt% PES, 5 wt% PVP-K-30, 5 wt% DEG, 59~69 wt% NMP and 0-10 wt% PANCMACDAMN, (M1-0%, M2-2.5%, M3-5%, M4-7,5% and M5-10%) respectively. The phase diagram for the used dope composition and the phase behavior is shown in Figure 7.3 in ESI. PVP powder was first added into the NMP/DEG mixture in a round bottom (RB) flask and the solution was stirred by a mechanical stirrer for at least 1 hour. After complete dissolution of PVP, PEG-Ag grafted PANCMACDAMN and PES were added and allowed to stir at a constant speed of 250~350 rpm for at least 24 h at 80° C, to obtain a completely dissolved homogeneous polymeric solution. All dope solutions from M0-M5 were used to fabricate the membranes. The dope solution was poured into the polymer tank and degassed at a vacuum pressure of -0.6 bar for 20 min. Nitrogen gas was purged into the dope tank to create an inert atmosphere and to push the polymer to the polymer pump. NMP and water were mixed in 80:20 volume ratio and poured into the bore liquid tank. The polymer solution and the bore liquid were pumped to the spinneret (OD 1.2 mm, ID 0.6 mm). The air gap was fixed at 10mm. The hollow fiber membranes were fabricated at around 25° C and at around 65% relative humidity with a take up speed of 0.25 m/s. The membrane turned opaque soon after coming into contact with water which indicates that the coagulation and precipitation of PES from the solution and finally a translucent, white hollow fiber membrane was formed. The membrane was then collected from the winder and left inside a water tank (post coagulation tank) for a minimum of 24 hrs to washout the residual NMP, DEG and PVP that was not removed from the solution at the point of coagulation. To keep the membranes wet, they were immersed into a post treatment solution of 40% ethanol and 60% glycerin before testing the clean water flux.

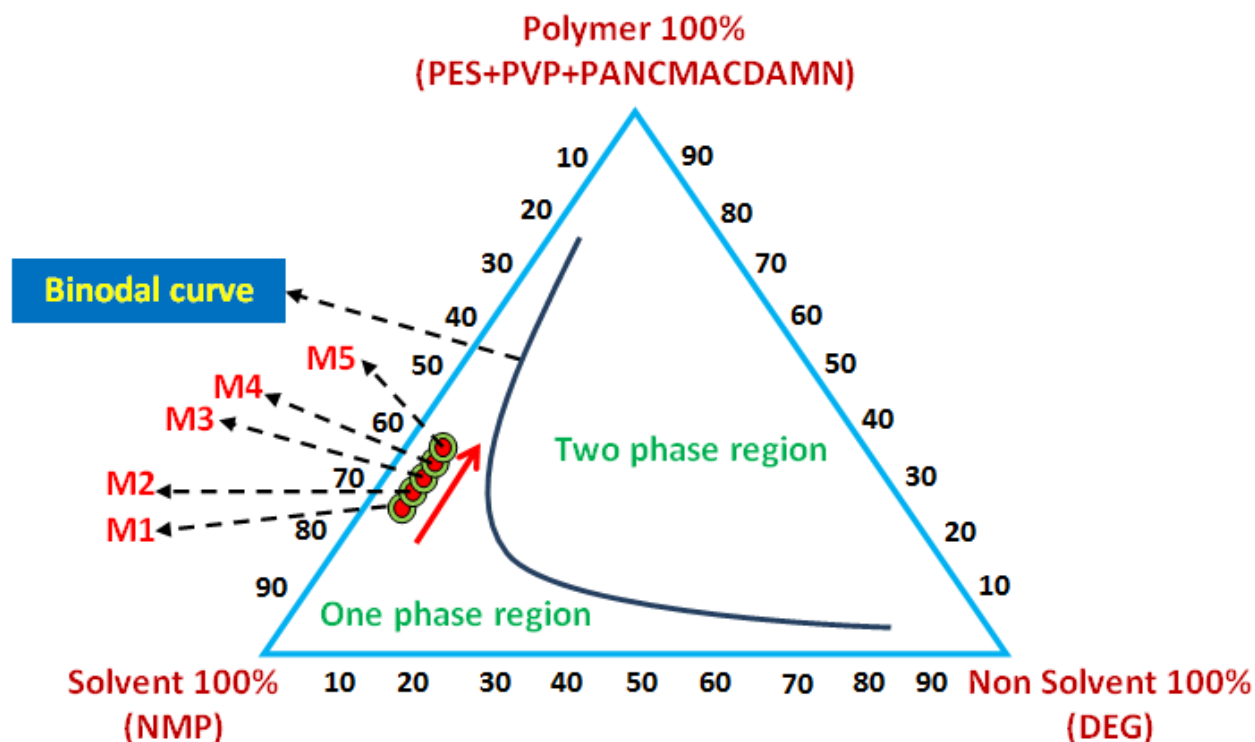


Figure 7.3: Phase diagram of the dope composition with optimization direction

7.3. RESULT AND DISCUSSION

7.3.1. FTIR ANALYSIS OF PANCMACDAMN

Structural confirmation: The structures of the new additive PANCMACDAMN and presence of the new additive in the modified PES membranes were studied by Fourier transform infrared (FTIR) spectroscopy and the results are presented in Figure 7.4. PES and PES/PEG-Ag grafted PANCMACDAMN hybrid hollow fibers were successfully fabricated by using the dry wet spinning process. FTIR analysis was used for the structural confirmation of incorporation of PEG-Ag grafted PANCMACDAMN into PES matrix. The FTIR spectrum is shown in Figure.7.4. And the successful incorporation of the copolymer into PES matrix is confirmed. The $-CH$ stretching vibration of the PES, PEG and PANCMACDAMN was observed around 2921cm^{-1} . The CN stretching peak for nitrile group of the co-polymer is observed at 2241cm^{-1} . The OH stretching vibration of the PEG is observed at 3492cm^{-1} and the carbonyl stretching vibrations of the acid groups in copolymer is observed at 1690cm^{-1} . All these peaks confirms the presence of PEG-Ag

grafted PANCMACDAMN in PES matrix. It is also observed that the peak intensity of the copolymer increases with increase in concentration.

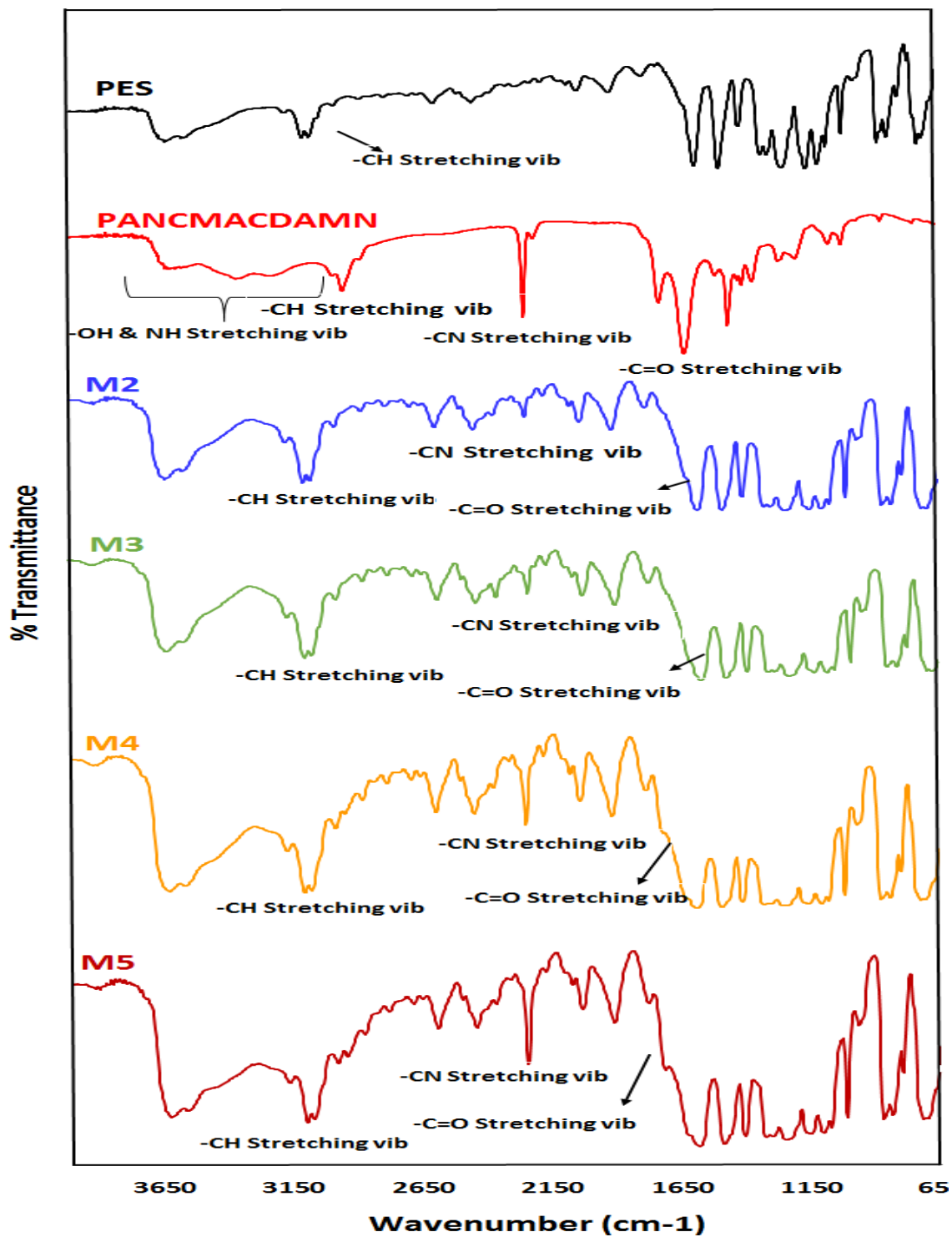


Figure 7.4: FTIR spectrum of the new additive PANCMACDAMN and presence of the new additive in the modified PES membranes

7.3.2. GPC ANALYSIS OF PANCMACDAMN

The molecular weight (M_w) and the molecular weight distribution of the synthesized polymer with respect to polystyrene standards was measured by using Gel permeation chromatography and the average of all the peaks is reported. The results are presented in Figure 7.5. From the analysis, the weight average molecular weight of the polymer was found to be around 95971 g/mol. The number average molecular weight was around 75800 g/mol. The polydispersity index (M_w/M_n) was calculated to be 1.27. This analysis confirms the high molecular weight of the synthesized polymer with controlled polymer width.

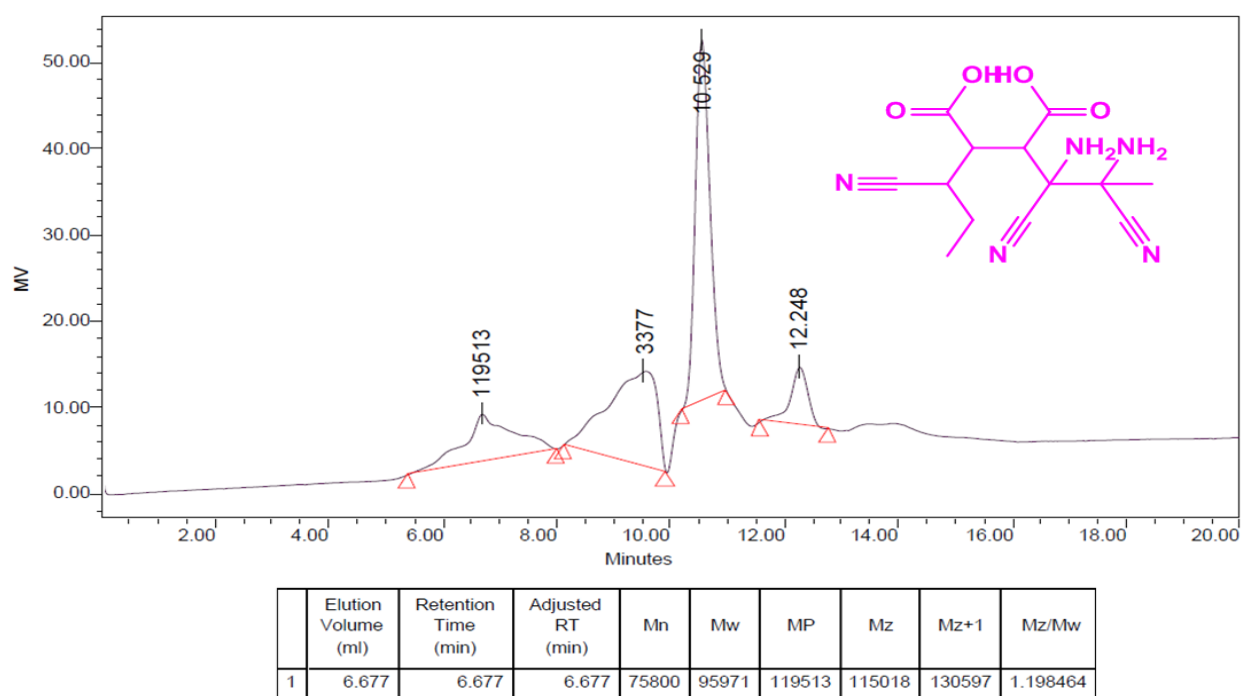


Figure 7.5 Gel permeation chromatography analysis of PANCMACDAMN

7.3.3. MORPHOLOGY OF HOLLOW FIBERS AND EDX ANALYSIS

The hollow fiber membranes fabricated through dry-wet spinning process had an average inner diameter of 0.6mm and an outer diameter of 1.2mm. The morphology of the cross section of all the prepared hollow fiber membranes were examined using SEM and the micrographs of the control sample (M1) and the best performing membrane sample (M4) are presented Figure 7.6.

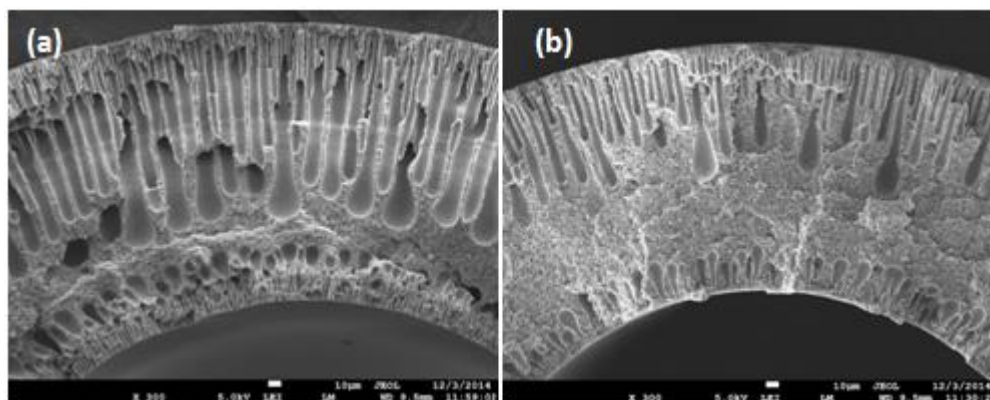


Figure 7.6: SEM image (cross section) of control membrane M1 (a) and modified (best performing) hollow fiber membranes sample M4 (b)

The morphology analysis shows that the hollow fibers exhibit different internal structures depending on their composition. M1 is the neat PES membrane which shows the presence of large number of macro voids in its internal structure. When the PANCMACDAMN concentration increases from 2.5 wt% to 10wt%, the void structure diminishes gradually and formation of uniform sponge like structures over the membrane cross section is observed. This can be explained by the increase in viscosity of the polymer solution with increase in PANCMACDAMN concentration. The increase in solution viscosity slows down the diffusion of non-solvent into the membrane which in turn decreases the rate of coagulation. The SEM image of the cross section and the presence of silver and its uniform distribution all over the best performing membrane sample M4 is evidenced from the elemental mapping shown in Figure 7.7.

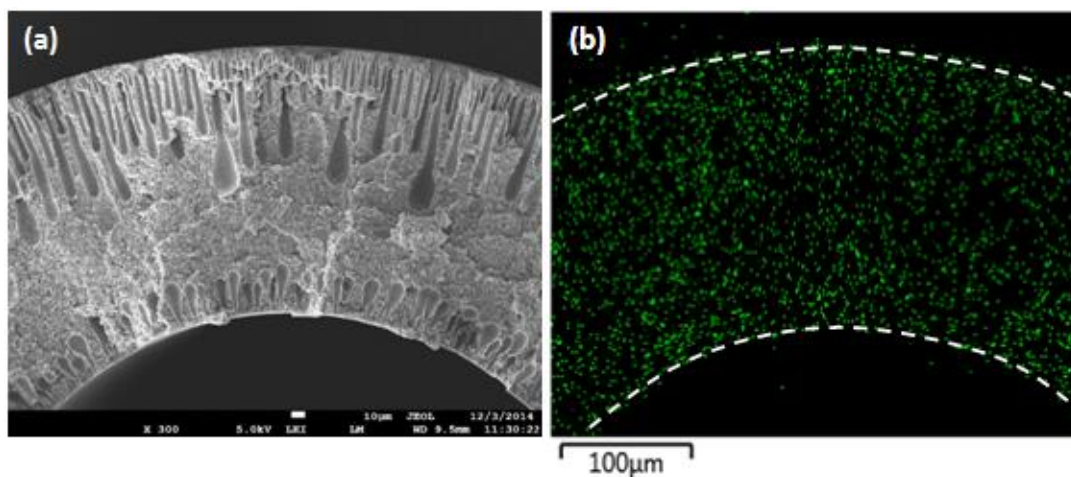


Figure 7.7: SEM image (cross section) (a) and Elemental mapping (b) of modified (best performing) hollow fiber membranes sample M4

7.3.4. LEACHING TEST FOR SILVER

After the thermal surface grafting process was performed as described earlier, the membranes were washed with excess DI water for 2 hours and dried at room temperature before testing. The dried samples M2, M3, M4 and M5 were immersed in DI water and ultra-sonicated at 37 kW for 60 mins. After ultra-sonication, the water was analyzed using inductively coupled plasma atomic emission spectroscopy (ICP-OES). The leached silver is found to be less than 2ppm for all the samples. This confirms that the silver is in strong covalent bonding with the functional groups of the PANCMACDAMN, which prevents the leaching of silver.

7.3.5. CONTACT ANGLE

The hydrophilicity of the membranes was measured by their water contact angle and the results are tabulated in Table 7.1. With M1 being the control, the rest of the samples shows a decrease in water contact angle with an increase in PANCMACDAMN concentration and reached the lowest at M5 with $14.2 \pm 2.3^\circ$. This test has proven the effectiveness of PEG-Ag grafted PANCMACDAMN in generating a more hydrophilic membrane with M5 having at least a 78.1% decrease in the contact angle from the control membrane (contact angle of control membrane is $64.6 \pm 3.2^\circ$).

7.3.6. PORE SIZE ANALYSIS

The average pore size of the control PES membrane (M1) and the PEG-Ag grafted PANCMACDAMN modified PES membrane samples M2, M3, M4 and M5 are also presented in Table 7.1. The experimental data indicate that the mean pore sizes of the membranes are gradually decreases with the PANCMACDAMN concentration. This may be due to the increase in viscosity and coagulation of the dope solution. Generally, pores in the membranes are formed by diffusion of non-solvent from coagulation bath into the membrane matrix and the de-solvation of casting solvent. If the solution viscosity increases, the diffusion of coagulant into the casting solution will be reduced and hence the macro voids can be reduced. The dense surface generally forms when a high ratio of the solvent out flow occurs compared to the non-solvent inflow. The lowest average pore size achieved is $0.05 \pm 0.025 \mu\text{m}$ for membrane sample M5 whereas the control membrane exhibited a mean pore size of $0.07 \pm 0.02 \mu\text{m}$.

Table 7.1 Pore size, contact angle and the clean water flux of the control PES membrane and the PEG-Ag grafted PANCMACDAMN modified PES membrane samples.

Sample ID	CAw (°)	Pore size (μm)	Clean water flux (LMH)
M1	64.6± 3.2	0.07 ± 0.02	477.6 ± 18.2
M2	49.1± 1.7	0.07 ± 0.02	666.2 ± 22
M3	32.4± 2.0	0.06 ± 0.025	858.6 ± 27.1
M4	18.7± 1.3	0.05 ± 0.02	1050.2 ± 24
M5	14.2± 2.3	0.04 ± 0.025	984.6 ± 14

7.3.7. ZONE INHIBITION TEST

In order to investigate the antibacterial activity of the membrane, zone of inhibition test was performed for the control membrane sample (M1) and the best performing membrane sample (M4). Figure 7.8 shows the zone of inhibition for the two different samples M1 and M4 (a) before protein filtration (b) after protein filtration. It can be easily identified that the membrane sample M4 exhibited positive results even after 12 hrs continuous filtration of protein solution whereas M1 does not show any inhibition zone. The width of the zone around the sample S4 was about 2.5 mm (before protein filtration) and 1.5-2mm (after protein filtration) respectively. This is attributed to the stable bactericidal property of composite membrane M4.

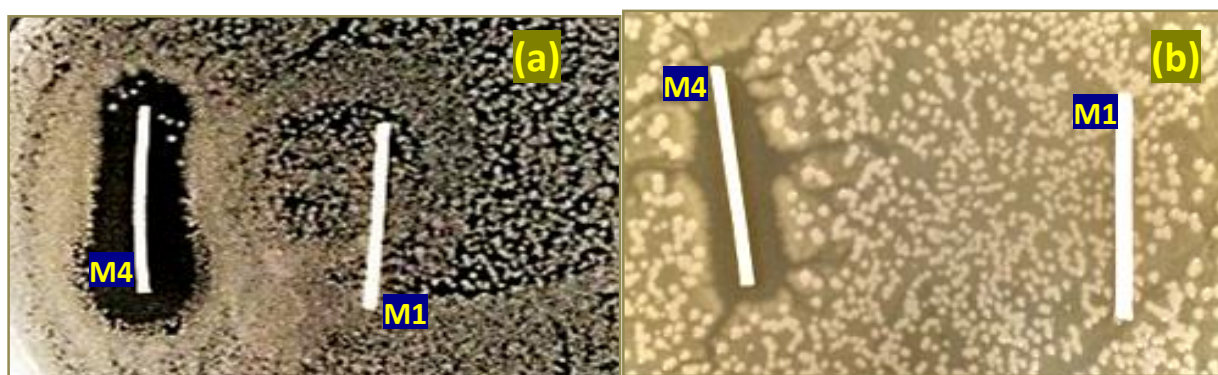


Figure 7.8: Zone of inhibition of control S1 and modified best performing membrane M4 (a) before protein filtration, (b) after protein filtration

7.3.8. CLEAN WATER FLUX

The membranes M1-M5 were tested to evaluate the clean water flux of the membrane by using a cross flow filtration setup at a constant feed pressure of 1bar and the results are presented in Table 7.1. All membranes were tested in the system under similar conditions with M1 as the control. The pure water flux of the membrane increased with increasing PEG-Ag attached PANCMACDAMN concentration. The highest flux achieved in this study was 1050.2 ± 24 LMH for the membrane sample M4 which is around 120% higher than the control membrane M1 (477.6 ± 18.2 LMH). This improvement is due to the increase in the membrane hydrophilicity as indicated by a decrease in its water contact angle. However, when compared to M3 and M4, sample M5 gives lower flux due to the slight reduction in membrane pore size or pore compression.

7.3.9. LONG TIME PERFORMANCE AND FOULING EVALUATION

In order to evaluate the effect of the PEG-Ag grafted PANCMADAMN on the membrane, the control M1 and the best performing membrane sample M4 were chosen on the basis of pure water flux permeability tests (Table 7.1 and Figure 7.9 (a)). A 12 hrs filtration test was conducted using 10ppm BAS in DI water as a feed solution through the two membrane samples. The results are summarized in Figure 7.9 (b). It is observed that the PEG-Ag grafted PANCMACDAMN modified membrane sample M4 gives a more stable flux compared to the control membrane sample M1. Figure 7.9 (c) shows the normalized permeability (J/J_0) or flux drop over time. The flux drop for the membrane M4 is only 14.29% of the initial flux after 9hrs protein separation whereas the flux drop for control membrane M1 is 60% for the same duration of operation. The obtained results highlight that the presence of negatively charged $-\text{OH}$, $-\text{NH}_2$ and $-\text{COOH}$ functional groups on the PEG-Ag grafted PANCMACDAMN can best repel the protein from the surface of the membrane. In order to evaluate the selectivity and the filtration efficiency of the membrane, the total organic carbon (TOC) of the feed BAS solution and permeate water were measured (4 samples were collected every 60 mins with 15mins frequency and the TOC was measured in order to get the average TOC removal over time). The percentage of TOC rejection was calculated and presented in Figure 7.9 (d).

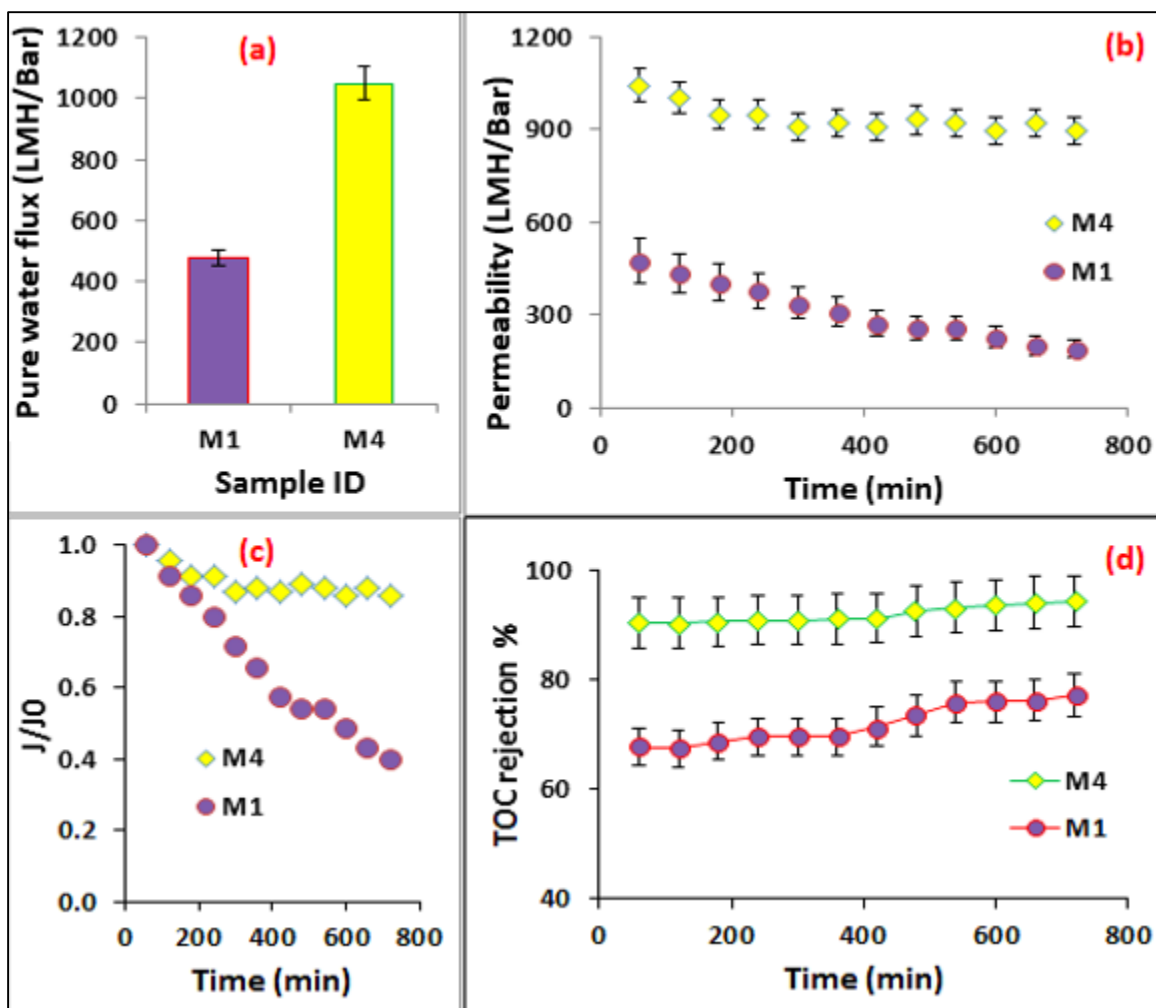


Figure 7.9: Pure water flux for the control membrane sample M1 and the best performing membrane sample M4 at 1bar feed pressure (a), water permeability during long time run with 10ppm BSA solution at 1bar feed pressure for the same samples (b), normalized water permeability for the BSA solution separation during long time run (c) and BSA protein (TOC) removal efficiency / selectivity of the membranes in % (d)

From the experimental data, it is found that the TOC removal of the membrane M4 is also higher and more stable compared to membrane M1. This may be due to the slight difference in the average pore sizes of the membrane. The pore size of the membrane sample M4 ($0.07 \pm 0.02 \mu\text{m}$) was slightly lower compared to sample S1 (0.05 ± 0.02). The increased TOC removal also confirms the increased hydrophilicity and zwitterionic effect of the PEG-Ag grafted PANCMACDAMN blended membranes M4 by negatively charged $-\text{OH}$, $-\text{COOH}$ and positively charged $-\text{NH}_2$

functional groups on the membrane surface. Recent studies have also shown that the negative surface charge of the membrane prevents the deposition of the negatively charged colloidal particles such as proteins, lipids and amino acids etc., on the membrane surface by electrostatic repulsion, which could slow down or reduce the membrane fouling¹³⁵⁻¹³⁸. On a related note, it is interesting to see from Figure 7.9 (d) that the increase in TOC removal efficiency of the control membrane M1 with time may be due to the pore constriction/pore blocking or development of fouling on the membrane surface³⁰⁹. Finally, a confocal laser scanning microscope (CLSM) analysis was conducted on the membrane samples to evaluate the protein absorption on the membrane surface and the images are presented in Figure 7.10. From the images it can be further confirmed that the protein absorption on the membrane M4 surface can be negligible however, the protein absorption on the control membrane M1 is high.

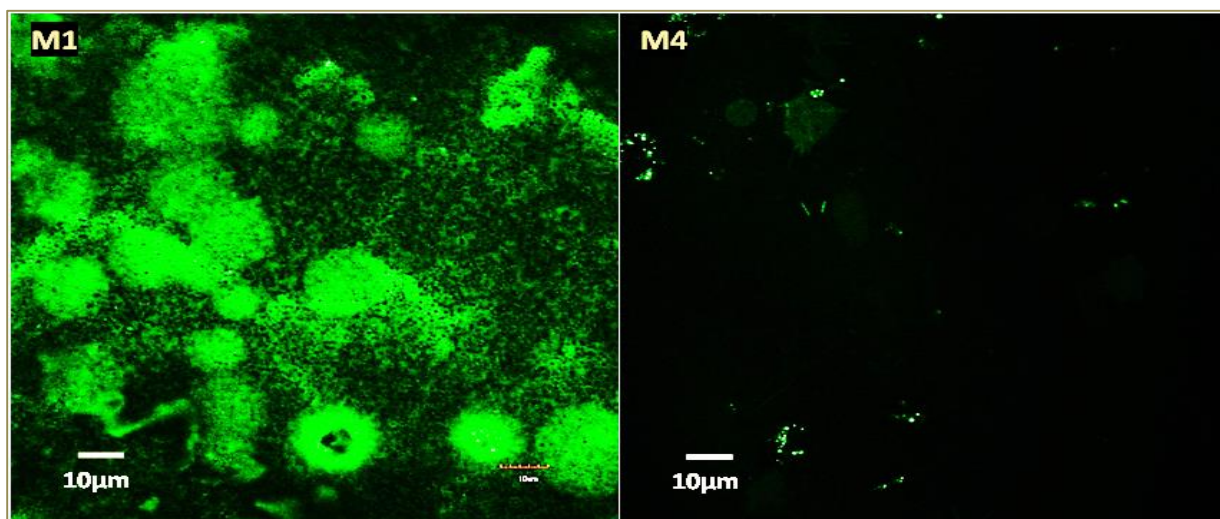


Figure 7.10: Confocal laser scanning (CLSM) image of control sample M1 and the best performing membrane sample M4

7.4. SUMMARY

In this chapter, a simple feasible method has been demonstrated to impart bio-fouling resistance to a membrane surface by developing a water insoluble unique copolymer additive, namely poly (acrylonitrile co maleic acid co diamino maleionitrile) (PANCMACDAMN) with highly hydrophilic electronegative carboxylic and amine functional groups. In addition, another highly hydrophilic hydroxyl group rich polyethylene glycol (PEG) and positively charged antibacterial compound silver (Ag) were covalently attached to the copolymer additive by simple thermal

CHAPTER: 7

grafting method. The final additive PEG-Ag attached PANCMACDAMN was used to modify polyethersulfone (PES) ultrafiltration (UF) membrane. Characterization tests indicate that the innovative surface chemistry increases the hydrophilicity of the membrane by reducing the water contact angle (CA_w) by 78.1% and increases its permeability by 120% compared to the control membrane. More importantly, the innovative surface chemistry prevents protein attachment to it and continuously exhibit inhibition to microbes even after a 720 min continuous filtration of protein solution.

8. Effect of hydroxyl (-OH), amine (-NH₂) and acid (-COOH) functionalized graphene on the antifouling properties of the prepared membranes

8.1. INTRODUCTION

The individual effects of hydroxyl (-OH) functional group (Chapter 5) and amine (-NH₂) functional groups (Chapter 6) and the combined effects of both amine (-NH₂) and hydroxyl (-OH) groups (Chapter 7) have been tested together with carboxylic (-COOH) functional groups and antimicrobial silver to evaluate their effect on the performance of the PES membrane in terms of hydrophilicity, water permeability, selectivity and membrane fouling. The experimental data have shown that the overall performances of the membranes are increased with the new additives. However, the thermal stability of these membrane are not improved and hence in this chapter highly thermally, chemically and physically stable graphene will be modified with hydroxyl (-OH), amine (-NH₂) and carboxyl (-COOH) functional groups for use as a hydrophilic additive to PES dope solution.

Graphene oxide-based membranes exhibit promising qualities in the field of desalination¹³³ and selective ion penetration¹⁶⁸. Graphene oxide-polymer hybrid material based membranes also exhibit excellent antifouling property¹²⁹ due to the interaction of contaminants with the delocalized p-electrons of the nanocarbons¹³⁰⁻¹³². In general, highly hydrophilic polymeric materials will have low mechanical and thermal stability and swell during continuous immersion in water³¹⁰. Thermal and mechanical properties of the polymeric membranes is increased by the addition of graphene and its derivatives¹⁶⁷ which imparts a strong rigid structure to the membrane material¹⁵².

In this chapter, a facile method to fabricate graphene-based composite membrane in real downstream application will be developed. In order to achieve this, the wettability of exfoliated

graphene nano platelets (xGnP) will be increased by amine (-NH₂) and carboxylation (-COOH) to an ultra-wetting level. While graphene oxide attains an increased level of hydrophilicity via -COOH and -OH functional groups, in this work a combination of -COOH and -NH₂ functional groups was chosen instead to modify the graphene for use in water filtration membrane applications. Amine modified graphene has recently been reported as an alternative to graphene oxide in biomedical³¹¹ and energy³¹² (battery) related applications. Carboxylic and amine functional groups have been shown to give significant improvements in the hydrophilicity of the membranes¹³⁴⁻¹³⁸ by inter molecular hydrogen bonding^{134,135,298,299}. The novelty in the present work is that, in addition to improved hydrophilicity due to the presence of amine and acid functional groups, the ultra-wetting modified graphene will also be covalently attached to an anhydride containing polymer matrix namely poly acrylonitrile-co-maleic anhydride (PANCMA) via a simple condensation reaction to form amic acid. This is made possible by the terminal -NH₂ groups of the functionalized graphene which are known to react readily with anhydrides to form strong, stable covalent bonds. The ultra-wetting graphene attached PANCMA will be thermally imidized to produce the final graphene-poly(acrylonitrile-co-maleimide) (G-PANCMi) polymer composite, which by virtue of the imide functionality, will have improved thermal and chemical stability. The ultra-wetting graphene modified G-PANCMi so formed will be used to fabricate a water filtration membrane by the simple phase inversion method^{313,314}.

This chapter is based on: *“Ultra-wetting graphene-based membrane”* by Prince J.A., Bhuvana S., Anbharasi V., Ayyanar N., Boodhoo K.V.K., Singh G., *Journal of Membrane Science* **500**, 76–85(2016).

8.2. EXPERIMENTAL METHODS

General characterization and experimental methods are described in chapter 4, some specific experiments with conditions particular to this chapter are discussed below.

8.2.1. MATERIALS

Acrylonitrile, maleic anhydride, ethylene diamine, and azobisisobutyronitrile (AIBN) were purchased from Sigma Aldrich with 99% purity. High purity ethanol, nitric acid (HNO₃), sulphuric acid (H₂SO₄), thionyl chloride (SOCl₂), N-N-Dimethyl acetamide (DMAc) and Fluorescein isothiocyanate (FITC) attached bovine serum albumin (BSA) were also purchased from Sigma Aldrich and used as received. The exfoliated graphene nanoplatelets (xGnP) were purchased from XG Sciences. The water used for the reaction was distilled and de-ionized (DI) with a Milli-Q plus system from Millipore, Bedford, MA, USA.

8.2.2. SYNTHESIS OF FUNCTIONALIZED xGnP

About 1 gram of the pristine xGnP was refluxed with an excess of acid mixture (H₂SO₄/HNO₃, 3:1) to introduce the acid and hydroxyl functionality on to the graphene surfaces. After successful oxidation, the functionalized xGnP was centrifuged, filtered and washed with excess water until the pH of the wash water was neutral. After thorough drying, the acid functionalized xGnP was further refluxed with 150ml of thionyl chloride at 80°C for 24 hrs. The excess thionyl chloride post-reaction was filtered off before 150ml of ethylene diamine was added to the reaction vessel operating under reflux for another 24hrs. The amine functionalized xGnP was finally separated out by centrifugation and washed with excess ethanol to remove the unreacted reagents.

8.2.3. SYNTHESIS OF xGnP GRAFTED PANCFI (G-PANCFI)

PANCFI was synthesized as per our previously reported procedure using azobisisobutyronitrile as an initiator¹³⁶. The synthesized PANCFI was allowed to react for 24 hrs with the amine functionalized xGnP in 500ml of DMAc at 80°C. The water formed as a result of this condensation reaction was removed by forming an azeotrope with toluene. This reaction leads to the formation of the product in amic acid form. This intermediate product was further subjected to thermal imidisation using a multistage heating of 120°C for 2hrs and 200°C for 1hr to obtain the final xGnP grafted PANCFI. Figure 8.1 shows the schematic representation of the synthesis of G-PANCFI.

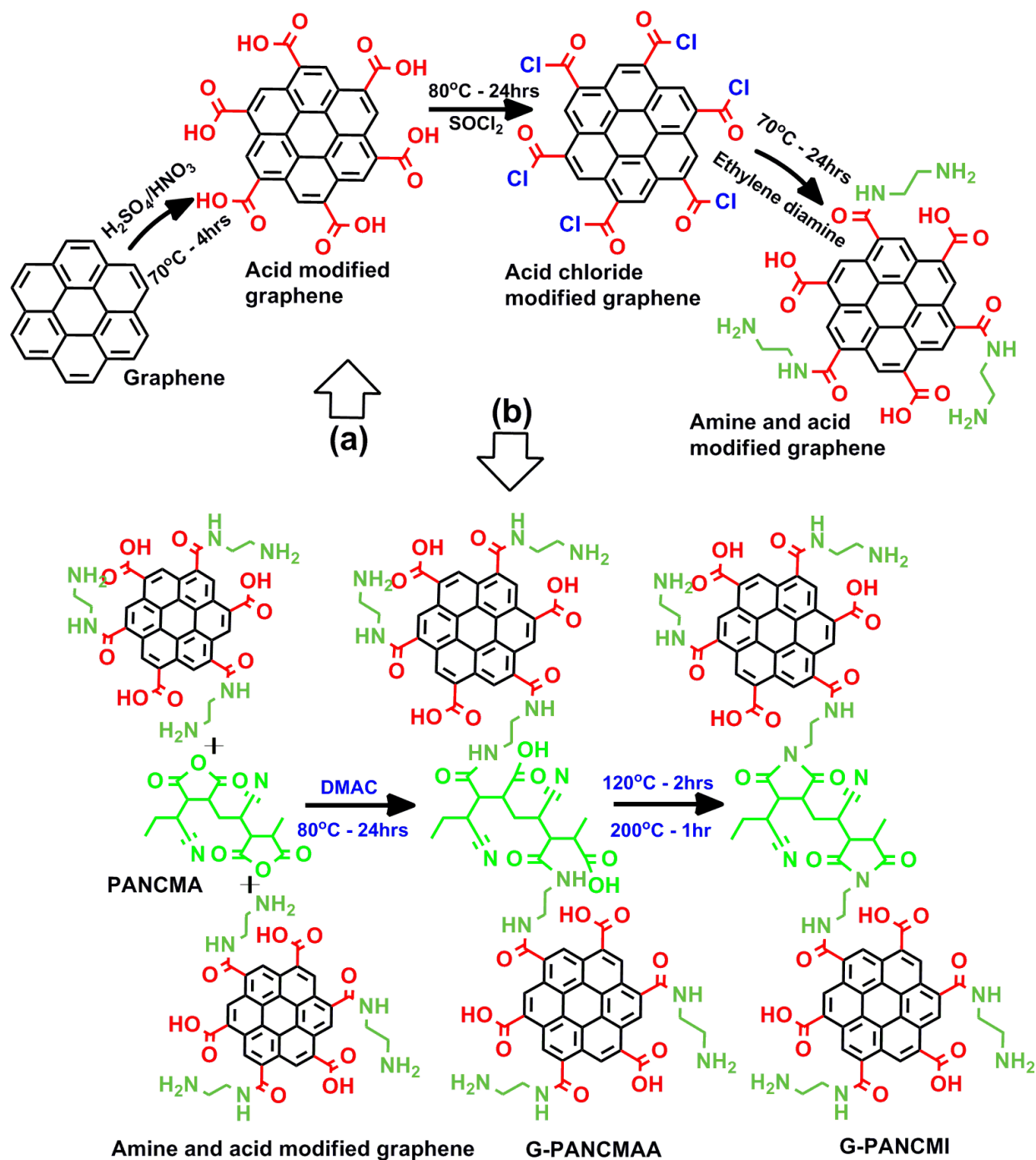


Figure.8.1. Synthesis of functionalized xGNP (a) Synthesis of G-PANCMMA (b)

8.2.4. PREPARATION OF FLAT SHEET MEMBRANE

The PANCMMA and G-PANCMPI ultrafiltration membranes were prepared by the simple phase inversion method^{313,314}. PANCMMA / G-PANCMPI were used as the base polymers, N-methyl-2-

pyrrolidone (NMP) was the base solvent, diethylene glycol (DEG) was used as a non-solvent and polyvinylpyrrolidone (PVP) was used as an additive (pore forming agent). The composition of the casting solution consists of 21 wt% PANCMA/G-PANCMCI, 5 wt% polyvinylpyrrolidone (PVP-K-30), 5 wt% Diethylene glycol (DEG), and 69 wt% N-methyl-2-pyrrolidone (NMP) respectively. The phase diagram of the dope compositions is presented in Figure.8.2. PVP powder was first added into the NMP /DEG mixture in a round bottomed (RB) flask and the solution was stirred by a mechanical stirrer for at least 1-1.5 hours. After complete dissolution of PVP, PANCMA/G-PANCMCI were added and allowed to stir at a constant speed of 250~350 rpm for at least 24 hrs at 80°C, to obtain a completely dissolved / dispersed homogeneous polymeric solution. The homogeneous polymer solution was used to fabricate ultrafiltration membrane by phase inversion method^{313,314}. To keep the membranes wet, they were immersed in a post treatment solution of 60% water and 40% glycerin before testing for clean water flux.

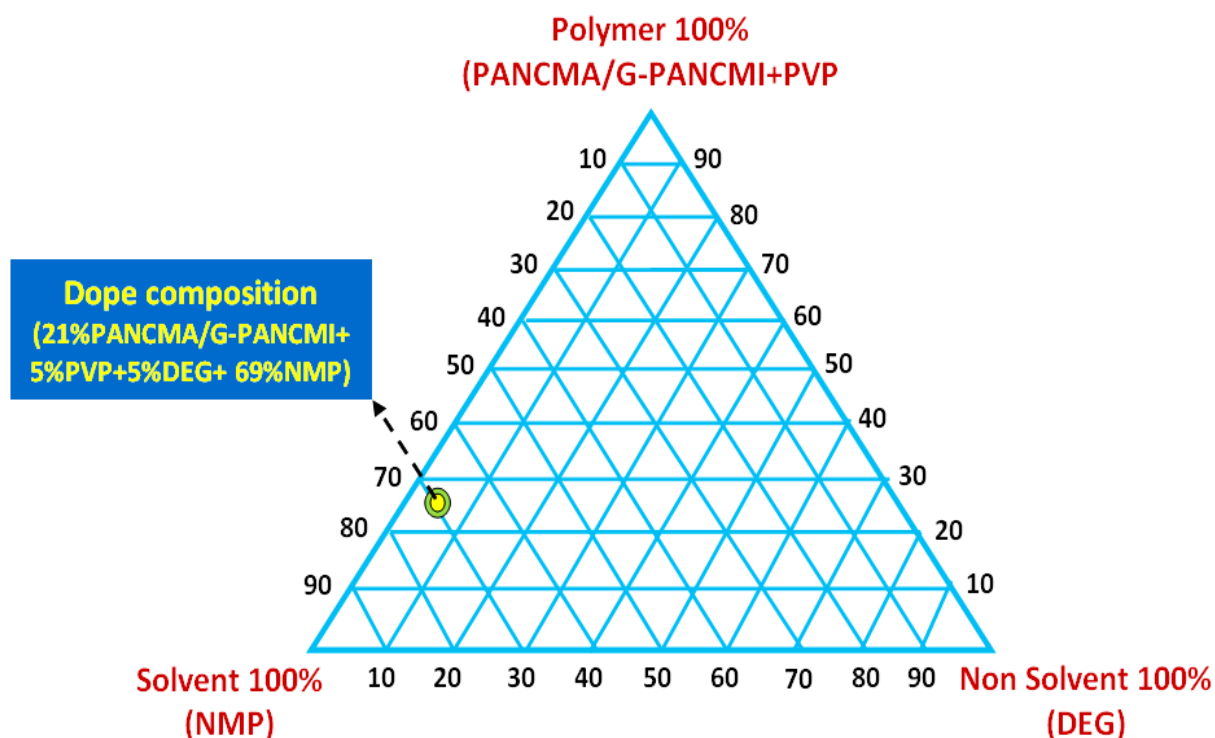


Figure.8.2. Phase diagram for the G-PANCMCI dope compositions

8.2.5. PREPARATION OF HOLLOW FIBER MEMBRANE BY DRY WET SPINNING

The control Polyethersulfone (PES) and xGnP grafted poly (acrylonitrile co maleimide) (G-PANCMi) modified PES-G-PANCMi hollow fiber ultrafiltration membranes were prepared by dry wet spinning method. PES was used as the base polymer, N-Methyl-2-pyrrolidone (NMP) was the base solvent, diethylene glycol (DEG) was used as a non-solvent, polyvinylpyrrolidone (PVP-k-30) was used as an additive (pore forming agent) and G-PANCMi was used as a hydrophilic additive. The composition of the casting solution consists of 21 wt% PES, 5 wt% PVP-K-30, 5 wt% DEG, 69 wt% NMP respectively 5% of G-PANCMi was added to the PES-G-PANCMi dope composition by replacing 5% of NMP where the NMP concentration was 64%. The phase diagram of the dope compositions is presented in Figure.8.3. PVP powder was first added into the NMP /DEG mixture in a round bottomed (RB) flask and the solution was stirred by a mechanical stirrer for at least 1-1.5 hours. After complete dissolution of PVP, PES and G-PANCMi were added and allowed to stir at a constant speed of 250~350 rpm for at least 24 h at 80° C, to obtain a completely dissolved / dispersed homogeneous polymeric solution. The dope solution was poured into the polymer tank and degassed at a negative pressure of -0.6 Bar for 15-20 min. Nitrogen gas was purged into the dope tank to create inert atmosphere and to push the polymer towards the polymer pump. NMP and water were mixed in 80:20 volume ratio (NMP: Water 80:20) was used as a bore liquid and poured into the bore liquid tank. The polymer solution and the bore liquid were pumped to the spinneret (OD 1.2 mm, ID 0.6 mm). The air gap was fixed at 50mm. The hollow fiber membranes were fabricated at around 25° C and at around 65-70% relative humidity with a take up speed of 0.21 m/s. The membranes were then collected from the winder and left inside a water tank (post coagulation tank) for 24 hrs to washout the residual NMP, DEG and PVP that was not removed from the solution at the point of fabrication process. In order to keep the membranes wet, the membranes were immersed into a post treatment solution of 40% water and 60% glycerin before testing the clean water flux.

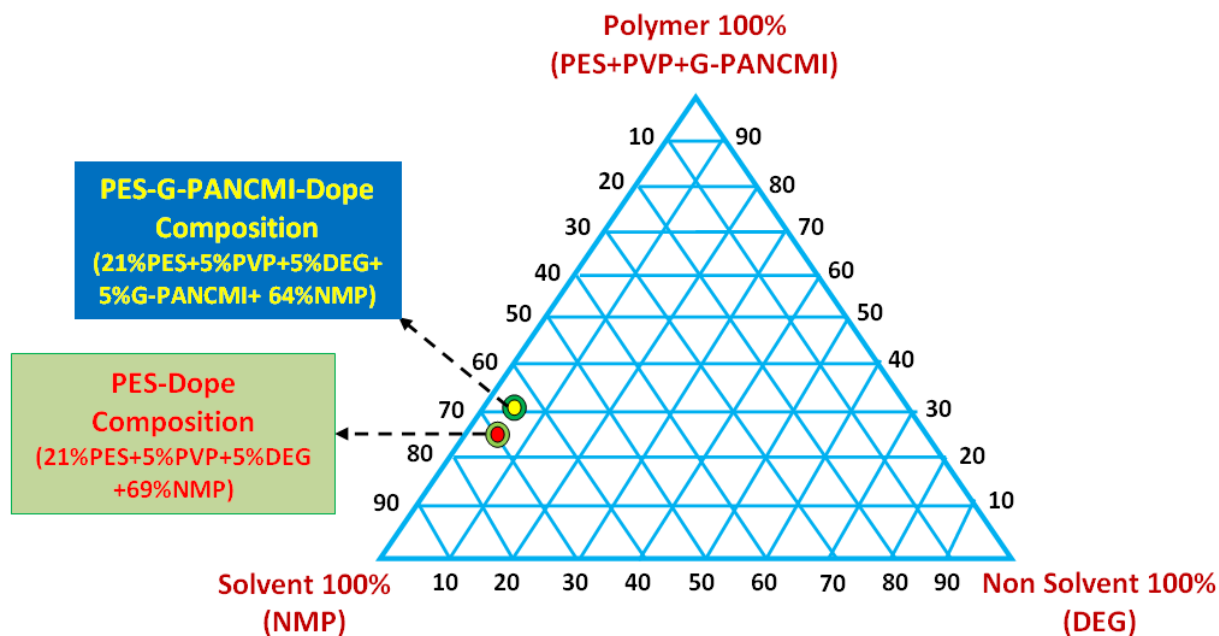


Figure.8.3. Phase diagram for the PES-G-PANCMI dope compositions

8.3. RESULTS AND DISCUSSION

8.3.1. FTIR ANALYSIS OF xGnP, PANCMMA AND G-PANCMMA

The structures of the modified xGnP, PANCMMA and G-PANCMMA were studied by Fourier transform infrared (FTIR) spectroscopy and the results are presented in Figure 8.4. The FTIR spectrum of amine modified xGnP shows a broad peak around 3436cm^{-1} for amine stretching vibration ($-\text{NH}$ stretching), a small peak at 2915cm^{-1} for the $-\text{CH}$ stretching vibrations of the ethylene moiety in ethylene diamine and a sharp and intense peak at 1672cm^{-1} for $-\text{NH}$ bending vibration. This confirms the attachment of ethylene diamine to xGnP. The FTIR spectrum of PANCMMA shows a small band at 2972cm^{-1} for the $-\text{CH}$ stretching vibration of the $-\text{CH}_2$ groups in maleic anhydride, a sharp peak at 2243cm^{-1} corresponding to the $-\text{C}-\text{N}$ stretching vibration of nitrile group and bands at 1784cm^{-1} and 1707cm^{-1} for the $-\text{C}=\text{O}$ stretching vibrations of the anhydride carbonyl groups. The FTIR spectrum of G-PANCMMA shows a broad band at 3219cm^{-1} corresponding to the $-\text{NH}$ stretching vibration of the diamine moiety, a small peak at 2931cm^{-1} for the $-\text{CH}$ stretching vibration, a sharp peak at 2245cm^{-1} corresponding to the $-\text{CN}$ stretching vibration of the nitrile group and two sharp peaks at 1770cm^{-1} and 1718cm^{-1} corresponding to the $\text{C}=\text{O}$ stretching vibrations of the imide carbonyl groups and finally a peak at 1386cm^{-1} for $-\text{C}-\text{N}$

C stretching vibration confirming the formation of imide functionality by the attachment of amine modified xGnP to PANCMA.

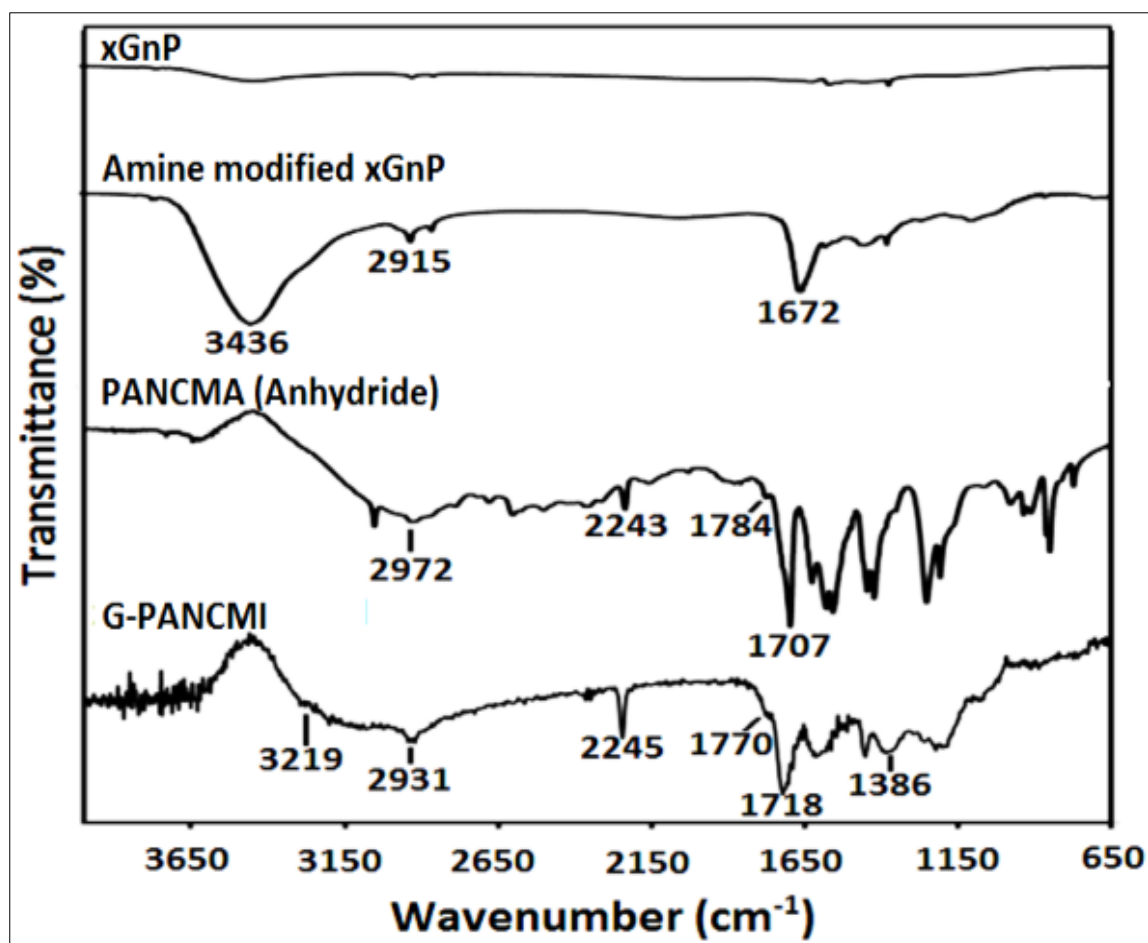


Figure.8.4. FTIR spectrum of xGnP, amine modified xGnP, PANCMA (anhydride) and G-PANCFMI

8.3.2. RAMAN SPECTRAL ANALYSIS OF xGnP, PANCMA AND G-PANCFMI

Figure 8.5 shows the Raman spectra of xGnP, aminated xGnP and G-PANCFMI. All the three compounds exhibited both the D band at around 1350 cm⁻¹ and G band at 1590 cm⁻¹. The intensity of D band in aminated xGnP is significantly larger compared to that of the xGnP which is ascribed to the disordered structure of the aminated xGnP by the amine treatment. This D band intensity is further increased in G-PANCFMI, which indicates the attachment of PANCFMI to the graphene structure. The G-band, which is ascribed to the ordered structure, is also increased due to amination and PANCFMI attachment. The attachment of polymer to the graphene structure is further

confirmed by the increase in ID/IG (ratio between the intensity of D band and G band) ratio from 0.23 to 0.56 and to 0.60 for xGnP, aminated xGnP and G-PANCMi respectively, indicating that the attached molecules are in between the platelet galleries, providing a disordered structure for xGnP.

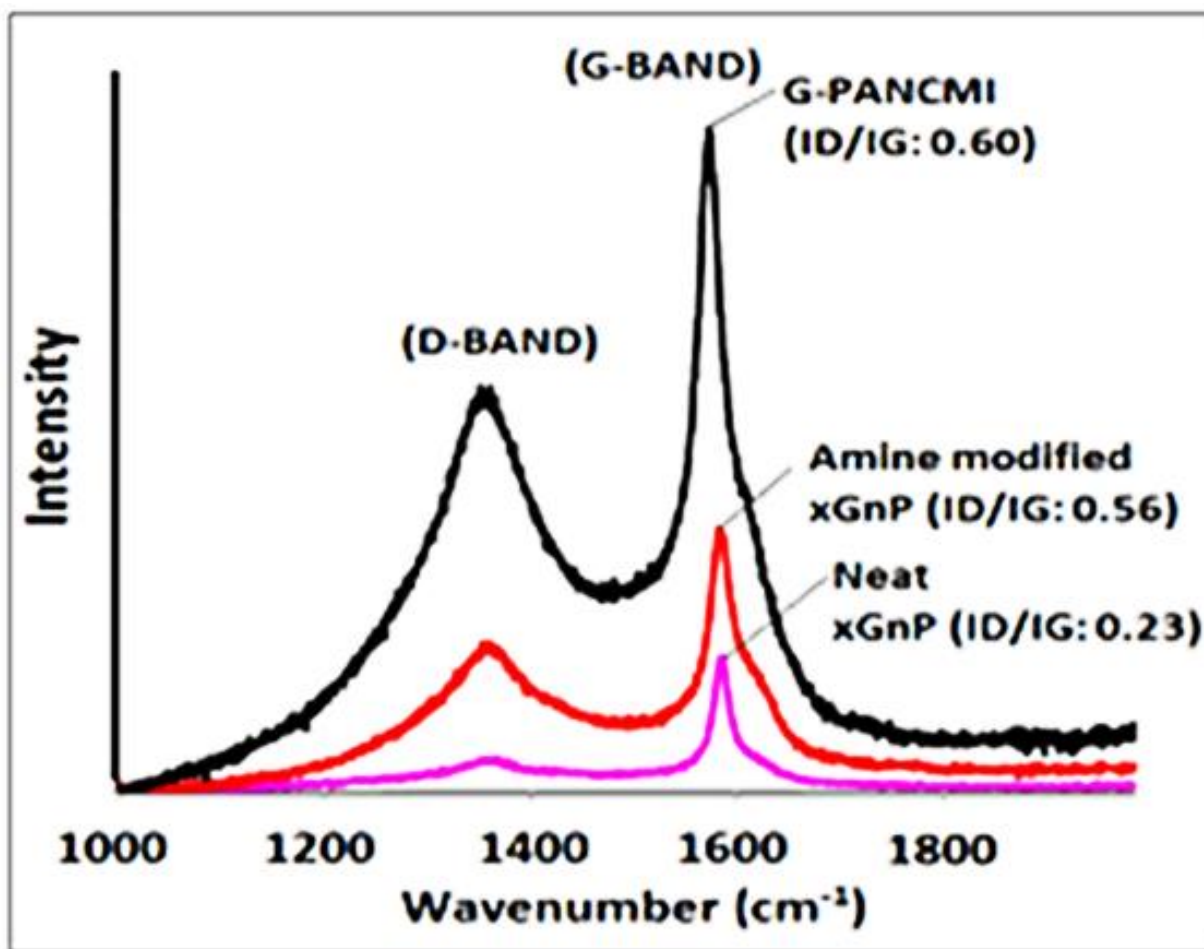


Figure 8.5 Raman spectroscopy analysis of unmodified graphene, amine and carboxylated graphene and G-PANCMi

8.3.3. ZETA POTENTIAL ANALYSIS

Figure 8.6 shows the zeta potential analysis of PANCMa and G-PANCMi. Zeta potential is a key indicator of surface charge as well as the stability of colloidal dispersions. The increased polarity and charge density of the modified graphene are due to the presence of oxygen containing

(carboxyl, hydroxyl) functional groups^{160,164}. It is known that, oxygen containing functionalities with low pka of 3-4 will lead to negative zeta potential. It is also observed that, at normal pH (of around 6-7), the G-PANCMi is more stable in dispersion than PANCMA as it exhibits high negative potential of about -40mv at this pH.

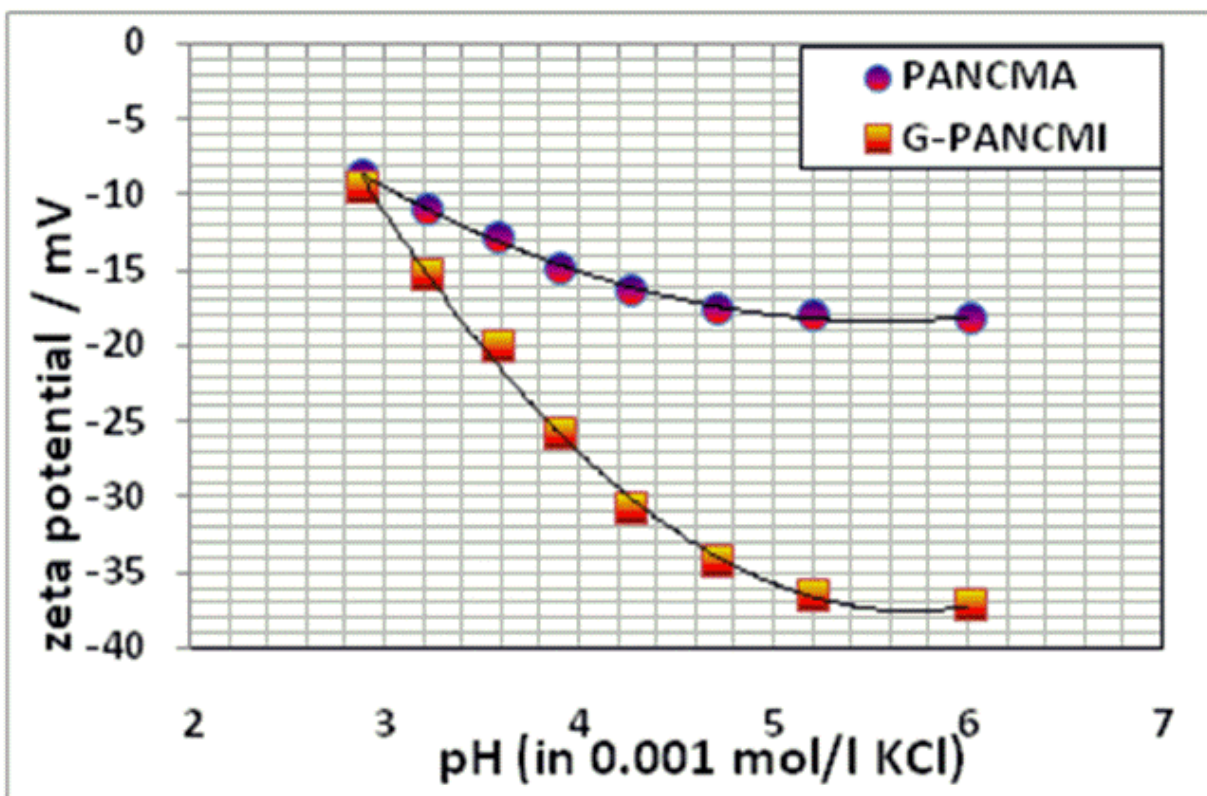


Figure 8.6 Zeta potential analysis

8.3.4. TGA ANALYSIS

The differences in thermal stability of PANCMA and G-PANCMi are highlighted in Figure 8.7. Compared to PANCMA, G-PANCMi shows excellent thermal stability. There is a slight weight loss at about 90°C for PANCMA, which may be due to loss of solvent or water molecules adsorbed onto it. The drastic weight loss for PANCMA occurs at about 190°C showing the complete degradation of PANCMA. In sharp contrast, G-PANCMi shows greater thermal stability up to a temperature of 400°C, confirming the improved thermal properties due to the presence of thermally rigid imide functionality and xGnP in the polymer matrix.

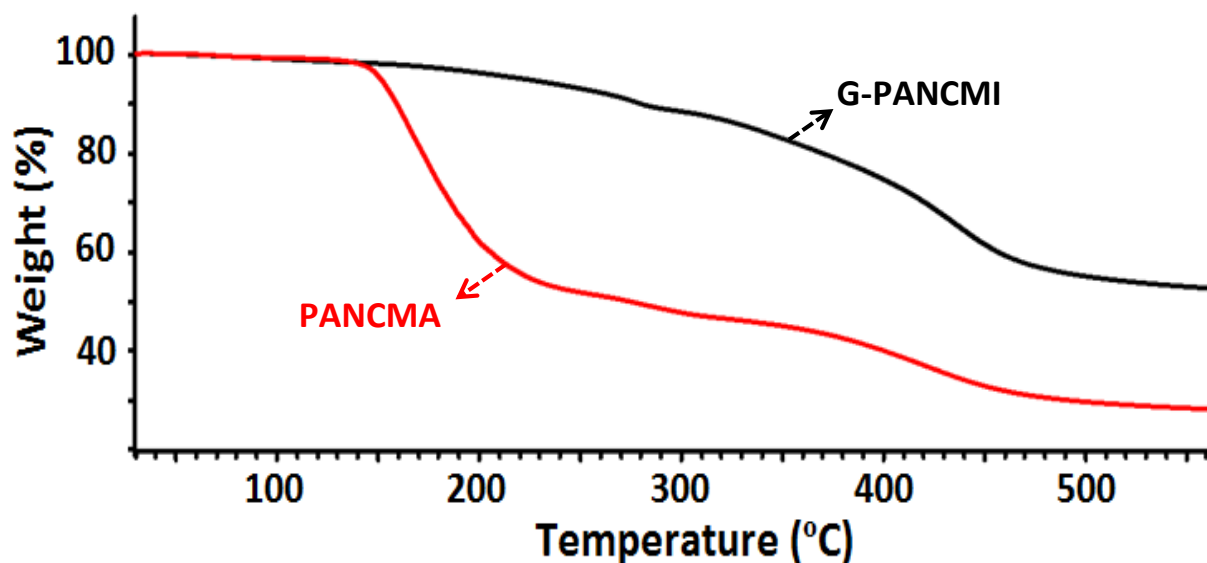


Figure 8.7 TGA analyses of PANCMA and G-PANCMII membranes

8.3.5. CONTACT ANGLE ANALYSIS AND DISPERSIBILITY TEST

In order to evaluate the hydrophilicity of the ultra-wetting graphene based membrane, the prepared membranes were tested for their water contact angle (CA_w) and the data are presented in Figure 8.8(a). It is observed that the water contact angle of the G-PANCMII membrane is reduced to zero (ultra-wetting level) which is 100% lower than that of the PANCMA membrane (average CA_w of PANCMA membrane is 63.3°). The contact angle reduction for the G-PANCMII membrane is due to the presence of highly hydrophilic carboxyl ($-COOH$), hydroxyl (OH) and amine ($-NH_2$) functional groups on the surface of the graphene Nano sheets attached G-PANCMII. In recent studies, these functional groups have been shown to give similar significant improvements in the hydrophilicity of polymeric membranes¹³⁴⁻¹³⁸. The contact angle reduction with time was also evaluated for both the PANCMA and G-PANCMII membranes and the data are presented in Figure 8.8 (b). The CA_w of G-PANCMII membrane is reduced to zero within one second (as it is difficult to take readings manually within a second, the images were video recorded for subsequent analysis), whereas PANCMA membrane took 420 seconds to reach $<5^\circ$. The rapid reduction in contact angle of G-PANCMII membrane further confirmed its ultra-wettability of the modified graphene.

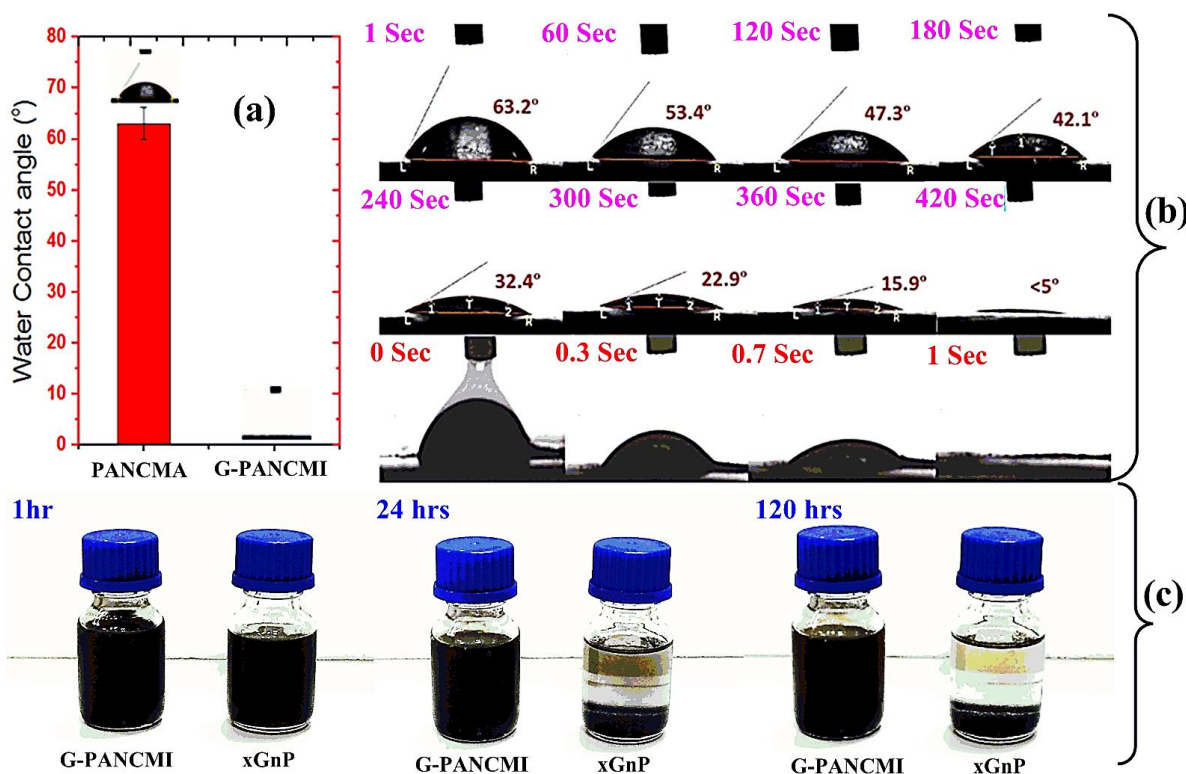


Figure.8.8. Average water contact angle (a), water contact angle reduction of the **PANCFMI** and **G-PANCFMI** membranes with time (b) and the dispersibility or stability of the unmodified (xGnP) and modified graphene (G-PANCFMI) in solution with time (c).

As the dispersibility of the xGnP attached to the polymer is critical to the fabrication of the water filtration membrane by phase inversion method, this parameter was visually evaluated for xGnP and G-PANCFMI. 1% solutions of xGnP and G-PANCFMI in DMAc were prepared in 50 ml glass bottles and ultrasonicated for 1 hr at 37 kHz. The ultrasonicated solutions were allowed to settle at a constant position at room temperature with relative humidity of 65-70%. Photos were captured 1 hour after ultrasonification and at every subsequent 24 hrs up to 120 hrs. The photos are presented in Figure 8.8c. The images clearly show that the xGnP completely settles down within a few hours whereas the G-PANCFMI remains dispersed, proving that the modified xGnP is more stable in solution for more than 120 hrs. This behavior of high dispersibility is due to the increased polarity and charge density of the surface of modified graphene containing carboxyl, hydroxyl and amine functional groups^{160,164}.

8.3.6. MORPHOLOGY ANALYSIS

The surface morphology and cross section of the PANCMA and ultra-wetting graphene based G-PANCM I membranes were examined using SEM (Figure 8.9). Although both membranes had an average thickness of 100 μ m, they exhibited different internal structures depending on their composition. The PANCMA membrane shows the presence of a large number of macro voids in its internal structure, whereas the ultra-wetting graphene modified G-PANCM I membranes is populated with more sponge-like structures in the cross section next to the internal surface. The presence of highly hydrophilic amine, hydroxyl and carboxylic groups in the ultra-wetting graphene increases the viscosity and the coagulation potential of the casting solution. This increase in coagulation will slow down the non-solvent/solvent exchange. As a result, less water will be drawn into the membrane, reducing the macro voids in the ultra-wetting graphene modified G-PANCM I membranes^{135,136,304}. A macro voids free sponge-like structure helps to enhance the porosity, water permeability and selectivity of the membrane. Moreover, the even distribution of ultra-wetting graphene Nano sheets can be identified in the cross section and on the outer surface of the G-PANCM I membrane. Also, the actual G-PANCM I membrane is black whereas the PANCMA membrane still remains white in color.

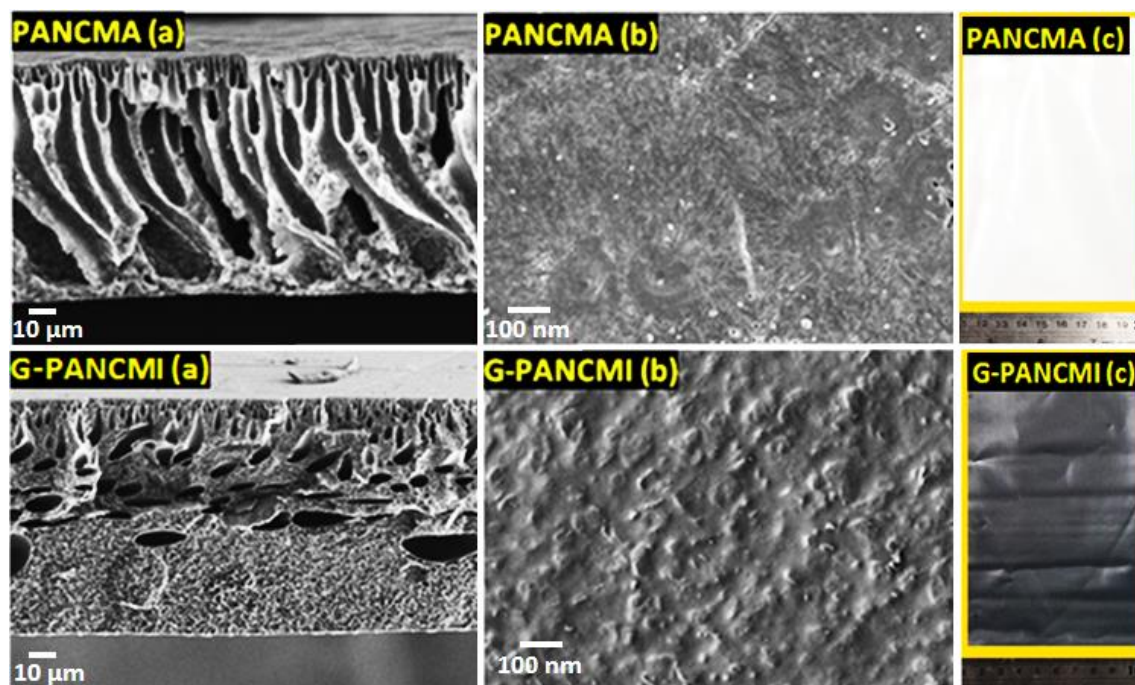


Figure.8.9. SEM images of PANCMA and G-PANCM I membranes (a) Cross section (b) Outer surface (c) Actual image of synthesized PANCMA and G-PANCM I membranes

8.3.7. PORE SIZE ANALYSIS

On examination of the average pore size of the PANCMA and G-PANCMII membranes, no significant difference is observed. The average pore size of PANCMI based membrane sample is $0.08 \pm 0.02\mu\text{m}$ and $0.07 \pm 0.02\mu\text{m}$ for the G-PANCMII based membrane.

8.3.8. CLEAN WATER FLUX TEST

The prepared PANCMA and G-PANCMII membranes were tested to evaluate the clean water flux by cross flow filtration method^{135,136} at constant feed water pressure of 100 kPa and the data are presented in Figure 8.10 (a). The PANCMA membrane gave a pure water flux of 435 ± 14 LMH. Even though the pore size is similar for both membranes, the G-PANCMII membrane gave higher pure water flux of 978 ± 27 LMH which is around 126% higher compared to the PANCMA membrane. This increase in pure water flux is due to the increase in hydrophilicity or wettability of the membrane by carboxylic, hydroxyl and amine functional groups which are attached to the graphene nanosheet¹³⁴⁻¹³⁸. These functional groups attract water towards the membrane surface by inter molecular hydrogen bonding which leads to an increase in permeability^{134,135,298,299}.

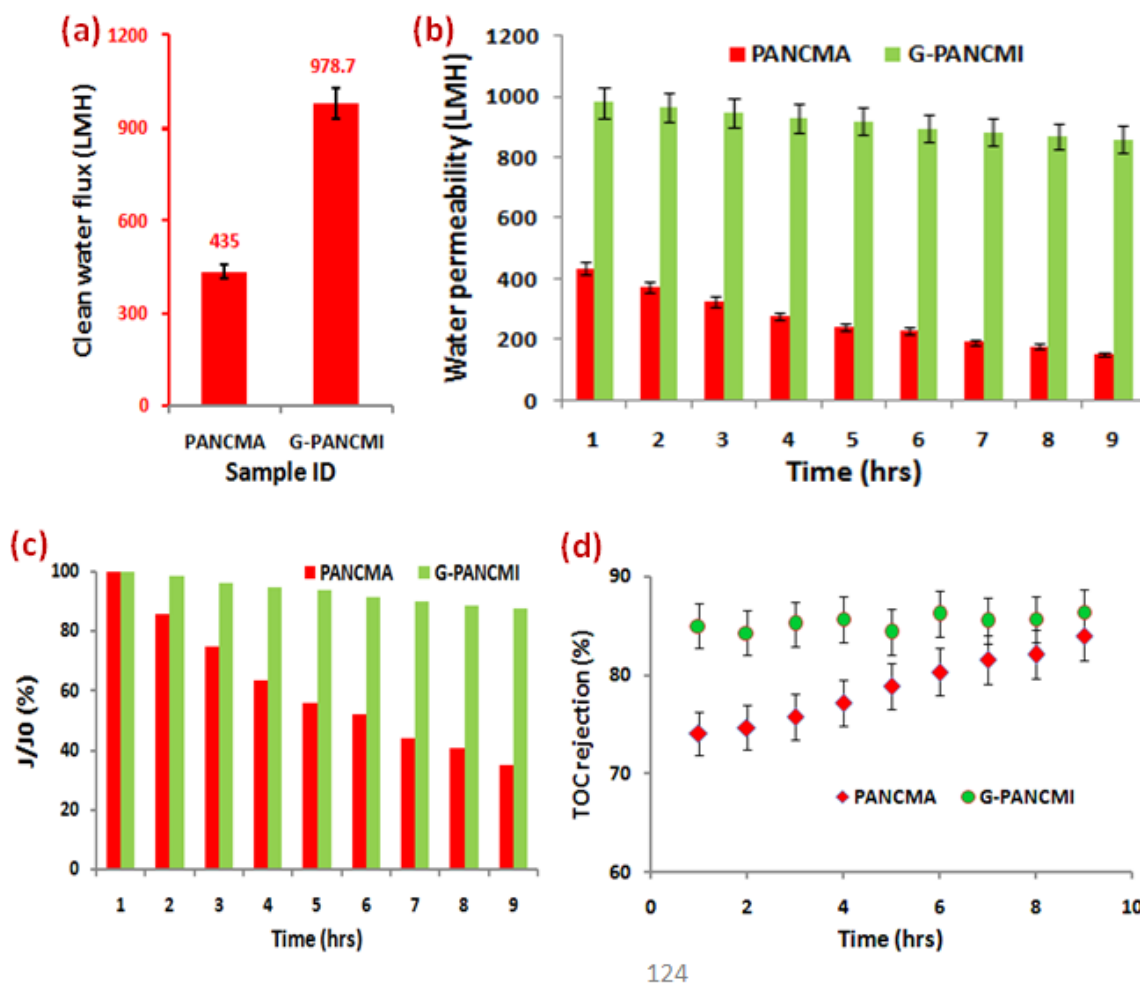


Figure.8.10. Pure water flux at 1bar feed pressure (a), water permeability during long time run with 10ppm BSA solution at 1bar feed pressure (b), normalized water permeability for the BSA solution separation during long time run (c) and BSA protein (TOC) removal efficiency in % (d)

8.3.9. LONG TIME PERFORMANCE AND FOULING EVALUATION

To evaluate the antifouling efficiency of the membrane, a 9hrs filtration test was conducted using 10ppm BAS in DI water as a feed solution. The results are summarized in Figure 8.10 (b). It is observed that the G-PANCMi membrane gives a more stable flux compared to PANCMA membrane samples. Figure 8.10 (c) shows the normalized permeability or flux drop over time. The flux drops for the G-PANCMi membrane is only 12.3% of the initial flux after 9hrs protein separation whereas the PANCMA membrane flux drop is 64.3% for the same duration of operation. The obtained results highlight that the presence of negatively charged $-\text{COOH}$ and $-\text{NH}_2$ in the

ultra-wetting graphene based G-PANCMCI membrane can best repel the protein from the surface of the membrane.

In order to evaluate the selectivity and the filtration efficiency of the membrane, the total organic carbon (TOC) of the feed BAS solution and permeate water were measured. Four samples were collected every 60mins with 15mins frequency and the TOC was measured in order to get the average TOC removal over time. Percentage of TOC rejection was calculated and presented in Figure 8.10 (d). From the experimental data, it is found that the TOC removal of the G-PANCMCI membrane is also higher and more stable compared to PANCMCI membrane. This may be due to the slight difference in the average pore sizes of the membrane. The pore size of the membrane sample M4 ($0.08 \pm 0.02\mu\text{m}$) was slightly lower compared to sample S1 ($0.07 \pm 0.02\mu\text{m}$). This result also confirms the increased hydrophilicity or wettability of the ultra-wetting graphene based G-PANCMCI membranes by negatively charged $-\text{OH}$ and $-\text{COOH}$ on the membrane surface. Recent studies have also shown that the negative surface charge of the membrane prevents the deposition of the negatively charged colloidal particles such as proteins, lipids and amino acids etc., on the membrane surface by electrostatic repulsion, which could slow down or reduce the membrane fouling¹³⁵⁻¹³⁸. A similar effect is also apparent in the present work, as depicted in the illustration shown in Figure 8.11(a). The electrostatic repulsion between the membrane surface and protein and hydrogen bonding between H_2O and $-\text{NH}_2$ and $-\text{COOH}$ of the G-PANCMCI membrane are also highlighted in the graphical abstract. On a related note, it is interesting to see from Figure 8.10 (d) that the increase in TOC removal efficiency of the control PANCMCI membrane with time may be due to the pore constriction/pore blocking or development of fouling on the membrane surface³⁰⁹. A confocal laser scanning (CLSM) analysis was conducted on the membrane samples to evaluate the protein absorption on the membrane surface and the images are presented in Figure 8.11 (b).

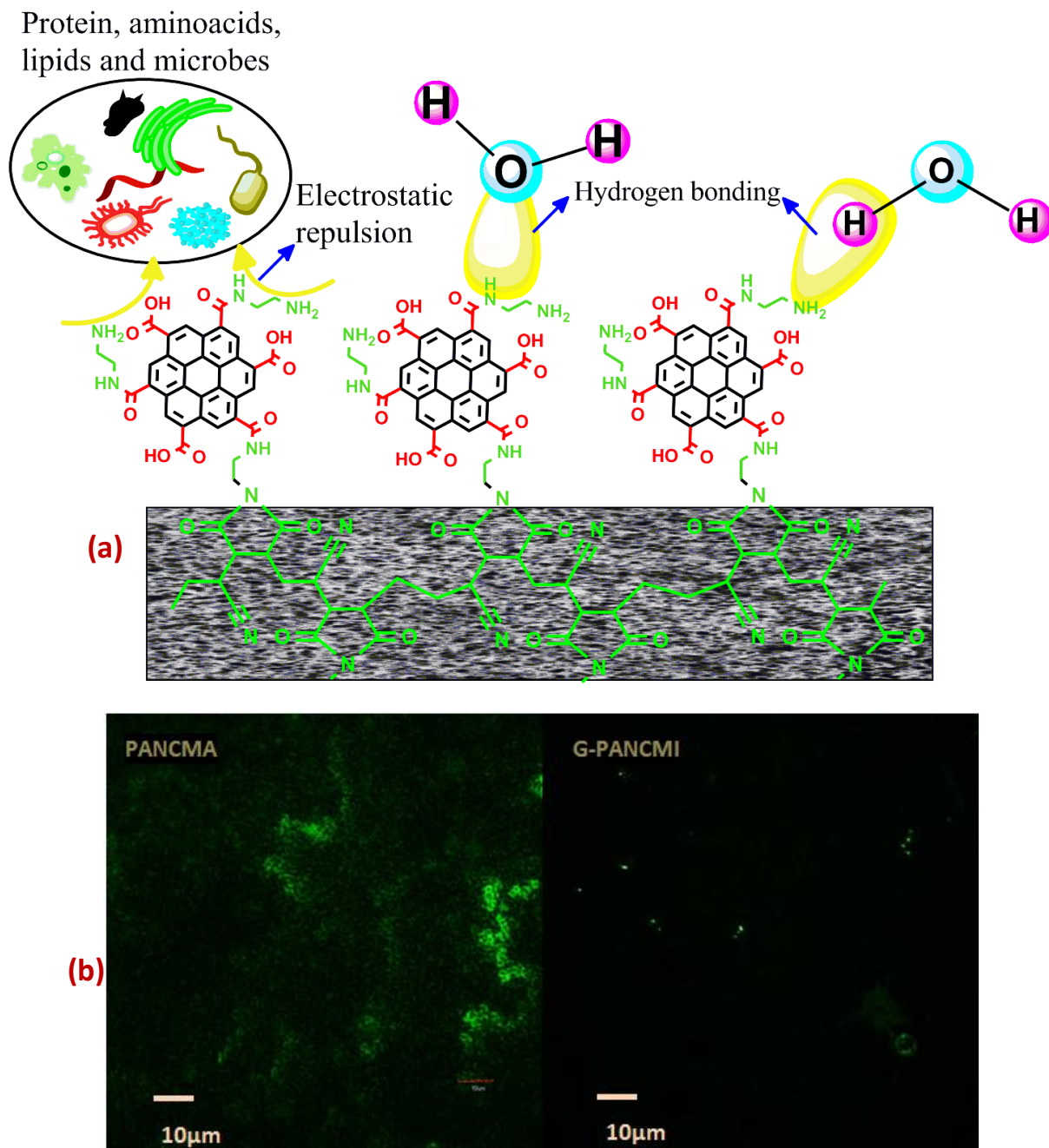
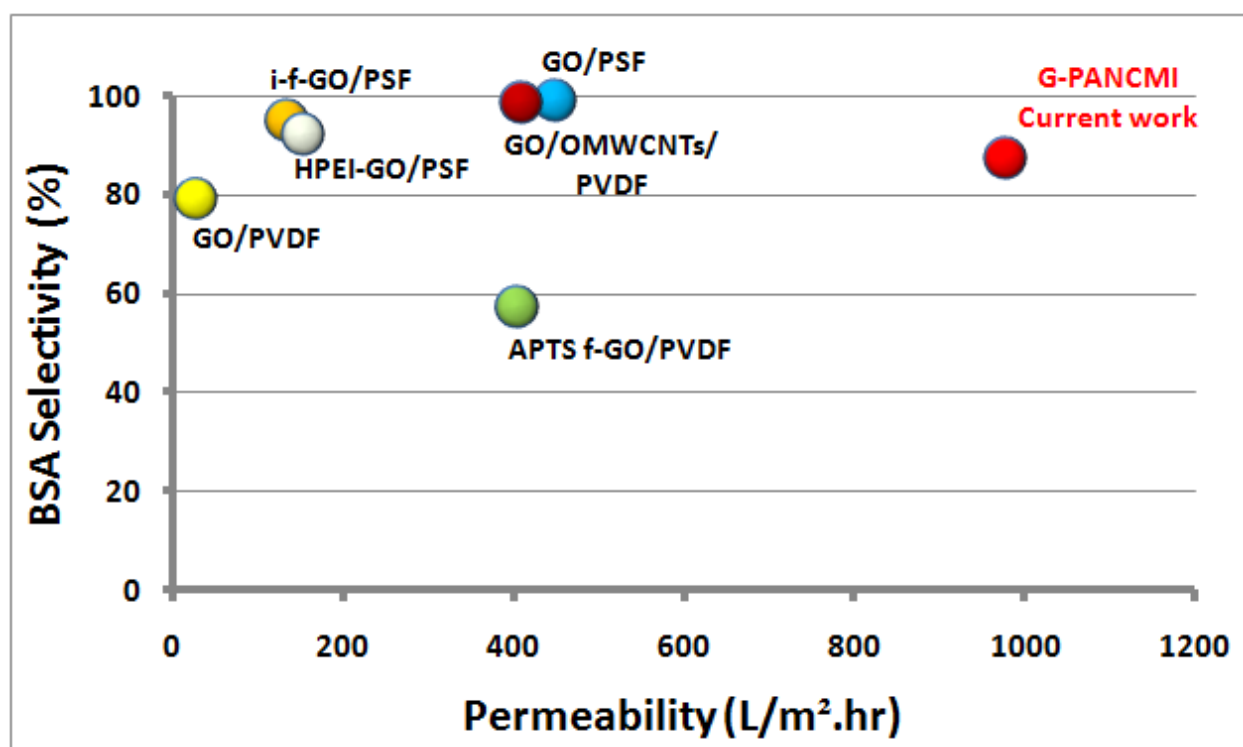


Figure.8.11. Schematic representation of hydrogen bonding and protein repulsion of the novel membrane (a) and confocal laser analysis of the membrane after protein filtration (b)

From the images it can be further confirmed that the protein adsorption on the G-PANcMI membrane surface can be negligible in contrast to the relatively high protein adsorption on the PANcMA membrane. Finally the performance of the ultra-wetting graphene based membrane was

compared against different current state of art polymer-graphene oxide (GO) composite ultrafiltration membranes in terms of permeability and BSA selectivity and the data are presented in Figure 8.12. From the data it can be easily identified that the ultra-wetting graphene based membrane gives at least 2 times higher permeability compared to the best performing current state of art membranes without much change in the selectivity^{132,315-319}. Based on our findings, it can be concluded that the ultra-wetting graphene offers the distinct potential to be an ideal material with significantly improved properties for new generation water filtration membranes.



- C. Zhao et al., 2013³¹⁵, ● H. Zhao et al., 2013¹³², ● L. Yu et al., 2013³¹⁶,
● J. Lee et al., 2013³¹⁷, ● Z. Xu et al., 2014³¹⁸, ● J. Zhang et al., 2013³¹⁹,

Figure 8.12: Comparison of the performance of the ultra-wetting graphene based membrane against different current state of art polymer-graphene oxide (GO) composite ultrafiltration membranes in terms of permeability and BSA selectivity

8.3.10. OILY WASTE WATER TREATMENT

In order to evaluate the effect of our novel ultra-wetting graphene based G-PANCMi on the wettability/hydrophilicity of other commercially well-known materials, a 5% of G-PANCMi was blended with polyethersulfone (PES) dope solution as a hydrophilic additive to produce ultrafiltration membranes for oily waste water treatment and compared against the membrane without G-PANCMi. The prepared membranes were characterized for their morphology, water and oil contact angle, liquid entry pressure of oil, water permeability or pure water flux and finally the prepared membranes were subjected to a continuous 8 hrs filtration test of oily waste water.

The surface morphology and cross section of the PES and ultra-wetting graphene modified PES-G-PANCMi based hollow fiber membranes were examined using SEM and presented in Figure 8.13. (a) cross section, (b) outer surface and (c) shows the actual image of the prepared PES and PES-G-PANCMi hollow fiber membranes. Both membranes had an average inner diameter of 0.6mm and an outer diameter of 1.2mm. However, the hollow fiber membranes exhibit different internal structures depending on their composition. The PES membrane shows the presence of a large number of macro voids in its internal structure, whereas the ultra-wetting graphene modified PES-G-PANCMi hollow fiber membranes has a lower macro voids with more sponge-like structures in the cross section next to the internal surface. This may be due to the increase in viscosity and the coagulation value of the casting solution due to the presence of highly hydrophilic amine and carboxylic groups in the ultra-wetting graphene which slow down the nonsolvent/solvent exchange. As a result less water is drawn into the membrane which leads to the sponge like structure. Sponge like structure helps to enhance the water permeability and selectivity. In addition, the even distribution of ultra-wetting graphene nano sheets can be identified in the cross section and on the outer surface of the PES-G-PANCMi modified membrane.

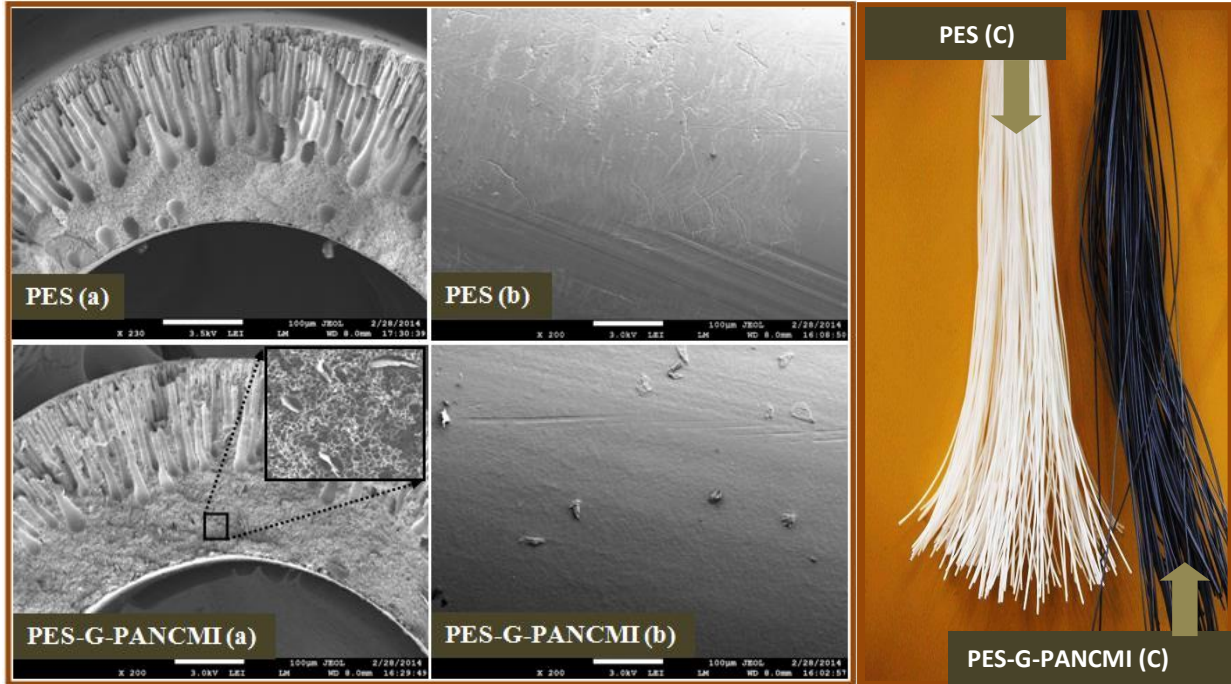


Figure.8.13. SEM images of PES and PES-G-PANCMCI membranes (a) Cross section (b) Outer surface (c) Actual image of synthesized PES and PES-G-PANCMCI membranes

The average pore size of the PES membrane and the ultra-wetting graphene modified PES-G-PANCMCI membranes were measured. The experimental data indicate that there is no significant difference in the mean pore size of both PES and PES-G-PANCMCI membranes. The average pore sizes of PES membrane is $0.07 \pm 0.02\mu\text{m}$ and $0.07 \pm 0.03\mu\text{m}$ for the PES-G-PANCMCI membrane.

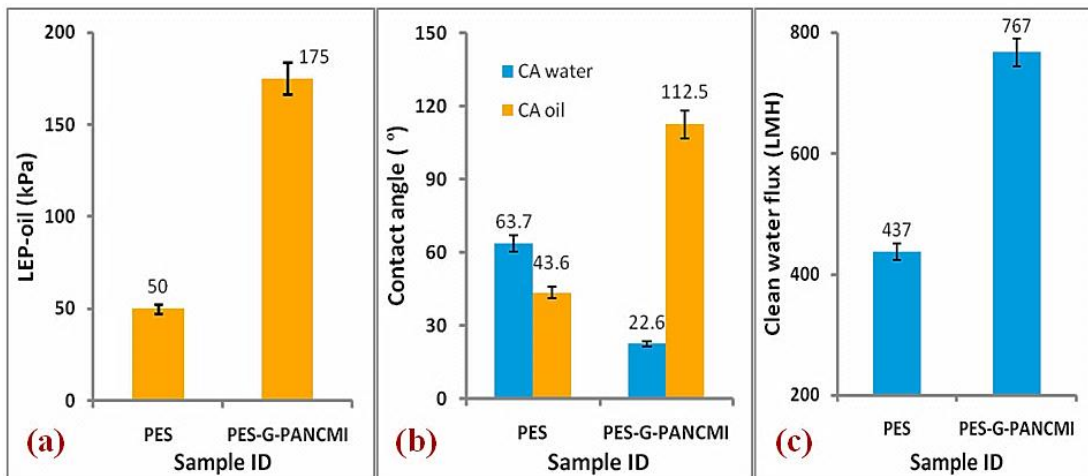


Figure.8.14. (a) Liquid entry pressure of oil (LEP_{oil}) analysis, (g) Water and oil contact angle and (c) Clean water flux of the PES and PES-G-PANCMCI membrane samples

CHAPTER: 8

Figure.8.14. shows average LEP_{oil} , water and oil contact angles and clean water flux of the membranes together with its error range. The experimental data indicates that the G-PANCMIs play an important role in the wettability of the PES-G-PANCMIs membrane. The water contact angle of the PES membrane is reduced by 64.5% from $63.7 \pm 3.8^\circ$ to $22.6 \pm 2.5^\circ$, by adding 5% of G-PANCMIs. The addition of 5% G-PANCMIs also helps to increase the oil contact angle of the PES membrane from $43.6 \pm 3.5^\circ$ to $112.5 \pm 3.2^\circ$ which is 158% higher compared to that of the PES membrane sample. More importantly, the liquid entry pressure (LEP_{oil}) increases from 50 ± 10 kPa of PES membrane to 175 ± 25 kPa of PES-G-PANCMIs membrane with ultra-wetting graphene, which is 350% increase. Moreover, the addition of 5wt% G-PANCMIs to PES increases the water permeability by 43% without any change in the selectivity and the same trend was found during the long term experiment with oily wastewater filtration. Based on our findings we conclude that the ultra-wetting graphene will be an ideal new generation material for water filtration membranes.

The prepared PES membrane and the ultra-wetting graphene modified PES-G-PANCMIs ultrafiltration membrane were tested to evaluate the clean water flux of the membrane using a cross flow filtration method. Figure.8.14. (c) shows the clean water flux for both membranes at a constant feed water pressure of 100 kPa (1bar). The PES membrane gave a pure water flux of 437 ± 18 LMH. Even though their pore size are similar for both membrane, the ultra-wetting graphene modified PES-G-PANCMIs based membrane gave higher pure water flux of 767 ± 23 LMH which is around 43% higher compared to the PES based membrane. This increase in pure water flux is due to the increase in hydrophilicity / wettability of the membrane.

To evaluate the performance of the prepared membrane in oil water separation, a long time (8 hrs) filtration test was conducted using 200ppm oil (oil emulsion) in DI water for the control PES membrane and the PES-G-PANCMIs membrane individually, and the results are summarized in Figure 8.15 (a) Permeability (flux drop) and (b) oil removal efficiency of the membrane samples PES&PES-G-PANCMIs. It is observed that the ultra-wetting graphene modified PES-G-PANCMIs membrane gives stable flux compared to PES based membrane.

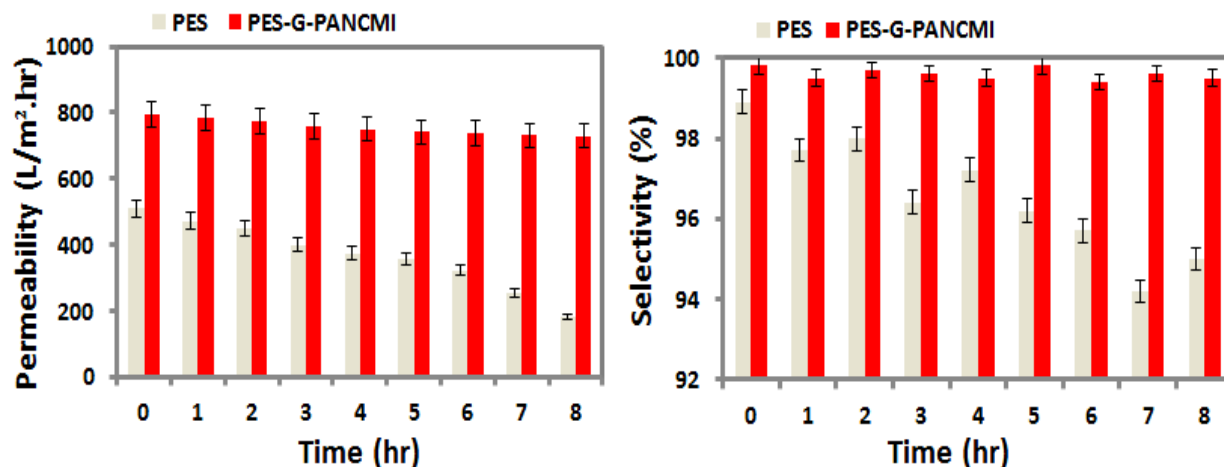


Figure 8.15 (a) Permeability (flux drop) and (b) oil removal efficiency of the membrane samples PES&PES-G-PANCMi in a long time study of 8 hrs

The flux drops for the PES-G-PANCMi membrane is only 9.2 (<10) % of the initial flux after 8 hrs oil emulsion in water separation whereas the PES membrane's flux drop is 65% for the same duration of operation. The obtained results highlight that the presence of G-PANCMi helps to reduce fouling (oil deposition) on the membrane surface. In order to evaluate the oil-emulsion selectivity of the membrane, the total organic carbon (TOC) of the feed oil-emulsified solution and permeate were measured. Percentage of oil emulsion rejection (selectivity) was calculated and presented in Figure 8.15 (b). From the data, it is found that the oil emulsion removal of the PES-G-PANCMi membrane is also higher and stable compared to the control PES membrane. These result further confirms the increased hydrophilicity of the PES membranes by G-PANCMi. Based on our findings, we conclude that the ultra-wetting graphene offers the distinct potential to be an ideal material with significantly improved properties for new generation water filtration membranes.

8.4. SUMMARY

In this chapter, a simple and feasible fabrication method is devised to bring the high end nano carbon based material to real downstream applications. In order to achieve this objective, the wettability of graphene was initially increased to an ultra-wetting level by incorporating amine and carboxyl functionality onto the graphene. The amine and carboxylated graphene was then covalently attached to a polymer matrix to fabricate a water filtration membrane. The characterization of the modified supported graphene based membrane indicates that significantly

CHAPTER: 8

higher hydrophilicity than previously expected is achieved, with the water contact angle reduced to zero. The ultra-wetting graphene increases the water permeability of the membrane by 1.26 times without any changes in the selectivity. Based on our findings, we conclude that the ultra-wetting graphene will be an ideal material for new generation water filtration membranes.

This study, also evaluated the effect of incorporation of our novel ultra-wetting graphene based G-PANCMi on the wettability/hydrophilicity of other commercially well-known materials, a 5% of G-PANCMi was blended with polyethersulfone (PES) dope solution to produce ultrafiltration membranes and tested for oily waste water treatment. The experimental data indicates that by incorporating 5wt% of this G-PANCMi, the the water contact angle of the PES membrane can be reduced by 64.5%. It also helps to increase the oil contact angle of the PES membrane by 158% compared to that of the PES membrane sample. More importantly, the liquid entry pressure (LEP_{oil}) can be significantly increased by adding this G-PANCMi as an additive to the PES membrane.

9. Performance comparison of all the developed membranes

9.1. SUMMARY OF RESULTS

In this thesis, a novel concept was proposed and practised to prevent bio-fouling by developing a self-cleaning membrane surface having additional enhanced hydrophilicity via newly synthesized water insoluble highly hydrophilic polymeric additive blended with the PES dope solution and bring them to the membrane matrix. In order to develop a self-cleaning surface, highly hydrophilic, negatively charged carboxylic (-COOH), hydroxyl (-OH) and amine (-NH₂) functional groups rich double bonded (alkenes) monomers (acrylonitrile, maleic acid/anhydride and diaminomaleio nitrile) were carefully chosen and polymerized by simple atom transfer radical polymerisation (ATRP) method to obtain highly hydrophilic water insoluble polymeric additives, as detailed in Chapters 5, 6 and 7 respectively. The antimicrobial silver nanoparticles were covalently anchored to the prepared additives. These new additives were then blended with PES dope solution to prepare the hollow fiber ultrafiltration membranes by dry wet spinning process.

The new surface chemistry so produced has been shown to be responsible for the self-cleaning property of the membrane surface. The mechanism of the self-cleaning process is shown in the Figure 9.1. From the schematic it can be clearly understood that, when the bacteria approaches the novel membrane surface, the antimicrobial silver kills them by rupturing their negatively charged plasma wall, which leads to the leakage of negatively charged protein molecules through the ruptured bacterial cell wall. At the same time, the highly hydrophilic, negatively charged acid, and hydroxyl functionalities prevents the deposition of these protein molecules onto the membrane surface by electrostatic repulsion. Thus, the membrane can exhibit the self-cleaning property. In addition, since the AgNPs are embedded (covalently attached) in the polymeric matrix of the additives, the leaching of AgNPs has been shown to be completely prevented.

In Chapter 8, another method was introduced to improve the performance of the PES membranes with the above functional groups incorporated highly hydrophilic graphene. In general, highly hydrophilic polymeric additives will have low mechanical and thermal stability. In order to

overcome these issue in this chapter, highly thermally and mechanically stable graphene was chosen and modified with above highly hydrophilic functional groups. The modified graphene was then attached to a highly hydrophilic water insoluble poly acrylonitrile co maleic acid and imidized by thermal imidization process. The imide and the graphene backbone will give high thermal and mechanical strength and the functional groups will enhance the surface property/wettability. These functional groups prevent the deposition of protein molecules onto the membrane surface by same electrostatic repulsion mechanism.

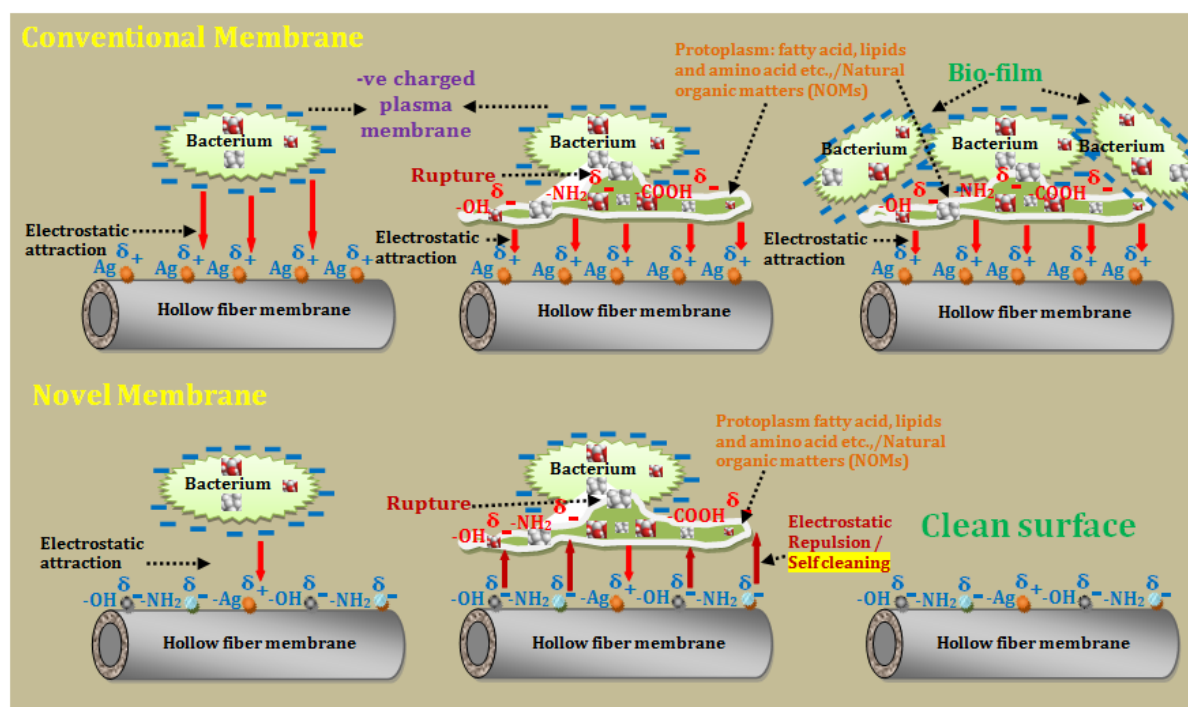


Figure.9.1. Schematic representation of self-cleaning mechanism of the new membranes

In this thesis, all together 4 new additives were newly synthesized and blended with PES dope solution and they include PEG-Ag attached PANCMMA, PEI-Ag attached PANCMMA, PANCMACDAMN and G-PANCMMA. The detailed synthesis, characterization methods and the performance evaluations of each additive are presented in Chapters 5, 6, 7 and 8 respectively. The membrane performance at a constant additive concentration of 5 wt% (5% is the optimum concentration for most of the membranes prepared in this thesis) are summarized in Table 9.1, in terms of hydrophilicity, permeability and selectivity

CHAPTER: 9

Table 9.1, Performance of various membrane prepared in this thesis in terms of hydrophilicity, permeability and selectivity

Sl.NO	Base membrane material	Additive	Additive concentration (wt %)	Hydrophilicity (CA_w) (°)	Permeability (LMH)	Selectivity (%)	Flux Drop (%)	Feed water
1	PES	0	0	62.6 ± 3.7	477	75	45-65*	**
2	PES	PANCMA-PEG-AG	5	15.3 ± 1.2	702	96.2	19.4	Surface water
3	PES	PANCMA-PEI-Ag	5	$32.7^\circ \pm 2.1$	687	81.2	16.3	Sodium alginate
4	PES	PANCMA-CDAMN-PEG-Ag	5	14.2 ± 2.3	858	91.9	14.3	BSA
5	PES / G-PANCFI	G-PANCFI	5	0.0 ± 0.0	978	99.6	9.2	Oil-water emulsion / BSA

*Tested with different waste water: **Challenged with all the listed feed water

9.2. COMPARISON OF VARIOUS MEMBRANE PREPARED IN THIS THESIS

In order to compare the effect of various functional groups (-COOH, -OH and -NH₂) containing materials (polymeric additives) on the performance of the PES ultrafiltration membrane, the improved hydrophilicity, water permeability and selectivity of the all prepared membranes including the control PES membrane and the membrane prepared only by using the novel additive (in the case of G-PANCFI) (in terms of % improvement) were analyzed and summarized in Figure 9.2. From the figure it can be seen that all the new additives blended membranes give better performance compared to the control membrane in terms of hydrophilicity, water permeability and selectivity.

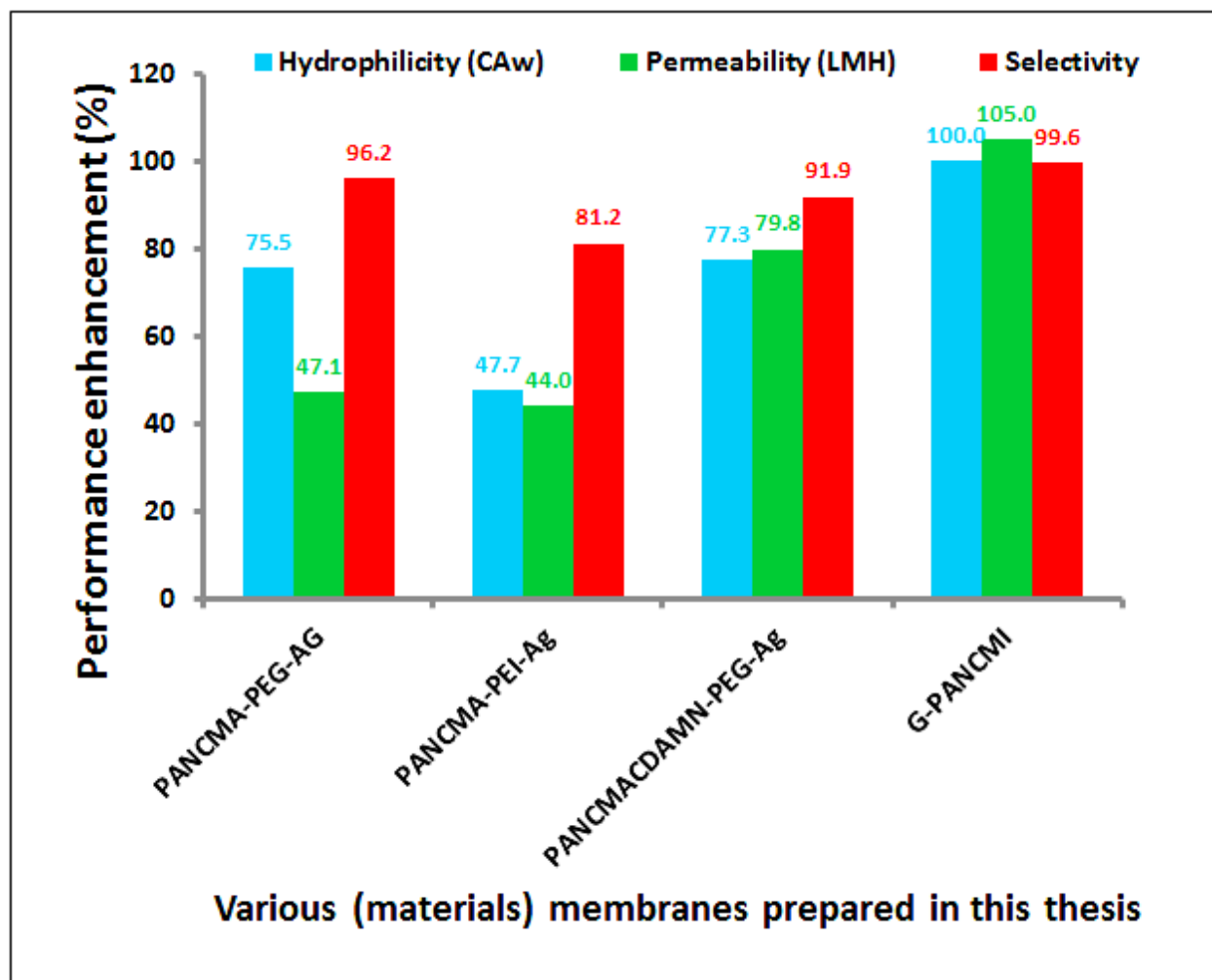


Figure.9.2. Comparison of various membranes prepared in this thesis

9.2.1. HYDROPHILICITY

When comparing the hydrophilicity of all prepared membranes, the water contact angle of the membranes is reduced significantly on incorporation of these new additives in the membrane structure. For instance, PEG-Ag attached PANCMA increase the wettability of the membrane by reducing the CA_w by 75.5% compared to the control PES membrane, Similarly, PEI-Ag attached PANCMA and PEG-Ag attached PANCMACDAMN gave reductions in contact angles of 47.7% and 77.3% respectively compared to the control membrane. Finally, the membrane prepared with

G-PANCMCI gives a water contact angle of zero (0°) which is 100% reduction compared to the control PES membrane.

On the basis of the above data, the effects of different additives on the hydrophilicity of the prepared membranes can be summarized as follows:

G-PANCMCI > PANCMACDAMN > PEG-Ag attached PANCMA > PEI-Ag attached PANCMA

9.2.2. WATER PERMEABILITY

In terms of water permeability, the membrane with additives containing $-\text{COOH}$, $-\text{OH}$ and $-\text{NH}_2$ functional groups demonstrates significant improvements in comparison with the control PES membrane. A schematic representation of inter molecular hydrogen bond formation by these hydrophilic functional groups and water is shown in Figure 9.3 below.

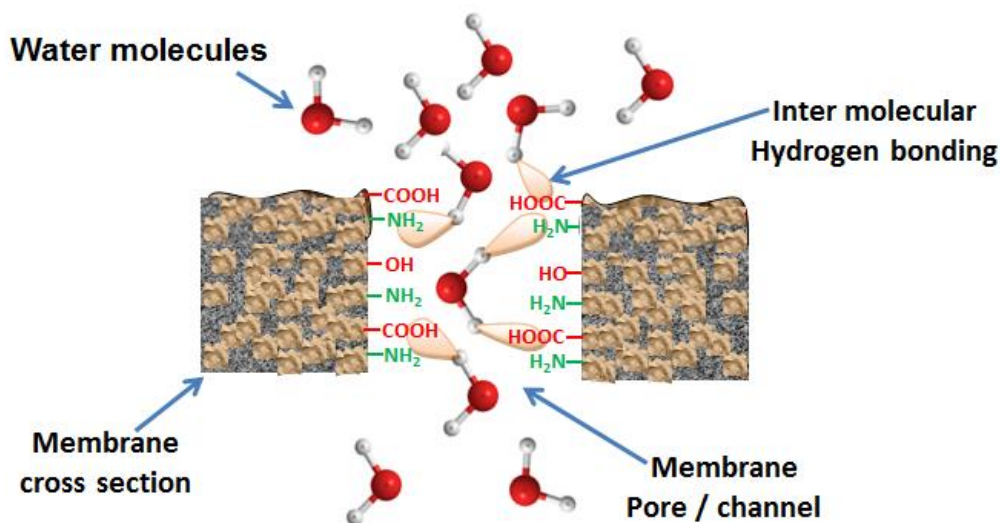


Figure 9.3. Schematic representation of water transportation through membrane surface by intermolecular hydrogen bonding between hydrophilic groups and water.

The PEG-Ag attached PANCMA increase the water permeability by 47.1%, PEI-Ag attached PANCMA 44.0% and PEG-Ag attached PANCMACDAMN also helps to increase the water permeability of the PES membrane by 79.8% compared to the control membrane. The membrane prepared with G-PANCMCI gives the highest water permeability of 105.0% compared to the control PES membrane.

The effects of different additives on the water permeability of the prepared membranes are as follows:

***G-PANCM1 >PEG-Ag attached PANCMACDAMN >> PEG-Ag attached PANCMA
>PEI-Ag attached PANCMA***

9.2.3. SELECTIVITY

The selectivity of the membranes were tested using different feed water spiked with protein solution/reservoir water/ oil emulsion and the data were discussed in individual chapters. Here the overall selectivity of the membranes are compared against the control PES membrane to compare the effect of different additives on the selectivity of the membrane. From the analysis it was found that the PEG-Ag attached PANCMA blended PES membrane's selectivity was 96.2% (reservoir water) whereas the control PES membrane selectivity was only 75% when tested with same reservoir water. Similarly, for PES membrane modified with PEI-Ag attached PANCMA, the membrane selectivity was found to be 81.2% whereas the control PES membrane selectivity was less than 70% while tested with protein solution. Another modification of PES with PEG-Ag attached PANCMACDAMN improved the membrane selectivity to 91.9% whereas the control PES membrane selectivity was less than 80% while tested with protein solution. Finally, PES membrane modified with G-PANCM1, showed the highest selectivity of 99.6% whereas the control PES membrane's selectivity was only less than 85% when tested with oil emulsion. However, the G-PANCM1 based membrane was found to have selectivity of around 85% for protein solution and 99.6% for oil water emulsion.

The effects of different additives on the selectivity of the prepared membranes are as follow

G-PANCM1 > PEG-Ag attached PANCMA > PANCMACDAMN > PEI-Ag attached PANCMA

9.2.4. EFFECT OF FUNCTIONAL GROUPS ON THE ANTI-FOULING PROPERTIES

Finally, the effect of functionalizing PES membranes with various functional groups (-OH, -COOH and -NH₂) on the anti-fouling (organic fouling) efficiency of the PES membrane was investigated by studying the permeability drop or flux drop (in %) of the membranes over time

using various feed water (reservoir water, protein solution, polysaccharide solution and oil-water emulsion). Carboxyl (-COOH) functional group rich PANCMA was used as a base additive and PANCMA was further grafted with various hydrophilic polymers to evaluate their effect on the PES membrane. In chapter 5, the PES membrane was functionalized with -COOH and -OH functional groups by blending PEG-Ag grafted PANCMA to PES and the membranes were challenged with reservoir water in a 66 hrs continuous experiment. The flux drop for the control PES membrane is much higher (45.3% of the initial flux) compared to the -COOH and -OH functionalized PES-PANCMA-PEG-Ag membrane (19.4% of the initial flux). In chapter 6, the PES membrane was functionalized with -COOH and -NH₂ functional groups by blending PEI-Ag grafted PANCMA to PES and membranes were tested with sodium alginate (a polysaccharide) solution. The flux drop for the -COOH and -NH₂ modified membrane is lower (16.3% of the initial flux) than the control PES membrane (55.3% of the initial flux). Similarly, in chapter 7, the PES membrane was functionalized with three different (-COOH, -OH and -NH₂) functional groups by blending PANCMACDAMN polymer to PES membranes and the membranes were tested with bovine serum albumin (BSA) solution. The flux drop for the PES membrane functionalized with three different (-COOH, -OH and -NH₂) functional groups is only 14.29% of the initial flux after 12 hrs protein separation whereas the flux drop for control PES membrane is 60% for the same duration of operation. Finally, in chapter 8, the PES membrane was modified by blending functionalized graphene grafted PANCMA with PES and the membranes were tested with oil-water emulsion. The flux drops for the PES-G-PANCMCI membrane is only 9.2 (<10) % of the initial flux after 8 hrs oil emulsion in water separation whereas the PES membrane's flux drop is 65% for the same duration of operation.

From the experimental data, it is clear that functionalization of PES membranes with hydrophilic functional groups (-COOH, -OH and -NH₂) helps to improve the antifouling properties of the PES membrane by improving the hydrophilicity and zwitterionic effect. More particularly the combination of all three functional groups are giving better anti-fouling properties than just one or two functional groups.

10. Conclusions and Recommendations

10.1. CONCLUSIONS

In general, PES ultrafiltration membranes are modified by blending either hydrophilic additives or antibacterial compounds (most commonly silver) with the dope solution. However, these hydrophilic additives are normally water soluble and hence, the elution of these additives is unavoidable during harsh operations. It has been proven that silver can kill the bacteria by rupturing the plasma membrane. However, once the plasma membrane ruptures, the negatively charged protoplasm compounds deposits onto the positive surface of the membrane by electrostatic attraction which will eventually inactivate the silver ion/particle. Furthermore, as the silver nanoparticles are typically just blended in, they tend to leach out into the permeate water due to the harsh operating conditions.

In this thesis, a novel concept was proposed and experimentally proved to prevent bio-fouling by developing a self-cleaning membrane surface having additional enhanced hydrophilicity via newly synthesized water insoluble highly hydrophilic polymeric additives blended with PES dope solution. The self-cleaning capability arises from a neutral surface which contains positive charged antimicrobial silver nanoparticles and highly negatively charged functional groups. In order to develop a self-cleaning surface, highly hydrophilic, carboxyl (-COOH), hydroxyl (-OH) and amine (-NH₂) functional groups rich double bonded (alkenes) monomers were carefully chosen and polymerized by atom transfer radical polymerization method to obtain highly hydrophilic water insoluble polymeric additives. The antimicrobial silver nanoparticles were covalently anchored to the prepared additives by thermal grafting method. The new surface chemistry will be responsible for the self-cleaning surface. When the bacteria approaches the novel membrane surface, the antimicrobial silver will kill them by rupturing their negatively charged plasma wall (which leads to the leakage of negatively charged protein molecules through the ruptured bacterial cell wall), whereas the highly hydrophilic, negatively charged hydroxyl and carboxyl functionalities will prevent the deposition of these protein molecules onto the membrane surface by hydrophobic hydrophilic repulsion and electrostatic repulsion. Thereby, the membrane can exhibit the self-cleaning property.

In total, four new additives were used in this thesis: PEG-Ag attached PANCMA, PEI-Ag attached PANCMA, PEG-Ag attached PANCMA CDAMN and amine and carboxylated graphene attached PANCMI (G-PANCMI). These new additives were blended with PES dope solution to prepare the hollow fiber ultrafiltration membranes by dry wet spinning process. In addition, the additive G-PANCMI alone was used to produce membrane without PES. All prepared membranes were characterized thoroughly and their performances were evaluated in terms of hydrophilicity, water permeability, and selectivity with various types of feed water. The antifouling properties of the membrane was measured by flux drop method.

In chapter 5, it was shown that highly hydrophilic carboxylic (-COOH) functional groups rich water insoluble poly (acrylonitrile-co-maleic acid) (PANCMA) blended with covalently attached highly hydrophilic hydroxyl (-OH) rich polyethylene glycol (PEG) and antimicrobial silver nanoparticles (Ag) in the PES dope solution resulted in significantly increased membrane hydrophilicity. This finding was based on the reduction of the water contact angle of the pure PES UF membrane by around 75.5% (from 62.6 ± 3.7 to $15.3 \pm 1.2^\circ$) for the modified membrane containing 5% of PANCMA. As a result of the increased hydrophilicity, the pure water flux increased by about 36% from 513 LMH for the pure PES membrane to 702 LMH for the same modified membrane. An antibacterial study based on the zone of inhibition test clearly highlighted the improved antibacterial properties of the modified membrane compared to the pure PES membrane. Long time tests with reservoir water also gave promising results whereby the PANCMA modified membrane exhibited a lower flux drop giving a stable flux compared to the control PES membrane.

In chapter 6, a novel concept was proposed to prevent bio-fouling by developing a killing and self-cleaning membrane surface and experimentally proved. In order to develop a self-cleaning surface the functional groups on the surfaces were carefully chosen. Negatively charged carboxylic group (-COOH) rich, hydrophilic water insoluble PANCMA was chosen as a base additive. Instead of PEG (Chapter 5), amine (-NH₂) rich PEI was chosen as another additive and positively charged antimicrobial silver (Ag⁺) was chemically attached to it by thermal grafting. This Ag grafted PEI was attached to the base PANCMA additive to get the final additive PANCMA-PEI-Ag. 5% of the modified PANCMA-PEI-Ag was then blended with PES dope solution to prepare the hollow fiber ultrafiltration membranes by dry wet spinning process. The innovative surface chemistry helps to reduce the contact angle of the PANCMA-PEI-Ag modified membrane by at least a 48% and

increase the pure water flux by 39.4% compared to the control membrane. The flux drop for the novel membrane was also lower (16.3% of the initial flux) than the control membrane (55.3% of the initial flux) during the long term experiments with protein solution. Moreover, the novel membrane continued to exhibit inhibition to microbes even after 1320 min of protein filtration.

Chapter 7 further confirmed the novel concept to prevent bio-fouling by developing a killing and self-cleaning membrane surface having additional enhanced hydrophilicity via a new polymeric additive poly (acrylonitrile co maleic acid co di-amino maleionitrile) (PANCMAVDAMN). This co-polymer formed from negatively charged carboxylic (-COOH) and amine (-NH₂) rich alkene monomers including maleic anhydride, diamino maleionitrile and acrylonitrile imparts important hydrophilic functionalities to the membrane together with covalently attached PEG via the presence of carboxylic (-COOH), amine (-NH₂) and hydroxyl (-OH) groups in their structure. The presence of positively charged antimicrobial silver (Ag⁺) contributes to the antimicrobial properties of the membrane. The improvements in properties for the modified membrane include:

- (1) A reduction in the contact angle of the modified membrane by at least a 78.1% from 64.6± 3.2° for the control membrane to 14.2±2.3° for the modified membrane was achieved.
- (2) An increase in water flux, with the highest flux achieved in this study being 1050.23± 24 LMH for the novel additive modified membrane which is around 120% higher than the control membrane (477.62± 18.2 LMH) due to the increased hydrophilicity was achieved. The flux drop (after 720 min of protein filtration) for the novel membrane is also lower (14.29% of the initial flux) than the control membrane (around 60% of the initial flux) during the long term experiments with protein solution.
- (3) The selectivity is also improved (around 20%) for the new additive modified membrane.

Chapter 8 discussed a novel method to produce carboxylic, hydroxyl and amine functionalised graphene attached PANCMI and its effect on the PES membrane. In this chapter, highly thermally and mechanically stable graphene was chosen and modified with above functional groups. The modified graphene was then covalently attached to a highly hydrophilic water insoluble poly acrylonitrile co maleic acid and imidized by thermal imidization process. The rigid imide and the graphene backbone will give high thermal and mechanical strength while, the highly hydrophilic functional groups will enhance the surface wettability and prevent the deposition of protein onto the membrane surface. The functionalized graphene attached G-PANCMI was used as an additive

to fabricate the membrane. The experimental data indicate that the G-PANCMIs play an important role in the wettability of the PES-G-PANCMi membrane. The water contact angle of the PES membrane is reduced by 64.5% from $63.7 \pm 3.8^\circ$ to $22.6 \pm 2.5^\circ$, by adding 5% of G-PANCMi. The addition of 5% G-PANCMi also helps to increase the oil contact angle of the PES membrane from $43.6 \pm 3.5^\circ$ to $112.5 \pm 3.2^\circ$ which is 158% higher compared to that of the PES membrane sample. More importantly, the liquid entry pressure (LEP_{oil}) increases from 50 ± 10 kPa of PES membrane to 175 ± 25 kPa of PES-G-PANCMi membrane with ultra-wetting graphene, which is 350% increase. This increase in LEP_{oil} is due to the increased hydrophilicity or oleophobicity. Moreover, the addition of 5wt% G-PANCMi to PES increases the water permeability by 43% without any change in the selectivity and the same trend was found during the long term experiment with oily wastewater filtration. Finally, G-PANCMi based ultrafiltration membrane was prepared without PES. The characterization of the modified supported graphene (G-PANCMi) based membrane indicated that significantly higher hydrophilicity than previously expected can be achieved, with the water contact angle reduced to zero. The ultra-wetting graphene increases the water permeability of the membrane by 126% without compromising its selectivity.

Based on the experimental data the overall performances of the additives are in the following order: ***G-PANCMi > PEG-Ag attached PANCMCADAMN > PEG-Ag attached PANCMMA > PEI-Ag attached PANCMMA.***

Synthesis of self-cleaning ultrafiltration membrane with long lasting properties opens up a viable solution for bio-fouling in ultrafiltration application for wastewater purification and based on the findings in this study, it can be concluded that the ultra-wetting graphene will be an ideal material for new generation water filtration membranes.

10.2 RECOMMENDATIONS

Based on the experimental results obtained, the discussions presented and the conclusions made from this research, the following recommendations may be interesting for future investigation related to this topic:

- 1) Further investigations on the synthesis of G-PANCMi are needed to simplify the modification methods and to reduce the material cost for industrial applications. In the present study, graphene was first modified with concentrated acids to bring $-COOH$ and $-OH$ groups on the surface and

followed by thionyl chloride and ethylene diamine to modify with amine functional groups. Thionyl chloride modification is a tedious process and hence other simple methods have to be developed for amine modification and the synthesis of G-PANCMi.

2) The present work should be extended to explore the fabrication of G-PANCMi based hollow fiber membrane for application in large/pilot scale membrane filtration units to evaluate the life time validation of the membrane in an actual industrial environment. The present study is only based on the lab scale analysis and the maximum operation period was less than a month. Hence, in order to evaluate the long term performance of the membrane, a pilot scale production process has to be developed and the membranes need to be tested in an actual industrial setup to validate the life time of the membrane.

3) The present study should be extended to look into the possibility of using other positively charged polymeric materials, metal ions, metal oxides and metal complexes instead of silver nanoparticles as used in the current study. Apart from Ag, there are several other materials which can be studied with negatively charged hydroxyl, carboxylic and amine functional groups. The possible materials that can be tested are noble metals such as Hg, Cu, Cd, Cr, Pb, Co, Au, Zn, Fe, Mn, Mo and Sn. In addition to this materials, other polymeric materials with positive charge also can be tested.

4) Other membrane fabrication methods such as temperature induced phase separation (TIPS) and melt spinning may be explored for the synthesis of G-PANCMi hollow fiber membrane.

The current membrane development method is non-solvent induced phase separation (NIPS), instead of NIPS, TIPS can be explored. In TIPS method, the material loading can be increased in the final membrane matrix which will help to improve the mechanical strength of the membrane.

5) Dense membrane development (membranes with small pore size) can be explored by using G-PANCMi for other application like nanofiltration (NF), reverse osmosis (RO) and gas separation application. The current study focused on the development of hollow fiber ultrafiltration (UF) membrane and the new material G-PANCMi shows very good performance for this application. Other applications can be studied.

References

- 1 Prüss-Üstün A, B. R., Gore F, Bartram J. Safer water, better health: costs, benefits and sustainability of interventions to protect and promote health. Report No. ISBN 978 92 4 159643 5, (Geneva, 2008).
- 2 (UNEP)., U. N. E. P. (UNEP, Nairobi, Kenya., 2008.).
- 3 Shannon, M. A. *et al.* Science and technology for water purification in the coming decades. *Nature* **452**, 301-310 (2008).
- 4 Burbano, A. A. A., Samer S.; Pearce, William R. The State of Full-scale RO/NF Desalination - Results from a Worldwide Survey (PDF). *J. - Am. Water Works* **99**, Number **4**, 116-127 (April 2007).
- 5 Tripathi, B. P., Dubey, N. C., Choudhury, S. & Stamm, M. Antifouling and tunable amino functionalized porous membranes for filtration applications. *Journal of Materials Chemistry* **22**, 19981-19992, doi:10.1039/C2JM34172G (2012).
- 6 Mallevialle, J., Odendall, P.E., and Wiesner, M.R. (McGraw-Hill, New York, 1996).
- 7 Nollet, J. A. (Paris., 1748.).
- 8 Nollet J.A., (Paris, Recherchessur les causes du bouillonnement des liquides,).
- 9 Lonsdale, H. K. The growth of membrane technology. *Journal of Membrane Science* **10**, 81-181, doi:[http://dx.doi.org/10.1016/S0376-7388\(00\)81408-8](http://dx.doi.org/10.1016/S0376-7388(00)81408-8) (1982).
- 10 Traube, M., Archiv fur Anatomie, Leipzig. (Archiv fur Anatomie, Leipzig., 1867).
- 11 Hassler, G. L., July 1954. The use of molecular oilfilms in a pressure method for obtaining irrigation water from the sea unpublished report. . (July 1954.).
- 12 Glater, J. The early history of reverse osmosis membrane development. *Desalination* **117**, 297-309, doi:[http://dx.doi.org/10.1016/S0011-9164\(98\)00122-2](http://dx.doi.org/10.1016/S0011-9164(98)00122-2) (1998).
- 13 Loeb, S., Sourirajan, S. . (1960.).
- 14 Loeb, S., Sourirajan, S. . . Saline Water Conversion-II. In: Advances in Chemistry Series 38. (Washington, , 1963).
- 15 Loeb, S., Sourirajan, S. . . High flow porous membranes for separating water from saline solutions. US patent (1964).
- 16 Brandt, D. C., Leitner, G.F., Leitner, W.E. Amjad, Z. (ed.), . (Van Nostrand Reinhold, New York. , 1993.).
- 17 Bøddeker, K. W. Commentary: Tracing membrane science. *Journal of Membrane Science* **100**, 65-68, doi:[http://dx.doi.org/10.1016/0376-7388\(94\)00223-L](http://dx.doi.org/10.1016/0376-7388(94)00223-L) (1995).
- 18 Baker, R. W. *Membrane Technology and Applications*. 2nd Edition edn, (John Wiley & Sons, Ltd., 2004).
- 19 Pendergast, M. M. & Hoek, E. M. V. A review of water treatment membrane nanotechnologies. *Energy & Environmental Science* **4**, 1946-1971, doi:10.1039/C0EE00541J (2011).

- 20 Phillip, W. A., O'Neill, B., Rodwogin, M., Hillmyer, M. A. & Cussler, E. L. Self-Assembled Block Copolymer Thin Films as Water Filtration Membranes. *ACS Applied Materials & Interfaces* **2**, 847-853, doi:10.1021/am900882t (2010).
- 21 Anselme, C., and E.P. Jacobs. Ultrafiltration. . (ed J. Mallevalle, P.E. Odendaal, M. R. Wiesner.) (. American Water Works Association Research Foundation. Lyonnaise des Eaux. Water Research Commission of South Africa., McGraw-Hill. , 1996.).
- 22 Kang, S.-K. & Choo, K.-H. Use of MF and UF membranes for reclamation of glass industry wastewater containing colloidal clay and glass particles. *Journal of Membrane Science* **223**, 89-103, doi:[http://dx.doi.org/10.1016/S0376-7388\(03\)00311-9](http://dx.doi.org/10.1016/S0376-7388(03)00311-9) (2003).
- 23 Cheryan, M. *The Ultrafiltration Handbook*. (Technomic, 1986).
- 24 Youn, K.-S., Hong, J.-H., Bae, D.-H., Kim, S.-J. & Kim, S.-D. Effective clarifying process of reconstituted apple juice using membrane filtration with filter-aid pretreatment. *Journal of Membrane Science* **228**, 179-186, doi:<http://dx.doi.org/10.1016/j.memsci.2003.10.006> (2004).
- 25 Blanpain, P., Hermia, J. & Lenoël, M. Mechanisms governing permeate flux and protein rejection in the microfiltration of beer with a Cyclopore membrane. *Journal of Membrane Science* **84**, 37-51, doi:[http://dx.doi.org/10.1016/0376-7388\(93\)85049-3](http://dx.doi.org/10.1016/0376-7388(93)85049-3) (1993).
- 26 Czekaj, P., López, F. & Güell, C. Membrane fouling during microfiltration of fermented beverages. *Journal of Membrane Science* **166**, 199-212, doi:[http://dx.doi.org/10.1016/S0376-7388\(99\)00261-6](http://dx.doi.org/10.1016/S0376-7388(99)00261-6) (2000).
- 27 Czekaj, P., López, F. & Güell, C. Membrane fouling by turbidity constituents of beer and wine: characterization and prevention by means of infrasonic pulsing. *Journal of Food Engineering* **49**, 25-36, doi:[http://dx.doi.org/10.1016/S0260-8774\(00\)00181-3](http://dx.doi.org/10.1016/S0260-8774(00)00181-3) (2001).
- 28 Nagata, N., Herouvis, K. J., Dziejulski, D. M. & Belfort, G. Cross-flow membrane microfiltration of a bacteriol fermentation broth. *Biotechnology and Bioengineering* **34**, 447-466, doi:10.1002/bit.260340405 (1989).
- 29 Sakai, K., Ozawa, K., Ohashi, K., Yoshida, R. & Sakurai, H. Low-temperature plasma separation by cross-flow filtration with microporous glass membranes. *Industrial & Engineering Chemistry Research* **28**, 57-64, doi:10.1021/ie00085a012 (1989).
- 30 Cheryan, M. *Ultrafiltration and Microfiltration*. (Technomic Publishing Company, Inc. , 1998).
- 31 Kim, J. J., Yoon, H., Hong, J., Lee, T. & Wilf, M. Evaluation of new compact pretreatment system for high turbidity seawater: Fiber filter and ultrafiltration. *Desalination* **313**, 28-35, doi:<http://dx.doi.org/10.1016/j.desal.2012.11.031> (2013).
- 32 Knops, F., van Hoof, S., Futselaar, H. & Broens, L. Economic evaluation of a new ultrafiltration membrane for pretreatment of seawater reverse osmosis. *Desalination* **203**, 300-306, doi:<http://dx.doi.org/10.1016/j.desal.2006.04.013> (2007).
- 33 Wolf, P. H., Sivers, S. & Monti, S. UF membranes for RO desalination pretreatment. *Desalination* **182**, 293-300, doi:<http://dx.doi.org/10.1016/j.desal.2005.05.006> (2005).

- 34 Merrilee Galloway, J. M., Membrane Technology,, . Ultrafiltration for seawater reverse osmosis pretreatment,. **Volume 2004**, , Pages 5-8 (January 2004).
- 35 Zhang, J. D. *et al.* Pilot testing of outside-in UF pretreatment prior to RO for high turbidity seawater desalination. *Desalination* **189**, 269-277, doi:<http://dx.doi.org/10.1016/j.desal.2005.07.009> (2006).
- 36 Tchobanoglous, G. *et al.* Ultrafiltration as an advanced tertiary treatment process for municipal wastewater. *Desalination* **119**, 315-321, doi:[http://dx.doi.org/10.1016/S0011-9164\(98\)00175-1](http://dx.doi.org/10.1016/S0011-9164(98)00175-1) (1998).
- 37 Ravazzini, A. M., van Nieuwenhuijzen, A. F. & van der Graaf, J. H. M. J. Direct ultrafiltration of municipal wastewater: comparison between filtration of raw sewage and primary clarifier effluent. *Desalination* **178**, 51-62, doi:<http://dx.doi.org/10.1016/j.desal.2004.11.028> (2005).
- 38 Chakrabarty, B., Ghoshal, A. K. & Purkait, M. K. Ultrafiltration of stable oil-in-water emulsion by polysulfone membrane. *Journal of Membrane Science* **325**, 427-437, doi:<http://dx.doi.org/10.1016/j.memsci.2008.08.007> (2008).
- 39 Chakrabarty, B., Ghoshal, A. K. & Purkait, M. K. Cross-flow ultrafiltration of stable oil-in-water emulsion using polysulfone membranes. *Chemical Engineering Journal* **165**, 447-456, doi:<http://dx.doi.org/10.1016/j.cej.2010.09.031> (2010).
- 40 Yi, X. S. *et al.* Hydrodynamics behaviour of oil field wastewater advanced treatment by ultrafiltration process. *Desalination* **305**, 12-16, doi:<http://dx.doi.org/10.1016/j.desal.2012.06.012> (2012).
- 41 Majewska-Nowak, K. & Winnicki, T. Decolorization of dye solutions by continuous ultrafiltration. *Desalination* **60**, 59-66, doi:[http://dx.doi.org/10.1016/0011-9164\(86\)80005-4](http://dx.doi.org/10.1016/0011-9164(86)80005-4) (1986).
- 42 Aouni, A. *et al.* Reactive dyes rejection and textile effluent treatment study using ultrafiltration and nanofiltration processes. *Desalination* **297**, 87-96, doi:<http://dx.doi.org/10.1016/j.desal.2012.04.022> (2012).
- 43 Huang, J.-H. *et al.* Micellar-enhanced ultrafiltration of methylene blue from dye wastewater via a polysulfone hollow fiber membrane. *Journal of Membrane Science* **365**, 138-144, doi:<http://dx.doi.org/10.1016/j.memsci.2010.08.052> (2010).
- 44 Del Hoyo, P., Moure, F., Rendueles, M. & Diaz, M. Demineralization of animal blood plasma by ion exchange and ultrafiltration. *Meat science* **76**, 402-410, doi:[10.1016/j.meatsci.2006.06.014](http://dx.doi.org/10.1016/j.meatsci.2006.06.014) (2007).
- 45 R.W. Baker. *Membrane Technology and Applications*,. 3 edn, (Wiley, 2012).
- 46 Peng Lee, K. & Mattia, D. Monolithic nanoporous alumina membranes for ultrafiltration applications: Characterization, selectivity–permeability analysis and fouling studies. *Journal of Membrane Science* **435**, 52-61, doi:<http://dx.doi.org/10.1016/j.memsci.2013.01.051> (2013).

- 47 Narong, P. & James, A. E. Efficiency of ultrafiltration in the separation of whey suspensions using a tubular zirconia membrane. *Desalination* **219**, 348-357, doi:<http://dx.doi.org/10.1016/j.desal.2007.04.057> (2008).
- 48 Djafer, L., Ayril, A. & Ouagued, A. Robust synthesis and performance of a titania-based ultrafiltration membrane with photocatalytic properties. *Separation and Purification Technology* **75**, 198-203, doi:<http://dx.doi.org/10.1016/j.seppur.2010.08.001> (2010).
- 49 Cui, J., Zhang, X., Liu, H., Liu, S. & Yeung, K. L. Preparation and application of zeolite/ceramic microfiltration membranes for treatment of oil contaminated water. *Journal of Membrane Science* **325**, 420-426, doi:<http://dx.doi.org/10.1016/j.memsci.2008.08.015> (2008).
- 50 Xu, Z.-L. & Alsahy Qusay, F. Polyethersulfone (PES) hollow fiber ultrafiltration membranes prepared by PES/non-solvent/NMP solution. *Journal of Membrane Science* **233**, 101-111, doi:<http://dx.doi.org/10.1016/j.memsci.2004.01.005> (2004).
- 51 Malaisamy, R., Mohan, D. R. & Rajendran, M. Polyurethane and sulfonated polysulfone blend ultrafiltration membranes. I. Preparation and characterization studies. *Journal of colloid and interface science* **254**, 129-140 (2002).
- 52 Wang, D., Li, K. & Teo, W. K. Preparation and characterization of polyvinylidene fluoride (PVDF) hollow fiber membranes. *Journal of Membrane Science* **163**, 211-220, doi:[http://dx.doi.org/10.1016/S0376-7388\(99\)00181-7](http://dx.doi.org/10.1016/S0376-7388(99)00181-7) (1999).
- 53 Lohokare, H. R., Muthu, M. R., Agarwal, G. P. & Kharul, U. K. Effective arsenic removal using polyacrylonitrile-based ultrafiltration (UF) membrane. *Journal of Membrane Science* **320**, 159-166, doi:<http://dx.doi.org/10.1016/j.memsci.2008.03.068> (2008).
- 54 Qin, J.-J., Li, Y., Lee, L.-S. & Lee, H. Cellulose acetate hollow fiber ultrafiltration membranes made from CA/PVP 360 K/NMP/water. *Journal of Membrane Science* **218**, 173-183, doi:[http://dx.doi.org/10.1016/S0376-7388\(03\)00170-4](http://dx.doi.org/10.1016/S0376-7388(03)00170-4) (2003).
- 55 Bo, D. & Kun, Z. Preparation and properties of polyimide ultrafiltration membranes. *Journal of Membrane Science* **60**, 63-73, doi:[http://dx.doi.org/10.1016/S0376-7388\(00\)80324-5](http://dx.doi.org/10.1016/S0376-7388(00)80324-5) (1991).
- 56 Shen, L.-Q., Xu, Z.-K., Liu, Z.-M. & Xu, Y.-Y. Ultrafiltration hollow fiber membranes of sulfonated polyetherimide/polyetherimide blends: preparation, morphologies and anti-fouling properties. *Journal of Membrane Science* **218**, 279-293, doi:[http://dx.doi.org/10.1016/S0376-7388\(03\)00186-8](http://dx.doi.org/10.1016/S0376-7388(03)00186-8) (2003).
- 57 Hosch, J. & Staude, E. Preparation and investigation of chemically modified porous polyamide ultrafiltration membranes. *Journal of Membrane Science* **121**, 71-82, doi:[http://dx.doi.org/10.1016/0376-7388\(96\)00166-4](http://dx.doi.org/10.1016/0376-7388(96)00166-4) (1996).
- 58 Qiu, C., Nguyen, Q. T. & Ping, Z. Surface modification of cardo polyetherketone ultrafiltration membrane by photo-grafted copolymers to obtain nanofiltration membranes. *Journal of Membrane Science* **295**, 88-94, doi:<http://dx.doi.org/10.1016/j.memsci.2007.02.040> (2007).

- 59 MUELLER U., W. M., , . *Ceramic membranes – case related protocol for optimal operational conditions to treat filter backwash*. (TECHNEAU, 2007 , 5/02/2007).
- 60 Leob, S. S. S. Sea water demineralization by means of an osmosis membrane. *Adv. in Chem. Ser.* **38** (1963).
- 61 Mahon, H. I. (Google Patents, 1966).
- 62 Mahon, H. I. (Google Patents, 1966).
- 63 Strathmann, H. Membrane separation processes: Current relevance and future opportunities. *AIChE Journal* **47**, 1077-1087, doi:10.1002/aic.690470514 (2001).
- 64 Chung, T.-S., Qin, J.-J. & Gu, J. Effect of shear rate within the spinneret on morphology, separation performance and mechanical properties of ultrafiltration polyethersulfone hollow fiber membranes. *Chemical Engineering Science* **55**, 1077-1091, doi:[http://dx.doi.org/10.1016/S0009-2509\(99\)00371-1](http://dx.doi.org/10.1016/S0009-2509(99)00371-1) (2000).
- 65 Zeman, L. J. a. Z., A.L. . . *Microfiltration and ultrafiltration: Principles and Applications*. (Marcel Dekker, INC., 1996).
- 66 Judd, S. a. J., B. . (Elsevier., 2003).
- 67 Aptel, P., & C.A Buckley. . *Categories of membrane operations Water Treatment Membrane Processes.*, (American Water Works Association Research Foundation. Lyonnaise des Eaux. Water Research Commission of South Africa. , 1996).
- 68 M. Mulder. *Basic principles of membrane technology*. (Dordrecht: Kluwer Academic Publishers, , 1996.).
- 69 C.J. Geankoplis. Membrane separation processes: In transport processes and unit operations., (Prentice-Hall., 1995).
- 70 Cano, G. *et al.* Determination of pressure and velocity fields in ultrafiltration membrane modules used in drinking water production. *Journal of Membrane Science* **431**, 221-232, doi:<http://dx.doi.org/10.1016/j.memsci.2012.11.082> (2013).
- 71 Colas, F., Bonn elye, V. & Abidine, N. Development of a new hollow-fiber module for large ultrafiltration plants. *Desalination* **148**, 389-394, doi:[http://dx.doi.org/10.1016/S0011-9164\(02\)00735-X](http://dx.doi.org/10.1016/S0011-9164(02)00735-X) (2002).
- 72 Chang, S., Fane, A. G., Waite, T. D. & Yeo, A. Unstable filtration behavior with submerged hollow fiber membranes. *Journal of Membrane Science* **308**, 107-114, doi:<http://dx.doi.org/10.1016/j.memsci.2007.09.047> (2008).
- 73 Groendijk, L. & de Vries, H. E. Development of a mobile water maker, a sustainable way to produce safe drinking water in developing countries. *Desalination* **248**, 106-113, doi:<http://dx.doi.org/10.1016/j.desal.2008.05.044> (2009).
- 74 Al-Bastaki, N. & Abbas, A. Permeate recycle to improve the performance of a spiral-wound RO plant. *Desalination* **158**, 119-126, doi:[http://dx.doi.org/10.1016/S0011-9164\(03\)00442-9](http://dx.doi.org/10.1016/S0011-9164(03)00442-9) (2003).
- 75 M.F.A. Goosen, S. S. S., H.A. Hinai, S.A. Obeidani, R.A. Belushi, D. Jackson., Fouling of reverse osmosis and ultrafiltration membranes: a critical review. *Sep. Sci. Technol* **39** (10) (2005).

- 76 Geraldes, V. t., Semião, V. & de Pinho, M. N. Flow management in nanofiltration spiral wound modules with ladder-type spacers. *Journal of Membrane Science* **203**, 87-102, doi:[http://dx.doi.org/10.1016/S0376-7388\(01\)00753-0](http://dx.doi.org/10.1016/S0376-7388(01)00753-0) (2002).
- 77 Li, F., Meindersma, W., de Haan, A. B. & Reith, T. Optimization of commercial net spacers in spiral wound membrane modules. *Journal of Membrane Science* **208**, 289-302, doi:[http://dx.doi.org/10.1016/S0376-7388\(02\)00307-1](http://dx.doi.org/10.1016/S0376-7388(02)00307-1) (2002).
- 78 Zhao, Y. H., Zhu, X. Y., Wee, K. H. & Bai, R. Achieving highly effective non-biofouling performance for polypropylene membranes modified by UV-induced surface graft polymerization of two oppositely charged monomers. *The journal of physical chemistry. B* **114**, 2422-2429, doi:10.1021/jp908194g (2010).
- 79 Jarusutthirak, C. & Amy, G. Role of Soluble Microbial Products (SMP) in Membrane Fouling and Flux Decline. *Environmental Science & Technology* **40**, 969-974, doi:10.1021/es050987a (2006).
- 80 Asatekin, A., Kang, S., Elimelech, M. & Mayes, A. M. Anti-fouling ultrafiltration membranes containing polyacrylonitrile-graft-poly(ethylene oxide) comb copolymer additives. *Journal of Membrane Science* **298**, 136-146, doi:<http://dx.doi.org/10.1016/j.memsci.2007.04.011> (2007).
- 81 Koros, W., J., Y.H. Ma and T., Shimidzyu T. . Terminology for Membranes and Membrane Processes; IUPAC Recommendations 1996. *Journal of membrane science* **120** (1996).
- 82 Flemming, H. C. Mechanistic aspects of reverse osmosis membrane biofouling and prevention. (1993).
- 83 Kelly, S. T. & Zydney, A. L. Mechanisms for BSA fouling during microfiltration. *Journal of Membrane Science* **107**, 115-127, doi:[http://dx.doi.org/10.1016/0376-7388\(95\)00108-O](http://dx.doi.org/10.1016/0376-7388(95)00108-O) (1995).
- 84 McDonogh, R. M., Bauser, H., Stroh, N. & Chmiel, H. Concentration polarisation and adsorption effects in cross-flow ultrafiltration of proteins. *Desalination* **79**, 217-231, doi:[http://dx.doi.org/10.1016/0011-9164\(90\)85007-W](http://dx.doi.org/10.1016/0011-9164(90)85007-W) (1990).
- 85 Nyström, M., Pihlajamäki, A. & Ehsani, N. Characterization of ultrafiltration membranes by simultaneous streaming potential and flux measurements. *Journal of Membrane Science* **87**, 245-256, doi:[http://dx.doi.org/10.1016/0376-7388\(94\)87031-4](http://dx.doi.org/10.1016/0376-7388(94)87031-4) (1994).
- 86 Ricq, L., Narçon, S., Reggiani, J.-C. & Pagetti, J. Streaming potential and protein transmission ultrafiltration of single proteins and proteins in mixture: β -lactoglobulin and lysozyme. *Journal of Membrane Science* **156**, 81-96, doi:[http://dx.doi.org/10.1016/S0376-7388\(98\)00341-X](http://dx.doi.org/10.1016/S0376-7388(98)00341-X) (1999).
- 87 Bachmann, R. T. & Edyvean, R. G. J. Biofouling: an historic and contemporary review of its causes, consequences and control in drinking water distribution systems. *Biofilms* **2**, 197-227, doi:doi:10.1017/S1479050506001979 (2005).
- 88 Rana, D. & Matsuura, T. Surface Modifications for Antifouling Membranes. *Chemical Reviews* **110**, 2448-2471, doi:10.1021/cr800208y (2010).

- 89 Katsikogianni, M. & Missirlis, Y. F. Concise review of mechanisms of bacterial adhesion to biomaterials and of techniques used in estimating bacteria-material interactions. *European cells & materials* **8**, 37-57 (2004).
- 90 Flint, S. H., Bremer, P. J., & Brooks, J. D. . Biofilms in dairy manufacturing plant-Description, current concerns and methods of control. *Biofouling* **11(1)** (1997a).
- 91 Characklis, W. G., Marshall, K.C. . *Biofilms.*, (John Wiley & Sons, New York., 1990).
- 92 Lewandowski, Z. & Beyenal, H. Biofilm monitoring: a perfect solution in search of a problem. *Water science and technology : a journal of the International Association on Water Pollution Research* **47**, 9-18 (2003).
- 93 Vadillo-Rodríguez, V., Busscher, H. J., Mei, H. C. v. d., Vries, J. d. & Norde, W. Role of lactobacillus cell surface hydrophobicity as probed by AFM in adhesion to surfaces at low and high ionic strength. *Colloids and Surfaces B: Biointerfaces* **41**, 33-41, doi:<http://dx.doi.org/10.1016/j.colsurfb.2004.10.028> (2005).
- 94 Palmer, J., Flint, S. & Brooks, J. Bacterial cell attachment, the beginning of a biofilm. *Journal of industrial microbiology & biotechnology* **34**, 577-588, doi:10.1007/s10295-007-0234-4 (2007).
- 95 Cogan, N. G. & Chellam, S. Regularized Stokeslets solution for 2-D flow in dead-end microfiltration: Application to bacterial deposition and fouling. *Journal of Membrane Science* **318**, 379-386, doi:<http://dx.doi.org/10.1016/j.memsci.2008.03.012> (2008).
- 96 Van Houdt, R. & Michiels, C. W. Biofilm formation and the food industry, a focus on the bacterial outer surface. *Journal of Applied Microbiology* **109**, 1117-1131, doi:10.1111/j.1365-2672.2010.04756.x (2010).
- 97 Ivnitsky, H. *et al.* Characterization of membrane biofouling in nanofiltration processes of wastewater treatment. *Desalination* **185**, 255-268, doi:<http://dx.doi.org/10.1016/j.desal.2005.03.081> (2005).
- 98 Jefferson, K. K. What drives bacteria to produce a biofilm? *FEMS microbiology letters* **236**, 163-173, doi:10.1016/j.femsle.2004.06.005 (2004).
- 99 Dang, H. & Lovell, C. R. Bacterial primary colonization and early succession on surfaces in marine waters as determined by amplified rRNA gene restriction analysis and sequence analysis of 16S rRNA genes. *Applied and environmental microbiology* **66**, 467-475 (2000).
- 100 Goldman, G., Starosvetsky, J. & Armon, R. Inhibition of biofilm formation on UF membrane by use of specific bacteriophages. *Journal of Membrane Science* **342**, 145-152, doi:<http://dx.doi.org/10.1016/j.memsci.2009.06.036> (2009).
- 101 Kang, S.-T., Subramani, A., Hoek, E. M. V., Deshusses, M. A. & Matsumoto, M. R. Direct observation of biofouling in cross-flow microfiltration: mechanisms of deposition and release. *Journal of Membrane Science* **244**, 151-165, doi:<http://dx.doi.org/10.1016/j.memsci.2004.07.011> (2004).
- 102 Baker, J. S. & Dudley, L. Y. Biofouling in membrane systems — A review. *Desalination* **118**, 81-89, doi:[http://dx.doi.org/10.1016/S0011-9164\(98\)00091-5](http://dx.doi.org/10.1016/S0011-9164(98)00091-5) (1998).

- 103 Le-Clech, P., Chen, V. & Fane, T. A. G. Fouling in membrane bioreactors used in wastewater treatment. *Journal of Membrane Science* **284**, 17-53, doi:<http://dx.doi.org/10.1016/j.memsci.2006.08.019> (2006).
- 104 Percival, S. L., Knapp, J. S., Wales, D. S. & Edyvean, R. G. J. The effect of turbulent flow and surface roughness on biofilm formation in drinking water. *J Ind Microbiol Biotech* **22**, 152-159, doi:10.1038/sj.jim.2900622 (1999).
- 105 D'Souza, N. M. & Mawson, A. J. Membrane cleaning in the dairy industry: a review. *Critical reviews in food science and nutrition* **45**, 125-134, doi:10.1080/10408690490911783 (2005).
- 106 te Poele, S. & van der Graaf, J. Enzymatic cleaning in ultrafiltration of wastewater treatment plant effluent. *Desalination* **179**, 73-81, doi:<http://dx.doi.org/10.1016/j.desal.2004.11.056> (2005).
- 107 Xiong, Y. & Liu, Y. Biological control of microbial attachment: a promising alternative for mitigating membrane biofouling. *Applied microbiology and biotechnology* **86**, 825-837, doi:10.1007/s00253-010-2463-0 (2010).
- 108 Simões, M., Simões, L. C., Machado, I., Pereira, M. O. & Vieira, M. J. Control of Flow-Generated Biofilms with Surfactants: Evidence of Resistance and Recovery. *Food and Bioproducts Processing* **84**, 338-345, doi:<http://dx.doi.org/10.1205/fbp06022> (2006).
- 109 Ceryan, M. L. (UK: Technomic Publishing Co., Inc, 1998).
- 110 Krack, R. Chemical agents and costs in cleaning and disinfection of membrane equipment, Fouling and Cleaning in Pressure Driven Membrane Process. (1995).
- 111 Liu, C. X., Zhang, D. R., He, Y., Zhao, X. S. & Bai, R. Modification of membrane surface for anti-biofouling performance: Effect of anti-adhesion and anti-bacteria approaches. *Journal of Membrane Science* **346**, 121-130, doi:<http://dx.doi.org/10.1016/j.memsci.2009.09.028> (2010).
- 112 Zodrow, K. *et al.* Polysulfone ultrafiltration membranes impregnated with silver nanoparticles show improved biofouling resistance and virus removal. *Water Research* **43**, 715-723, doi:<http://dx.doi.org/10.1016/j.watres.2008.11.014> (2009).
- 113 Kim, S. H., Kwak, S.-Y., Sohn, B.-H. & Park, T. H. Design of TiO₂ nanoparticle self-assembled aromatic polyamide thin-film-composite (TFC) membrane as an approach to solve biofouling problem. *Journal of Membrane Science* **211**, 157-165, doi:[http://dx.doi.org/10.1016/S0376-7388\(02\)00418-0](http://dx.doi.org/10.1016/S0376-7388(02)00418-0) (2003).
- 114 Akar, N., Asar, B., Dizge, N. & Koyuncu, I. Investigation of characterization and biofouling properties of PES membrane containing selenium and copper nanoparticles. *Journal of Membrane Science* **437**, 216-226, doi:<http://dx.doi.org/10.1016/j.memsci.2013.02.012> (2013).
- 115 Shah, P. & Murthy, C. N. Studies on the porosity control of MWCNT/polysulfone composite membrane and its effect on metal removal. *Journal of Membrane Science* **437**, 90-98, doi:<http://dx.doi.org/10.1016/j.memsci.2013.02.042> (2013).

- 116 Liu, M., Wei, Y.-M., Xu, Z.-L., Guo, R.-Q. & Zhao, L.-B. Preparation and characterization of polyethersulfone microporous membrane via thermally induced phase separation with low critical solution temperature system. *Journal of Membrane Science* **437**, 169-178, doi:<http://dx.doi.org/10.1016/j.memsci.2013.03.004> (2013).
- 117 Hu, J. *et al.* Plasma-grafted alkaline anion-exchange membranes based on polyvinyl chloride for potential application in direct alcohol fuel cell. *Journal of Power Sources* **196**, 4483-4490, doi:<http://dx.doi.org/10.1016/j.jpowsour.2011.01.034> (2011).
- 118 Souzy, R., Boutevin, B. & Ameduri, B. Synthesis and Characterizations of Novel Proton-Conducting Fluoropolymer Electrolyte Membranes Based on Poly(vinylidene fluoride-ter-hexafluoropropylene-ter- α -trifluoromethacrylic acid) Terpolymers Grafted by Aryl Sulfonic Acids. *Macromolecules* **45**, 3145-3160, doi:10.1021/ma3001912 (2012).
- 119 Sun, H., Liu, S., Ge, B., Xing, L. & Chen, H. Cellulose nitrate membrane formation via phase separation induced by penetration of nonsolvent from vapor phase. *Journal of Membrane Science* **295**, 2-10, doi:<http://dx.doi.org/10.1016/j.memsci.2007.02.019> (2007).
- 120 Zavastin, D. *et al.* Preparation, characterization and applicability of cellulose acetate-polyurethane blend membrane in separation techniques. *Colloids and Surfaces A: Physicochemical and Engineering Aspects* **370**, 120-128, doi:<http://dx.doi.org/10.1016/j.colsurfa.2010.08.058> (2010).
- 121 Zhao, W. *et al.* Modification of polyethersulfone membrane by blending semi-interpenetrating network polymeric nanoparticles. *Journal of Membrane Science* **369**, 258-266, doi:<http://dx.doi.org/10.1016/j.memsci.2010.11.065> (2011).
- 122 Razmjou, A., Mansouri, J. & Chen, V. The effects of mechanical and chemical modification of TiO₂ nanoparticles on the surface chemistry, structure and fouling performance of PES ultrafiltration membranes. *Journal of Membrane Science* **378**, 73-84, doi:<http://dx.doi.org/10.1016/j.memsci.2010.10.019> (2011).
- 123 Celik, E., Park, H., Choi, H. & Choi, H. Carbon nanotube blended polyethersulfone membranes for fouling control in water treatment. *Water research* **45**, 274-282, doi:<http://dx.doi.org/10.1016/j.watres.2010.07.060> (2011).
- 124 Kong, J. & Li, K. Oil removal from oil-in-water emulsions using PVDF membranes. *Separation and Purification Technology* **16**, 83-93, doi:[http://dx.doi.org/10.1016/S1383-5866\(98\)00114-2](http://dx.doi.org/10.1016/S1383-5866(98)00114-2) (1999).
- 125 Deshmukh, S. P. & Li, K. Effect of ethanol composition in water coagulation bath on morphology of PVDF hollow fibre membranes. *Journal of Membrane Science* **150**, 75-85, doi:[http://dx.doi.org/10.1016/S0376-7388\(98\)00196-3](http://dx.doi.org/10.1016/S0376-7388(98)00196-3) (1998).
- 126 Kumar, M., Payne, M., Poust, S. & Zilles, J. in *Biomimetic Membranes for Sensor and Separation Applications Biological and Medical Physics, Biomedical Engineering* (ed Claus Hélix-Nielsen) Ch. 3, 43-62 (Springer Netherlands, 2012).
- 127 Tang, C. Y., Zhao, Y., Wang, R., Hélix-Nielsen, C. & Fane, A. G. Desalination by biomimetic aquaporin membranes: Review of status and prospects. *Desalination* **308**, 34-40, doi:<http://dx.doi.org/10.1016/j.desal.2012.07.007> (2013).

- 128 Kaufman, Y., Berman, A. & Freger, V. Supported lipid bilayer membranes for water purification by reverse osmosis. *Langmuir : the ACS journal of surfaces and colloids* **26**, 7388-7395, doi:10.1021/la904411b (2010).
- 129 Hu, M. & Mi, B. Enabling Graphene Oxide Nanosheets as Water Separation Membranes. *Environmental Science & Technology* **47**, 3715-3723, doi:10.1021/es400571g (2013).
- 130 Qiu, S. *et al.* Preparation and properties of functionalized carbon nanotube/PSF blend ultrafiltration membranes. *Journal of Membrane Science* **342**, 165-172, doi:<http://dx.doi.org/10.1016/j.memsci.2009.06.041> (2009).
- 131 Maphutha, S., Moothi, K., Meyyappan, M. & Iyuke, S. E. A carbon nanotube-infused polysulfone membrane with polyvinyl alcohol layer for treating oil-containing waste water. *Scientific reports* **3**, 1509, doi:10.1038/srep01509 (2013).
- 132 Zhao, H., Wu, L., Zhou, Z., Zhang, L. & Chen, H. Improving the antifouling property of polysulfone ultrafiltration membrane by incorporation of isocyanate-treated graphene oxide. *Physical Chemistry Chemical Physics* **15**, 9084-9092, doi:10.1039/C3CP50955A (2013).
- 133 Cohen-Tanugi, D. & Grossman, J. C. Water Desalination across Nanoporous Graphene. *Nano Letters* **12**, 3602-3608, doi:10.1021/nl3012853 (2012).
- 134 Jin, F. *et al.* High-performance ultrafiltration membranes based on polyethersulfone-graphene oxide composites. *RSC Advances* **3**, 21394-21397, doi:10.1039/C3RA42908C (2013).
- 135 Prince, J. A. *et al.* Self-cleaning Metal Organic Framework (MOF) based ultra filtration membranes - A solution to bio-fouling in membrane separation processes. *Sci. Rep.* **4**, doi:10.1038/srep06555 (2014).
- 136 Prince, J. A., Bhuvana, S., Boodhoo, K. V. K., Anbharasi, V. & Singh, G. Synthesis and characterization of PEG-Ag immobilized PES hollow fiber ultrafiltration membranes with long lasting antifouling properties. *Journal of Membrane Science* **454**, 538-548, doi:<http://dx.doi.org/10.1016/j.memsci.2013.12.050> (2014).
- 137 Knoell, T. *et al.* Biofouling potentials of microporous polysulfone membranes containing a sulfonated polyether-ethersulfone/polyethersulfone block copolymer: correlation of membrane surface properties with bacterial attachment. *Journal of Membrane Science* **157**, 117-138, doi:[http://dx.doi.org/10.1016/S0376-7388\(98\)00365-2](http://dx.doi.org/10.1016/S0376-7388(98)00365-2) (1999).
- 138 Khulbe, K. C., Feng, C. & Matsuura, T. The art of surface modification of synthetic polymeric membranes. *Journal of Applied Polymer Science* **115**, 855-895, doi:10.1002/app.31108 (2010).
- 139 Kumar, M., Grzelakowski, M., Zilles, J., Clark, M. & Meier, W. Highly permeable polymeric membranes based on the incorporation of the functional water channel protein Aquaporin Z. *Proceedings of the National Academy of Sciences* **104**, 20719-20724, doi:10.1073/pnas.0708762104 (2007).

- 140 Sun, G., Chung, T.-S., Jeyaseelan, K. & Armugam, A. Stabilization and immobilization of aquaporin reconstituted lipid vesicles for water purification. *Colloids and Surfaces B: Biointerfaces* **102**, 466-471, doi:<http://dx.doi.org/10.1016/j.colsurfb.2012.08.009> (2013).
- 141 Novoselov, K. S. *et al.* Electric field effect in atomically thin carbon films. *Science* **306**, 666-669, doi:10.1126/science.1102896 (2004).
- 142 Zhu, Y. *et al.* Carbon-based supercapacitors produced by activation of graphene. *Science* **332**, 1537-1541, doi:10.1126/science.1200770 (2011).
- 143 Lee, C. *et al.* Frictional characteristics of atomically thin sheets. *Science* **328**, 76-80, doi:10.1126/science.1184167 (2010).
- 144 Chen, S. *et al.* Oxidation resistance of graphene-coated Cu and Cu/Ni alloy. *ACS nano* **5**, 1321-1327, doi:10.1021/nn103028d (2011).
- 145 Kim, K. S. *et al.* Chemical vapor deposition-grown graphene: the thinnest solid lubricant. *ACS nano* **5**, 5107-5114, doi:10.1021/nn2011865 (2011).
- 146 Prasai, D. *et al.* Graphene: corrosion-inhibiting coating. *ACS nano* **6**, 1102-1108, doi:10.1021/nn203507y (2012).
- 147 Garaj, S. *et al.* Graphene as a subnanometre trans-electrode membrane. *Nature* **467**, 190-193, doi:10.1038/nature09379 (2010).
- 148 O'Hern, S. C. *et al.* Selective molecular transport through intrinsic defects in a single layer of CVD graphene. *ACS nano* **6**, 10130-10138, doi:10.1021/nn303869m (2012).
- 149 Rafiee, J. *et al.* Wetting transparency of graphene. *Nature materials* **11**, 217-222, doi:10.1038/nmat3228 (2012).
- 150 Li, Z. *et al.* Effect of airborne contaminants on the wettability of supported graphene and graphite. *Nature materials* **12**, 925-931, doi:10.1038/nmat3709 (2013).
- 151 Ruan, M. *et al.* Epitaxial graphene on silicon carbide: Introduction to structured graphene. *MRS Bulletin* **37**, 1138-1147, doi:10.1557/mrs.2012.231 (2012).
- 152 Leenaerts, O., Partoens, B. & Peeters, F. M. Graphene: A perfect nanoballoon. *Applied Physics Letters* **93**, 193107, doi:<http://dx.doi.org/10.1063/1.3021413> (2008).
- 153 Gai, J.-G., Gong, X.-L., Wang, W.-W., Zhang, X. & Kang, W.-L. An ultrafast water transport forward osmosis membrane: porous graphene. *Journal of Materials Chemistry A* **2**, 4023-4028, doi:10.1039/C3TA14256F (2014).
- 154 Suk, M. E. & Aluru, N. R. Water Transport through Ultrathin Graphene. *The Journal of Physical Chemistry Letters* **1**, 1590-1594, doi:10.1021/jz100240r (2010).
- 155 Allemann, R. K., Young, N. J., Ma, S., Truhlar, D. G. & Gao, J. Synthetic Efficiency in Enzyme Mechanisms Involving Carbocations: Aristolochene Synthase. *Journal of the American Chemical Society* **129**, 13008-13013, doi:10.1021/ja0722067 (2007).
- 156 Konatham, D., Yu, J., Ho, T. A. & Striolo, A. Simulation Insights for Graphene-Based Water Desalination Membranes. *Langmuir : the ACS journal of surfaces and colloids* **29**, 11884-11897, doi:10.1021/la4018695 (2013).
- 157 Koenig, S. P., Wang, L., Pellegrino, J. & Bunch, J. S. Selective molecular sieving through porous graphene. *Nat Nano* **7**, 728-732,

- doi:<http://www.nature.com/nnano/journal/v7/n11/abs/nnano.2012.162.html#supplementary-information> (2012).
- 158 Taherian, F., Marcon, V., van der Vegt, N. F. A. & Leroy, F. What Is the Contact Angle of Water on Graphene? *Langmuir* **29**, 1457-1465, doi:10.1021/la304645w (2013).
- 159 Shih, C. J. *et al.* Breakdown in the wetting transparency of graphene. *Physical review letters* **109**, 176101 (2012).
- 160 Dreyer, D. R., Park, S., Bielawski, C. W. & Ruoff, R. S. The chemistry of graphene oxide. *Chemical Society Reviews* **39**, 228-240, doi:10.1039/B917103G (2010).
- 161 Loh, K. P., Bao, Q., Eda, G. & Chhowalla, M. Graphene oxide as a chemically tunable platform for optical applications. *Nat Chem* **2**, 1015-1024 (2010).
- 162 Avouris, P. & Dimitrakopoulos, C. Graphene: synthesis and applications. *Materials Today* **15**, 86-97, doi:[http://dx.doi.org/10.1016/S1369-7021\(12\)70044-5](http://dx.doi.org/10.1016/S1369-7021(12)70044-5) (2012).
- 163 Compton, O. C. & Nguyen, S. T. Graphene Oxide, Highly Reduced Graphene Oxide, and Graphene: Versatile Building Blocks for Carbon-Based Materials. *Small* **6**, 711-723, doi:10.1002/sml.200901934 (2010).
- 164 Wajid, A. S. *et al.* Erratum to ‘Polymer-stabilized graphene dispersions at high concentrations in organic solvents for composite production’ [Carbon 50 (2012) 526–534]. *Carbon* **50**, 2065, doi:<http://dx.doi.org/10.1016/j.carbon.2012.01.002> (2012).
- 165 Marmur, A. Soft contact: measurement and interpretation of contact angles. *Soft Matter* **2**, 12-17, doi:10.1039/B514811C (2006).
- 166 Rafiee, J. *et al.* Wetting transparency of graphene. *Nature materials* **11**, 217-222, doi:<http://www.nature.com/nmat/journal/v11/n3/abs/nmat3228.html#supplementary-information> (2012).
- 167 Vickery, J. L., Patil, A. J. & Mann, S. Fabrication of Graphene–Polymer Nanocomposites With Higher-Order Three-Dimensional Architectures. *Advanced Materials* **21**, 2180-2184, doi:10.1002/adma.200803606 (2009).
- 168 Sun, P. *et al.* Selective Ion Penetration of Graphene Oxide Membranes. *ACS nano* **7**, 428-437, doi:10.1021/nn304471w (2013).
- 169 Rahimpour, A. *et al.* Novel functionalized carbon nanotubes for improving the surface properties and performance of polyethersulfone (PES) membrane. *Desalination* **286**, 99-107, doi:<http://dx.doi.org/10.1016/j.desal.2011.10.039> (2012).
- 170 Zhao, C., Xue, J., Ran, F. & Sun, S. Modification of polyethersulfone membranes – A review of methods. *Progress in Materials Science* **58**, 76-150, doi:<http://dx.doi.org/10.1016/j.pmatsci.2012.07.002> (2013).
- 171 Van der Bruggen, B. Chemical modification of polyethersulfone nanofiltration membranes: A review. *Journal of Applied Polymer Science* **114**, 630-642, doi:10.1002/app.30578 (2009).
- 172 Koh, M., Clark, M. M. & Howe, K. J. Filtration of lake natural organic matter: Adsorption capacity of a polypropylene microfilter. *Journal of Membrane Science* **256**, 169-175, doi:<http://dx.doi.org/10.1016/j.memsci.2005.02.016> (2005).

- 173 Agenson, K. O. & Urase, T. Change in membrane performance due to organic fouling in nanofiltration (NF)/reverse osmosis (RO) applications. *Separation and Purification Technology* **55**, 147-156, doi:<http://dx.doi.org/10.1016/j.seppur.2006.11.010> (2007).
- 174 Bolong, N., Ismail, A. F., Salim, M. R., Rana, D. & Matsuura, T. Development and characterization of novel charged surface modification macromolecule to polyethersulfone hollow fiber membrane with polyvinylpyrrolidone and water. *Journal of Membrane Science* **331**, 40-49, doi:<http://dx.doi.org/10.1016/j.memsci.2009.01.008> (2009).
- 175 Mosqueda-Jimenez, D. B., Narbaitz, R. M. & Matsuura, T. Manufacturing conditions of surface-modified membranes: effects on ultrafiltration performance. *Separation and Purification Technology* **37**, 51-67, doi:<http://dx.doi.org/10.1016/j.seppur.2003.07.003> (2004).
- 176 Wang, Y.-Q., Su, Y.-L., Sun, Q., Ma, X.-L. & Jiang, Z.-Y. Generation of anti-biofouling ultrafiltration membrane surface by blending novel branched amphiphilic polymers with polyethersulfone. *Journal of Membrane Science* **286**, 228-236, doi:<http://dx.doi.org/10.1016/j.memsci.2006.09.040> (2006).
- 177 Klaysom, C., Ladewig, B. P., Lu, G. Q. M. & Wang, L. Preparation and characterization of sulfonated polyethersulfone for cation-exchange membranes. *Journal of Membrane Science* **368**, 48-53, doi:<http://dx.doi.org/10.1016/j.memsci.2010.11.006> (2011).
- 178 Lu, D., Zou, H., Guan, R., Dai, H. & Lu, L. Sulfonation of Polyethersulfone by Chlorosulfonic Acid. *Polym. Bull.* **54**, 21-28, doi:10.1007/s00289-005-0361-x (2005).
- 179 Sanchez, J. Y. *et al.* Extrusion: An environmentally friendly process for PEMFC membrane elaboration. *Electrochimica Acta* **53**, 1584-1595, doi:<http://dx.doi.org/10.1016/j.electacta.2007.04.022> (2007).
- 180 Blanco, J. F., Nguyen, Q. T. & Schaetzel, P. Novel hydrophilic membrane materials: sulfonated polyethersulfone Cardo. *Journal of Membrane Science* **186**, 267-279, doi:[http://dx.doi.org/10.1016/S0376-7388\(01\)00331-3](http://dx.doi.org/10.1016/S0376-7388(01)00331-3) (2001).
- 181 Guan, R., Zou, H., Lu, D., Gong, C. & Liu, Y. Polyethersulfone sulfonated by chlorosulfonic acid and its membrane characteristics. *European Polymer Journal* **41**, 1554-1560, doi:<http://dx.doi.org/10.1016/j.eurpolymj.2005.01.018> (2005).
- 182 Guan, R., Dai, H., Li, C., Liu, J. & Xu, J. Effect of casting solvent on the morphology and performance of sulfonated polyethersulfone membranes. *Journal of Membrane Science* **277**, 148-156, doi:<http://dx.doi.org/10.1016/j.memsci.2005.10.025> (2006).
- 183 Bai, P. *et al.* Modification of a polyethersulfone matrix by grafting functional groups and the research of biomedical performance. *Journal of biomaterials science. Polymer edition* **21**, 1559-1572, doi:10.1163/092050609x12519805626158 (2010).
- 184 Deng, B. *et al.* Microfiltration membranes prepared from polyethersulfone powder grafted with acrylic acid by simultaneous irradiation and their pH dependence. *Radiation Physics and Chemistry* **77**, 898-906, doi:<http://dx.doi.org/10.1016/j.radphyschem.2008.02.008> (2008).

- 185 Wang, D. *et al.* Preparation and characterization of functional carboxylic polyethersulfone membrane. *Journal of Membrane Science* **374**, 93-101, doi:<http://dx.doi.org/10.1016/j.memsci.2011.03.021> (2011).
- 186 Li, L. & Wang, Y. Sulfonated polyethersulfone Cardo membranes for direct methanol fuel cell. *Journal of Membrane Science* **246**, 167-172, doi:<http://dx.doi.org/10.1016/j.memsci.2004.08.015> (2005).
- 187 Kochan, J., Wintgens, T., Melin, T. & Wong, J. Characterization and filtration performance of coating-modified polymeric membranes used in membrane bioreactors. *Chem. Pap.* **63**, 152-157, doi:10.2478/s11696-008-0096-x (2009).
- 188 Ma, X., Su, Y., Sun, Q., Wang, Y. & Jiang, Z. Enhancing the antifouling property of polyethersulfone ultrafiltration membranes through surface adsorption-crosslinking of poly(vinyl alcohol). *Journal of Membrane Science* **300**, 71-78, doi:<http://dx.doi.org/10.1016/j.memsci.2007.05.008> (2007).
- 189 Pontié, M., Durand-Bourlier, L., Lemordant, D. & Lainé, J. M. Control fouling and cleaning procedures of UF membranes by a streaming potential method. *Separation and Purification Technology* **14**, 1-11, doi:[http://dx.doi.org/10.1016/S1383-5866\(98\)00054-9](http://dx.doi.org/10.1016/S1383-5866(98)00054-9) (1998).
- 190 Bae, T.-H., Kim, I.-C. & Tak, T.-M. Preparation and characterization of fouling-resistant TiO₂ self-assembled nanocomposite membranes. *Journal of Membrane Science* **275**, 1-5, doi:<http://dx.doi.org/10.1016/j.memsci.2006.01.023> (2006).
- 191 Kochkodan, V., Tsarenko, S., Potapchenko, N., Kosinova, V. & Goncharuk, V. Adhesion of microorganisms to polymer membranes: a photobactericidal effect of surface treatment with TiO₂. *Desalination* **220**, 380-385, doi:<http://dx.doi.org/10.1016/j.desal.2007.01.042> (2008).
- 192 Malaisamy, R. & Bruening, M. L. High-flux nanofiltration membranes prepared by adsorption of multilayer polyelectrolyte membranes on polymeric supports. *Langmuir : the ACS journal of surfaces and colloids* **21**, 10587-10592, doi:10.1021/la051669s (2005).
- 193 Bruening, M. & Dotzauer, D. Polymer films: Just spray it. *Nat Mater* **8**, 449-450 (2009).
- 194 Aravind, U. K., Mathew, J. & Aravindakumar, C. T. Transport studies of BSA, lysozyme and ovalbumin through chitosan/polystyrene sulfonate multilayer membrane. *Journal of Membrane Science* **299**, 146-155, doi:<http://dx.doi.org/10.1016/j.memsci.2007.04.036> (2007).
- 195 Çifci, C. & Polat, Ş. Polymer-Enhanced Ultrafiltration of Fe(III) and Cu(II) Aqueous Solutions Using Poly(Vinyl Alcohol)-Alginate Acid/Cellulose Membranes. *Journal of Macromolecular Science, Part A* **46**, 682-687, doi:10.1080/10601320902938939 (2009).
- 196 Pontié, M., Cowache, P., Klein, L. H., Maurice, V. & Bedioui, F. Preparation and characterization of an electronically conductive and chemically modified ultrafiltration type membrane. *Journal of Membrane Science* **184**, 165-173, doi:[http://dx.doi.org/10.1016/S0376-7388\(00\)00619-0](http://dx.doi.org/10.1016/S0376-7388(00)00619-0) (2001).

- 197 De Bartolo, L. *et al.* Influence of membrane surface properties on the growth of neuronal cells isolated from hippocampus. *Journal of Membrane Science* **325**, 139-149, doi:<http://dx.doi.org/10.1016/j.memsci.2008.07.022> (2008).
- 198 Chu, L.-Y., Wang, S. & Chen, W.-M. Surface Modification of Ceramic-Supported Polyethersulfone Membranes by Interfacial Polymerization for Reduced Membrane Fouling. *Macromolecular Chemistry and Physics* **206**, 1934-1940, doi:10.1002/macp.200500324 (2005).
- 199 Liu, S. X., Kim, J.-T., Kim, S. & Singh, M. The effect of polymer surface modification via interfacial polymerization on polymer–protein interaction. *Journal of Applied Polymer Science* **112**, 1704-1715, doi:10.1002/app.29606 (2009).
- 200 Zhao, J., Wang, Z., Wang, J. & Wang, S. Influence of heat-treatment on CO₂ separation performance of novel fixed carrier composite membranes prepared by interfacial polymerization. *Journal of Membrane Science* **283**, 346-356, doi:<http://dx.doi.org/10.1016/j.memsci.2006.07.004> (2006).
- 201 Mansourpanah, Y., Madaeni, S. S. & Rahimpour, A. Preparation and investigation of separation properties of polyethersulfone supported poly(piperazineamide) nanofiltration membrane using microwave-assisted polymerization. *Separation and Purification Technology* **69**, 234-242, doi:<http://dx.doi.org/10.1016/j.seppur.2009.07.025> (2009).
- 202 Jahanshahi, M., Rahimpour, A. & Peyravi, M. Developing thin film composite poly(piperazine-amide) and poly(vinyl-alcohol) nanofiltration membranes. *Desalination* **257**, 129-136, doi:<http://dx.doi.org/10.1016/j.desal.2010.02.034> (2010).
- 203 Buch, P. R., Jagan Mohan, D. & Reddy, A. V. R. Preparation, characterization and chlorine stability of aromatic–cycloaliphatic polyamide thin film composite membranes. *Journal of Membrane Science* **309**, 36-44, doi:<http://dx.doi.org/10.1016/j.memsci.2007.10.004> (2008).
- 204 Hilal, N. & Kochkodan, V. Surface modified microfiltration membranes with molecularly recognising properties. *Journal of Membrane Science* **213**, 97-113, doi:[http://dx.doi.org/10.1016/S0376-7388\(02\)00516-1](http://dx.doi.org/10.1016/S0376-7388(02)00516-1) (2003).
- 205 Zhao, C., Liu, X., Rikimaru, S., Nomizu, M. & Nishi, N. Surface characterization of polysulfone membranes modified by DNA immobilization. *Journal of Membrane Science* **214**, 179-189, doi:[http://dx.doi.org/10.1016/S0376-7388\(02\)00524-0](http://dx.doi.org/10.1016/S0376-7388(02)00524-0) (2003).
- 206 Yamagishi, H., Crivello, J. V. & Belfort, G. Development of a novel photochemical technique for modifying poly (arylsulfone) ultrafiltration membranes. *Journal of Membrane Science* **105**, 237-247, doi:[http://dx.doi.org/10.1016/0376-7388\(95\)00063-I](http://dx.doi.org/10.1016/0376-7388(95)00063-I) (1995).
- 207 He, D., Susanto, H. & Ulbricht, M. Photo-irradiation for preparation, modification and stimulation of polymeric membranes. *Progress in Polymer Science* **34**, 62-98, doi:<http://dx.doi.org/10.1016/j.progpolymsci.2008.08.004> (2009).

- 208 Norrman, K., Kingshott, P., Kaeselev, B. & Ghanbari-Siahkali, A. Photodegradation of poly(ether sulphone) Part 1. A time-of-flight secondary ion mass spectrometry study. *Surface and Interface Analysis* **36**, 1533-1541, doi:10.1002/sia.1980 (2004).
- 209 Pieracci, J., Crivello, J. V. & Belfort, G. Photochemical modification of 10 kDa polyethersulfone ultrafiltration membranes for reduction of biofouling. *Journal of Membrane Science* **156**, 223-240, doi:[http://dx.doi.org/10.1016/S0376-7388\(98\)00347-0](http://dx.doi.org/10.1016/S0376-7388(98)00347-0) (1999).
- 210 Pieracci, J., Wood, D. W., Crivello, J. V. & Belfort, G. UV-Assisted Graft Polymerization of N-vinyl-2-pyrrolidinone onto Poly(ether sulfone) Ultrafiltration Membranes: Comparison of Dip versus Immersion Modification Techniques. *Chemistry of Materials* **12**, 2123-2133, doi:10.1021/cm9907864 (2000).
- 211 Pieracci, J., Crivello, J. V. & Belfort, G. UV-Assisted Graft Polymerization of N-Vinyl-2-pyrrolidinone onto Poly(ether sulfone) Ultrafiltration Membranes Using Selective UV Wavelengths. *Chemistry of Materials* **14**, 256-265, doi:10.1021/cm010565+ (2001).
- 212 Taniguchi, M. & Belfort, G. Low protein fouling synthetic membranes by UV-assisted surface grafting modification: varying monomer type. *Journal of Membrane Science* **231**, 147-157, doi:<http://dx.doi.org/10.1016/j.memsci.2003.11.013> (2004).
- 213 Kaeselev, B., Pieracci, J. & Belfort, G. Photoinduced grafting of ultrafiltration membranes: comparison of poly(ether sulfone) and poly(sulfone). *Journal of Membrane Science* **194**, 245-261, doi:[http://dx.doi.org/10.1016/S0376-7388\(01\)00544-0](http://dx.doi.org/10.1016/S0376-7388(01)00544-0) (2001).
- 214 Taniguchi, M., Kilduff, J. E. & Belfort, G. Low fouling synthetic membranes by UV-assisted graft polymerization: monomer selection to mitigate fouling by natural organic matter. *Journal of Membrane Science* **222**, 59-70, doi:[http://dx.doi.org/10.1016/S0376-7388\(03\)00192-3](http://dx.doi.org/10.1016/S0376-7388(03)00192-3) (2003).
- 215 Abu Seman, M. N., Khayet, M., Bin Ali, Z. I. & Hilal, N. Reduction of nanofiltration membrane fouling by UV-initiated graft polymerization technique. *Journal of Membrane Science* **355**, 133-141, doi:<http://dx.doi.org/10.1016/j.memsci.2010.03.014> (2010).
- 216 Gupta S, S. Y., Bhattacharya A. Studies on permeation of bovine serum albumin (BSA) through photo-modified functionalized asymmetric membrane. *J Macromol Sci A* **90-6** (2009).
- 217 Wei, X., Wang, R., Li, Z. & Fane, A. G. Development of a novel electrophoresis-UV grafting technique to modify PES UF membranes used for NOM removal. *Journal of Membrane Science* **273**, 47-57, doi:<http://dx.doi.org/10.1016/j.memsci.2005.11.049> (2006).
- 218 Hilal, N., Al-Khatib, L., Atkin, B. P., Kochkodan, V. & Potapchenko, N. Photochemical modification of membrane surfaces for (bio)fouling reduction: a nano-scale study using AFM. *Desalination* **158**, 65-72, doi:[http://dx.doi.org/10.1016/S0011-9164\(03\)00434-X](http://dx.doi.org/10.1016/S0011-9164(03)00434-X) (2003).
- 219 Susanto, H., Balakrishnan, M. & Ulbricht, M. Via surface functionalization by photograft copolymerization to low-fouling polyethersulfone-based ultrafiltration membranes.

- Journal of Membrane Science* **288**, 157-167, doi:<http://dx.doi.org/10.1016/j.memsci.2006.11.013> (2007).
- 220 Susanto, H. & Ulbricht, M. Photografted Thin Polymer Hydrogel Layers on PES Ultrafiltration Membranes: Characterization, Stability, and Influence on Separation Performance. *Langmuir : the ACS journal of surfaces and colloids* **23**, 7818-7830, doi:10.1021/la700579x (2007).
- 221 Zhou, M. *et al.* High-Throughput Membrane Surface Modification to Control NOM Fouling. *Environmental Science & Technology* **43**, 3865-3871, doi:10.1021/es9003697 (2009).
- 222 Zhou, M. *et al.* High throughput synthesis and screening of new protein resistant surfaces for membrane filtration. *AIChE Journal* **56**, 1932-1945, doi:10.1002/aic.12104 (2010).
- 223 Zhu, L.-P., Xu, Y.-Y., Wei, X.-Z. & Zhu, B.-K. Hydrophilic modification of poly(phthalazine ether sulfone ketone) ultrafiltration membranes by the surface immobilization of poly(ethylene glycol) acrylates. *Desalination* **242**, 96-109, doi:<http://dx.doi.org/10.1016/j.desal.2008.03.034> (2009).
- 224 Ulbricht, M., Riedel, M. & Marx, U. Novel photochemical surface functionalization of polysulfone ultrafiltration membranes for covalent immobilization of biomolecules. *Journal of Membrane Science* **120**, 239-259, doi:[http://dx.doi.org/10.1016/0376-7388\(96\)00148-2](http://dx.doi.org/10.1016/0376-7388(96)00148-2) (1996).
- 225 Hilal, N., Al-Khatib, L., Al-Zoubi, H. & Nigmatullin, R. Atomic force microscopy study of membranes modified by surface grafting of cationic polyelectrolyte. *Desalination* **184**, 45-55, doi:<http://dx.doi.org/10.1016/j.desal.2005.02.071> (2005).
- 226 Béquet, S. *et al.* From ultrafiltration to nanofiltration hollow fiber membranes: a continuous UV-photografting process. *Desalination* **144**, 9-14, doi:[http://dx.doi.org/10.1016/S0011-9164\(02\)00281-3](http://dx.doi.org/10.1016/S0011-9164(02)00281-3) (2002).
- 227 Goma-Bilongo, T., Akbari, A., Clifton, M. J. & Remigy, J. C. Numerical simulation of a UV photografting process for hollow-fiber membranes. *Journal of Membrane Science* **278**, 308-317, doi:<http://dx.doi.org/10.1016/j.memsci.2005.11.013> (2006).
- 228 Shen, Y. J. *et al.* Gas-initiation under UV and liquid-grafting polymerization on the surface of polysulfone hollow fiber ultrafiltration membrane by dynamic method. *Journal of environmental sciences (China)* **17**, 465-468 (2005).
- 229 Furtado Filho, A. A. M. & Gomes, A. S. Copolymerization of Styrene onto Polyethersulfone Films Induced By Gamma Ray Irradiation. *Polym. Bull.* **57**, 415-421, doi:10.1007/s00289-006-0574-7 (2006).
- 230 Deng, B. *et al.* Microfiltration membranes with pH dependent property prepared from poly(methacrylic acid) grafted polyethersulfone powder. *Journal of Membrane Science* **330**, 363-368, doi:<http://dx.doi.org/10.1016/j.memsci.2009.01.010> (2009).
- 231 Schulze, A., Marquardt, B., Went, M., Prager, A. & Buchmeiser, M. R. Electron beam-based functionalization of polymer membranes. *Water science and technology : a journal*

- of the International Association on Water Pollution Research **65**, 574-580, doi:10.2166/wst.2012.890 (2012).
- 232 Gancarz, I., Poźniak, G. & Bryjak, M. Modification of polysulfone membranes 1. CO2 plasma treatment. *European Polymer Journal* **35**, 1419-1428, doi:[http://dx.doi.org/10.1016/S0014-3057\(98\)00240-7](http://dx.doi.org/10.1016/S0014-3057(98)00240-7) (1999).
- 233 Castro Vidaurre, E. F., Achete, C. A., Simão, R. A. & Habert, A. C. Surface modification of porous polymeric membranes by RF-plasma treatment. *Nuclear Instruments and Methods in Physics Research Section B: Beam Interactions with Materials and Atoms* **175–177**, 732-736, doi:[http://dx.doi.org/10.1016/S0168-583X\(00\)00659-5](http://dx.doi.org/10.1016/S0168-583X(00)00659-5) (2001).
- 234 Tyszler, D. *et al.* Reduced fouling tendencies of ultrafiltration membranes in wastewater treatment by plasma modification. *Desalination* **189**, 119-129, doi:<http://dx.doi.org/10.1016/j.desal.2005.06.019> (2006).
- 235 Saxena, N., Prabhavathy, C., De, S. & DasGupta, S. Flux enhancement by argon–oxygen plasma treatment of polyethersulfone membranes. *Separation and Purification Technology* **70**, 160-165, doi:<http://dx.doi.org/10.1016/j.seppur.2009.09.011> (2009).
- 236 Kull, K. R., Steen, M. L. & Fisher, E. R. Surface modification with nitrogen-containing plasmas to produce hydrophilic, low-fouling membranes. *Journal of Membrane Science* **246**, 203-215, doi:<http://dx.doi.org/10.1016/j.memsci.2004.08.019> (2005).
- 237 Iwa, T., Kumazawa, H. & Bae, S. Y. Gas permeabilities of NH₃-plasma-treated polyethersulfone membranes. *Journal of Applied Polymer Science* **94**, 758-762, doi:10.1002/app.20961 (2004).
- 238 Steen, M. L., Jordan, A. C. & Fisher, E. R. Hydrophilic modification of polymeric membranes by low temperature H₂O plasma treatment. *Journal of Membrane Science* **204**, 341-357, doi:[http://dx.doi.org/10.1016/S0376-7388\(02\)00061-3](http://dx.doi.org/10.1016/S0376-7388(02)00061-3) (2002).
- 239 Batsch, A., Tyszler, D., Brügger, A., Panglisch, S. & Melin, T. Foulant analysis of modified and unmodified membranes for water and wastewater treatment with LC-OCD. *Desalination* **178**, 63-72, doi:<http://dx.doi.org/10.1016/j.desal.2004.11.029> (2005).
- 240 Li, L., Yan, G. & Wu, J. Modification of polysulfone membranes via surface-initiated atom transfer radical polymerization and their antifouling properties. *Journal of Applied Polymer Science* **111**, 1942-1946, doi:10.1002/app.29204 (2009).
- 241 Yong Bo Shen, Y. T. Z., Jian Hua Qiu, Yan Wu Zhang, Hao Qin Zhang. Hydrophilic Modification of PES Hollow Fiber Membrane via Surface-Initiated Atom Transfer Radical Polymerization
565-570, doi:10.4028/www.scientific.net/AMR.150-151.565 (2010).
- 242 Liu, S. X., Kim, J. T. & Kim, S. Effect of polymer surface modification on polymer-protein interaction via hydrophilic polymer grafting. *Journal of food science* **73**, E143-150, doi:10.1111/j.1750-3841.2008.00699.x (2008).
- 243 Li, D. F., Chung, T.-S., Wang, R. & Liu, Y. Fabrication of fluoropolyimide/polyethersulfone (PES) dual-layer asymmetric hollow fiber membranes

- for gas separation. *Journal of Membrane Science* **198**, 211-223, doi:[http://dx.doi.org/10.1016/S0376-7388\(01\)00658-5](http://dx.doi.org/10.1016/S0376-7388(01)00658-5) (2002).
- 244 Li, Y. & Chung, T.-S. Silver ionic modification in dual-layer hollow fiber membranes with significant enhancement in CO₂/CH₄ and O₂/N₂ separation. *Journal of Membrane Science* **350**, 226-231, doi:<http://dx.doi.org/10.1016/j.memsci.2009.12.032> (2010).
- 245 Cao, X., Tang, M., Liu, F., Nie, Y. & Zhao, C. Immobilization of silver nanoparticles onto sulfonated polyethersulfone membranes as antibacterial materials. *Colloids and Surfaces B: Biointerfaces* **81**, 555-562, doi:<http://dx.doi.org/10.1016/j.colsurfb.2010.07.057> (2010).
- 246 Shah, T. N., Goodwin, J. C. & Ritchie, S. M. C. Development and characterization of a microfiltration membrane catalyst containing sulfonated polystyrene grafts. *Journal of Membrane Science* **251**, 81-89, doi:<http://dx.doi.org/10.1016/j.memsci.2004.10.037> (2005).
- 247 Cowan, S. & Ritchie, S. Modified Polyethersulfone (PES) Ultrafiltration Membranes for Enhanced Filtration of Whey Proteins. *Separation Science and Technology* **42**, 2405-2418, doi:10.1080/01496390701477212 (2007).
- 248 Reddy, A. V. R. *et al.* Fouling resistant membranes in desalination and water recovery. *Desalination* **183**, 301-306, doi:<http://dx.doi.org/10.1016/j.desal.2005.04.027> (2005).
- 249 Belfer, S., Fainctain, R., Purinson, Y. & Kedem, O. Surface characterization by FTIR-ATR spectroscopy of polyethersulfone membranes-unmodified, modified and protein fouled. *Journal of Membrane Science* **172**, 113-124, doi:[http://dx.doi.org/10.1016/S0376-7388\(00\)00316-1](http://dx.doi.org/10.1016/S0376-7388(00)00316-1) (2000).
- 250 Wulff, G. Molecular Imprinting in Cross-Linked Materials with the Aid of Molecular Templates—A Way towards Artificial Antibodies. *Angewandte Chemie International Edition in English* **34**, 1812-1832, doi:10.1002/anie.199518121 (1995).
- 251 Zhao, C. *et al.* BPA transfer rate increase using molecular imprinted polyethersulfone hollow fiber membrane. *Journal of Membrane Science* **310**, 38-43, doi:<http://dx.doi.org/10.1016/j.memsci.2007.10.042> (2008).
- 252 Pichon, V. & Chapuis-Hugon, F. Role of molecularly imprinted polymers for selective determination of environmental pollutants—A review. *Analytica Chimica Acta* **622**, 48-61, doi:<http://dx.doi.org/10.1016/j.aca.2008.05.057> (2008).
- 253 Mu, L.-J. & Zhao, W.-Z. Hydrophilic modification of polyethersulfone porous membranes via a thermal-induced surface crosslinking approach. *Applied Surface Science* **255**, 7273-7278, doi:<http://dx.doi.org/10.1016/j.apsusc.2009.03.081> (2009).
- 254 Shi, Q. *et al.* Trypsin-enabled construction of anti-fouling and self-cleaning polyethersulfone membrane. *Bioresource Technology* **102**, 647-651, doi:<http://dx.doi.org/10.1016/j.biortech.2010.08.030> (2011).
- 255 Shi, Q. *et al.* Graft polymerization of methacrylic acid onto polyethersulfone for potential pH-responsive membrane materials. *Journal of Membrane Science* **347**, 62-68, doi:<http://dx.doi.org/10.1016/j.memsci.2009.10.006> (2010).

- 256 Lin, Y. C., Brayfield, C. A., Gerlach, J. C., Rubin, J. P. & Marra, K. G. Peptide modification of polyethersulfone surfaces to improve adipose-derived stem cell adhesion. *Acta biomaterialia* **5**, 1416-1424, doi:10.1016/j.actbio.2008.11.031 (2009).
- 257 Wang, H., Yu, T., Zhao, C. & Du, Q. Improvement of hydrophilicity and blood compatibility on polyethersulfone membrane by adding polyvinylpyrrolidone. *Fibers Polym* **10**, 1-5, doi:10.1007/s12221-009-0001-4 (2009).
- 258 Mosqueda-Jimenez, D. B., Narbaitz, R. M. & Matsuura, T. Effects of preparation conditions on the surface modification and performance of polyethersulfone ultrafiltration membranes. *Journal of Applied Polymer Science* **99**, 2978-2988, doi:10.1002/app.22993 (2006).
- 259 Zhao, W. *et al.* Fabrication of antifouling polyethersulfone ultrafiltration membranes using Pluronic F127 as both surface modifier and pore-forming agent. *Journal of Membrane Science* **318**, 405-412, doi:<http://dx.doi.org/10.1016/j.memsci.2008.03.013> (2008).
- 260 Zhu, L.-P. *et al.* Amphiphilic graft copolymers based on ultrahigh molecular weight poly(styrene-alt-maleic anhydride) with poly(ethylene glycol) side chains for surface modification of polyethersulfone membranes. *European Polymer Journal* **44**, 1907-1914, doi:<http://dx.doi.org/10.1016/j.eurpolymj.2008.03.015> (2008).
- 261 Rahimpour, A., Madaeni, S. S., Amirinejad, M., Mansourpanah, Y. & Zeresghi, S. The effect of heat treatment of PES and PVDF ultrafiltration membranes on morphology and performance for milk filtration. *Journal of Membrane Science* **330**, 189-204, doi:<http://dx.doi.org/10.1016/j.memsci.2008.12.059> (2009).
- 262 Riedl, K., Girard, B. & Lencki, R. W. Influence of membrane structure on fouling layer morphology during apple juice clarification. *Journal of Membrane Science* **139**, 155-166, doi:[http://dx.doi.org/10.1016/S0376-7388\(97\)00239-1](http://dx.doi.org/10.1016/S0376-7388(97)00239-1) (1998).
- 263 Wang, Y.-Q., Su, Y.-L., Ma, X.-L., Sun, Q. & Jiang, Z.-Y. Pluronic polymers and polyethersulfone blend membranes with improved fouling-resistant ability and ultrafiltration performance. *Journal of Membrane Science* **283**, 440-447, doi:<http://dx.doi.org/10.1016/j.memsci.2006.07.021> (2006).
- 264 Chen, W. *et al.* Separation of oil/water emulsion using Pluronic F127 modified polyethersulfone ultrafiltration membranes. *Separation and Purification Technology* **66**, 591-597, doi:<http://dx.doi.org/10.1016/j.seppur.2009.01.009> (2009).
- 265 Zhu, L. P. *et al.* Improved protein-adsorption resistance of polyethersulfone membranes via surface segregation of ultrahigh molecular weight poly(styrene-alt-maleic anhydride). *Colloids and surfaces. B, Biointerfaces* **57**, 189-197, doi:10.1016/j.colsurfb.2007.01.021 (2007).
- 266 Wang, M., Wu, L. G., Zheng, X. C., Mo, J. X. & Gao, C. J. Surface modification of phenolphthalein poly(ether sulfone) ultrafiltration membranes by blending with acrylonitrile-based copolymer containing ionic groups for imparting surface electrical properties. *Journal of colloid and interface science* **300**, 286-292, doi:10.1016/j.jcis.2006.03.042 (2006).

- 267 Reddy, A. V. R. & Patel, H. R. Chemically treated polyethersulfone/polyacrylonitrile blend ultrafiltration membranes for better fouling resistance. *Desalination* **221**, 318-323, doi:<http://dx.doi.org/10.1016/j.desal.2007.01.089> (2008).
- 268 Rahimpour, A. & Madaeni, S. S. Improvement of performance and surface properties of nano-porous polyethersulfone (PES) membrane using hydrophilic monomers as additives in the casting solution. *Journal of Membrane Science* **360**, 371-379, doi:<http://dx.doi.org/10.1016/j.memsci.2010.05.036> (2010).
- 269 Susanto, H. & Ulbricht, M. Characteristics, performance and stability of polyethersulfone ultrafiltration membranes prepared by phase separation method using different macromolecular additives. *Journal of Membrane Science* **327**, 125-135, doi:<http://dx.doi.org/10.1016/j.memsci.2008.11.025> (2009).
- 270 Khayet, M., Suk, D. E., Narbaitz, R. M., Santerre, J. P. & Matsuura, T. Study on surface modification by surface-modifying macromolecules and its applications in membrane-separation processes. *Journal of Applied Polymer Science* **89**, 2902-2916, doi:10.1002/app.12231 (2003).
- 271 Wang, T., Wang, Y.-Q., Su, Y.-L. & Jiang, Z.-Y. Antifouling ultrafiltration membrane composed of polyethersulfone and sulfobetaine copolymer. *Journal of Membrane Science* **280**, 343-350, doi:<http://dx.doi.org/10.1016/j.memsci.2006.01.038> (2006).
- 272 Shi, Q. *et al.* A facile method for synthesis of pegylated polyethersulfone and its application in fabrication of antifouling ultrafiltration membrane. *Journal of Membrane Science* **303**, 204-212, doi:<http://dx.doi.org/10.1016/j.memsci.2007.07.009> (2007).
- 273 Alsari, A. M., Khulbe, K. C. & Matsuura, T. The effect of sodium dodecyl sulfate solutions as gelation media on the formation of PES membranes. *Journal of Membrane Science* **188**, 279-293, doi:[http://dx.doi.org/10.1016/S0376-7388\(01\)00395-7](http://dx.doi.org/10.1016/S0376-7388(01)00395-7) (2001).
- 274 Zhang, L., Chowdhury, G., Feng, C., Matsuura, T. & Narbaitz, R. Effect of surface-modifying macromolecules and membrane morphology on fouling of polyethersulfone ultrafiltration membranes. *Journal of Applied Polymer Science* **88**, 3132-3138, doi:10.1002/app.12000 (2003).
- 275 Li, L. *et al.* Preparation and characterization of poly(acrylonitrile-acrylic acid-N-vinyl pyrrolidinone) terpolymer blended polyethersulfone membranes. *Journal of Membrane Science* **349**, 56-64, doi:<http://dx.doi.org/10.1016/j.memsci.2009.11.018> (2010).
- 276 Su, Y. *et al.* Modification of polyethersulfone ultrafiltration membranes with phosphorylcholine copolymer can remarkably improve the antifouling and permeation properties. *Journal of Membrane Science* **322**, 171-177, doi:<http://dx.doi.org/10.1016/j.memsci.2008.05.047> (2008).
- 277 Mansourpanah, Y., Madaeni, S. S., Adeli, M., Rahimpour, A. & Farhadian, A. Surface modification and preparation of nanofiltration membrane from polyethersulfone/polyimide blend—Use of a new material (polyethyleneglycol-triazine). *Journal of Applied Polymer Science* **112**, 2888-2895, doi:10.1002/app.29821 (2009).

- 278 Rahimpour, A., Madaeni, S. S. & Mehdipour-Ataei, S. Synthesis of a novel poly(amide-imide) (PAI) and preparation and characterization of PAI blended polyethersulfone (PES) membranes. *Journal of Membrane Science* **311**, 349-359, doi:<http://dx.doi.org/10.1016/j.memsci.2007.12.038> (2008).
- 279 Yi, Z., Zhu, L., Xu, Y., Jiang, J. & Zhu, B. Polypropylene Glycol: The Hydrophilic Phenomena in the Modification of Polyethersulfone Membranes. *Industrial & Engineering Chemistry Research* **50**, 11297-11305, doi:10.1021/ie201238c (2011).
- 280 Amirilargani, M., Saljoughi, E. & Mohammadi, T. Improvement of permeation performance of polyethersulfone (PES) ultrafiltration membranes via addition of Tween-20. *Journal of Applied Polymer Science* **115**, 504-513, doi:10.1002/app.30814 (2010).
- 281 Sotto, A. *et al.* Effect of nanoparticle aggregation at low concentrations of TiO₂ on the hydrophilicity, morphology, and fouling resistance of PES-TiO₂ membranes. *Journal of colloid and interface science* **363**, 540-550, doi:10.1016/j.jcis.2011.07.089 (2011).
- 282 Mansourpanah, Y., Madaeni, S. S., Rahimpour, A., Farhadian, A. & Taheri, A. H. Formation of appropriate sites on nanofiltration membrane surface for binding TiO₂ photocatalyst: Performance, characterization and fouling-resistant capability. *Journal of Membrane Science* **330**, 297-306, doi:<http://dx.doi.org/10.1016/j.memsci.2009.01.001> (2009).
- 283 Prashantha, K. & Park, S. G. Nanosized TiO₂-filled sulfonated polyethersulfone proton conducting membranes for direct methanol fuel cells. *Journal of Applied Polymer Science* **98**, 1875-1878, doi:10.1002/app.21970 (2005).
- 284 Wei, Q., Li, J., Qian, B., Fang, B. & Zhao, C. Preparation, characterization and application of functional polyethersulfone membranes blended with poly (acrylic acid) gels. *Journal of Membrane Science* **337**, 266-273, doi:<http://dx.doi.org/10.1016/j.memsci.2009.03.055> (2009).
- 285 Li, Y., Chung, T.-S., Cao, C. & Kulprathipanja, S. The effects of polymer chain rigidification, zeolite pore size and pore blockage on polyethersulfone (PES)-zeolite A mixed matrix membranes. *Journal of Membrane Science* **260**, 45-55, doi:<http://dx.doi.org/10.1016/j.memsci.2005.03.019> (2005).
- 286 Li, Y., Guan, H.-M., Chung, T.-S. & Kulprathipanja, S. Effects of novel silane modification of zeolite surface on polymer chain rigidification and partial pore blockage in polyethersulfone (PES)-zeolite A mixed matrix membranes. *Journal of Membrane Science* **275**, 17-28, doi:<http://dx.doi.org/10.1016/j.memsci.2005.08.015> (2006).
- 287 Kusworo, T. D., Ismail, A. F., Mustafa, A. & Matsuura, T. Dependence of membrane morphology and performance on preparation conditions: The shear rate effect in membrane casting. *Separation and Purification Technology* **61**, 249-257, doi:<http://dx.doi.org/10.1016/j.seppur.2007.10.017> (2008).
- 288 Maximous, N., Nakhla, G., Wong, K. & Wan, W. Optimization of Al₂O₃/PES membranes for wastewater filtration. *Separation and Purification Technology* **73**, 294-301, doi:<http://dx.doi.org/10.1016/j.seppur.2010.04.016> (2010).

- 289 Maximous, N., Nakhla, G., Wan, W. & Wong, K. Performance of a novel ZrO₂/PES membrane for wastewater filtration. *Journal of Membrane Science* **352**, 222-230, doi:<http://dx.doi.org/10.1016/j.memsci.2010.02.021> (2010).
- 290 Ulbricht, M., Schuster, O., Ansorge, W., Ruetering, M. & Steiger, P. Influence of the strongly anisotropic cross-section morphology of a novel polyethersulfone microfiltration membrane on filtration performance. *Separation and Purification Technology* **57**, 63-73, doi:<http://dx.doi.org/10.1016/j.seppur.2007.02.012> (2007).
- 291 Rahimpour, A., Madaeni, S. S., Ghorbani, S., Shokravi, A. & Mansourpanah, Y. The influence of sulfonated polyethersulfone (SPES) on surface nano-morphology and performance of polyethersulfone (PES) membrane. *Applied Surface Science* **256**, 1825-1831, doi:<http://dx.doi.org/10.1016/j.apsusc.2009.10.014> (2010).
- 292 Berger, T. J., Spadaro, J. A., Bierman, R., Chapin, S. E. & Becker, R. O. Antifungal properties of electrically generated metallic ions. *Antimicrobial agents and chemotherapy* **10**, 856-860 (1976).
- 293 Balazs, D. J. *et al.* Inhibition of bacterial adhesion on PVC endotracheal tubes by RF-oxygen glow discharge, sodium hydroxide and silver nitrate treatments. *Biomaterials* **25**, 2139-2151 (2004).
- 294 Melaiye, A. & Youngs, W. J. Silver and its application as an antimicrobial agent. *Expert Opinion on Therapeutic Patents* **15**, 125-130, doi:doi:10.1517/13543776.15.2.125 (2005).
- 295 Stobie, N. *et al.* Prevention of Staphylococcus epidermidis biofilm formation using a low-temperature processed silver-doped phenyltriethoxysilane sol-gel coating. *Biomaterials* **29**, 963-969, doi:10.1016/j.biomaterials.2007.10.057 (2008).
- 296 Qian, X.-F. *et al.* The preparation and characterization of PVA/Ag₂S nanocomposite. *Materials Chemistry and Physics* **68**, 95-97, doi:[http://dx.doi.org/10.1016/S0254-0584\(00\)00288-1](http://dx.doi.org/10.1016/S0254-0584(00)00288-1) (2001).
- 297 Chou, W.-L., Yu, D.-G. & Yang, M.-C. The preparation and characterization of silver-loading cellulose acetate hollow fiber membrane for water treatment. *Polymers for Advanced Technologies* **16**, 600-607, doi:10.1002/pat.630 (2005).
- 298 Hoek, E. M. V., Kaner, R. B., GUILLEN, G. R. & Farrell, T. P. (Google Patents, 2014).
- 299 Martín, A. *et al.* Enhanced ultrafiltration PES membranes doped with mesostructured functionalized silica particles. *Desalination* **357**, 16-25, doi:<http://dx.doi.org/10.1016/j.desal.2014.10.046> (2015).
- 300 Kumar, A., Vemula, P. K., Ajayan, P. M. & John, G. Silver-nanoparticle-embedded antimicrobial paints based on vegetable oil. *Nat Mater* **7**, 236-241, doi:http://www.nature.com/nmat/journal/v7/n3/suppinfo/nmat2099_S1.html (2008).
- 301 Guggenbichler, J. P., Boswald, M., Lugauer, S. & Krall, T. A new technology of microdispersed silver in polyurethane induces antimicrobial activity in central venous catheters. *Infection* **27 Suppl 1**, S16-23 (1999).

- 302 Kang, S., Hoek, E. M. V., Choi, H. & Shin, H. Effect of Membrane Surface Properties During the Fast Evaluation of Cell Attachment. *Separation Science and Technology* **41**, 1475-1487, doi:10.1080/01496390600634673 (2006).
- 303 Nie, F.-Q. *et al.* Preparation and characterization of polyacrylonitrile-based membranes: Effects of internal coagulant on poly(acrylonitrile-co-malefic acid) ultrafiltration hollow fiber membranes. *Desalination* **160**, 43-50, doi:[http://dx.doi.org/10.1016/S0011-9164\(04\)90016-1](http://dx.doi.org/10.1016/S0011-9164(04)90016-1) (2004).
- 304 Khayet, M., Feng, C. Y., Khulbe, K. C. & Matsuura, T. Preparation and characterization of polyvinylidene fluoride hollow fiber membranes for ultrafiltration. *Polymer* **43**, 3879-3890, doi:[http://dx.doi.org/10.1016/S0032-3861\(02\)00237-9](http://dx.doi.org/10.1016/S0032-3861(02)00237-9) (2002).
- 305 Young, T.-H., Cheng, L.-P., Lin, D.-J., Fane, L. & Chuang, W.-Y. Mechanisms of PVDF membrane formation by immersion-precipitation in soft (1-octanol) and harsh (water) nonsolvents. *Polymer* **40**, 5315-5323, doi:[http://dx.doi.org/10.1016/S0032-3861\(98\)00747-2](http://dx.doi.org/10.1016/S0032-3861(98)00747-2) (1999).
- 306 Ahmad, A. L. Y., N.H. Mat ; Derek, C.J.C. ; Lim, J.K. ; . Microfiltration of *Chlorella* sp.: Influence of material and membrane pore size. *Membrane Water Treatment* **2**, 143-155, doi:10.12989/mwt.2013.4.2.143 (2013).
- 307 Liu, P.-S., Chen, Q., Wu, S.-S., Shen, J. & Lin, S.-C. Surface modification of cellulose membranes with zwitterionic polymers for resistance to protein adsorption and platelet adhesion. *Journal of Membrane Science* **350**, 387-394, doi:<http://dx.doi.org/10.1016/j.memsci.2010.01.015> (2010).
- 308 Subramani, A. & Hoek, E. M. V. Direct observation of initial microbial deposition onto reverse osmosis and nanofiltration membranes. *Journal of Membrane Science* **319**, 111-125, doi:<http://dx.doi.org/10.1016/j.memsci.2008.03.025> (2008).
- 309 Katsoufidou, K., Yiantsios, S. G. & Karabelas, A. J. Experimental study of ultrafiltration membrane fouling by sodium alginate and flux recovery by backwashing. *Journal of Membrane Science* **300**, 137-146, doi:<http://dx.doi.org/10.1016/j.memsci.2007.05.017> (2007).
- 310 Liu, T. *et al.* Synergistic strengthening of polyelectrolyte complex membranes by functionalized carbon nanotubes and metal ions. *Sci. Rep.* **5**, doi:10.1038/srep07782 <http://www.nature.com/srep/2015/150114/srep07782/abs/srep07782.html#supplementary-information> (2015).
- 311 Singh, S. K. *et al.* Amine-Modified Graphene: Thrombo-Protective Safer Alternative to Graphene Oxide for Biomedical Applications. *ACS nano* **6**, 2731-2740, doi:10.1021/nn300172t (2012).
- 312 Cao, L., Sun, Q., Gao, Y., Liu, L. & Shi, H. Novel acid-base hybrid membrane based on amine-functionalized reduced graphene oxide and sulfonated polyimide for vanadium redox flow battery. *Electrochimica Acta* **158**, 24-34, doi:<http://dx.doi.org/10.1016/j.electacta.2015.01.159> (2015).

- 313 Prince, J. A. *et al.* Effect of hydrophobic surface modifying macromolecules on differently produced PVDF membranes for direct contact membrane distillation. *Chemical Engineering Journal* **242**, 387-396, doi:<http://dx.doi.org/10.1016/j.cej.2013.11.039> (2014).
- 314 Matsuura, T. *Synthetic Membranes and Membrane Separation Processes*. (CRC Press December 17, 1993).
- 315 Zhao, C., Xu, X., Chen, J. & Yang, F. Effect of graphene oxide concentration on the morphologies and antifouling properties of PVDF ultrafiltration membranes. *Journal of Environmental Chemical Engineering* **1**, 349-354, doi:<http://dx.doi.org/10.1016/j.jece.2013.05.014> (2013).
- 316 Yu, L. *et al.* Preparation and characterization of HPEI-GO/PES ultrafiltration membrane with antifouling and antibacterial properties. *Journal of Membrane Science* **447**, 452-462, doi:<http://dx.doi.org/10.1016/j.memsci.2013.07.042> (2013).
- 317 Lee, J. *et al.* Graphene oxide nanoplatelets composite membrane with hydrophilic and antifouling properties for wastewater treatment. *Journal of Membrane Science* **448**, 223-230, doi:<http://dx.doi.org/10.1016/j.memsci.2013.08.017> (2013).
- 318 Xu, Z. *et al.* Organosilane-functionalized graphene oxide for enhanced antifouling and mechanical properties of polyvinylidene fluoride ultrafiltration membranes. *Journal of Membrane Science* **458**, 1-13, doi:<http://dx.doi.org/10.1016/j.memsci.2014.01.050> (2014).
- 319 Zhang, J. *et al.* Synergetic effects of oxidized carbon nanotubes and graphene oxide on fouling control and anti-fouling mechanism of polyvinylidene fluoride ultrafiltration membranes. *Journal of Membrane Science* **448**, 81-92, doi:<http://dx.doi.org/10.1016/j.memsci.2013.07.064> (2013).